UNIVERSITY OF BIRMINGHAM

Gold Nanoparticles: Synthesis, Characterisation and their Effect on Pseudomonas Flourescens

By

Yusuf Nur

A thesis submitted to

The University of Birmingham

for the Degree of

DOCTOR OF PHILOSOPHY

School of Geography, Earth and Environmental Sciences

The University of Birmingham

April 2013

Abstract

As recently developed products with many unknown aspects, the effect of nanoparticles on the natural environment is of growing concerns among environmental scientists and the wider community. Both the fate and behaviour of the nanoparticles in the environment and their effects on the living organisms need to be better understood in order to maintain environmental health and ensure the sustainability of the important nanotechnology industry.

This dissertation focused on the effects of gold nanoparticles on the environmentally relevant bacteria, Pseudomonas fluorescens, as a model of the planktonic bacterial biomass in the environment.

A bottom - up chemical method was deployed to synthesise constrained gold nanoparticles of a variety of sizes and with two different coating agents (citrate and polyvinylpyrrolidone (PVP)) followed by a series of characterisation steps both pre and post bacterial exposure. Citrate capped gold NPs were synthesized by citrate reduction of $HAuCl_4.3H_2O$ at 100 ^oC. The synthesis of AuNPs capped with PVP was carried out at both room temperature and 70 ^oC to compare the effect of the temperature on the quality of the final NPs. Nanoparticles were characterised by measuring their relevant physicochemical properties. Among the determined properties are size, shape, zeta potential, surface charge and stability in environmentally relevant ionic strength and in bacterial growth media.

The freshly synthesized gold nanoparticles remained stable for at least six months. The citrate capped gold nanoparticles (AuNPs) were less stable in environmentally relevant ionic strength solutions and in bacterial growth media than the PVP capped gold nanoparticles. The citrate capped gold NPs formed aggregates which are much bigger than 100 nm in the solutions of ionic strength as low as 16 mM and in full strength of bacterial growth Media

(Minimal Davis Media) while the PVP capped gold NPs remained stable in size and in shape in the above mentioned solutions and in solutions of ionic strength as high as 80 mM.

Fully characterised gold NPs were incubated in the bacterial exposure media minimal Davis media (MDM). The effects of the gold nanoparticles on the bacteria were investigated both via measurements of bacterial growth inhibition (optical density at 595 nm) and by visual examination of the structural damage of the bacterial membrane using transmission electron microscope (TEM).

The citrate capped AuNPs of (14 nm core size) of 10 ppm final concentration in the exposure media had no measureable effect on the bacterial growth as no inhibition was recorded when compared with control samples. Similarly no membrane damages were shown by the TEM images of the bacterial cells incubated with citrate capped NPs, while similar concentration and comparable sizes of PVP capped gold NPs have affected the bacterial growth. This effect was manifested through the reduction of optical density and was demonstrated by the transmission electron microscope (TEM) images in the form of membrane damage including blebbing formation, tubular structures on the surface of the outer membrane of the bacterial cells and, in severe cases, the complete bursting of bacterial cells. It was found out that gold ions inhibit completely the bacterial growth as shown by optical density measurements.

In conclusion, this research has confirmed the effect of gold nanoparticles on the planktonic bacteria Pseudomonas fluorescens. The importance of the surface chemistry of the nanoparticles on the bacteria was clearly shown since NPs with similar concentration and core size but with different coating agents showed different effect on the bacteria.

Acknowledgements

There are lots of people whom I want to take this opportunity to thank for their valuable support in the course of my PhD project. My first and foremost gratitude goes to my supervisor, Professor Jamie Lead for his honest and friendly guidance, his extremely useful ideas and endless professional support throughout the project. Thank you very much for your valuable time and immeasurable patience. My special thanks also go to my co-supervisors Dr Jerome Duvel and Professor Herman van Leeuwen for their excellent ideas and support. I am extremely thankful to all of my colleagues in the Environmental Health Research group in the School of Geography, Earth and Environmental Science at the University of Birmingham, especially, to Mrs Milla Tajamaya for her useful discussions and mutual moral support needed for the continuation of the PhD project, Dr Mohammed Baalousha for his support with atomic force microscope (AFM) images and Dr Ruth Merrifield for her initial training with the analytical equipments in the laboratory. I owe special thanks to the group of Microscopic Centre at the University of Birmingham for both the training and technical support of the imaging of my samples. The data of this project will be incomplete without the support of Dr Stephen Baker for the ICPM-MS measurements, thank you infinitely for your help. I am also very grateful to my friend and previous colleague, Mr Khaled Ghazel, for his continuous encouragement and support with the structure of the dissertation.

I would particularly like to thank the Natural Environmental Research Council (NERC) for the funding of my project.

Finally, I am extremely grateful to my family for their patience, compromise, continuous moral support and understanding during the last three and a half years in which most of my time and energy was devoted to the completion of this project.

Table of Contents

List of abbreviations

β	angular aperture
δ	distance between two objects
μ	refractive index
AFM	atomic force microscope
AuNPs	gold nanoparticles
CNT	carbon nanotube
CVD	chemical vapor deposition
DLS	dynamic light scattering
DVLO	Derjaguin, Verwe, Landau, and Overbeek
E	field strength
EDS	energy dispersive X-ray spectrometer
EDX	energy dispersive x-ray
EPS	extracellular polymeric substances
ESA	electrostatic analyser
F_C	centrifugal acceleration
FFF	Field flow fractionation
ICP-MS	Inductively Coupled Plasma Mass Spectrometry
K	stiffness of the lever.
kDa	kilodalton
KV	kilovolt
K_w	water constant
LED	light emitting diodes
LSPR	localised surface Plasmon resonance
MDM	Minimal Davis Media
MRI	magnetic resonance imaging
MTB	magnetotactic bacteria

MWCNTs	multi-walled carbon nanotubes
N	rotational speed
NOM	natural organic matter
NPS	nanoparticles
OD	optical density
OECD	Organization for Economic Cooperation and Development
PEG	polyethylene glycol
PGPR	plant growth-promoting rhizobacteria
PGPR	plant growth-promoting rhizobacteria
PPb	part per billion
PPM	part per million
PVP	polyvinylpyrrolidone
PVPNPs	polyvinylpyrrolidone nanoparticles
r	radius
REFNANO	Reference materials for engineered nanoparticle
RF	radio frequency
SRHA	Suwannee River humic acid
STM	scanning tunneling microscopy
SWCNTs	single-walled carbon nanotubes
TEM	transmission electron microscope
TOC	total organic carbon
UV_VIS	ultraviolet-visible spectroscopy
WPMN	Working Party on Manufactured Nanomaterials
Z	deflection distance
ζ	zetapotentia
λ	wavelength
ώ	angular speed

List of figures

List of tables

Chapter 1: Introduction

Nanoparticles (NPs) are building blocks of nanotechnology and are referred to a natural, incidental or manufactured material containing particles, in an unbound state or as an aggregate or as an agglomerate and where, for 50% or more of the particles in the number size distribution, one or more external dimensions is in the size range 1 nm – 100 nm (European, 2011). It is important to understand that the abovementioned definition of the nanoparticles is mainly for regulation purpose and there are other definitions given by other institutions (SCENIHR, 2007, Dowling, 2005). Throughout the thesis the European Union definition will be used. The source of NPs can be both natural and anthropogenic (man-made). Natural nanoparticles have been present in the environment for millions of years and they have been generated by a number of natural processes including weathering, erosion, volcanic eruption, hydrolysis and biological activities. Recently, however, several sources have resulted in an increase in anthropogenic nanoparticle formation (Pratim and Chang-Yu, 2005): among the different activities that contributed to the augmentation of the nanoparticles in the environment are: coal fired combustions, transportations, welding processes followed by more recent processes where engineered nanoparticles are designed and produced deliberately (see Figure 1-1).

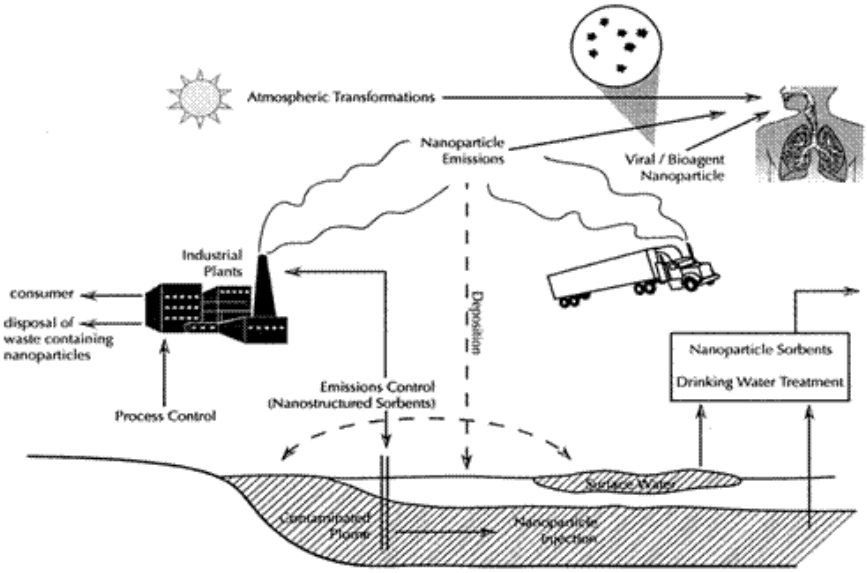

Figure 1-1: Schematic diagram illustrating source, release and the presence of the nanoparticles in the environment (Pratim and Chang-Yu, 2005). Reprinted with the permission from copyright 2005 Taylor and Francis.

Engineered nanoparticles are the backbone of modern nanotechnology where research and development are growing very fast and attract substantial funding both from public and private sectors (Joner et al., 2008). Particles in the nanometer-size (10^{-9} m) range have gained much attention due to their fascinating electrical, optical, magnetic and catalytic properties associated with their nanoscale dimensions (Christof, 2001). Those fascinating, unique and novel properties make nanomaterials pysicochemically different and often superior to both the atomic and bulk materials of the same element. For instance, copper which is opaque at macroscale becomes completely transparent to visible light at the nanoscale (Zong et al., 2005, Shanmin and et al., 2003); stable materials like aluminium turn combustible (Shafirovich et al., 2006, Shafirovich et al., 2007); Gold, which is rarely insoluble in water at the macroscale, becomes more soluble in the nanoscale (Paolo Pengo, 2003). While a known insulator, silicon, becomes a conductor of electrical current at nanoscale (Hu et al., 2003), A material such as platinium, which is chemically inert at normal scales, can serve as a potent chemical catalyst at nanoscales (Luo et al., 2005, Tian et al., 2007). They have many applications varying from communications to catalysts, computing chips, nanomechanical

parts, photo sensors, novel platform for specific delivery of therapeutic agents, cosmetics and ant-aging drugs and they are attracted by a wide range of scientific researches in different fields of science (Figure 1-2) (Ferrari, 2005, Templeton et al., 1999).

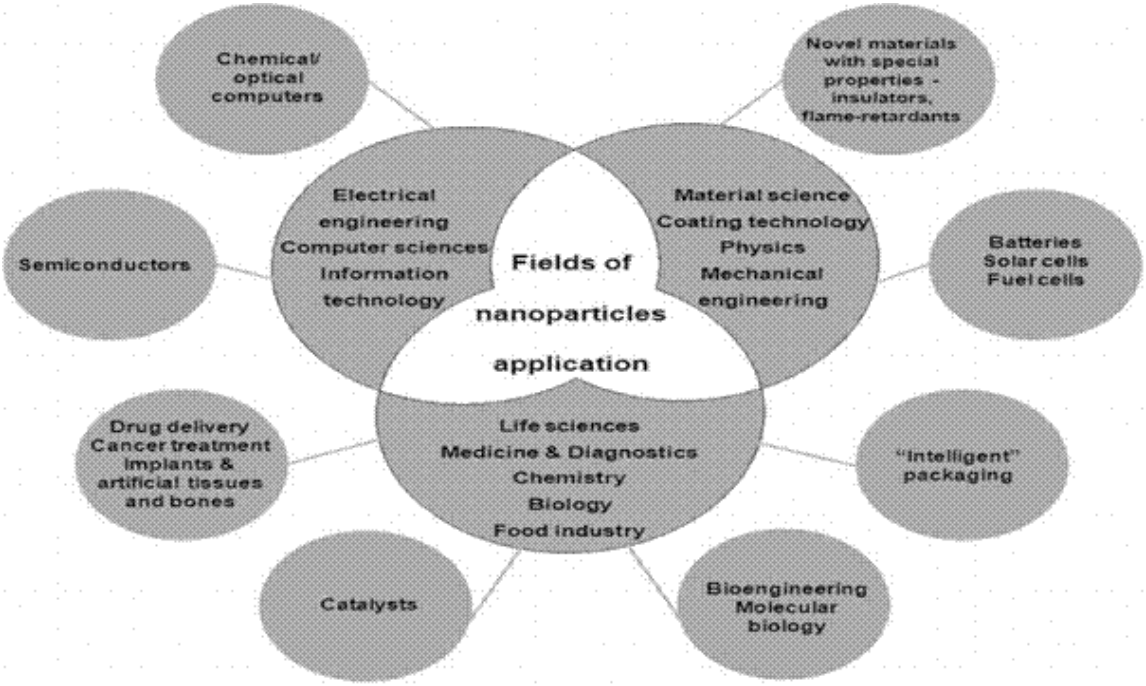

Figure 1-2: Different fields of application for nanaoparticles (Krumov et al., 2009). Reprinted with the permission from copyright 2009 John and Willey

Therefore, both the number and type of the manufactured nanoparticles have amplified tremendously with the development of this new technology. Consequently, their concentration in the natural environment has increased proportionally since enormous amounts of products are being commercialised and marketed through the world and finally released directly or indirectly into the environment (Ray et al., 2009, Flahaut, 2010). This undesired presence of manufactured nanoparticles in the environment may augment if the recycling processes, waste management and monitoring activities are not effective enough to relinquish the leakage of nanoparticles into the environment. Although we may have some knowledge about the properties of synthesised nanoparticles during the synthesis process and in the commercial products, our understanding of their fate and behaviour in the natural

environment is still quite limited due to the complexity of the system and the need for further understanding is eminent (Ju-Nam and Lead, 2008). They can interact with other naturally occuring nanosized particles and produce new particles with unknown properties. Their surface chemistry may change due to the relevant environmental conditions.

However, there is growing awareness and increasing interest in the fate, behaviour and environmental impact of the nano-scaled materials. To avoid past mistakes of the chemicals and different products (plastics, asbestos) designed and used without any clear understanding of their possible impact on the environment, researchers of today are now more than ever willing to understand the effects of nanomaterials on the environment before their use becomes widespread (Theodore, 2005). Once NPs are released they may end up in the different compartments of the environment which are: air, water, soil and living organisms. Since the physicochemical properties of these compartments are quite different, the NPs are more likely to behave differently in each compartment. Information about the NPs behaviour in any compartment will increase our understanding of the nanomaterials in the environment which, in turn, is essential to study any effects caused by the NPs in the environment including living organisms such microorganisms.

1.1 Aims and Objectives

The overall aim of this PhD project is to investigate the effect of gold nanoparticles as a model of engineered NPs on environmental abundant planktonic bacteria. The objectives of this study are:

1. to synthesise and fully characterise well constrained gold NPs.

2. to study the fate and behaviour of gold NPs in bacteria growth media.

3. to investigate the effect of the nanoparticles core size on planktonic bacteria.

4. to investigate the effect of the coating agents (surface chemistry) of the NPs on the bacteria.

During the first stage of the investigation, gold nanoparticles of different sizes and different coating agents will be synthesised and thoroughly characterised using a variety of different but complementing analytical and imaging techniques. Prior to the exposure of the NPs to the planktonic bacteria, their behaviour in liquid bacteria growth media are studied in terms of size, shape, aggregation, overall charge and surface plasmon resonance. In media characterisation step of the NPs is essential to study whether the NPs keep their original physicochemical properties in the media. Then fully characterised gold nanoparticles were used to test the effect of both size and coating agent on planktonic bacteria. The chosen strain for this study is pseudomonas fluorescens SBW25, a widespread, bacterium which is very helpful for both plants (agriculture) and humans (it produces antibiotics). Special care is taken to the core size of nanoparticles so that the possible effect of coating agents can be determined and compared. Increasing knowledge about these kinds of systems extends our understanding of the effect of the NPs core size and their surface chemistry on bacteria and can facilitate the prediction of the effect of similar nanoparticles on similar bacteria.

1.2 Outline of the dissertation

This PhD thesis consists of seven chapters whose topics are summarised below:

Chapter 1 introduces the concept of nanoparticles and describes both the aims and objectives of the thesis. It also gives clear outline of the thesis chapters as follows.

Chapter 2 highlights a general background of nanoparticles. After a detailed description of the types and origin of the nanoparticles, their fate and behaviour in natural environment is examined. After that, outlined are the possible difficulties imposed by the complex natural system which may make almost impossible to gain accurate understanding of their expected effects on the living organisms. Special attention is devoted to the effect of the nanoparticles on the bacterial biomass which is an integral part of the environment.

Chapter 3 addresses the variety of methods used to perform the project. It gives a short description of gold nanoparticles syntheses methods followed by characterisation techniques. Metal nanoparticles can be prepared by physical methods like evaporation of a metal in a vacuum or laser ablation, or by chemical methods involving the reduction of metal salts. All nanoparticles used in this project are prepared by the chemical method. After the reduction of gold ions into gold atoms, the resulting gold nanoparticles need to be stabilised. This can be achieved either sterically using relatively big molecules such as polymers or by charge. In this project, Sterically stabilised gold nanoapraticles are synthesised using PVP as coating agents and NaOH as reducing agents in room temperature while charge stabilisation of the gold nanoparticles is achieved by using sodium citrate as capping agents as was introduced by Turkevich (Turkevich, 1951) and modified by Frens (Frens, 1973) and others (Kumar et al., 2006). The synthesised NPs are fully characterised using a variety of analytical and imaging techniques. Among the techniques used to elucidate the physicochemical properties of the nanoparticles are transmission electronic microscopy (TEM), atomic force microscopy (AFM), dynamic light scattering (DLS), and ultraviolet-visible spectroscopy (UV_VIS). To study the bacterial growth and to investigate the effect of the NPs on the bacteria, optical densities of bacteria treated with NPs and untreated bacteria are recorded and compared. TEM and imaging of the outer membrane of the bacteria will help to visualise any membrane

damage caused by the NPs. Similarly, fixation and sectioning techniques of the bacteria cells followed by TEM imaging will serve to observe internalisation of the nanoparticles in the bacterial cells.

Chapter 4 presents the results of the synthesised gold nanoparticles. The focus is to synthesise a wide range of sizes of gold nanoparticles with different coating agents. Two coating agents (PVP and sodium citrate) are used and for each one a range of different sizes are achieved and fully characterised. This chapter investigates the physicochemical properties of the synthesised gold nanoparticles in terms of size, shape, charge and electrophoretic mobility and tries to discover any patterns in the data. Special attention will be devoted to the quality of the data in terms of monodispersity, roundness and stability.

Chapter 5 investigates the stability of goldnanoparticles in the bacteria growth media (Minimal Davis Media) through complete post exposure characterisation in terms of relevant physicochemical properties. The effect of the fully characterised NPs on the bacteria is also studied in this chapter. The growth inhibition of the bacteria caused by the NPs is studied by recording the optical density (OD) of the bacterial population with spectrophotometer. This chapter aims to visualise the distribution and stability of the NPs in the bacteria suspension media using TEM image measurements.

Chapter 6 studies the interaction of the synthesised and characterised gold nanoparticles on the bacterial outer membrane. TEM and images of treated bacteria with different types of gold NPs are used to observe any membrane damage caused by the NPs. Internalisation of the gold NPs in the bacterial body is also studied though fixation and sectioning techniques.

Chapter 7 summarises the general findings of the PhD project and draws analysis of the results followed by some useful suggestions for future work in the field of the fate and

behaviour of nanoparticles in natural environment especially the interaction of the NPs on the bacterial biomass which forms an integral part of the environment.

Chapter 2: Research Background

2.1 Types and the origin of the nanoparticles (NPs)

To have an idea of the scale of the nanostructured materials, Figure 2-1 below puts the size of nanoscale regime materials into perspective and compares them with some well-known objects. There are a number of ways, based on different aspects, that NPs can be classified into groups. Considering their origin, they can be divided into natural and anthropogenic (man-made) which, in turn, can be subdivided into accidental and engineered or manufactured NPs (see Table 2-1 below) or they can be further separated, based on their chemical composition, into organic (carbon containing) and inorganic(Nowack and Bucheli, 2007).

As the name clearly implies, natural NPs are a group of nanosized materials which are generated by the action of natural processes and have been present in the natural environment for a very long time since the origin of the planet Earth. In addition to natural NPs, earlier human activities like mining, agriculture, forest burning and constructions have tremendously increased the concentration of accidental nanoparticles into the environment especially into the atmosphere. Despite the fact that NPs have been present in the environment for millions of years as natural and later as accidental NPs, it was not until quite recently that their interest in both pure and applied sciences have been extensively exploited due to the discovery of their promising, novel and applicable properties which make them attractive for a vast number of products in a wide range of scientific researches and for many sectors of the modern technology.

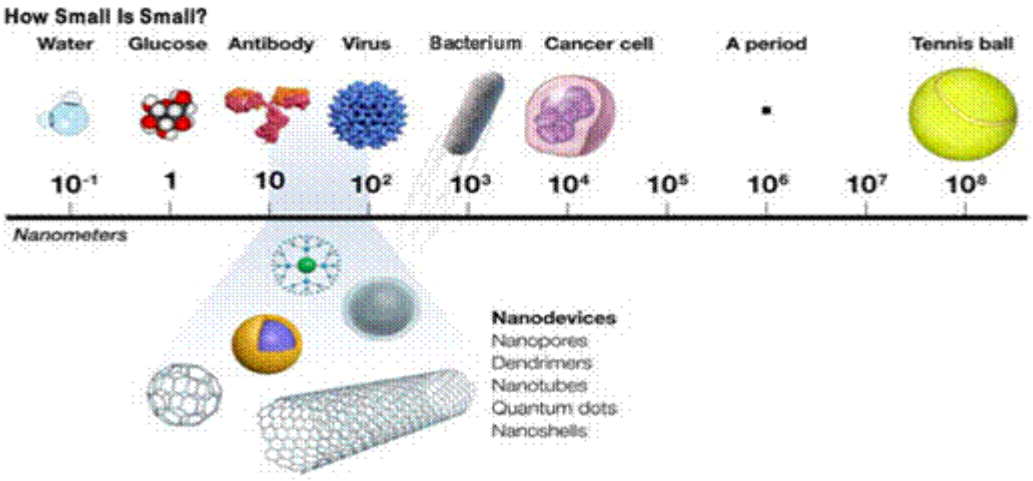

Figure 2-1: Schematic representation of the size of some objects in nanometers scale.
(http://publications.nigms.nih.gov/chemhealth/cool.htm, 2011)

Nanostructured materials behave differently and are often superior in properties to bulk materaials due to two primary factors: surface effects (enhanced surface phenomena caused by the very high surface area to volume ratio. Most atoms are on or near the surface thus they can be weakly bonded and more reactive) and quantum effects (discontinuity in behaviour caused by the confined delocalised electrons on the surface of the NPs due to their small dimensions) (Roduner, 2006). Those properties affect the overall physicochemical properties of the nanoscale materials in a way that they demonstrate novel and unprecedented properties. Nanotechnology takes the advantage and exploits these aforementioned unique properties of nanoscale matter to design, translate and apply science to plenty of useful products. This new technology forms the basis of a wide interdisciplinary area of research development and industrial activity that has been growing fast throughout the world for the past few decades (Aitken et al., 2006).The importance of nanotechnology in today's modern society is clearly explained by both the variety of scientific and technological applications using nanoparticles (Fabrega et al., 2009) and by the magnitude of the exponentially growing investments in this field, allocated by public and private sectors worldwide.

Quantifying the accurate scale of these investments is not an easy task but some forecasts have estimated the worldwide market for nanotechnology related products at around £ 105 billion in 2005 and £ 700 billion in 2010 (Taylor, June 2002,) and about $1 trillion by 2011-2015(Roco, 2005).The USA is the leading country in this relatively new field of technology followed by countries like China, Japan, the European Union and South Korea. The above mentioned prediction made by Roco in 2005 for a worldwide nano-products value of $ 1 trillion by 2011-2015 still appears to hold in 2011(see Figure 2-2) which shows that the market is doubling every three year as a result of successive introduction of new nanoscale products (Roco, 2011)

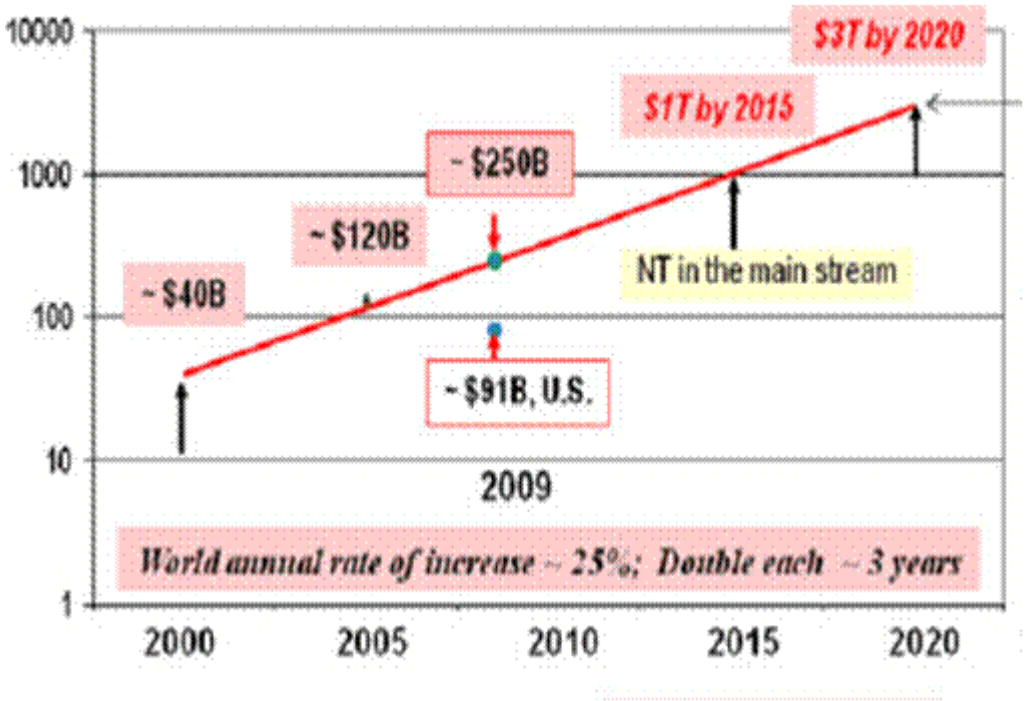

Figure 2-2: market timeline : projection for the worldwide products that incorporate nanotechnology (Roco, 2011). Reprinted with the permission of copyright@ 2011, Springer science and business B.V.

Although the term nanoparticle (see chapter 1 for its definition) is a general term used for nanoscale materials, there are a number of different types of nanoparticles. It is the task of the

following sections to attempt to give detailed description of the natural, accidental and engineered nanoparticles in terms of their properties, types and synthesis routes followed by their fate and behavior in the natural environment with special attention being paid to both aquatic environment and biomass population.

Table 2-1: Classification of nanaparticles *(Nowack and Bucheli, 2007).*

Type		Formation		Examples
Natural	C-containing	Biogenic	Organic colloids	Humic, fulvic acids
			Organisms	Viruses
		Geogenic	Soot	Fullerenes
		Atmospheric	Aerosols	Organic acids
		Pyrogenic	Soot	CNT
				Fullerenes
				Nanoglobules, onion-shaped nanospheres
	Inorganic	Biogenic	Oxides	Magnetite
			Metals	Ag, Au
		Geogenic	Oxides	Fe-oxides
			Clays	Allophane
		Atmospheric	Aerosols	Sea salt
Anthropogenic (manufactured, engineered)	C-containing	By-product	Combustion by-products	CNT
				Nanoglobules, onion-shaped nanospheres
		Engineered	Soot	Carbon Black
				Fullerenes
				Functionalized CNT, fullerenes
			Polymeric NP	Polyethyleneglycol (PEG) NP
	Inorganic	By-product	Combustion by-products	Platinum group metals
		Engineered	Oxides	TiO_2, SiO_2
			Metals	Ag, iron
			Salts	Metal-phosphates
			Aluminosilicates	Zeolites, clays, ceramics

2.1.1 Natural nanoparticles

Natural NPs are ubiquitous and they are distributed throughout the atmosphere, oceans, soil systems, terrestrial water systems (groundwater and surface water), and in and/or on most living organisms both at the micro and macro levels and have been present in the environment forever (Theng and Yuan, 2008, Hochella et al., 2008). They have been formed mainly by the effect of naturally occurring physical, chemical and biological processes such as hydrolysis, erosion, weathering, volcanic eruption, sea spray, photochemical reactions, growth nuclei in super-saturated fluids, plants roots on rocks, minerals and microrganisms. Forest fires, as volcanic eruptions, for instance, can spread ash and smoke over thousands of miles and lead to an increase in particulate matters, including NPs, exceeding ambient air quality standards (Sapkota et al., 2005).

In many environments , biogenetic nanoparticles are formed directly by microorganism to fulfil metabolic requirements (Suzuki et al., 2002, Schüler and Frankel, 1999) or as an indirect result of microbial activity (Glasauer et al., 2002, Hansel et al., 2004, Banfield et al., 2000). Dominant phases of the natural NPs include: Iron oxides/hydroxides, aluminum oxides/hydroxides, clay minerals (hydrated aluminosilicates of K, Mg, Fe etc.) and silica. Biological activities also assemble following the bottom up process- a wide range of carbon - containing NPs including humic substances, building molecules, functional enzymes, coal, and produce nanoorganisms such as bacteria, viruses, cells and their organelles. Though we usually associate air pollution with human activities such as transportation, industry, and charcoal burning, natural events such as dust storms, volcanic eruptions and forest fires can produce such vast quantities of nanoparticulate matter in the atmosphere that profoundly affect air quality worldwide (Buzea et al., 2007). Therefore, the exposure of human and other

living organisms to nanoscale particles is not as recent as the new field of nanotechnology which is more based on the ever increasing production of the engineered nanoparticles which are produced to serve for special purpose and may manifest different properties than above mentioned natural NPs.

2.1.2 Accidental nanoparticles

Human activities have been releasing different forms of nanoparticulate matter for millennia as by-products of some activities which were essential for their survival such as agriculture, construction, food cooking, mining and mineral processing. However, accidental NPs input to the environment has risen sharply and dramatically since the beginning of the Industrial Revolution in the mid 18^{th} century and after due to manufacturing emissions, nuclear waste generation and the combustion of fossil fuels (Wiesner et al., 2009). Diesel and automobile exhausts are the primary source of atmospheric nano-and microparticles in urban areas (2002). Since their productions are spontaneous, uncontrolled accidental nanoparticles are more likely to be polydisperse /heterogeneous and have irregular shapes. They contain sulfide, sulphate, nitrate, ammonium, organic carbon, elemental carbon and trace metals (Sioutas et al., 2005).

2.1.3 Engineered nanoparticles

The modern nanotechnology exploits the novel nanoscale properties of nanoparticles which has lead to the production of a vast amount of engineered NPs. Engineered NPs are deliberately manufactured by human activities to serve for special purposes and they are different from both incidental NPs that are produced as a side product of human activity, for example, from industrial processes or transport and from natural NPs, for example, humic

substances, produced from weathering, microbial action or chemical hydrolysis (Lead, 2010). Engineered NPs can be divided into a number of classes and not as a single homogeneous group. Based on their core materials, these manufactured nanomaterials can be classified into organic and inorganic. Organic NPs can be further defined as fullerenes (C60 and C70 and derivatives) and carbon nanotubes (multi-walled or single walled CNTs), while inorganic NPs can be sub-divided into metal oxides (of iron, zinc, titanium, cerium etc), metals (mainly silver and gold) and quantum dots (such as cadmiumselenides) (Ju-Nam and Lead, 2008). A brief description of the sources, applications and properties of each of these subgroups will be given in the next sections.

2.1.3.1 Production of engineered nanoparticles

Many different techniques have been developed and employed to generate metal nanoparticles, including gold nanoparticles. Those techniques for preparing nanoparticles have advanced rapidly over the recent decades and continue to evolve leading to more and improved control over the size and shape of the particles generated. Two fundamentally different approaches towards the controlled generation of nanostructures have evolved irrespective of the field or discipline (Shenhar and Rotello, 2003). The bottom up method (the chemical approach), where the atoms (produced from reduction of ions) are assembled to generate nanostructures, and the opposite approach, the top down method, also known as the physical method, where material is removed from the bulk material through grinding, milling, chemical methods or volatilisation of solid material followed by condensation of the vapour components, leaving only the desired nanostructures.

Both approaches can be implemented in either gas, liquid, supercritical fluids, solid states, or in vacuum. Most of the manufacturers are interested in the ability to control one or more of the following aspects of the nanoparticles: a) particle size b) particle shape c) size distribution

d) particle composition and e) degree of particle agglomeration. An important aspect of both approaches is the stabilisation of the particles to avoid aggregation and coalescence (Ju-Nam and Lead, 2008). Stabilization can occur in many different ways but primarily aggregation is prevented by electrostatic repulsion or steric hindrance. Two of the most important issues confronting nanocrystal synthesis are obtaining a purposeful control over the nanocrystal mean size and routinely producing narrow size distributions (Shields et al., 2010).

The synthesis of small, monodisperse nanoparticles is a major challenge in nanotechnology research. Similar particles experience increased driving forces to aggregate to diminish surface energy. So, protective coating or capping is necessary during synthesis to keep them in a finely dispersed state (Sardar et al., 2009). Both methods have inherent advantages. Top down assembly methods are currently superior for the possibility of interconnection and integration, as in electronic circuitry. Bottom-up assembly is very powerful in creating identical structures with atomic precision, such as the supramolecular functional entities in living organisms(2006). They can also be combined to achieve the material of specific physicochemical properties (Cigang and et al., 2006).

2.1.3.2 Examples of engineered nanoparticles

Since the invention of the nanotechnology few decades ago, different types of nanosized materials with different application have been produced and commercialised to take the advantage of their novel properties. The following sections will provide examples of the engineered nanoparticles, their synthesis processes and their applications.

2.1.3.2.1 Fullerenes and Carbon nanotubes

- **Fullerenes,** also called as Buckminsterfullerene, are spherical cages composed of 60, 70 or 80 carbon atoms, which are bound to three other atoms in sp^2 hybridation and each

atom has the remaining electron of the four outer shell electrons free. Unlike diamond (which is another allotrope of carbon), fullerenes can conduct electricity due to free electrons on its surface and in this respect has similar properties to graphite. Although fullerenes can be found spontaneously in the nature as by-products of combustion reactions, it was first synthesized in 1985 (Kroto et al., 1985). Since then, many processes for the production of fullerenes of different sizes have been developed including arcing of graphite, combustion of hydrocarbons, thermal and non-thermal plasma pyrolysis of coals and hydrocarbons and thermal decomposition of hydrocarbons (Huczko and Byszewski, 1998).

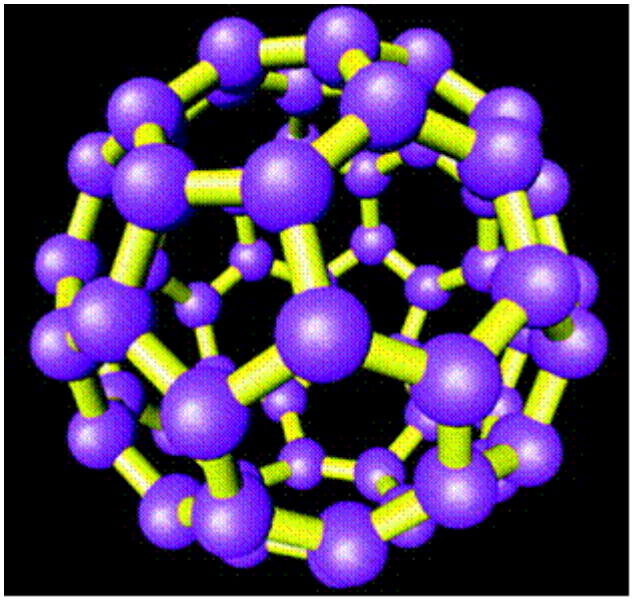

Figure 2-3: Structure of Fullerene C60 molecule. Purple balls represent the places of carbon atoms(Buseck, 2002). Reprinted with permission from copyright 2002 Elsevier.

Fullerenes have many applications, including lubrication, superconductors, semiconductors, photoconductors, optical limiters and atom encapsulation. Since fullerenes are empty structures with dimensions similar to several biologically active molecules, they can be filled with different substances and find medical applications. These include anti HIV- protease activity, photodynamic DNA cleavage, free radical scavenger, antimicrobial action and use of fullerenes as diagnostic agents (Mehta and Thakral, 2006, 2001).

- **Carbon nanotubes** are similar to fullerenes in structure and compositions but they have elongated shapes with 1- 2 nm in diameter. Using an arc-discharge evaporation method similar to that used for fullerene synthesis, they were first produced in 1991 (Iijima, 1991). Normally, carbon nanotubes are made of one sheet of graphite folded to form cylindrical single walled carbon nanotubes (SWCNT) (Iijima and Ichihashi, 1993) although multi walled carbon nanotubes (MWCN) (Iijima, 1991) can be formed by folding more than one sheet of graphite.

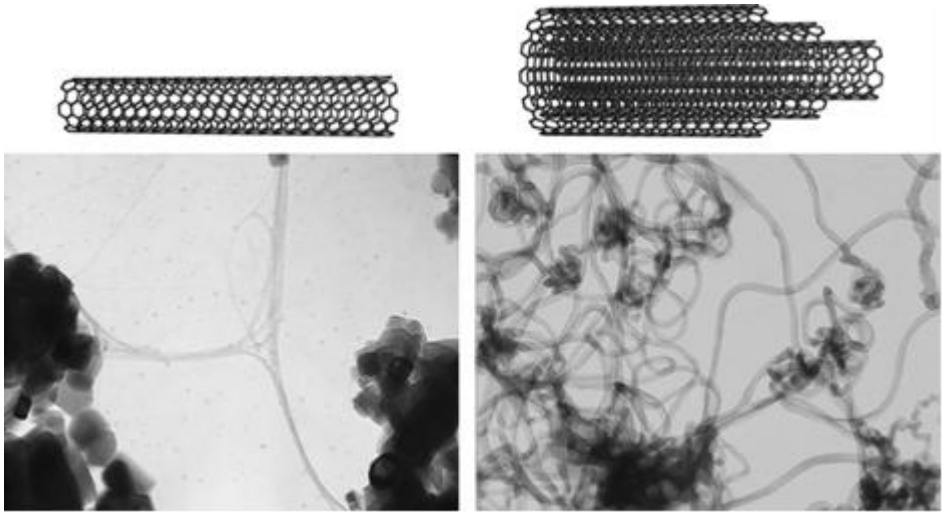

Figure 2-4: Representation of SWCNT and MWCN at the top and their TEM images at the bottom(Donaldson et al., 2006). Reprinted with permission from copyright 2006 Oxford University Press.

At present, the three main methods employed for CNT synthesis are arc-discharge, laser ablation, and chemical vapor deposition (CVD) (Trojanowicz, 2006). Carbon nanotubes are light, chemically stable, have high strength, high aspect ratio (long length compared to a small diameter) and remarkable optical properties (Hou et al., 2002, Tersoff and Ruoff, 1994) and, because of these useful properties, they become ideal material for many applications. Nanotubes have attracted a considerable amount of interest in the past few decades due to their potential applications in large numbers of academic and industrial areas for diverse application possibilities (Cao and Rogers, 2009) ranging from nanoscale circuits to low voltage devices (Philip Wong, 2005), to light-emitting devices (Freitag et al., 2006), thermal

heat sinks (Kordás et al., 2007), electrical interconnects (Close et al., 2008), chemical/biological sensors (Kim et al., 2007b), ultra-strong fibers (Baughman et al., 2002), high-power electrochemical capacitors, (Niu et al., 1997) gas storage components (Gadd et al., 1997, Rakhi et al., 2008), magnetic data storage devices and drug delivery systems (Bianco and Prato, 2003). Waste products from the above mentioned various applications and their disposal to the environment will undoubtedly increase the presence of carbon nanotubes with unknown fate and behavior in the natural environment.

2.1.3.2.2 Metal oxides NPs

Metal oxides NPs are synthesized in a variety of ways such as laser ablation, ion implantation, chemical vapour deposition (CVD), photolithography ,thermal decomposition, sol-gel process or hydrothermal reaction method (wolf, 2004). Nature is able to synthesize a variety of metal oxide nanomaterials as well under ambient conditions; the magnetic navigation device found in magnetotactic bacteria (MTB) is one such example (Lang et al., 2007). As in the case of most NPs, metal oxide NPs are stabilized through surface modifications and the main compounds used for modifying them are phosphonates or silanes (Grancharov et al., 2005). Metal oxides form a class of special interest among inorganic nanoparticles and due to their novel optical, electrical and magnetic properties (Shtykova et al., 2007) they have many applications including catalysis, sensors, electronic materials, biomedical diagnostics and environmental remediation (Oskam, 2006, Hoffmann et al., 1995, Kamat, 1993). Among metal oxide NPs, the following are those which have attracted most of the applications and, as a result, their concentrations in the natural environment are expected to be increasing.

Iron oxide: the most common forms of iron oxide NPs are maghemite, γ-Fe_2O_3 and magnetite, Fe_3O_4 and, because of their supermagnetic properties, they offer a high potential

for several biomedical applications, including tissue repair; drug delivery, magnetic resonance imaging (MRI) and hyperthermia (Arbab et al., 2003, Urs and et al., 2011, Widder et al., 1978, Perez, 2007). Various chemical routes have thus been proposed to synthesize ultra fine nanoparticles of Fe_2O_3, including the hydrothermal reaction method (Guardia et al., 2009), so l-gel process (Lu et al., 2002), chemical co-precipitation (Laurent et al., 2008) etc.

Titanium oxide. Four crystal forms of titanium dioxide are naturally found: rutile, anatase, brookite and TiO_2(B) (Wang et al., 2005) and they can be synthesized using the following techniques: co-precipitation, sol-gel synthesis process (Ramaswamy et al., 2008), chemical vapor deposition (Kawai-Nakamura et al., 2008), reverse micelle synthesis (Li et al., 2008), microemulsion synthesis process (Rashidzadeh, 2008) and hydrothermal reaction method (Kim et al., 2006). It is also worth knowing that the transformation behaviour from the amorphous to the anatase or rutile phase is influenced by the synthesis conditions (Madhusudan Reddy et al., 2001). Because of their attractive properties including high refractive index, light absorption/scattering as well as its chemical stability and relatively low-cost production titanium dioxide, NPs are exploited by a variety of fields (Kim et al., 2007a, Baldassari et al., 2005). Application fields of titanium oxide range from pigments (Pratsinis et al., 1996), to cosmetics, catalysts, (Chen and Yang, 1993) and photocatalysts (Rao and Dube, 1996), etc.

Cerium oxide: A number of attractive properties, such as quantum effects, magnetic properties and catalytic capabilities that cerium oxides display at nanoscale make them ideal for a variety of useful applications in both materials science (Lewis, 2000) and in biology (Kataoka et al., 2001).In material science, cerium oxide NPs are widely applied as catalysis in fuel cell technology (Logothetidis et al., 2003), catalytic wet oxidation (Larachi et al., 2002), engine exhaust catalysts (Dario and Bachiorrini, 1999) and photocatalytic oxidation of water

(Bamwenda and Arakawa, 2000) or as precursors for ceramics and electro-optic devices. In biology, magnetic cerium NPs provide contrast in magnetic resonance imaging (Wilhelm et al., 2002, Mornet et al., 2004)–and fluorescent quantum dots is an important tool for biomedical diagnostics (Perez et al., 2002) and cell imaging (Cha et al., 2003, Chen and Gerion, 2004). The above mentioned applications led to a steady increase of the production of cerium oxide NPs which relies - depending on the specific application of the product- on numerous different synthesis methods such as sol-gel, thermal decomposition, solvothermal oxidation, micro-emulsion methods, flame spray pyrolysis and microwave-assisted solvo-thermal process (Ju-Nam and Lead, 2008).

Zinc oxide: In recent years, nanoscale zinc oxides have received considerable attention due to their novel properties which are applicable in many fields including ultraviolet laser devices (Makino et al., 2002), piezoelectric nanogenerators (Wang and Song, 2006), chemical sensors (Müller and Weißenrieder, 1994), solar cells (Beek et al., 2004), antibacterial agents (Jones et al., 2008) and biomedical labels (Kuo et al., 2009). Zinc oxide is a wide-bandgap Semiconductor that displays luminescent properties in the near ultraviolet and visible region (Huang et al., 2001) and it can be doped with magnetic elements Co, Fe and Ni to store magnetic data. In the literature, several synthesis methods, such as thermal decomposition, chemical vapour deposition, laser ablation, spray pyrolysis, sol–gel method, hydrothermal synthesis, molecular beam epitaxy, etc. have been reported for the preparation of ZnO nanoparticles and films (Tarasenko et al., 2010). Surface modifications using appropriate organic compounds have also remarkably widened the existing applications or opened new ways of applying zinc oxide NPs (Guo et al., 2000).

2.1.3.2.3 Quantum dots:

Quantum dots (QD) are very special group of semiconductors due to their small sizes ranging from 2 -10 nm. The number of atoms inside them may vary from just few atoms to hundreds or thousands depending on their desired final size. They are defined as particles with physical dimensions smaller than the exciton Bohr radius (Chan et al., 2002) which is the distance between exited electron and the hole formed in the ground electronic state due to the excitation of the electron. QDs can be made from alloys of most semiconductor metals (e.g., CdS, CdSe, CdTe, ZnS, PbS) (Alivisatos, 1996, Bailey and Nie, 2003). The small size affects their electronic properties in a way that they form a special group of semiconductors which conducts electricity very fast. A quantum dot made of few atoms displays a big electronic band gap where the excitation of the electrons requires lots of energy and concurrently more energy in the form of fluorescence is released when electrons return to their rest state. This phenomenon gives the QDs optical properties which are different from the bulk material properties in the sense that their emission fluorescence wavelength can be altered by changing the size of the quantum dots. In principle, the smaller the quantum dots the more their fluorescence wavelength is shifted toward blue. QDs have been received as a new technology and, due to their unique electrical and optical properties, have many applications in a variety of fields including: electroluminescent displays like light emitting diodes (LED), solid-state lighting , solar cells, biotechnology and medicine (Jamieson et al., 2007).

2.1.3.2.4 Metals

Nanoscale metals have manifested a number of size – dependent interesting properties which makes them different from both bulk and atomic scale materials of the same metal. They have

fascinated the mankind since ancient times due to their attractive optical properties as decorative dyes in ornaments and artworks (Daniel and Astruc, 2003). Their more recent applications exploit many aspects of their unique nanoscale optical, electrical and chemical properties and range from catalysts (Jana et al., 1998), medical diagnostics (Mirkin et al., 1996), ant-bacterial uses to water purifications (Pradeep and Anshup, 2009). Among the variety of ways used to synthesize metal NPs, the following methods are widely applied to tune their size and shape into a specific purpose: electrochemical reduction (Lee et al., 2011, Hirsch et al., 2005), photochemical reduction (Eustis et al., 2005), vapour deposition (Pandey et al., 2011), and chemical reduction using a reducing agent (Brust et al., 1994, Turkevich, 1951, Frens, 1973).

2.1.3.2.4.1 Silver nanoparticles.

Among the different types of metal, nanoparticles silver is by far the most studied in the literature due to its wide and rapidly growing application in a number of scientific areas and in consumer products (Tolaymat et al., 2010) and its known toxic effects on the environment and human health (Khaydarov et al., 2011). Its areas of application vary from textile engineering , catalysts (Lewis, 1993), medicine (Salata, 2004), , water treatment (Solov'ev et al., 2007) and disinfecting to electronics (Lee and Jeong, 2005) and biotechnology (Niemeyer, 2001). Well designed silver nanoparticles of various shapes and sizes can be achieved through a variety of different synthesis approaches using numerous capping agents depending on their applications. Of the above mentioned synthesis approaches the following ones are the most applied methods: photochemical methods, laser ablation (Lee et al., 2001), microwave processing (Soto et al., 2005), thermal decomposition of silver axalate (Navaladian et al., 2006), reduction of both inorganic and organic agents and electron radiation (Bönnemann and Richards, 2001).

2.1.3.2.4.2 Gold nanoparticles

Elemental gold has many unique properties which have attracted and fascinated mankind since its discovery. Being very unreactive, gold does not turnish in the atmosphere and so keeps its attractive colour forever(Hutchings et al., 2008). That is one of the main reasons why gold has been used in shaping jewelleries. It has been used for many colourful, decorative, ceremonial and religious artifacts and has been a metal with a high monetary value. Colourful aqueous solutions of gold colloids date back to Roman times and were known to medieval alchemists as aurum potabile (Mellor, 1923). A Roman cup, called the Lycurgus cup, used nanosized (ca 50 nm) gold and silver alloys, with some Cu clusters to create different colours depending on whether it was illuminated from the front or the back. The cause of this effect was not known to those who exploited it. Michael Faraday was the first to recognise that the colour was due to the minute size of the gold particles (Faraday, 1857). On February 5, 1857, Michael Faraday delivered the Bakerian Lecture of the Royal Society in London entitled "Experimental Relations of Gold (and other metals) to Light". In his speech, he mentioned that known phenomena (the nature of the ruby glass) appeared to indicate that a mere variation in the size of its particles gave rise to a variety of resultant colours. Nearly a century later, electron microscope investigations on Faraday's ruby-coloured gold colloids have revealed that Faraday's fluid preparations contain particles of gold of average diameter (6 ± 2 nm) (Turkevich, 1951).

Although some scientists see the Faraday's experiment as a landmark in the history of nanoscience and nanotechnology (Peter and John Meurig, 2007) the chemical inertness of gold as a bulk metal appeared to provide very little opportunities to open up new and exciting chemistries (Hutchings et al., 2008). The new field of nanotechnology made it possible to discover the unique properties of matter when subdivided to the nanoscale. Gold at

nanoscale manifests a number of interesting physico-chemical properties that have fascinated many disciplines of science including: material scientists, catalysts, biologists, surface and synthetic chemists and theoreticians in great number. Today, in the 21st century, gold chemistry is based on solid ground regarding the preparation and characterisation of a wide variety of fundamental compounds with gold atoms and gold clusters as core units (Murray, 2000, Peter, 2000, Gagotsi, 2006). The fact that gold NPs have been studied in many different scientific fields has led not only to a deep understanding of many of the physico-chemical features that determine the characteristic behaviour of these nanoscale gold nanoaprticles but also to invent, test and validate reliable novel procedures for the preparation, synthesis and characterisation of gold nanoparticles of basically any desired size and shape.

The bottom up process described in section 2.1.3.1 is by far more common and effective (Sardar et al., 2009) and has become a popular method in current nano-science and nano-engineering. It has a number of potentially very attractive advantages. These include experimental simplicity down to the atomic size scale, the possibility of three-dimensional assembly and the potential for inexpensive mass fabrication (Brust and Kiely, 2002). The simplest and most common bottom up method employed for the production of the gold nanoparticles of different sizes is the reduction of Au(III) salt (usually $HAuCl_4$) by sodium citrate in water. In this method, pioneered by Turkevich and co-workers in 1951(Turkevich, 1951) and later refined by Frens in the 1970s (Frens, 1973) and more recently further developed by Kumar (Kumar et al., 2006). It is generally accepted that the $AuCl_4^-$ ions are first reduced to atomic gold (Au), the concentration of which rises quickly to the super-saturation level. Collision of the Au atoms leads to a sudden burst of nuclei formation which marks the start of the nucleation step. It is the attachment and coalescence of those nuclei which results in the growth and formation of desired nanoparticles (Pong et al., 2007). Figure

2-5 illustrates the reduction, nucleation and growth steps during the formation of the nanoparticles. It shows that the reduction and nucleation are fast (>200 ms) while growth step is the rate determining step since it is much slower than the antecedent nucleation step. Many times, difficulty in controlling the nucleation and growth steps, which are intermediate stages of particle formation process may result in a broad particles size distribution (Bellloni, 1996). In the presence of various reactive polymers in the reaction medium, that is, polymers having various functional groups, the growing metallic particles are stabilized by the adsorption of the polymer chains onto the surface of the growing metal fragments, thus lowering their surface energy and creating a barrier to further aggregation (King et al., 2003).

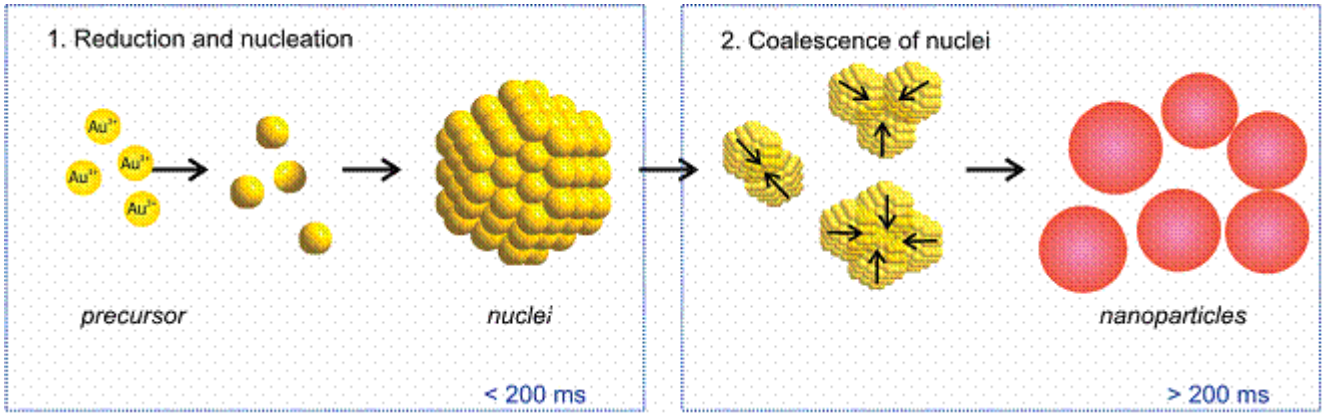

Figure 2-5: Schematic illustration for the deduced process of gold nanaoparticles formation . Reduction and nucleation are faster processes than coalescence of nuclei (Polte et al., 2010). Reprinted with the permission from copyright 2010 American chemical society.

One important factor for understanding the behaviour of the natural particles in the environment and the bioavailability of heavy metals loaded on them is their interaction with microorganisms associated with biomass population. The nanoparticles could possibly be immobilised, absorbed, reacted or retarded by biomass in the environment. Since one of the main objectives of this project is to study the effect gold nanoparticles on planktonic bacteria the following section 2.2 will give a general introduction of the overall fate and behaviour of NPs in the environment. Section 2.3 will be devoted to give a comprehensive introduction for

the chosen bacterial strain and section 2.4 will highlight the interaction of the NPs on this strain.

2.2 Fate and behaviour of the manufactured NPs in the environment

The abundant use of NPs and their final disposal into the environment have raised lots of concerns within the scientific community regarding their fate and behaviour in the natural environment and their possible impacts on the living organisms. Overall, the need for understanding the role of nanoparticles in the environment is important to perceive the extent to which we are changing the planet with the application of nanotechnology and to choose to address minimizing those changes (Wigginton et al., 2007).

Some important questions that need to be raised when addressing nanoscience in order for it to be fully understood are: will manufactured nanoparticles from industry and other sources enter the atmosphere, soils, sediments or water(Mueller and Nowack, 2008)? If so, how persistent will they be, and in what concentrations will they occur (Gottschalk et al., 2009) and what form will they take? It is quite clear that large scale use of NPs (Woodrow_Wilson_centre, 2007) suggests that their presence in the environment will increase (Navarro et al., 2008, Barnes et al., 2010). Another important point of consideration is that once nanoparticles originated from different sources get their way in the environment, their properties will not remain the same due to their interactions with water, soil, air or with living organisms such as plants, algae fungus and bacteria.

The key processes that govern nanoparticles behaviour in the aquatic environment are aggregation and dissolution, driven by size and surface properties of the materials which are mainly dependent on environmental factors such as temperature, ionic strength, pH, particle

concentration, and particle properties such as surface charge, size, coating agents, crystalinity , composition and shape (see Figure 2-6 below) (Dunphy Guzman et al., 2006, Filella and Buffle, 1993, Lecoanet et al., 2004) .

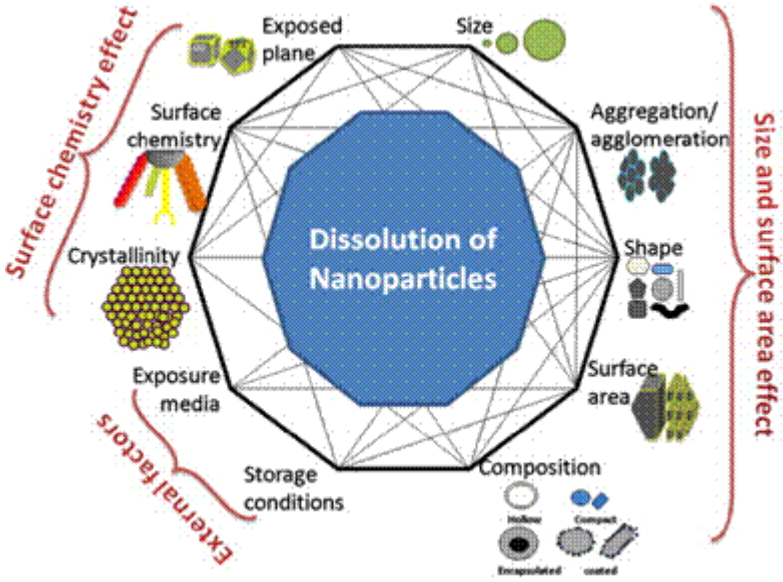

Figure 2-6: Schematic represantation of the key factors and processes that govern the behaviuor of the nanoparticles in the natural enviroement.(Misra et al., 2012). Reprinted with permission from copyright 2012 Elsevier.

Surface properties determine the stability and mobility of NPs in aquatic and terrestrial systems and their interactions with the living organisms(Navarro et al., 2008). That is why manufactured metallic NPs are for example coated with inorganic or organic agents such as citrate, PVP, polyethelene glycol (PEG), or surfactants such as sodium dodecyl sulfate to stabilize them in the suspensions (Mafuné et al., 2000). It is clear now that those coating agents will influence, if not determine, the surface chemistry of these NPs and have impact on their behaviour in the environment. The effect of pH on the metallic NPs was clarified by the silver nanoparticles which transformed in size or state (soluble silver and silver ions) within minutes in low pH aqueous nitric acid with similar acidity to the natural environment (Elzey and Grassian, 2010). The ionic strength and pH ranges typical of most soils and surface waters present conditions under which clusters or aggregates of TiO_2 with diameters

of several hundred nanometers to several micrometers are expected to form instead of monodisperse nano-TiO_2 (French et al., 2009).

On the other hand, naturally occurring organic materials may display disaggregation of NP such as nano-TiO_2 and thus in the natural aquatic environment, the dispersion and mobility of TiO_2 nanoparticles might occur to a much greater extent than predicted by laboratory measurements (Domingos et al., 2009b). Similar studies have indicated that Iron oxide NPs have been shown to change their solubility, stability, and aggregation behaviour in response to changes in pH and organic matter concentration with open, porous aggregates in the absence of standard Suwannee River humic acid (SRHA) and compact aggregates in the presence of SRHA (Baalousha et al., 2008). Organic substance may influence the behaviour of NPs in different ways. Humic substances are likely to form nanoscale coating on the surface of the solid NPs which stabilized the NPs through charge stabilisation (Tipping, 1981) while longer fibrils are more likely to form bridges between NPs and increase aggregation via bridging mechanisms (Buffle et al., 1998). Different environmental compartments differ in many aspects in terms of the aforementioned factors which determine the ultimate fate and behaviour of NPs. It is the task of the following subsections (2.2.1 and 2.2.2) to give clear introduction of the behaviour of NPs in both soil and water environments.

2.2.1 Nanoparticles in soil

Apart from the intrinsic characteristics of the nanoparticles which determine their behaviour, there is an equally important number of soil conditions which will have impact on their fate and behaviour. Soils are complicated structures of solid, liquid, gas, organic and inorganic components which result in the overall properties of different types of soils. Soil chemistry, pH, type of minerals and organic contents of the soil seem to have the most effect on the aggregations and transport of NPs in soil environment (Kretzschmar et al., 1997). In order to

fully understand the individual effects of the above mentioned factors and their combined impacts on the stability of nanoparticles and their ecotoxicology, detailed studies are necessary. Although there is a relatively substantial number of ecotoxicology and behaviour studies of nanoparticles in aquatic environment (Nel et al., 2006, M.N, 2006, Zhang et al., 2008, Keller et al., 2010) currently, few studies have to date focused on the toxicity of NPs in soil environment (Yang and Watts, 2005, Tong et al., 2007) and their transport in terrestrial environment with the aim of providing to the science community relevant data for making acceptable prediction for the NPs behaviour and exposure pathways(Xu et al., 2008). This indicates that this field of research is in its early stage and little information is available for a profound understanding of the NPs fate and behaviour in soil.

2.2.2 Nanoparticles in water:

Despite the fact that nanotechnology is apparently quite a recent technology, the fate, behaviour and the impact of nanoparticles on aquatic environment is becoming an increasing concern that needs to be prioritized in order to facilitate quantitative ecological risk assessment which is not yet available for environmental chemists (Klaine et al., 2008). Therefore, it has attracted many researches and has been relatively extensively studied. Consequently, our knowledge in this rapidly growing field has increased in the last decennia to a point that many researches in this field have pointed out the possible ecotoxicologial impacts of NPs on the aquatic organisms (Lovern et al., 2007, Li et al., 2010a, Adams et al., 2006). The ways of production and applications of nanoparticles in a variety of fields including consumer products make it inevitable that nanoparticles and their by-products end up in the aquatic environment (rivers, lakes, ground water, coastal waters) (Christian G, 2004) through rain events, runoff, leaching , industrial waste and all urban water sewage.

Once NPs are in the aquatic environment, their fate and behaviour will be mainly determined by both their own properties and relevant environmental factors. As noted previously, dissolution, aggregation and subsequent sedimentation determine the ultimate fate of NPs. The main sinks and receptors of aquatic NPs are therefore sediments in which there are living benthic organisms (Klaine et al., 2008). Different waters will affect similar NPs in different ways depending on a number of factors such as pH, ionic strength, inorganic species, organic matter and others. Seawater and freshwater are the extremes of the aquatic mesocosms in terms of water properties including ionic strength and total organic carbon(TOC) which are two important factors for the stabilisation or aggregation of NPs.

2.2.2.1 Fate and behaviour of NPs in freshwater

Freshwater is a term generally used for the naturally - occurring water sources on the surface of the Earth such as lakes, ponds, rivers and icecaps and ground water like underground streams and aquifers. To define water as freshwater, it needs to have the concentration of dissolved salts less than 500 parts per million (ppm). General characteristics of different types of freshwater such as ionic strength, pH, natural organic matter, ionic composition and their combined effects will result in many transformations of nanoparticles such as reactions with biomacromolecules, redox reactions, aggregation, and dissolution which will alter the fate, transport, and toxicity of nanomaterials. (Lowry et al., 2012). Although many studies have focused on the individual effects of the above mentioned factors, only few studies have addressed the behaviour of NPs in more complex aquatic matrices (Keller et al., 2010, Findlay et al., 1996, Gao et al., 2009). The pH of the aquatic media may influence the surface charge of the particles through protonation and deprotonation processes in various ways. The pH around the zero point charge of the particles will reduce repulsion forces between particles which keep them separate and subsequently facilitate aggregation as pointed out by

different studies (Piccapietra et al., 2011, Keller et al., 2010). The amount of dissolved ions in the media will determine the overall ionic strength wherein NPs are exposed. Nanoparticles, which owe their stability to the charge stabilization caused by (Liu and Hurt, 2010) repelling surface charges such as citrate coated NPs will show more aggregation than sterically stabilized NPs where bulk uncharged organic materials are adsorbed on their surfaces. Under high ionic strength conditions, the electrical double layer around the charge NPs shrinks and zeta potential approaches to zero value which facilitates fast agglomeration (Elimelech et al., 1995).

Natural organic matter (NOM) is ubiquitous in the freshwater and it can either increase or decrease the stability of NPs depending on the type of organic materials as stated in the previous section (section 2.2). Nanoparticles entering fresh water will inevitable interact and being transformed by water abundant organic matter naturally. This includes proteins, polysaccharides, and humic substances (HS) (Lowry et al., 2012, Kiser et al., 2012). Initial interaction of the NPs and organic matter and their subsequent mobility and behaviour in the environment is mainly dependent on the nature of coating agents on the surface of the NPs (Saleh et al., 2008). Coating of organic materials on the surface of the nanoparticles will influence on the speciation of the nanoparticles. Liu and Hurt have, for example, shown the decrease of ionic silver Ag+ when citrate-capped Ag NPs were coated with humic or fulvic acids (Liu and Hurt, 2010). Since the ions show apparent toxicity on many organisms the decrease of ions will influence the toxicity of the NPs in aquatic environment. Recently published data aiming to understand the interaction of the organic compounds in the freshwater and the gold nanoparticles has indicated that the colloidal stability of the NPs in the absence of NOM is a function of capping agent, pH, ionic strength, and electrolyte valence. In the presence of NOM, the capping agent is a less important determinant of stability, and the adsorption of NOM is a controlling factor (Stankus et al., 2010). The effect

of coating agents on the stability and ion release of silver nanoparticles in natural surface water was investigated and the results have shown that sterically stabilized silver nanoparticles can persist longer as individual particles in natural water systems and thus will release silver more quickly and to a greater extent than would particles that aggregate quickly after entering the water (Li and Lenhart, 2012).This finding points out that sterically stabilsised NPs release more ions and thus are more hazardous to the aquatic organisms than charge stabilised NPs (citrate capped NPs) which are more likely to aggregate in environmental relevant conditions.

Studies have shown that the size of small aggregates of NPs in waters with high total organic matter and low ionic strength will remain stable in water column and that no sedimentation takes place (Keller et al., 2010, Hyung et al., 2006). Aggregation or lack of it of nanoparticles determines the particles size and the fraction of ions in the water which are exposed to any aquatic organisms living inside the water column (Fabrega et al., 2011). In general aggregation is an important toxicity factor of all different types of nanoparticles (Wick et al., 2007). Stability of nanoparticles in the water column increases the toxicity of the NPs while the aggregation mitigates their potential toxicity due to decreasing available surface area of the NPs and their reduced mobility (Kvitek et al., 2008, Bradford et al., 2009).

2.2.2.2 Fate and behaviour of NPs in Marine water

Most of the Earth's surface is water that is accumulated in ocean basins and covers 72% of the Earth’s surface. Due to the weathering process of rocks on the Earth’s surface, it contains more dissolved ion and has lower freezing point and higher density than freshwater. It conducts electricity better and is more basic. Coastal runoff and atmospheric deposition may contribute to the contamination of marine environment with chemical wastes including NPs. The abovementioned properties will apparently affect the behavior of NPs

differently than freshwater. Experimental evidences have highlighted that even a small increase of salinity of freshwater by adding seawater will increase aggregation followed by sedimentation and therefore less nanoscale colloidal concentration are left in the water column (Stolpe and Hassellöv, 2007). Similar investigation has concluded that singly dispersed 20 nm core size, citrate capped AgNPs in seawater and waters with greater than 20 mmol L− 1 sodium chloride were unstable and formation of aggregates were recorded due to the charge screening by greater salt concentrations and the presence of divalent cations in the seawater (Chinnapongse et al., 2011). High aggregation rate and less dissolution of AgNPs in seawater as compared with deionised water was also reported (Chen and Zhang, 2013). The zeta potential of the AgNPs in the seawater was less negative than in the deionised water. Zeta potential is measure of stability of the NPs, the higher the absolute value of the zeta potential of the particles the higher the repulsion forces between them and less likely that they form aggregates. Similar results were reported for TiO_2 nanoparticles in seawater for which rapid aggregation occurred in suspensions of TiO_2 NPs to form micrometer size particle(Ates et al., 2013). Overall, the stability of NPs decreases in line with increasing salinity over the course of their transport along an estuary passing ultimately to the sea, due to a decrease in the repulsion forces by surface charge screening of counter-ions in the diffuse double layer(Lapresta-Fernández et al., 2012).

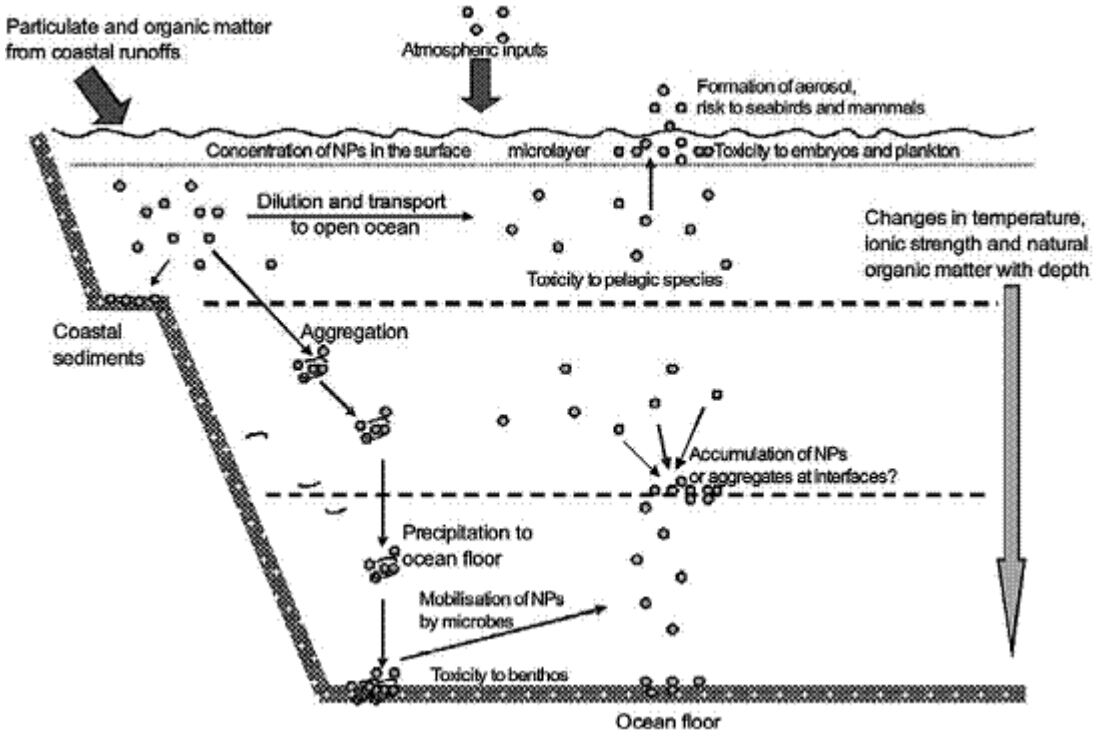

Figure 2-7: Schematic diagram outlining the possible fate of nanoparticles (NPs) in the marine environment and the organisms at risk of exposure *(Klaine et al., 2008). Reprinted with permission from copyright 2008 SETAC*

2.2.3 Ecotoxicology and the effect of nanoparticles on bacteria population

Results from ecotoxicological studies have suggested possible ways that NPs can affect planktonic bacteria in different environmental mesocosms. A good summary of the performed researches on the toxicity of different types of the NPs on bacteria are given in Table 2-2 below adopted from the critical review of Kleine et al (Klaine et al., 2008). Literature review in the table was updated with more recent literature for all nanoparticles in the table. Table 2-2 clearly outlines that different NPs have different toxic effects on the types of bacterial species studied. Some NPs like silver, carbon containing fullurenes and carbon nanotubes manifest antibacterial effects on bacteria while others like Silicon oxide and gold have mild or low toxicity. The toxicity of NPs are found to be mainly size or surface area dependent (Nel et al., 2006).

Table 2-2: Toxic effects of nanomaterials on bacteria adopted from Klaine et al and updated with more recent references (Klaine et al., 2008).

Nanomaterial	Toxic effects	References
Carbon-containing fullerenes		
C60 water suspension (nC60)	Antibacterial to a broad range of bacteria	**(**Lyon et al., 2006, Sayes et al., 2004)
C60 encapsulated in polyvinylpyrrolidone	Antibacterial to a broad range of bacteria	(Kai et al., 2003)
fullerene (C60)	Slight cell membrane damage on E. coli	(Wang et al., 2012)
Hydroxylated fullerene	Bactericidal for Gram-positive bacteria	(Rozhkov et al., 2003)
Carboxyfullerene (malonic acid derivatives)	Bactericidal for Gram-positive bacteria due to fullerene insertion into the cell wall; inhibitory or ineffective against Gram-negative	(Mashino et al., 1999, Biswas and Wu, 2005, Tsao et al., 2001)
Fullerene derivatives with pyrrolidine groups	Inhibits the growth of *Escherichia coli* by interfering with energy metabolism	(Mashino et al., 1999, Mashino et al., 2003a, Mashino et al., 2003b)
Other derivatives of C60	Inhibit the growth of *Mycobacteria*; antimutagenic in *Salmonella typhimurium*; antibacterial	(Babynin et al., 2002, Bagrii and Karaulova, 2001, Bosi et al., 2000)
Carbon nanotubes		
Single-walled	Antibacterial to *E. coli*, cell membrane damage	(Kang et al., 2007, Wei and et al., 2007)
Single-walled	Inactivate bacterial cells of Escherichia coli, Pseudomonas aeruginosa, Bacillus subtilis, and Staphylococcus epidermis	(Kang et al., 2009)
Multiwalled	Cytotoxic to microbes	(Biswas and Wu, 2005)
Metallic		
Quantum dots	Penetrate cells by oxidative damage to membrane; uncoat-ed quantum dots toxic to *E. coli* and *Bacillus subtilis*	(Kloepfer et al., 2005, Kirchner et al., 2005, Hardman, 2006)
Quantum dots	QDs enhanced the level of the reactive oxygen species in the bacterial cells and augmented the percentage of the cells with damaged and leaky membranes	*(Slaveykova et al., 2009)*
Quantum dots	*QDs disrupted the function of the cell membranes of E.coli*	*(Lai et al., 2013)*
Silver	Bactericidal; viricidal	(Morones et al., 2005a, Sondi and Salopek-Sondi, 2004)
		(Lai et al., 2013)
Silver	Membrane disruption at 2ppm citrate capped AgNPs	(Arnaout and Gunsch, 2012)
Silver	Inhibition of bacterial growth, antibacterial efficient of 98%	(Liu et al., 2013)

Table 2-1: Continues		
Silver	*Bacteroidetes* and *Proteobacteria* were sensitive to Ag NPs treatment	(Sun et al., 2013)
Silver	susceptibility of *N. europaea* to inhibition by AgNPs	(Yuan et al., 2012)
Silver	induced high toxicity on Escherichia coli, Bacillus subtilis and Agrobacterium tumefaciens	(Wang et al., 2012)
Gold	Low toxicity to *E. coli* and *Staphylococcus aureus*	(Nyberg et al., 2008, Zharov et al., 2006, Goodman et al., 2004)
Gold	had hardly any effect on Escherichia coli, Bacillus subtilis and Agrobacterium tumefaciens	(Wang et al., 2012)
Metal oxides		
Magnetite	Low toxicity to *Shewanella oneidensis*	(De Windt et al., 2006)
TiO2	Accelerates solar disinfection of *E. coli* through photocata-lytic activity and reactive oxygen species (ROS); surface coatings photocatalytically oxidize *E. coli*, *Micrococcus luteus*, *B. subtilis*, and *Aspergillus niger*	(Rincon and Pulgarin, 2004b, Rincon and Pulgarin, 2004a, Wolfrum et al., 2002)
TiO2	TiO2 particle mixture showed high antibacterial action against S. aureus even at a low concentration.	(Asahara et al., 2009)
MgO	Antibacterial activity against *B. sutbilis* and *S. Aureus*	(Huang et al., 2005)
CeO2	Antimicrobial effect on *E. coli*	(Thill et al., 2006)
CeO2	Strain and size dependent growth inhibition	(Pelletier et al., 2010)
ZnO	Antibacterial activity against *E. coli* and *B. Subtilis*	(Sawai et al., 1995, Sawai et al., 1996)
ZnO	Damages cell membrane and inhibits the growth of E.coli	(Padmavathy and Vijayaraghavan, 2011)
SiO2	Mild toxicity due to ROS production	(Adams et al., 2006)

The data in Table 2-2 shows that silver is by far the most toxic nanoparticles in the list. All tested silver NPs have shown certain toxicity on the target bacterium while the toxicity of gold nanoparticles seems to be the lowest in the rank. Among the different types of the nanomaterials listed in Table 2-2 silver nanoparticles have so far been the most studied group in terms of ecotoxicology due to the long term known ant-microbial activity of ~~the~~ silver.

Silver nanoparticles can easily be synthesised and their surface chemistry can be modified by using different coating agents. The effects of these functionalised silver nanoparticles on different organisms were studied by a number of researchers and detailed review of the effect of silver NPs on different aquatic invertebrate, vertebrate and prokaryote species was given by Fabrega et al ((Fabrega et al., 2011).

Although the effect of gold nanoparticles on the bacteria was not studied as extensively as silver NPs, there is an increasing list of researches that are aimed to investigate the possible effect of gold NPs of different sizes and surface coatings on the environmental bacteria. Since the topic of this thesis is to study the effect of gold On *Pseudomonas fluorescens* the available literature of the effect of gold nanoparticles on bacterial populations was presented and summarised in separate Table 2-3 below.

Table 2-3: Toxicity of AuNPs on different strains of bacteria.

Name of the bacteria	Size of the AuNPs (nm)	Shape of the AuNPs	Coating agent	Toxicity	References
E. coli	2	Spherical	quaternary ammonium-functionalized (cation)	moderately toxic	(Goodman et al., 2004)
E. coli	2	Spherical	carboxylate-substituted (anion)	quite nontoxic	(Goodman et al., 2004)
Strapylococcus Capitis	15 ± 1.2	Spherical	Sodium citrate	No significant effect	(Amin et al., 2009)
E.coli	15 ± 1.2	Spherical	Sodium citrate	No significant effect	(Amin et al., 2009)
Streptococcus mutans	80	Spherical	PVP	growth inhibition at gold concentration of 197µg/l	(Hernández-Sierra et al., 2008)
Salmonella typhimurium	16	Spherical	Citrate	Not toxic or mutagenic	(Shuguang Wang et al., 2011)
E.coli	5	Spherical	Dextrose or Glutathione	Nontoxic	(Chatterjee et al., 2011)
E.coli	20 – 30	Spherical	Citrate, polyallylamine hydrochloride (PAH)	Citrate capped no toxicity, PAH capped caused cell lysis.	(Zhou et al., 2012)
E.coli	5 – 30	Spherical	(Yeast extract Peptone Dextrose)	MIC_{80} = 128	(Ahmad et al., 2013)

Data in Table 2-3 indicate that most reports of the toxicity of gold NPs on bacteria have found the lack of significant toxic effects on many bacterial strains. In contrast to those reports, there are few groups which have reported that gold nanoparticles can be toxic to the target bacteria depending mainly on the coating agents of the NPs (Goodman et al., 2004, Hernández-Sierra et al., 2008). The abovementioned researches did not provide a clear census on the ecotoxicology of the gold NPs on the environmental bacteria and the need for further research is eminent in order to understand the effect of gold on bacterial population. The following subsections will provide a short introduction of the forms of bacterial population and their role in the natural environment.

2.3 Bacterial population in the environment

Bacterial populations are omnipresent living organisms which means that they can be found everywhere in the environment including places with extreme conditions like hot springs, polar ices and even in the radioactive nuclear waste (Dunne, 2002, Allison, 2000). They colonise and grow in all different environmental compartments introduced in the previous sections. Planktonic bacteria exist as unicellular organisms in the environment and every cell behaves as a small independent organism which is invisible with the naked eye. They can only be seen with the aid of microscope. When the cells grow and reach certain size they divide into two identical new cells (see Figure 2-8 below). In this way, the population increases in number as long as there are favourable environmental conditions for the bacteria growth including enough supply of food in the near environment, right temperature and pH.

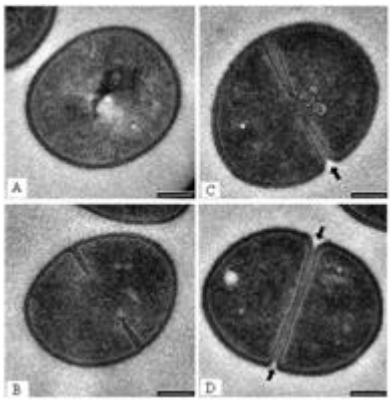

Figure 2-8: Visualising bacterial cell division stages using thin-section TEM(Touhami et al., 2004).

To get energy from the organic food, bacterial cells need to decompose the molecules in one of the following two respiration processes. Similar to higher level organisms (plants and animals), Aerobic bacteria need oxygen to extract energy from the available raw organic materials and, for this reason, aerobic bacterial populations colonise and thrive in environmental compartments where there is a good supply of air. In contrast, anaerobic bacteria can survive without oxygen and they live in non-oxygenated areas as under Earth crust but also on the surface of the Earth.

Apart from the unicellular planktonic bacteria described above, another prevailing structure of bacteria survival that forms in almost all environmental compartments is the biofilm structure explained below.

2.3.1 Biofilm

Biofilms are defined as matrix-enclosed bacterial populations adherent to each other and/or to surfaces or interfaces. This definition includes microbial aggregates and floccules and also adherent populations within the pore spaces of porous media (Costerton et al., 1995). A "film" is a thin coating. "Bio" refers to the living nature of this film. In other words, a biofilm is a thin coating comprised of living material. Unlike the more familiar planktonic lifestyle, in which bacteria float or swim freely, in biofilms, bacterial communities surround themselves

with a complex extracellular polysaccharides (EPS) matrix, better known as ‘slime. As it grows thicker, the film often includes many bacterial species and the matrix develops a complex structure (Dunne, 2002, Allison, 2000, Callow and Callow, 2006). Different cells in the biofilm have different tasks in the community and, in this way, they support each other to survive in hostile conditions like antibiotics, antiseptics, highly reactive chemical biocides, dehydration and nutrient depletion (Costerton et al., 1999).

Biofilm development is a series of complex but discrete and well-regulated steps. The exact molecular mechanisms differ from organism to organism, but the stages of biofilm development are similar across a wide range of micro-organisms (O'Toole, 2003, Kaplan et al., 2003). The sequential stages of biofilm development on different surfaces can be recognised as consisting of five stages.(Percival, 2000) (See Figure 2-9 below for a simplified representation of the development stages of bacterial biofilm):

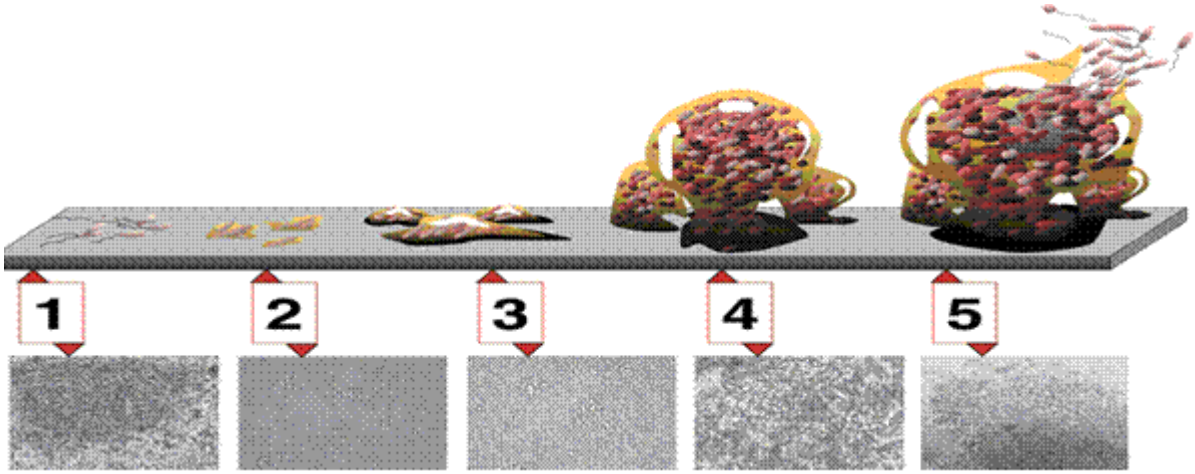

Figure 2-9: Biofilm formation steps (Monroe, 2007). Stage 1, initial attachment; stage 2, irreversible attachment; stage 3, maturation I; stage 4, maturation II; stage 5, dispersion.

Although many people associate bacteria with adverse effects like diseases and infections, most bacterial populations are extremely useful for both our life and the well - being of the environment. Despite the rapid growth of our knowledge about the development and

differentiation of bacterial biofilms on one hand and about the infectious diseases caused by biofilm on the other ~~side~~ in the last two decades, there are relatively few published materials studying the transport of the nanoparticles through biofilms (Tong et al., 2010). The limited studies currently available fail to identify any significant effects at the microbial level of nanoparticles in more complex systems (Neal, 2008).

2.3.2 Role of bacterial population in the environment

Bacterial population in the natural environment, whether it is planktonic unicellular form or more complex biofilm structures, has an important role in the productivity and function of the ecosystem. The most important role of a bacterial population is its ability to decompose organic materials and release useful nutrients for plants. Organic nitrogen in the dead organisms and their excretion are converted into ammonium which is an inorganic form of nitrogen through a process called ammonification in soil living fungi and bacteria called decomposers. Ammonium cannot be used directly by plants unless it is converted into nitrates by nitrifying bacteria (Belser, 1979, Kuenen and Robertson, 1994, Abeliovich, 1992). In this way, many useful plants including crops depend on bacteria and live symbiotically with bacteria in order to gain basic nutrients for their growth. Apart from the important nitrification process explained above, there are some free - living bacterial groups called plant growth-promoting rhizobacteria (PGPR) which protect plants from deadly pathogens (Babalola, 2010, Kloepper et al., 1980, Lugtenberg and Kamilova, 2009). These beneficial bacteria can be used to improve crop production and reduce the consumption of pesticides. Similarly, bacteria plays an important role for both carbon (Heimann and Reichstein, 2008, Davidson and Janssens, 2006) and phosphorus cycle (Ammerman, 2003b, Ammerman, 2003a) in the ecosystem.

Practical application of the degradation ability of the bacterial population is the sewage treatment plants where especially cultured bacteria provide necessary enzymes to reduce waste materials. Since bacteria reproduce in the sewage plant and increases in number, so is the amount of enzymes produced to decompose waste materials. This application is the cheapest available alternative for the abovementioned purpose and can be applied for any process where organic waste causes problems such as food processing systems, remediation of oil contaminated soils, contaminated aquifers, fish ponds and many more.

Both the very important role of bacteria population in the environment and its useful applications mentioned above justify the reason why many environmental scientists are concerned with the effect of human activity including nanotechnology on the environmental bacteria. To increase our knowledge of the environmental problems caused by NPs, this project aims to study the effect of gold nanoparticles on widespread environmental bacteria: Pseudomonas flourescens. It is the task of the next two sections to give a detailed introduction of the Pseudomonas flourescens and the summary of the published literature on the effect of the nanoparticles on this bacterial strain.

2.3.3 Pseudomonas fluorescens

Pseudomonas flourescens are gram negative bacteria and they belong to RNA- homology group I in the genus pseudomonas (Stanier et al., 1966, Palleroni et al., 1973). Other members of this group include Pseudomonas putida, Pseudomonas aureginosa, Pseudomonas syringae, (Palleroni, 1974). One of the main characteristics of the Pseudomonas flourescens is their ability to synthesise a yellow greenish water - soluble fluorescent pigment called pyoverdines (Stanier et al., 1966). These clearly visible fluorescent pigments attracted scientists to use them as taxonomic markers for the classification of different strains of Pseudomonas flourescens. (Winkelman, 1991). The main physiological function of

pyoverdines is based on their ability to fix iron (Meyer and Hornsperger, 1978) and make it available for these mainly aerobic pseudomonas species where the transport of oxygen is essential for their respiration process. Structurally, pyoverdines has three main domains (Meyer, 2000): a quinoline chromophone (responsible for the colour), an acryl chain and peptide chain which are important structures for the taxonomy purpose since different strains of pseudomonas flourescens have different peptidic chains (Kilz et al., 1999). Like other members of the Pseudomonas genus, it is a motile bacterium by means of polar flagella.

Pseudomonas flourescens are widely found in many different habitats in the environment. They can grow and flourish in water, soil and on plant leaves and roots. The fact that they can colonise a variety of different habitats in the environment indicates that they have simple flexible nutritional requirements. They can metabolise a wide range of different organic compounds as carbon sources (Dooren de Jong, 1926). Many strains of Pseudomonas flourescens are plant growth-promoting rhizobacteria (PGPR). They promote the growth of a different variety of plants by colonising their roots and producing antibacterial substances which stops the effect of the plant pathogens microorganisms. It is recognised that the compound responsible for the abovementioned mutualism is the pyroverdine pigment (Choi et al., 2008). Economically, the application of Pseudomonas flourescens on agricultural crops has increased, offering a green way of controlling deadly plant pathogens which can replace the traditional environmental non-friendly pesticides (Dey et al., 2004).

To gain a basic and preliminary understanding of the general problem of the NPs' interaction with bacterial population, the abundance of Pseudomonas flourescens in the environment makes them suitable organisms for the study of NPs in the environment since they are more likely to encounter and interact with them than the other less abundant organisms. Despite

their abundance in the environment, there are few studies available regarding the interaction of nanoparticles with Pseudomonas flourescens.

2.4 Pseudomonas flourescens and nanoparticles.

It is important to understand the effect of the NP on the microbiota once released in the environment. Unicellular planktonic bacteria can be used as a model to investigate the bacteria-NPs interaction at cellular level and at molecular level. Researches on planktonic bacteria may provide useful information about structural changes of the bacterial cell membrane and possible internalisation of NPs. Previous studies have reported the interaction in terms of intermolecular forces such as electrostatic forces, van der waals and hydrophopic interaction (McWhirter et al., 2002, Parikh and Chorover, 2006). Due to their antimicrobial activities, the effect of titanium dioxide NPs (Wei et al., 1994, Block et al., 1997) and silver-NPs on both gram-positive and gran-negative varieties of bacteria are widely studied. However, among the wealth of information available in the field of nanoparticles toxicity on the microbiota, only very few studies have dealt with Pseudomonas flourescens despite its abundance in the environment. See Table 2-4 below for summary of the published literature on the effects of engineered nanoparticles on Pseudomonas flourescens).

Table 2-4: Published literature on the effect of engineered NPs on pseudomonas flourescens.

Name of the NPs	Size of the AuNPs (nm	Coating agent	Shape of the AuNPs	Nominal conc	Toxicity	References
AgNPs	65 + 30	citrate	Spherical triangular	0 – 2000 ppb	Toxicity of AgNPs was pH dependent., presence of organic matter mitigated AgNPs toxicity	(Fabrega et al., 2009)
ZnO	≤ 50 nm	oxide	ND	1 -200 mm MIC = 24 µM	Increased cell death, abnormal cell morphology	(Tayel et al., 2011)
CuO	30 nm	oxide	ND	6 mg/l	ROS and DNA damage	(Bondarenko et al., 2012)
Al_2O_3, TiO, ZnO	60, 50, 20 respectively	oxide	ND	20mg/l	Mortality 70%, 0% and 100% respectively	(Jiang et al., 2009)

Toxicity of nanoscaled zinc, titanium , aluminium and silicon oxides on Pseudomonas flourescens were reported ((Jiang et al., 2009). Similarly, the effect of silver nanoparticles on the Pseudomonas flourescens were studied and the sign of toxicity at high concentration (2000 ppm) of the NPs (Fabrega et al., 2009) was found. Copper oxide NPs have caused the production of reactive oxygen species followed by DNA damage of Pseudomonas flourescens. Therefore, further work is needed to understand the effect of the engineered NPs on the environmental relevant Pseudomonas flourescens bacterium. As it was highlighted in chapter1 (introduction), it is the overall aim of this project to investigate the effect and interaction of gold nanoparticles of different sizes and coating agents on Pseudomonas flourescens.

Chapter 3: Theory of the characterisation Techniques for Gold Nanoparticles

Aiming to have well defined gold nanoparticles, the first part of this project was assigned to synthesize monodisperse batches of gold nanoparticles with systematically varying sizes and with two coating agents: PVP and citrate. After the synthesis of gold nanoparticles, complementing modern analytical and imaging techniques have been employed for the full characterisation of the nanoparticles as prepared, in bacterial growth media and after exposure to bacteria. Among important pysicochemical properties of the NPs include: the size, shape, charge, solubility, surface Plasmon resonance and surface chemistry (Filella and Buffle, 1993, Elzey and Grassian, 2010). In this project we characterise the freshly synthesised gold NPs by measuring their size, shape, zetapotential, surface Plasmon resonance, surface charge, stability overtime, and stability in a range of ionic strengths.

Due to the complexity and diversity in nature of the aforementioned physicochemical properties, It is obvious that they cannot be determined by using only one analytical technique so a multi-method approach has been chosen (Lead and Wilkinson, 2006). The following sections will be devoted to give a detailed introduction of the theoretical background of the characterization techniques of the NPs operated to elucidate the forgoing physicochemical properties of the gold NPs. Since the second part of the project aims to study the interaction of AuNPs on planktonic bacteria short description of the bacterial growth quantification techniques and sterilization techniques used during this project will be also be provided.

3.1.1 Centrifugation and ultracentrifugation

Theoretically, the centrifugal acceleration can be described by the following equation (Herivel, 1960).

$$F_C = \varpi^2 r$$ **Equation 3-1**

Where F_C is the centrifugal acceleration of the particles which rotate angular speed of ώ (rad/s) in a rotor with radius r (m). Using F = ma and substituting acceleration with Equation 3-1 the force that applies on the particles can be given in Equation 3-2 below

$$F = m\varpi^2 r$$ **Equation 3-2**

Where m stands for the mass of the particles and F is the centrifugal forces acting on the particles. Here, the force is directly proportional to both the mass and the square of the angular speed of the rotating particles in the suspension. For the sake of the practicality, the angular speed is, many times, given in terms of rotational speed which is expressed in round per minute (rpm). Since in one minutes there are 60 seconds and in one round there are 2π rads, the angular speed is related to the rotational speed N through Equation 3-3 below

$$\varpi = \frac{2\pi}{60} N$$ **Equation 3-3**

The equation for centrifugal force can then be change into following Equation 3-4 through substitution of ώ to the above relationship.

$$F = mr\left(\frac{2\pi}{60}N\right)^2$$ **Equation 3-4**

Whenever a suspension or pure liquid in a container is rotated around a central point, a centrifugal force, which can be 1000 times greater than the gravitational force is generated (Wallace, 1998). The effect of this force is to drive denser particles in the suspension away from the centre of the rotation toward the outside wall of the container and subsequently accelerate them to the bottom of the container as precipitate in the form of a pellet (Wilson and Walker, 2010). The top layer which is mainly the liquid and the suspended substances which are less dense than the liquid is called supernatant. The rate of sedimentation of the particles depends not only the magnitude of the centrifugal force and the diameter of the rotor driven by an electrical motor around a fixed axis but also the shape, size and density of the particles and viscosity of the liquid (Wallace, 2007). This means particles suspended in a same type of liquid can be separated according to their density by applying fractional centrifugation process. During this process, the size of the centrifugal force is altered through changing of the rotational speed of the rotor and in this way density separation of the components in the suspension is achieved. To compare different rotors, the amount of acceleration which they can provide is used instead of the rotational speed since rotors of the same speed will provide different acceleration and thus different centrifugal forces if their diameters differ from each other.

3.1.2 Transmission Electron Microscopy (TEM)

Transmission electron microscopy was first invented and constructed by Max Knoll and Ernst Ruska in Germany in 1932 (Knoll and Ruska, 1932). It took only about four years

before the first commercial TEM appeared in the market in 1936. Around that time, the lower limit of the resolution of light microscope which uses light waves to image objects was already achieved and scientific community seriously needed a much higher resolution for their researches (Knoll and Ruska, 1932). The resolving power of an optical instrument is its ability to separate two objects which are very close to each other. The resolution of the traditional light microscope depends on the wave length of the type of light rays used through the classical Rayleigh criterion (Inoue and Spring, 1997, Kapitza, 1994).

$$\delta = \frac{0.61\lambda}{\mu \sin \beta}$$ **Equation 3-5**

Where δ is the distance between two objects, λ = is the wavelength of the light beam, μ is the refractive index of the medium (usually air, water or oil) and β is the half of the angular aperture of the lens. Given that the refractive index of certain medium and aperture of a lens of a certain microscope do not change during an experiment, the maximum resolution that can be achieved with light microscope is mainly determined by the wave length in the sense that the shorter the wave length of the light the higher the resolution which can be achieved. Therefore, according to the aforementioned relationship, the highest theoretically possible resolution which can be achieved by conventional light (optical) microscope is around 0.2 mm (O'Keefe, 1956, Born and Wolf, 1999) as correctly predicted by Ernst Abbe in 1870.

In the case of the transmission electron microscope, electron beam is used for imaging of the objects under study and is accelerated through vacuum medium with refractive index equal to 1; the angular aperture is so small that the value of sin(β) can be approximated by the size of

the angle β itself. With these two valid assumptions for TEM, the resolution can be approximated to (Williams and Carter, 1996).

$$\delta = \frac{0.61\lambda}{\beta}$$ **Equation 3-6**

The wavelength of a beam of electrons is inversely proportional to its speed caused by the applied potential difference. In 1925 Broglie derived an equation showing this relationship (Equation 3-7) which can be used to calculate the wavelength of the electron beam accelerated in a certain predetermined electrical field.

$$\lambda = \frac{1.22}{E^{1/2}}$$ **Equation 3-7**

Where λ is the wavelength of the light and E is field strength. By substituting the value of λ from Equation 3-7 into Equation 3-6, we can calculate the theoretical resolution of the TEM.

TEM has normally much higher resolution than traditional light microscope due to the short wave length of the highly energetic electron beams used in the TEM to get images of the object under study. Modern high resolution TEM is capable of imaging the position of individual atoms in a crystal (Voyles et al., 2002, Singhal et al., 1997) with resolutions below angstrom scale (Nellist et al., 2004) while the resolution of light microscope is at the scale of micrometer. The source of the electron beams in the TEM is tungsten filaments cathode. The electrons are accelerated in a vacuum by potential difference varying from 40 to 100 KV depending on the type of TEM and are focused on the target sample by

electromagnetic lenses. The beam of electrons interact with the sample (Williams and Carter, 1996) and only transmitted fraction of electrons reach on the viewing screen which is coated with electron beam sensible fluorescent substances. It is on the viewing screen where bright dark images are produced depending on the intensity of the beam reaching on the areas of the image (Figure 3-1).

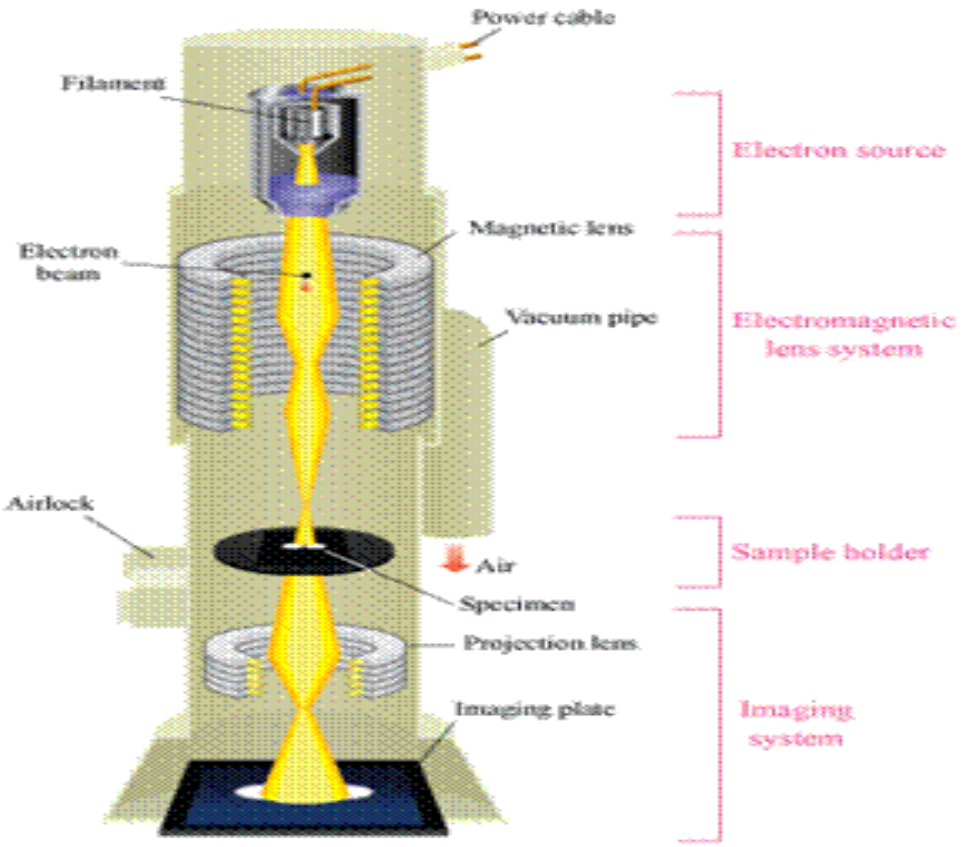

Figure 3-1: Schematic diagram of the basics of TEM(AtomicWorld, 2012)

3.1.3 Atomic Force Microscopy (AFM)

Atomic force microscopy is one of the most popular and useful tools available for research community to image the surface of materials at the nanoscale. The precursor of the AFM, the so called scanning tunneling microscopy (STM) was only limited to study samples which conduct electricity since the STM required the conductivity of the samples (Binnig et al.,

1982b, Binnig et al., 1982a, Binnig and Rohrer, 1987). This limitation was resolved when in 1985 the AFM was proposed and invented by Binnig, Quate, and Gerber (Binnig et al., 1986). The main difference between STM and AFM is the fact that the first measures the tunnelling current between the tip and surface of the sample while the second instrument measures the force interaction between the tip and the sample (Meyer, 1992, Pool, 1990). With the AFM, atomic resolution can be achieved (Mizes et al., 1987) and its possible that single atoms in both insulating and conducting materials can be imaged (Albrecht et al., 1988). Apart from the controller unit, the main parts of the AFM machine are cantilever with a very sharp tip made mainly from Si or Si_3N_4, the laser beam generator and photodiode detector (Jalili and Laxminarayana, 2004). During the imaging process with AFM, the interaction between the tip of the cantilever and the surface introduces the deflection of the movement of the tip. This deflection causes that the laser beam which was directed on the back of the tip is reflected into different position on a photodiode detector (Hutter and Bechhoefer, 1993) (see Figure 3-2 below).

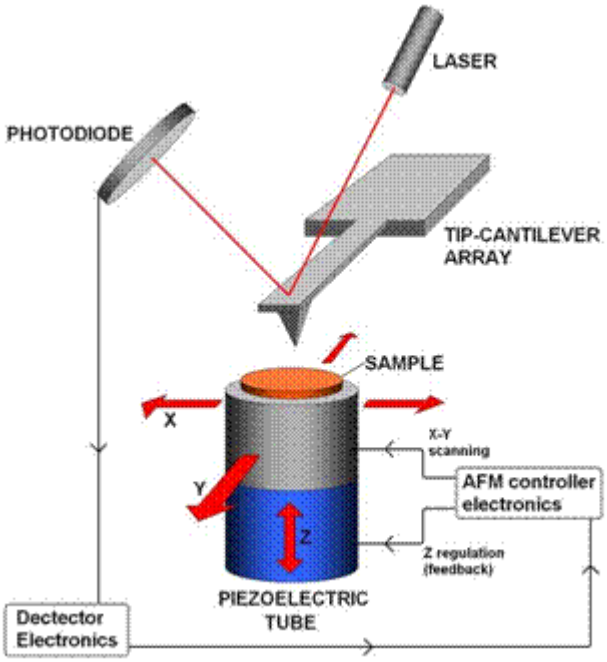

Figure 3-2: Block presentation of the internal components of the AFM(Pharm_virginia, 2012)

This upside down movement of the tip can be used to trace the surface of the sample and generate its topographic map (Basso et al., 1998). How the deflection of the cantilever is related to the Van der Waals attraction/ repulsion forces between the tip and the sample surface can be represented by Hook's law (Dürig et al., 1986) (Equation 3-8 below) and illustrated in Figure 3-3 below.

$F = kZ$	**Equation 3-8**

Where F is the force, Z is the deflection distance and K stands for the stiffness of the lever.

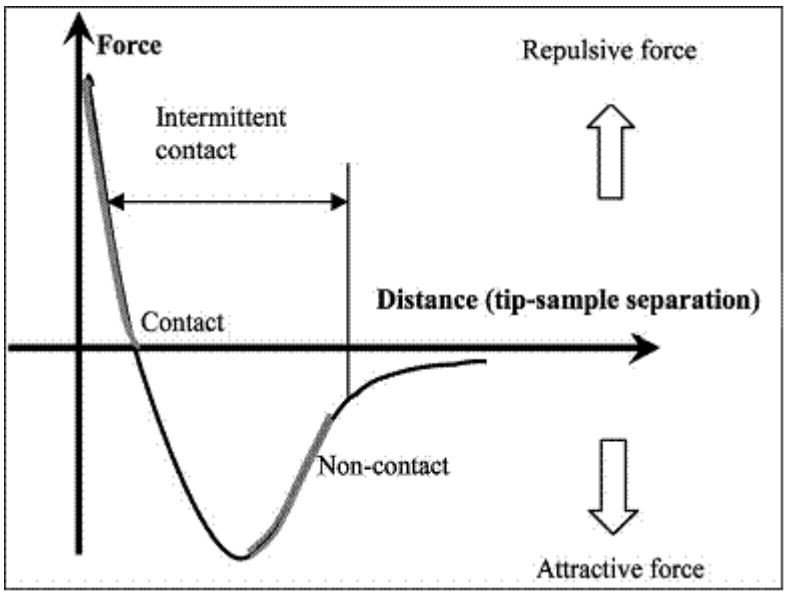

Figure 3-3: Interatomic force variation versus distance between AFM tip and sample(Jalili and Laxminarayana, 2004). Reprinted with permission from copyright 2004 Elsevier.

Among the different modes of the AFM, the contact, non-contact and tapping modes are mostly applied in determining the size and the shape of the materials in the nanoscale (Dufrêne, 2002). These modes differ mainly in the distance between the tip of the cantilever and the surface atoms of the samples. In the contact mode the tip in contact with the surface

atoms of the sample creates repulsive interatomic forces caused by the electron clouds of the touching atom (Blackman et al., 1990) while by non-contact AFM mode the cantilever tips oscillates near the surface of the sample and the change of this vibration caused by the interatomic forces is detected and translated into topographical images of the sample surface. The distance between the tip and surface atoms in tapping mode is somewhere between the other two modes explained above and changes as the tip comes into contact with the surface of the sample under study. Due to its versatility, AFM has been applied in many branches of sciences including surface science, material science, nanoscience and biology (Butt et al., 2005, Yang et al., 2007).

3.1.4 Dynamic Light Scattering (DLS)

Dynamic light scattering (DLS) also known as photon correlation spectroscopy (PCS) is one of the most applied measuring techniques used in determining the size of nanoparticles in liquid media(Berne and Pecora, 2000). This technique uses the scattering of light from particles in a liquid media. Due to the random Brownian motion of the particles caused by the bombardment of the continuous motion of the liquid media surrounding the particles(Tscharnuter, 2006).

The movement of the particles cause Doppler Effect to the wavelength of the incoming light and thus to the scattered light (Angus et al., 1969). The intensity fluctuation of the light scattered, which is related to the size of the particles, gives fluctuating speckle. A photon correlator continuously monitors the speckle fluctuation which can be used to calculate the time-dependent intensity correlation function (Berne and Pecora, 2000). The correlation function which decreases with time is related to the size of the particles as the larger particles

are much slower than smaller ones and scattering intensity fluctuates more slowly. The rate of decay of the correlation function provides information about line width (Γ́) of the scattering light which is related to the diffusion coefficient (D) through Equation 3-9 below.

$$\Gamma = Dq^2 \qquad \textbf{Equation 3-9}$$

q stands for the numerical value of the vector describing the scattered light and is related to a number of both instrumental and light properties as described in Equation 3-10 below.

$$q = \frac{4\pi\eta_0}{\lambda}\sin(\theta/2) \qquad \textbf{Equation 3-10}$$

Where θ is the angle of scattering measurement, λ is the wavelength of the laser beam, η_0 is the refractive index of the liquid media. The above two equation can be used to find the diffusion coefficient of the particles. By assuming that the particles are spherical in shape, we can use the classical Stokes-Einstein Equation 3-11 (Einstein, 1905) which provides a relation between diffusion coefficient of the particles in motion and their size radius.

$$D = \frac{K_B T}{6\pi\eta A} \qquad \textbf{Equation 3-11}$$

D stands for the diffusion coefficient, T is the absolute temperature in degrees Kelvin of the sample, K_B is the distribution Boltzmann constant, η is the viscosity of the solvent and A is the radius of the spherical particles.

3.1.5 Zetapotential

Apart from hydrodynamic diameter measurements described above, DLS instrument from Malvern is used to measure the electrophoretic mobility of the particles in an electric field which in turn can be used to calculate the Zetapotential of the samples by applying either Smoluchowski or Huckel Henry (Smoluchowski, 1903) equations depending on the nature of the media. Zeta potential is a good indicator of the repulsion forces between particles and is used to estimate the stability of nanoparticles in the media (Eilers and Korff, 1940). By nature, equally charged particles in a media tend to repel each other due to repulsive electrostatic force in contrast, there is also Van der waals attraction force between particles regardless their charge which mainly depends on the distance of the particles (Hamaker, 1937). It is the combined effect of these two opposing forces which determines whether particles aggregate or not as explained by the classical DVLO theory (Derjaguin, Landau, Verwey and Overbeek theory)(Deryagin and Landou, 1941, Verwey and Overbeek, 1948) which can be summarised in Equation 3-12 (Malvern, 2001).

$$V_T = V_R + V_A + V_S \qquad \textbf{Equation 3-12}$$

Here, V_T is the total potential of the particles, V_R is repulsive potential caused by equal charges of equal sign on the particles, V_A is the van der Waals attractive potential and V_S is the solvent's potential energy which is less important than the other two potential.

Since particles are in continuous movement due to the Brownian motion, they can come too close together if they have enough kinetic energy to overcome the effect of the repulsive forces and then Van der Waals forces pull particles together to form aggregates (see Figure 3-4 below) (Honigmann, 1970).

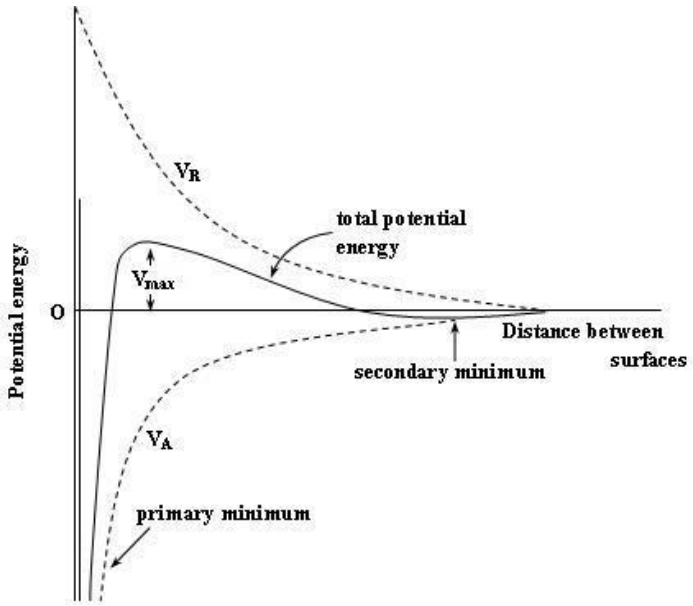

Figure 3-4: Repulsion and attraction potential as function of the distance from the charged particle(Honigmann, 1970)

To understand the scientific meaning of zetapotential, consider of a negatively charged spherical particles in a dispersion media, the positively charged ions in the media will be attracted to the surface to counter-balance the charge. This generates potential difference around the particles which can be illustrated in Figure 3-5. Since the particle is in Brownian motion, the strongly attracted positive ions will move with the particles forming the stern or stationary layer while less bonded ions will form a dynamic diffusive layer. The imaginary

plane between the bulk and the diffusive layer is called slipping plane (see Figure 3-5) and the electrical potential difference between this plane and a point in the bulk media far away from the negatively charged particle is defined as zetapotential. As mentioned earlier in this section, Zeta potential cannot be measured directly from the solution but it is calculated from the electrophoretic mobility (EPM) which is the rate of migration of charged particles in stationary liquid medium due to the effect of an applied external electric field. DLS instrument has ability to measure the EPM by filling the NPs solution in to a cell and applying external electric field. How fast particles move is directly proportional to the strength of the external applied electric field, the viscosity of the liquid medium and the charge and the size of the particles. There are two opposing forces acting on these moving particles which are the electric field force and the drag forces due to the viscosity of the liquid. When these two forces are in equilibrium the particles gain steady speed. Equation 3-13 below shows the relationship between the velocity of the particles and the strength of the electric field.

$$\vec{V} = \mu\vec{E} \qquad \textbf{Equation 3-13}$$

Where $\vec{V}$ stands for the velocity of the particles in cm/s , $\vec{E}$ is the strength of the electric field in V/cm and μ is the electrophoretic mobility and its unit is thus $cm^2/Vsec$. Henry equation establishes the link between the zeta potential and elctrophoretic mobility (Henry, 1931).

$$\mu_E = \frac{2\varepsilon z f k(a)}{3\eta}$$ **Equation 3-14**

Where μE is the elctrophoretic mobility, ε stands for dielectric constant, Z is the zeta potential, η is the viscosity of the media, K is Debye-Huckel constant and fk(a) is the Henry function. In most practical situations, where particle size is bigger than the thickness of the double layer and there is sufficient electrolyte concentration, simplified Marian Smoluchowski's approximation (Smoluchowski, 1918) with fk(a) = 1.5 can be used instead to calculate zeta potential from elctrophoretic mobility using Equation 3-15.

$$\mu = \frac{\zeta \varepsilon}{\eta}$$ **Equation 3-15**

Here μ is the electrophoretic mobility, ε is the electric permitivity , η stands for the viscosity of the surrounding liquid, ζ is the zeta potential, with a simple algebraic manipulation, ζ can be made the subject of the formula and calculated from the electrophoretic mobility of the charged particles.

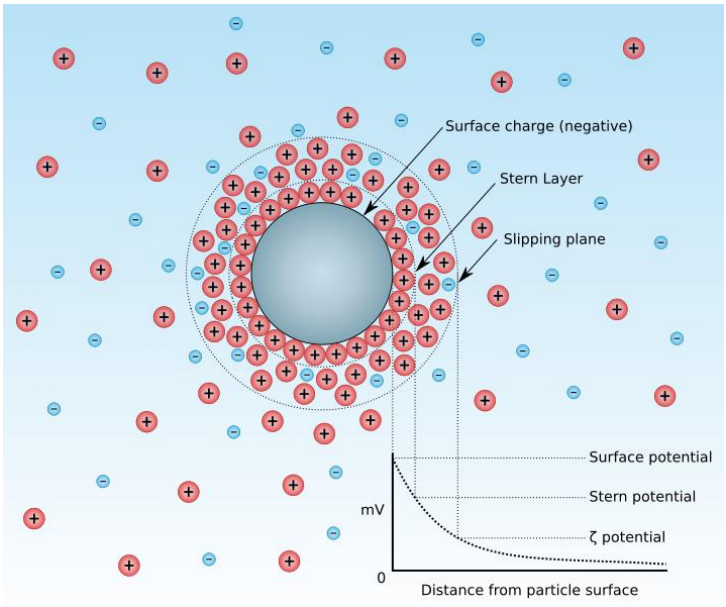

Figure 3-5: Schematic diagram illustrating the charge distribution around a charged spherical particles in dispersion media. it shows both the stern layer and slipping plane plus how the potential changes with the distance from the charged particle (Wikipedia 2012).

3.1.6 Surface Plasmon Resonance (SPR) spectroscopy.

The free conductive valence electrons on the surface of the metals oscillate naturally due to the storing attraction effect of the positive charge of the atomic nuclei. This oscillation causes an electron density waves (surface Plasmon) with characteristic frequency on the surface of the metal. The nature of the force between electrons and nuclei is coulomb forces which is indirectly proportional to the charges separation distance and directly proportional to the strength of the charges. The separation distance of the charges (electrons and nuclei) in the metal is given by Equation 3-16 below.

$$S = \sqrt[3]{N} \qquad \textbf{Equation 3-16}$$

Where n is the charge density.

The stored potential energy between separated charges is calculated with Equation 3-17.

$$U = K\frac{e^2}{S}$$ **Equation 3-17**

Here, K is constant, e stands for the charge of the electrons and S is the separation distance between charges.

The oscillation of the electrons around the positively charged nuclei can be treated like classical harmonic oscillator and below can be used for the energy of harmonic oscillator.

$$U = \frac{1}{2}M\varpi_P^2\ s^2$$ **Equation 3-18**

$\acute{\omega}_p$ is the frequency of the harmonic oscillator. Using the last three equations and rearranging them for the frequency of oscillation the following equation can be derived which gives the frequency of the oscillating electron density (surface Plasmon) waves.

$$\varpi_p = \sqrt{2k\frac{ne^2}{m}}$$ **Equation 3-19**

If the frequency of incident light photons matches the natural characteristic frequency ($\acute{\omega}_p$) of the electron density waves of the metal, the energy of the photons is absorbed (Pockrand et al., 1978) and surface plasmon resonance (SPR) occurs (Gordon Ii and Ernst, 1980) for planar surface and localised surface plasmon resonance (LSPR) for nanoscale sized metals (see Figure 3-6 below).

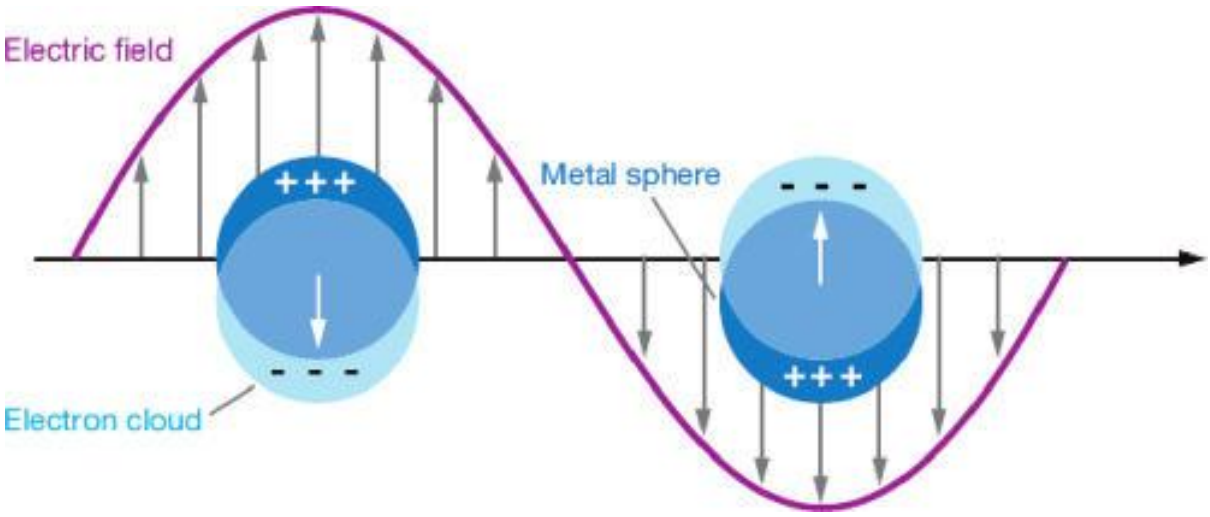

Figure 3-6: Localised Surface plasmon resonance (LSPR) of conductive electron density wave excited by light wave. Electrons clouds around the particles are repelled by the electric field of the light waves (Willets and Van Duyne, 2007). Reprinted with the permission from copyright Annual Review of analytical chemistry.

The wavelength of the maximum absorption depends on the type , shape, size and the environmental surrounding of the nanoparticles (Kreibig and Vollmer, 1995) In the most metal nanoparticles this maximum absorbance which causes the localised surface Plasmon resonance falls in the ultraviolet region of the electromagnetic spectrum. In the case of gold and silver nanoparticles, the resonance takes places in the visible region due to interband transitions. This absorption wave can be recorded with UV-Vis spectrometer to identify the type of metal in the sample or to study any changes in the surrounding media. To quantify the amount of light absorbed by sample, the concept absorbance A is used which is defined as.

$$A_\lambda = \log_{10}(I_0 / I) \qquad \textbf{Equation 3-20}$$

Where Io and I stand for respectively the intensity of the light at certain wavelength (λ) before and after it has passed through the sample under study. Absorbance is a fraction of two intensities so it has no unit but many times it is reported in absorbance unit (AU). Figure 3-7 gives a diagram representation of the typical dauble beam Uv_vis spectroscopy.

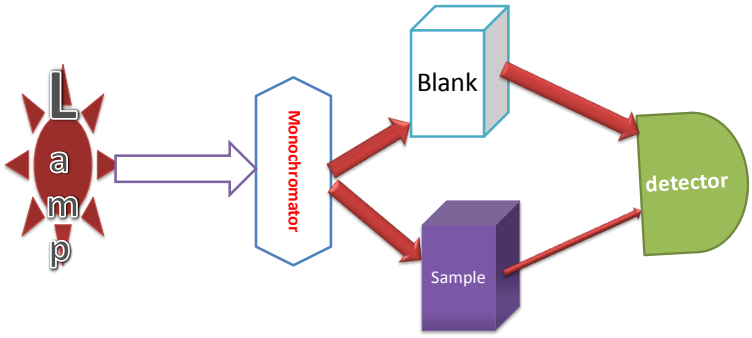

Figure 3-7: Simplified Schematic representation of the main parts of Uv-vis spectrophotometer showing the light sources the monochromater, reference and sample holder and the detector.

3.1.7 Field Flow Fractionation (FFF)

Field flow fractionation is a very versatile sizing and separation technique which has many applications in the different scientific areas including food chemistry, medicines, biology and environmental science (Wittgren and Wahlund, 1997, Petteys and Schimpf, 1998, Chmelik, 2007). The range of sizes that can be separated may vary from 0.001 to 100 µm (Dulog and Schauer, 1996) which is the whole range of colloidal, macromolecules (Ratanathanawongs Williams et al., 2006), nanoparticles (Lohrke et al., 2008, Baalousha et al., 2011) and particulates (Kirkland et al., 1990) in different carried solvents. What makes FFF so versatile to separate a wide range of sizes is because of the variety of different nature fields which can be used to achieve separation (Shendruk and Slater, 2012). The one main difference between the different separation types of the commercial FFF is the nature of the applied field which can be either electric field (Giddings et al., 1974), temperature gradient (Caldwell et al., 1972), sedimentation field (Giddings et al., 1975) or crossflow (Giddings et al., 1976). FFF instruments contains similar components (carrier, pump, injection port, separation channel, detector and computer see Figure 3-8 below) of the traditional liquid chromatography (Myers, 1997) though the basic separation principles are, as will be explained later , different.

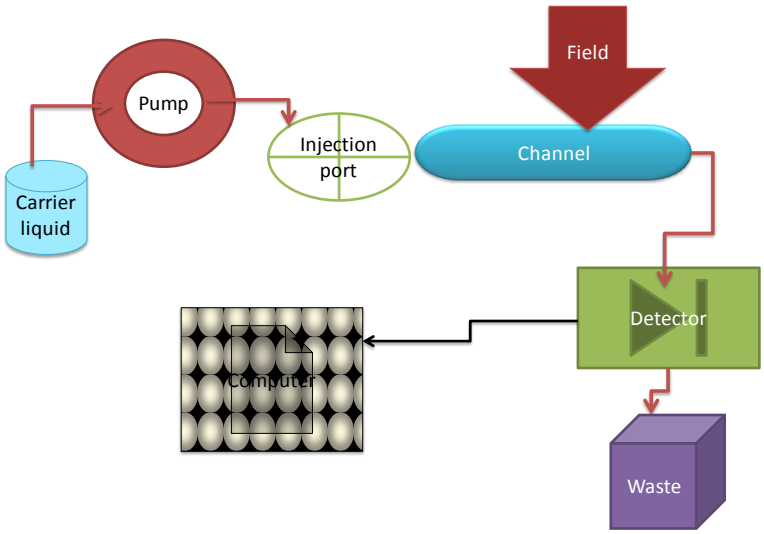

Figure 3-8: Schematic diagram of field flow fractioning with all main parts illustrated (FFF)

A detailed theory of the relevant principles of the FFF has been given in a number of papers (Myers, 1997, Giddings, 1993a, Giddings et al., 1977, Giddings, 1966). Here, only a short introduction of the basics of cross-flow normal mode of the FFF is given, which is suitable for the NPs in this project. Of the number of assumptions applied to develop a theoretical concept of the FFF retention the main ones are: the uniformity of the field across the channel, and the lack of interaction between particles and between wall particles interaction (Messaud et al., 2009).

FFF separation is achieved due to the combined effect of two opposing transport processes (Giddings, 1966). An applied cross-flow which is perpendicular to the liquid flow direction pushes the particles in the samples toward the accumulation wall (Bos and Tijssen, 1995). This is followed by continuous diffusion of the particles from the accumulation wall due to concentration gradient set up by the cross flow where the highest concentration are by the wall. The thickness of the cloud of particles L can be related to the above mentioned main processes through Equation 3-21.

$$L = \frac{D}{U}$$ **Equation 3-21**

D is the diffusion coefficient and U is the side way velocity caused by the cross flow. If the thickness L is divided by the thickness of the channel (w) an alternative dimensionless parameter λ can be defined as follows.

$$\lambda = \frac{L}{w}$$ **Equation 3-22**

Combining Equation 3-21 and Equation 3-22 and solving for λ provides Equation 3-23.

$$\lambda = \frac{DU}{W}$$ **Equation 3-23**

From the theory of FFF (Giddings, 1973, Giddings et al., 1976), λ is related to experimental parameter R (void volume/ retained volume) through Equation 3-24 below.

$$R = 6\lambda\left[\coth(1/2\lambda) - 2\lambda\right]$$ **Equation 3-24**

Experimentally, R can be obtained by the ratio of the void time t0 and the retention tr(Messaud et al., 2009). Then Equation 3-23 can be used to give λ. With the λ so obtained, Equation 3-21 is applied to calculate the value for the diffusion coefficient of the particles

which in turn can provide the size diameter of the particles through classical Stokes-Einstein equation.

$$D = \frac{K_B T}{6\pi\eta A}$$ **Equation 3-25**

D stands for the diffusion coefficient, T is the absolute temperature in degrees Kelvin of the sample, K_B is the distribution Boltzman constant, η is the viscosity of the solvent and A is the radius of the spherical particles.

There are two modes of operations for FFF techniques with different separation mechanisms determined by the size of the particles to be separated (Shendruk and Slater, 2012). In the normal Brownian dominated mode, submicron and nanosized particles are separated by the balance of the two transportation processes explained earlier in this section. While for bigger particles, the diffusion process is negligible and particles roll on the bed of the channel so a sterical interaction between the particles and the surface of the channel determines the separations and this mode is called steric mode. Since bigger particles roll faster than smaller ones the separation is opposite to the normal mode (Reschiglian et al., 2005) (see Figure 3-9 for further illustration). The shape of the flow in the channel is parabolic with maximum speed in the centre (Giddings, 1993b) see Figure 3-9 below. Since smaller particles diffuse faster, they will reach further away from the wall into the area of the higher laminar velocity and they are transported faster and detected earlier than the bigger particles which are situated near the wall where the laminar flow of the carrier fluid has the lowest velocity (Caldwell et al., 1979).

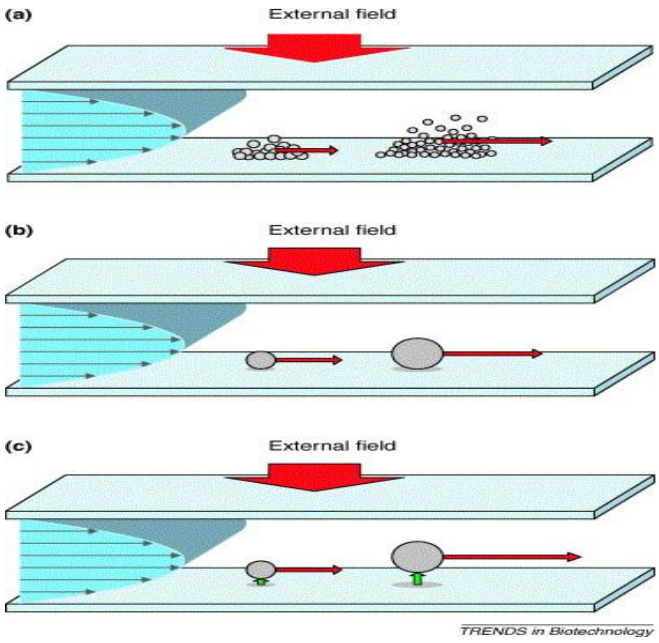

Figure 3-9: Separation of particles of different sizes with different modes of the FFF 9 (a) is normal, Brownian dominated mode, (b) is the steric mode and (c) is hyperlayer mode *(Reschiglian et al., 2005). Reprinted with the permission from copyright 2005 Elsevier.*

3.1.8 Inductively Coupled Plasma Mass Spectrometry (ICP-MS)

ICP-MS can be applied to measure traces of nearly most of the elements in the periodic table; it is an extremely powerful analysis method for metal (Hirner, 2006) and non-metallic (Wuilloud and Altamirano, 2006) elemental measurements. The combinations of low detection limit, lower than part per trillion (Ray et al., 2004, Moldovan et al., 2004), and the short measurement time (Montaser, 1998, Nelms, 2005) make it suitable for many fields in both research and applied science (Ammann, 2007) and superior to other types of elemental analysis instruments such as atomic absorption spectrometer (AAS) and inductively coupled plasma –optical emission spectrometer (ICP-OES) (Thomas, 2004, Jarvis, 1988). Examples of the fields where ICP-MS has been applied include environmental(Butler et al., 2011), biomedical, forensic (Ulrich et al., 2004), food industry, life sciences (Bettmer et al., 2006) and many more. Samples used for ICP-MS can be any state liquid, solid or gas.

Historically, the first papers about ICP-MS were published in 1980 (Houk et al., 1980) followed by the first commercial ICP-MS introduced by Perkin Elmer SCIEX in 1983 (Rakhi et al., 2008). Generic components for most ICP-MS components which are similar to other mass spectrometers include: Sample introduction system, ICP torch and radio frequency (RF) coil, Interface, Vacuum system, electrical lenses (electrostatic analyser ESA), quadrupole mass filter and detector (PerkinElmer, 2011) (see Figure 3-10 below for illustration). In the ICP-MS, ions are generated in the induction system and introduced in the vacuum area of the mass spectrometer, and then they are accelerated by electrostatic lenses. The separation of ions on the basis of their mass/charge ratio is achieved through a mass analyser filter (quadrupole) and they are finally detected by an electron multiplier at the far end of the mass spectrometer system. To find the concentration of the element under study, its electrical signal from the detector is compared with a signal given by a certified reference material used to calibrate the system (Zeisler et al., 2006).

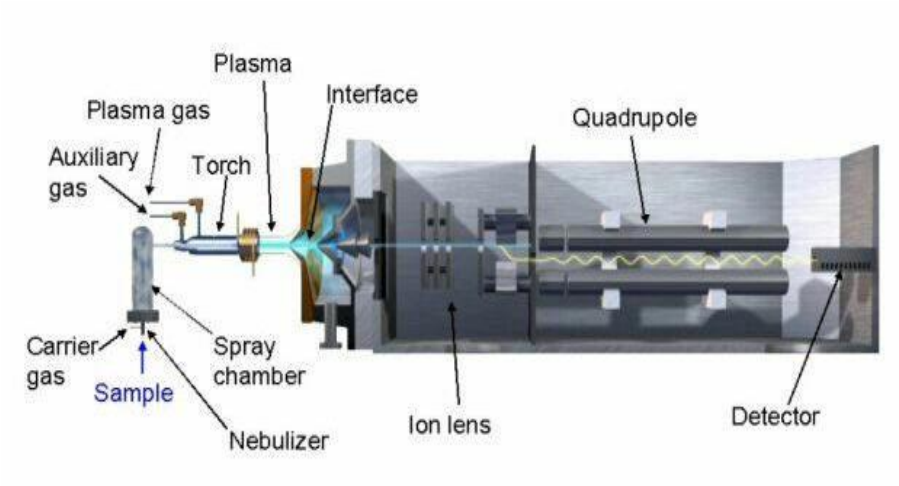

Figure 3-10: A diagram showing the cross section of the different components of modern quadrupole ICPMS(Wum, 2012)

3.1.9 Potentiometric Titrations Method

Potentiometric titration is an analytical method where an electrochemical cell measures the potential difference between two electrodes immersed in a sample. One of the electrodes is a

stable reference electrode while the other one is the indicator electrode. Although potentiometric titration can be applied to different types of reaction such as redox, complexion, precipitation and many more the most popular reaction is the acid base titration.

Certain volume (V) of an acid with unknown concentration of H^+ is titrated with volume v of base with known concentration of OH^- . The potential difference between the two electrodes is then given in the form of pH due to the calibration that was conducted prior to the measurement. The change of the pH against the volume of titrant used can be recorded and plotted as a graph (see Figure 3-11 below). The inflection point of the graph is where maximum change occurs and corresponds to the end point of the reaction.

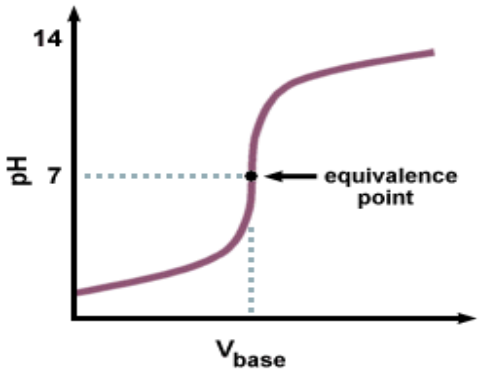

Figure 3-11: Titration of acid with strong alkali.(Floridauniversity, 2012)

Another alternative way of finding the end point of the reaction is the applying of the Gran method which is explained in the following paragraphs. The section of the titration curve before the end point in the acidic region applies that the concentration of the hydrogen ions can be calculated using **Equation 3-26** below (Gran, 1950).

$$\left[H^+\right] = \frac{v_0\left[H^+\right]_0 - vb\left[OH^-\right]_0}{\left(v_0 + vb\right)} = 10^{-pH} \qquad \textbf{Equation 3-26}$$

Where v_0 and $[H^+]_0$ are the initial volume and the unknown concentration of H^+ ions of the acid solution respectively, v_b and $[OH^-]$ are the volume of the base added and the concentration of the OH^- ions. Manipulating Equation 3-26 slightly provides Equation 3-27 below.

$(v0+vb)*10^{-ph} = v0\left[H^+\right]_0 - vb\left[OH^-\right]_0$	**Equation 3-27**

If the part before the equal sign in Equation 3-27 is plotted against v_b a linear equation with slope of $[OH^-]_0$ will be found. The intercept of this linear relationship is $v_0 * [H^+]_0$ which is the number of moles of H^+ ions in the unknown original sample.

When the unknown is $[OH^-]$, the alkaline region of the titration curve can provide solution. In this region following Equation 3-28 applies for the initial concentration of the unknown OH^- concentration (Gran, 1950).

$-\left[OH^-\right] = \frac{v_0\left[H^+\right]_0 - vb\left[OH^-\right]_0}{\left(v_0+vb\right)} = -K_W 10^{pH}$	**Equation 3-28**

Where K_w is the water constant and is equal to $[H^+] * [OH^-] = 10^{-14}$. Similar manipulation as Equation 3-26 will provide a linear equation with gradient of $[OH^-]_0/Kw$ (Gran, 1952).

Chapter 4: Materials and Methodology

4.1 Introduction

This chapter describes the sample preparation techniques and analytical methods used to synthesise and characterise gold nanoparticles (AuNPs) of different capping agents (citrate and Polyvinyl pyrrolidone (PVP)) and sizes both as prepared and in bacterial growth media. In order to understand the effect of NPs on planktonic bacteria the properties of nanoparticles need to be fully understood so that the effect property relationship can be studied. It is important to examine and understand for example the stability of NPs in the bacteria growth media prior to their exposure to the actual bacteria since any change in the physicochemical properties of the NPs may cause unpredicted and hard to interpret results. The more we know about the properties of the nanoparticles the easier it will be for us to identify the nanoparticles property and bacterial response relationship (Stone et al., 2010). After a short introduction to the different synthesis method used to synthesise NPs, this chapter will give detailed description of how characterisation techniques are applied practically in this project. The last section of this unit will be devoted to microbiological analysis techniques including media preparation, sterilisation techniques, staining, fixation, sectioning and bacteria quantification methods.

4.2 Synthesis of gold nanoparticles

This section introduces different synthesis methods used in this project to produce high quality gold nanoparticles with different sizes and different surface chemistry. To modify the surface chemistry of the nanoparticles two different coating agents were used as will be explained in the following sections.

4.2.1 Materials

The following chemicals were of analytical grade and have been purchased from Sigma Aldrich: tetrachloroauric acid ($HAuCl_4.3H_2O$), trisodium citrate dehydrate, NaOH, HNO_3, HCl, NaCl, Polyvinyl pyrrolidone (molecular weight =10,000; hereafter referred to PVP) and were used as received from the supplier without further purification. The water used for all reactions and preparation procedures were milli-Q quality R > 18 MΩ cm, and was obtained by filtering through Millipore cartridges. All glassware used in these synthesis processes were thoroughly cleaned three times in aqua regia (3 parts HCl: 1 part HNO_3), rinsed with ultra high purity water (resistivity 18.2 MΩ·cm) and air dried.

4.2.2 Synthesis of AuNPs capped with Citrate

AuNPs were prepared by citrate reduction of $HAuCl_4.3H_2O$ according to the following procedure which is based on the Turkevich method(Turkevich, 1951) as modified by Frens (Frens, 1973) and others (Kumar et al., 2006).The required volume of an aqueous solution of $HAuCl_4.3H_2O$ was heated to the boiling point while stirring vigorously and then trisodium citrate was added quickly. The actual concentration of the solutions are summarised in Table 4-1. The ratio of the two chemicals was varied in order to produce the size of the desired nanoparticles (Table 4-1). An immediate colour change from pale yellow to deep red occurred within 10 minutes. The solutions were kept at the boiling point for 15 minutes to assure the completion of the reaction and finally allowed to cool to room temperature.

4.2.3 Synthesis of AuNPs capped with PVP

AuNPs stabilised by PVP were prepared using two different synthesis methods. The difference between them was mainly about the synthesis temperature and after synthesis

cleaning procedure as described below. One of the methods required the heating of a mixture of gold and PVP solutions up to 70 ^{o} C and it will be called hot method hereafter while the other synthesis method was carried out at room temperature and it will be referred to as cold method.

4.2.3.1 Cold process.

A detailed method of the process was given elsewhere (Zhou et al., 2009). Briefly, an aqueous solution of tetrachloroauric acid was added to a solution of polyvinylpyrrolidone (PVP) under vigorous stirring in room temperature. Then aliquots of NaOH, whose concentration was accurately known, was added to initiate the reduction of the gold ions which then was capped and stabilised by PVP (see Table 4-1). To achieve different sizes of AuNPs the ratio of gold precursor to capping agent were altered.

4.2.3.2 Hot process.

In preparing the nanoparticles of gold, the general procedure followed is summarised below. A known quantity of tetrachloroauric acid was weighed and dissolved in water. Then various amounts of PVP solution were added, as summarised in Table 4-1, to achieve different sizes of AuNPs. The final solution of $HAuCl_4.3H_2O$ and PVP in water was heated up to 70 ^{o}C for 3 hours. After cooling to room temperature, the solutions was washed with acetone and water with ratio (3 acetone: 1 water) and centrifuged 10 min at 4000 rpm to get rid of the access PVP. The so produced AuNPs were then redispersed in water and filtered with 100 nm filter paper.

Table 4-1: Experimental conditions and the concentrations on the reactant used for the synthesis of AuNPs capped by citrate and PVP10 separately.

Sample code	$HAuCl_4$ ml /(mM)	trisodium citrate (mM)	PVP (mM)	Molar ratio of $HAuCl_4$: Capping agent	Temperature (^0C)	Reducing agent
G1	100 ml 0.25 mM	1 ml 30. 4 mM		1.00 : 0.30	100	
G2	300 ml 1.06 mM	30 ml 40.8 mM		1.00 : 3.86	100	
G3	100 ml 1 mM	4 ml 38.8 mM		1.00 : 1.55	20	Sodium Borohydrate
G4	50 ml 5 mM		100 ml 1 mM	1.00 : 0.40	20	NaOH
G5	100ml 5 mM		200 ml 0.5 mM	1.0 0 : 0.10	20	NaOH
G6	100 ml 5 mM		200 ml 0.25 mM	1.00 : 0.05	20	NaOH
G7	20 ml 3.87 mM		180 ml 2.78 mM	1.00 : 6.467	70	
G8	20 ml 2.58 mM		180 ml 2.78 mM	1.00 : 9.70	70	

4.3 Sample Preparation

This section introduces pre analysis cleaning and preparative size separation techniques used to prepare nanoparticles and to clean all glassware used during the synthesis. Any excess capping agents and unreacted precursor ions need to be separated from NPs before they are analysed and characterised since they either may affect the quality of the analysis or may complicate the interpretation of the toxicity data of the nanoparticles. Similarly, bacterial cells need to be separated from the extracellular polymeric substances (EPS) prior to their fixation and sectioning for further imaging with transmission electron microscope (TEM) (see section 3.1.2).

4.3.1 Glassware Cleaning

All plastic and glassware used were treated with 10% nitric acid solution and thoroughly washed three times with utra high purity water (>18 Ω cm^{-1}) to prevent contamination between samples and between successive synthesis processes. The plastic and glassware were air dried prior to their usage. Gold nanoparticles adhere to reaction vessel walls strongly, so an aqua regia (1:3 concentrated nitric to hydrochloric acid) solution was used for their removal.

4.3.2 Ultrafiltration

Ultrafiltration is a separation method that uses pressure to squeeze liquid and dissolved chemicals through a porous membrane while molecules and particles which are bigger in size than the membrane pores are retained. Since the separation is based on the pore size, it can be used to achieve a size selected separation for cleaning and further analysis purposes (Timmer

et al., 1998, Trefry et al., 2010). Among the different materials used to synthesise ultrafiltration membrane polysulphone and cellulose acetate are the most common materials (Dhawan, 2012). Ultrafiltaration process can be used to clean up and remove excess reactants and to quantify dissolution.

The ultrafiltration system used in this project is Millipore stirred ultrafiltration cells model 8400 which can filter a liquid volume of up to 400 ml. A pressurized nitrogen gas of 25psi is used to drive the liquid through a cellulose membrane with molecular weight cut off of 1kD. Samples were washed to remove gold ions by ultrafiltering 50 ml of AuNPs suspension. The volume was reduced to 25 ml and was replenished to 50 ml. This process was repeated three times with 1 hour interval between the subsequent filtration to allow the NPs to reach equilibrium. For each samples replicates of unfiltered sample for total concentration and filtrate for dissolved ions were collected and acidified with concentrated nitric acid for further analysis of gold concentration by inductively coupled plasma mass spectometry ICP-MS (see section 3.1.8). The average mean values of each replicate were reported and the gold NP concentrations were calculated by difference. The analysis was performed using an Agilent 7500 ICP-MS instrument housed in an air conditioned room.

4.4 Characterisation of the synthesised gold Nanoparticles (AuNPs)

A number of analytical and imaging techniques have been used to fully characterise the synthesised AuNPs. The following subsections will introduce how these techniques were applied and the related sample preparation steps.

4.4.1 Centrifugation and ultracentrifugation

Centrifugation technique (an Eppendorf 5804 R) was used with maxmimum speed 5000 rpm to clean samples by removing access coating agents and to achieve size based separation of the nanoparticles. It is also used to separate bacterial cells from the growth media for further analysis such as fixation and sectioning.

Ultracentrifugation technique (Beckman coulter type SW40 with average rotation axis (r_{max}) of 112.7 mm and K factor of 137) was used as preparation steps prior to the imaging of the particles with TEM (see section 3.1.2 below) and AFM (see section 3.1.3). Either mica sheet or TEM grid is immersed inside ultracentrifuge tube containing highly diluted samples followed by one hour spinning process with 30,000 rpm. This extremely high rotational speed drives all particles on the surface of the mica/grid at the bottom of the ultracentrifuge tube.

4.4.2 Imaging NPs with Transmission Electron Microscopy (TEM)

In this project JEOL1200 TEM which has a resolution of up to 0.45 nm was used to visualize both the gold nanoparticles and bacteria samples. It produces bright dark field images and the acceleration voltage of this instrument can be varied from 60 V to 120 V. for most of the samples 80 V were operated. Images were collected digitally using a Gatan Dual Vision 300W digital camera. Nanoparticles were immobilised on a 300 mesh carbon-coated copper grid by immersing the grid in diluted solutions of nanoparticles and ultracentrifuging at 150,000 g for 1 hour. Subsequently, grids were washed with water of ultra high purity and left to dry at room temperature overnight prior to TEM analysis. For the simple systems (i.e. NP suspension at low ionic strength) measured here, this preparation method was suitable,

although other methods should be used for complex samples (Domingos et al., 2009a) (Baalousha et al., 2012b, Baalousha et al., 2012a). Sections on the grid were randomly chosen and all NPs located within those sections were counted. Mean particle size, shape factor and associated standard deviations were calculated from the observation of at least 100 particles using Gatan digital micrograph software. The shape factor of particles was calculated using Equation 4-1 below.

$$F_{circ} = \frac{4\pi A}{P^2}$$ **Equation 4-1**

Where P stands for perimeter and A for the area of the particles.

Additional size measurements and energy dispersive x-ray (EDX) analysis were carried out on a JEOL 2100 analytical TEM, which has a LaB6 electron gun and can be operated between 80 and 200kV. This instrument has a resolution of 0.19nm, an electron probe size down to 0.5 nm and a maximum specimen tilt of ±10 degrees along both axes. The instrument is equipped with an Oxford Instruments LZ5 windowless energy dispersive X-ray spectrometer (EDS) controlled by INCA software for the analysis of the EDX data.

4.4.3 Topography of the NPs measured with atomic force microscopy (AFM)

In this project, XE100 (AFM) from Park System was used to image the gold nanomaterials (see section 3.1.3 for theoretical description of the AFM) adsorbed on freshly cleaved mica sheet of 1 cm^2 surface. Prior to the measurement, the mica sheet was immersed in the AuNP solution in a centrifuge tube followed by ultracentrifugation process with 30,000 rounds per minute (rpm) for 1 hr. After that, it was gently rinsed with milli-q water and air dried for further analysis. The topographical sizes of more than 100 randomly selected particles were

scanned using non-contact mode of the AFM and analysed with XIE software provided with the instrument to study the topography and the shape of the particles and to estimate their size distribution.

4.4.4 Hydrodynamic and zeta potential measurement with dynamic light scattering (DLS)

The size and the zeta potential of gold nanoparticles synthesised during this project were continuously measured using dynamic light scattering from Malvern (see section 3.1.4) (He-Ne laser Malvern High performance Particle Sizer Model NanoZS90 HPPS 5001). This instrument measures the hydrodynamic diameter of sphere which diffuses the same speed as the nanoparticles measured (Malvern, 2007). Since the diffusion rate depends not only on the core size of the particles but also any surface structures including the capping agents, the size measured with DLS will be larger than the size of the same particle measured with electron microscopy (Malvern, 2012). The measurement of the size was performed by filling a plastic disposable cuvet with the sample. It takes about 2 minutes to optimize the measurement conditions and to stabilize the temperature of the sample around 25 ^{0}C (Malvern, 2004). Five replicates were measured and their average values were reported.

Apart from the size of individual NPs and zetapotential of the particles, this instrument was used to monitor the aggregation of AuNPs in different relevant media including the growth media of the bacteria and aqueous media of different ionic strength. In the case of the nanoparticles synthesized in this project where water media is used and particles sizes in lower nanometer scale Henery's function (see section 3.1.5) is applied to calculate zeta potential from electrophoretic mobliliy measured with DLS. The nanosizer software controls the instrument and allows for analyzing the data to either drive the size or the zeta potential information of the particles.

4.4.5 Surface Plasmon Resonance (SPR)

In this project, the localised surface Plasmon resonance (see section 3.1.6 for the theory) of the freshly synthesised gold nanoparticles were recorded to study the presence of gold which has its characteristic absorption peak at around 520 nm(Daniel and Astruc, 2003, Liz-MarzÃ¡n, 2005). The stability of NPs over a long period of time in both capping agents solution (6 months) and two weeks in Minimal Davis Media -which is the growth media of bacteria- were studied by recording their LSPR spectrum. The LSPR of gold nanoparticles of different sizes has also been recorded and compared among them to study any red shift of the maximum absorbance wave length of the gold particles in the sample due to the different sizes of the particles.

The instrument used for the measurement, collection and data analysis is 6800 Uv-vis spectrometer from Jenway (Figure 4-1 below). The main parts of this instrument are light source, sample holder, monochromator to select different wavelength of light, filter, detector and output (computer). It is a double beam spectrophotometer with highly stable optics of 1.5 nm spectral bandwidth. Jenway Flight Deck software was provided with it to collect, record, and display and analyse data. Solution spectra were obtained by measuring the absorption of dilute particle suspension at a wavelength in the range 200-700 nm in a quartz cell of 1 cm path length.

Figure 4-1: Double beam 6800 Uv-vis spectrometer from Jenway *(2012)*

4.4.6 Sizes as measured with Field Flow Fractionation (FFF)

FFF was one of the size measurement techniques used in this project to measure the hydrodynamic diameter of the gold nanoparticles synthesised in this project. Separation and sizing of gold nanoparticles were performed in an asymmetrical flow field-flow fractionation (from Postnova Analytics, Germany). 2 mM $NaNO_3$ solution was freshly prepared and used as carrier solution in this analysis. UV spectrometer was used for the detection of both the polystyrene standards (at 250 nm) and the eluated AuNPs (at 520 nm). Samples were diluted several times to verify the overloading effects of the samples. At least three independent replicates were analysed per sample and the data averaged.

4.4.7 Concentration of gold with Inductively Coupled Plasma Mass Spectrometry (ICP-MS)

In this, project, an Agilent 7500 ICP-MS instrument housed in an air conditioned room was used to measure the concentration of gold in the final solution of the synthesised goldNPs. To determine thes olubility of the AuNPs, samples were ultra-filtered using regenerated cellulose membrane with nominal pore sizes of 1 kDa. 50 ml of each sample was washed three times and ultra-filtered with equal volumes of milli-Q and between the consequent washings 1hour interval was allowed to leave gold nanoparticles to reach a steady state. Replicates of both the unfiltered sample and filtrate were collected and acidified with concentrated nitric acid for further analysis of gold concentration by ICP-MS. The average mean values of each replicate were reported and the gold NP concentrations were calculated by difference.

4.4.8 Surface charge of the particles measured with potentiometric titrations method

The surface-charge of all samples was determined using Titrando 809 from Metrohm with 2 dosing 800 units for titrant delivery. The initial pH values of the NPs capped by citrate and the PVP capped NPs which are prepared through hot process were slightly acidic and the actual values lie between 4.6 and 6.2. The high pH of the PVP capped samples reduced by NaOH is obviously due to the large concentration of free hydroxide ions from NaOH in the media. Pre-measured aliquots of nanoparticle solutions were dynamically titrated with volumes of 0.1 mM NaOH solution. The volume addition (10 µL – 200 µL) depended on the rate of pH increase; a stability criterion of 0.5mV/min over 50 seconds was set. Titrations were performed up to pH10 and then back titrations using the same criteria were 0.1 M HCl to pH4. Suitable blanks (without NPs) were run and Gran method was used to find the equivalent point of the acid base titrations as explained below (see section 3.1.9 for theoretical description of the method).

4.4.9 Studying the aggregation of AuNPs in solutions of different ionic strength.

To investigate the effect of ionic strength on the size of the AuNPs, sodium nitrate solutions of different concentrations were prepared. A stock solution of 1M $NaNO_3$ was made by weighing 8.499 g and dissolving in 100 ml of Milli-Q water. From this stock solution another more diluted stock solution of 100 mM of $NaNO_3$ (stock solution 2 hereafter SS2) was prepared. After period of trial and error it was found that citrate capped and PVP capped NPs need to be test in two different ranges of $NaNO_3$ concentrations due to lack of stability of citrate capped NPs in higher ionic strength. Citrate capped NPs were tested in a range of

NaNO3 concentrations varying from 0 mM to 20 mM while PVP capped NPs were investigated in higher concentrations of NaNO3 varying from 0 to 100 mM.

4.5 Bacterial growth and media preparation techniques

4.5.1 Media Preparation

The bacteria used in this project were pseudomonas fluorescens strain SBW25 provided by Professor Christopher Thomas from school of biomedical science at the University of Birmingham. A detailed description of the pseudomonas fluorescens was given in chapter2 (research background) section 2.3.3. Section 2.4 of the same chapter introduced the current knowledge of the interaction between these bacteria and the NPs in general with emphasis for the need of further research.

Pseudomonas agar base was used to grow bacteria on agar plates. To prepare growth media for the bacteria, 39.72 g of the agar were dissolved into 800 ml of distilled water and then 8 ml of glycerol were added to the boiling agar mixture followed by 15 minutes of sterilisation at 121 ^{o}C. After cooling down to 50 ^{o}C, the agar was poured into sterile Petri dishes in the clean laminar flow cabinet and stored at 4^{o}C inside fridge. Biweekly, bacteria cells were spread on these fresh agar nutrients to keep them alive. Prior to the investigation of the effect of gold NPs on bacteria their stability in a liquid bacterial growth media need to be tested. Minimal Davis Media is used for this purpose and ingredients in the media are summarised in Table 4-2 below.

Table 4-2: Minimal Davis Media (MDM)

Substance	Mass (g/l) for 5x concentrated stock media
K_2PO_4	3.1
KH_2PO_4	0.8
$(NH_4)_2SO_4$	4.4
MgSO4	0.4
$Na_3C_6H_5O_7.2H_2O$	2.2

This solution was autoclaved and appropriate dilution was made depending on the concentration of the desired final media. Glucose was dissolved in the media and sterilised by using 0.1µm filter. The total ionic strength of the 5x concentrated stock solution of the minimal Davis media was calculated using Equation 4-2 (Solomon, 2001) and was found to have value of 191 mM.

Equation 4-2

$$I = \sum_{i}^{r} C_i Z_i$$

4.5.2 pH-measurement

The pH of the freshly synthesised NPs solutions and bacteria growth media was measured using pH meter from Thermo Electron Corporation. Prior to the actual measurement of the sample pH, The pH meter was calibrated using standard buffers 4, 7 and 10 and between each two buffers the pH sensor was thoroughly washed with milli-Q water. The sensor was

kept in the sample until stable pH reading was shown on the display of the meter and then the results were recorded.

4.5.3 Sterilisation Techniques

Sterilisation is the process through which equipments or solutions are made microorganisms free either by destroying or trapping the microorganisms to separate from solution(Moisan et al., 2002). Among the techniques employed to achieve sterilisation include heating, filtering, radiating and using chemicals depending on the nature of the materials which are to be sterilised(Mendes et al., 2007).

In this project, all glassware and other autoclavable materials were sterilised in a steam autoclave at a temperature of 121^{o}C for 15 minutes and then cooled to room temperature rapidly. During preparation of Minimal Davis Media, all inorganic salts without glucose was dissolved and steam autoclaved while glucose solution was sterilised through membrane filters of nitrocellulose with pore size 0.1µm to remove any bacterial contaminations. When bacterial cells are needed to be centrifuged out of the media, sterile plastic centrifuge tubes were used. Any handling regarding the preparation of the media and sampling of the bacterial culture for the further analysis was carried out in a clean laminar flow cabinet. The floor of the cabinet was treated with 70% ethanol-water. Inoculating metallic loops are sterilised by heating them with the roaring blue Bunsen burner flame until they glow red and all bacterial cells are destroyed.

4.5.4 Routine preparation of bacterial specimen for examination in a Transmission Electron Microscope (T.E.M.)

4.5.4.1 : Chemical Fixation

Bacterial samples were grown in MDM media for a period of 12 hrs to reach the exponential growth phase. Similar concentration of Gold NPs of different coating agents and gold ions were exposed to the bacteria for a period of 5 hrs. Bacterial samples were centrifuged (see section 4.4.1 above) and cells were chemically fixed using 2.5% of gluteraldehyde in phosphate buffer solution for 1 hour. This step was followed by secondary fixation step where the bacterial cells were transferred in 1% tetroxide and kept for another one hour

4.5.4.2 Dehydration

Bacterial cells were then dehydrated using a series of gradually increasing alcohol solutions as summarised in Table 4-3 below.

Table 4-3: Concentrations of the alcohol used for dehydration of the bacterial cells.

Percentate alcohol	Duration (minutes)	Replicates
50% Alcohol	15	Twice
70%	15	Twice
90%	15	twice
100%	15	Twice

4.5.4.3 Embedding

After treating the cells with the above mentioned series alcohol concentration, propylene oxide /resin (1:1 ratio) was prepared on a rotator in a fume cupboard for 45 minutes. The resin was left on the rotator for another one hour. Samples were then placed just under the

surface of the resin in embedding moulds and vacuum was applied for 30 minutes. The resin was then polymerised at 60 ^{o}C for 16 hours.

4.5.4.4 Ultra Thin Sections

To obtain ultra thin sections (50 – 150 µm), diamond knife was used and sections were collected on TEM grid. . Samples were then stained with uranyl acetate before examination with the TEM (see section 3.1.2).

4.5.5 Quantification of Bacterial Growth

There are different ways of quantifying bacteria growth. One traditional quantification method is the bacterial colony counting method where the number of colony of bacterial sample on agar plate is counted. Simple comparison of the number of colony in samples treated with chemicals and the number of colony of untreated sample gives information about the bacterial growth inhibition effect of the chemicals under investigation. Another Alternative, faster method for bacteria quantification is the optical density measurement technique explained below.

The growth of the bacteria in the Minimal Davis Media (MDM) was monitored continuously in the whole growth period and phases by measuring the optical density of the bacterial suspension. The more cells are in the media the more cloudy the suspension becomes and the higher the absorbance of the light is. Optical density is measured with UV_Vis (see section 3.1.6 for a detailed description of this technique) and the wave length chosen was 595 nm which is the wave length where most of the light is absorbed by pseudomonas fluorescens (Fabrega et al., 2009).

Different techniques have been applied in biological suspensions to quantify bacterial biomass in the sample. The measurement is based on chemical, photometric and/or physical variables. Of the above mentioned properties, the most implemented one is the sensors that measure the turbidity of the culture such as optical density measurements. It is an easy, fast and non-destructive method (Toennies and Gallant, 1949) for estimation of the bacterial mass in a culture. Here, the amount of light absorbed by the culture is compared to a blank sample and the difference is related to the bacterial population in the culture (Clesceri et al., 1998) Linear trapezoidal method was applied to estimate the area under the growth curve of the bacterial culture. There are three steps in this method: first the area of each trapezoid is measured using Equation 4-3.

$$A = \frac{1}{2}(O1 + O2) * (t2 - t1)$$ **Equation 4-3**

Where A is the area of each trapezoid, O1 and O2 are optical density of the culture at time t1 and t2.

Then the area of all trapezoids are added together to give estimation for the area under the curve. Finally, the percentage growth inhibition was calculated using Equation 4-4

$I = \frac{A_b - A_s}{A_b} * 100$	**Equation 4-4:**

Where I is the percentage growth inhibition, A_s is the area under the sample curve and A_b is the area under the blank curve.

4.6 Statistical analysis of the samples.

The mean and standard deviation of the measurements were calculated using Equation 4-5 and Equation 4-6 below respectively (Miller and Miller, 1993). These equations are build in function of the excel software which automatically calculated and provides the values.

$$\bar{x} = \frac{\Sigma_n X_n}{n} \qquad \textbf{Equation 4-5}$$

Where n is the number of replicates in each measurement.

$$s = \sqrt{\frac{\sum_n \left(x_n - \bar{x} \right)^2}{(n-1)}} \qquad \textbf{Equation 4-6}$$

Similarly to carry out the significance tests between sizes measured with different techniques student t-test was calculated using the following equations. First of all pooled estimate of standard deviation was calculated from the two individual standard deviations using Equation 4-7 below.

$$s^2 = \frac{\left\{(n_1 - 1)s_1^2 + (n_2 - 1)s_2^1\right\}}{(n_1 + n_2 - 2)} \qquad \textbf{Equation 4-7}$$

Then t-value is calculated using the following equation

$$t = \frac{\left(\bar{x}_1 - \bar{x}_2 \right)}{s\sqrt{(\frac{1}{n_1} + \frac{1}{n_2})}}$$

Equation 4-8

To test correlation significance between two factors, t- values were calculated using Equation 4-9 below.

$$t = \frac{r\sqrt{n-2}}{\sqrt{1-r^2}}$$

Equation 4-9

Where n-2 is the degree of freedom and r is correlation coefficient. Then tdist (t, freedom, tail) function of the excel software was used for this purpose.

Chapter 5: Synthesis and Characterisation of Gold NPs

5.1 Introduction

Synthesised NPs with known properties can give a basic platform as test materials to understand the potential fate, behaviour and biological effects of nanomaterials on organisms and in ecosystems. NPs of the same elements with different coating agents can be synthesised to study how the surface coating affects their fate and behaviour in the environmental relevant conditions. Likewise, the size, shape and the charge of the nanoparticles can be tuned to study the property - response relationship of the environmental organisms. Although it is hard to reach a clear-cut consensus on the number of parameters that should be provided in ecotoxicology studies, scientists suggested that a minimum set of parameters should include the elemental composition of the particles, as well as surface morphology , and imaging by TEM (Bucher et al., 2004). Thus, the first aim of this PhD project is to synthesise a well defined AuNPs of range of sizes and with different coating agents. After synthesis, the particles need to be fully characterised using a number of techniques and their stability will be measured and monitored. Next sections will be devoted to describe the synthesis procedures and the analysis and interpretation of the characterisation results. It will be the task of the next chapter 5 to study the interaction of these synthesised and fully characterised AuNPs with environmental relevant bacteria Pseudomonas fluorescens.

5.2 Results and discussion.

Gold nanoparticles of a range of sizes with different capping agents were prepared using three different synthesis methods as fully described in chapter 4 section 4.2 and its subsections. Special attention was devoted on the quality of the product of the synthesis methods by comparing the properties of the nanoparticles in terms of size distribution, monodispersity, solubility and sphericity of the NPs. For the characterisation of the NPs, a multi-method approach was applied(Domingos et al., 2009a, Baalousha et al., 2012a, Baalousha et al., 2012b) where different but complementing modern analytical and imaging techniques were used to collect relevant and quality physicochemical data for the NPs.

5.2.1 Synthesis and growth of AuNPs

In the present work, the synthesis of AuNPs was carried out using two different capping agents: citrate and PVP. Samples with codes G1, G2 and G3 (see Table 4-1 in chapter 4 for the experimental conditions and the concentrations of the reactants used for each sample) used trisodium citrate. When the citrate solution was added into the boiling tetrachloroauric acid solution, an instantaneous colour change was observed. Upon addition of citrate, the initial yellow gold solution turned into a colourless solution which indicates that the gold ions are reduced into neutral Au atoms (Polte et al., 2010). Then the colourless solution became blue followed by a wine-red colour within 5 minutes which remained unchanged. This red colour indicates the formation of stable gold nanoparticles (Faraday, 1857, Turkevich, 1951, Frens, 1973). In like manner, the colour change and the growth of the samples G4, G5 and G6 (see Table 4-1 in chapter 4 for description of the samples) which were reduced by NaOH and stabilised with PVP manifested the same pattern as the above explained citrate capped nanoparticles with a similar time scale. However, the colour change of the samples G7 and

G8 reduced and capped by PVP and prepared using hot process method (see Chapter 4: section 4.2.3.2) was observed after heating the solution to 70 ^{o}C and waiting about 30 minutes. The total reaction time of these last samples was 3 hours. This slow change can be associated with the weak reducing effect of the PVP. Apart from the duration of the methods, there are a number of experimental conditions between the methods which needs to be considered. High temperature of around 70^{o}C is needed for PVP hot method followed by a extensive cleaning process with water-ethanol solution (3:1 ratio) for the removal of the excess PVP. For the other two methods the synthesis was conducted at room temperature with no further washing process. Practically, PVP hot synthesis (Chapter 4: section 4.2.3.2) method lasted longer, required higher temperature, more chemicals were used for cleaning and resuspending step and the result was less monodisperse than the other two synthesis methods as can be seen in Table 5-1 below.

5.2.2 Characterisation of AuNPs

For the characterisation of synthesised NPs, their main physicochemical properties have been measured and analysed. Among the properties which have been measured are size, shape, surface plasmon, monodispersity, surface charge, dissolution and stability in different environmental relevant conditions.

5.2.2.1 Presence of gold nanoparticles

In all three different synthesis methods summarised above and described in Chapter 4: section 4.2, the colours of the solutions have changed from yellow, due to gold ions from the precursor to ruby red which is a characteristic for the formation of gold material in nanoscale (see Figure 5-1 below). In PVP cold synthesis method (see above) and in citrate method, the colour change was faster. It lasted less than 10 minutes. However, in the PVP hot method

(see Chapter 4: section 4.2.3.2) the colour change was relatively longer with duration of approximately 30 minutes.

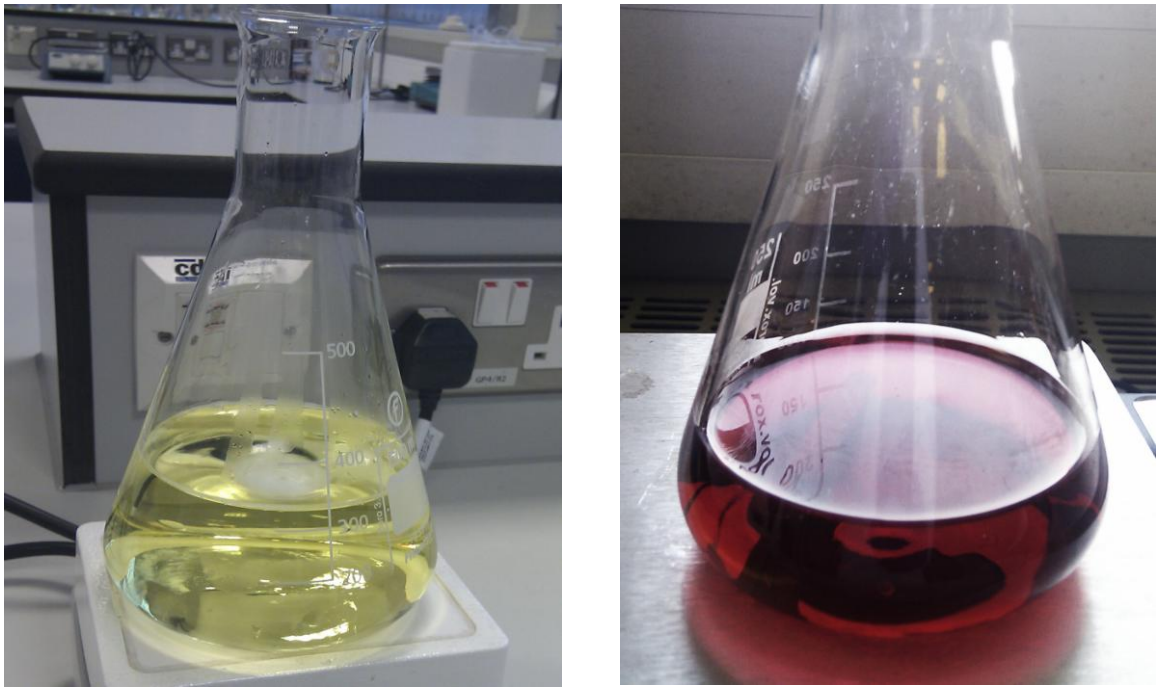

Figure 5-1: Yellow colour of the gold solution changed into ruby red during the formation of AuNPs.

The colour change manifested is caused by surface plasmon resonance (SPR) of the forming gold NPs. Therefore, the presence of gold NPs in the final suspensions was further confirmed by Uv-vis absorbance measurement which shows the NPs localised surface plasmon resonance (LSPR) behaviours. The spectra are given in Figure 5-2 and clearly indicate the characteristic sharp absorbance peak around 520 nm, which is a characteristic of gold (Daniel and Astruc, 2003, Liz-MarzÃ¡n, 2005). The narrow peak and absence of other peaks above 550 nm indicates the monodispersity of the particles.

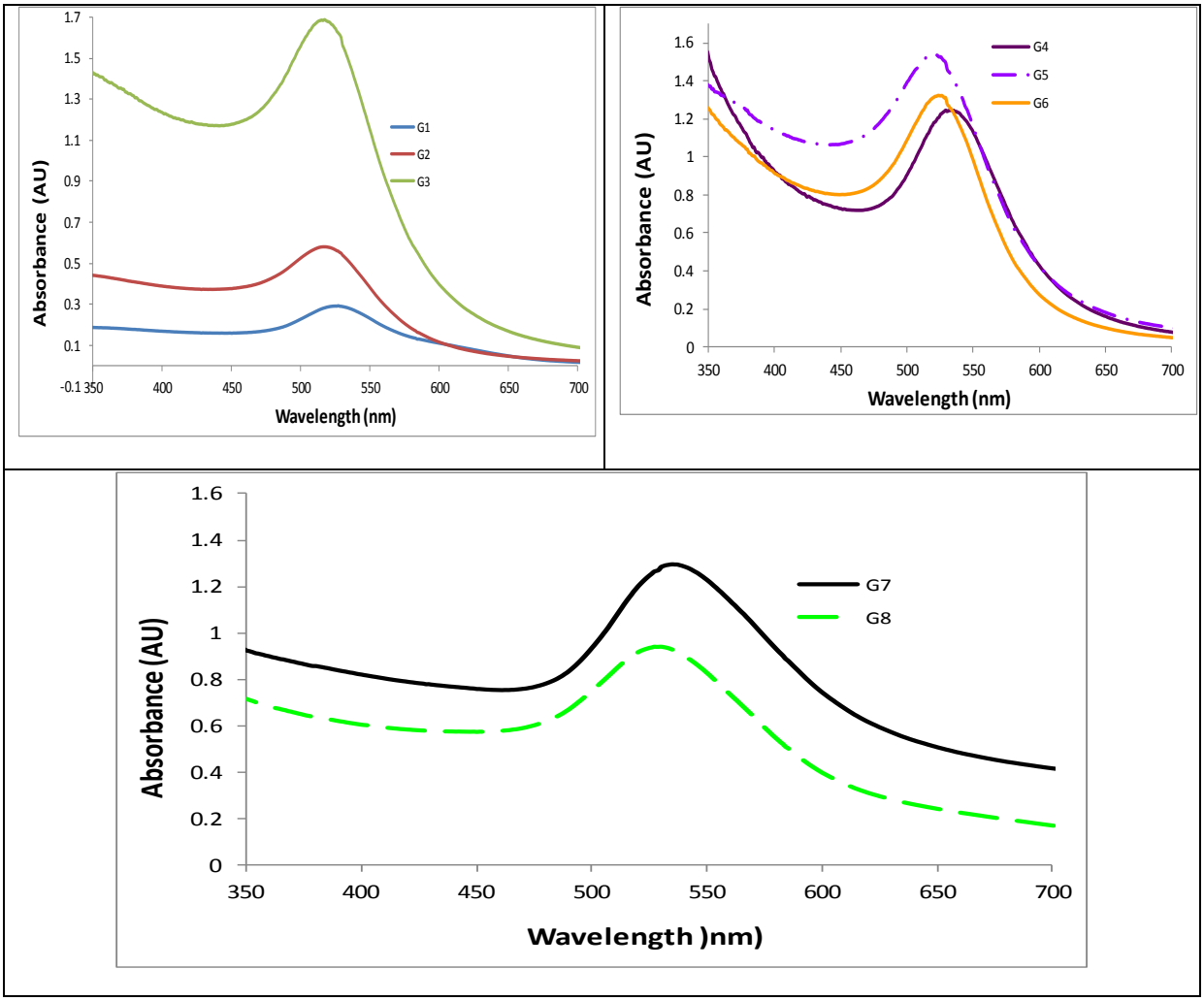

Figure 5-2: The surface plasmon resonance (SPR) of freshly prepared AuNPs and the maximum absorption takes place around 520 nm.

5.2.2.2 Size and size distribution

The size and size distribution of the NPs have been studied using a number of different but complementary imaging and size measurements techniques. Among the techniques used for the size measurements include dynamic light scattering (DLS), field flow fractionation (FFF), transmission electron microscope (TEM), atomic force microscope (AFM) and ultraviolet visible spectroscopy (Uv-vis). Detailed description of the practical application and the theoretical background of each technique were given in sections 4.4 and Chapter 3: of the

previous chapters. Results and measurements from these techniques are summarised in the following subsections.

5.2.2.2.1 DLS and FFF measured hydrodynamic sizes

DLS and FFF were used to quantify the hydrodynamic diameter which is the core size of the particles plus the size of the coating agents. For the samples measured, the sizes from the two techniques were fairly comparable as can be seen in Table 5-1.The hydrodynamic z-average values, measured with DLS, of samples vary from 11.55 nm to 41.77 nm for citrate stabilised samples and from 22.60 nm to 102 nm for PVP stabilised samples. All DLS data plus standard deviations of the measurement were recorded in Table 5-1. DLS diagrams are presented in Figure 5-4 and it shows that samples synthesized have different sizes. Figure 5-4 also shows that most of the samples are monomodal in distribution except the samples synthesised through PVP hot method which shows two distinct peaks for both measured samples (G7 and G8). Figure 5-3 represents the FFF raw data of the three standards showing their relative elution times and the UV_vis detector signal by 254 nm wavelength.

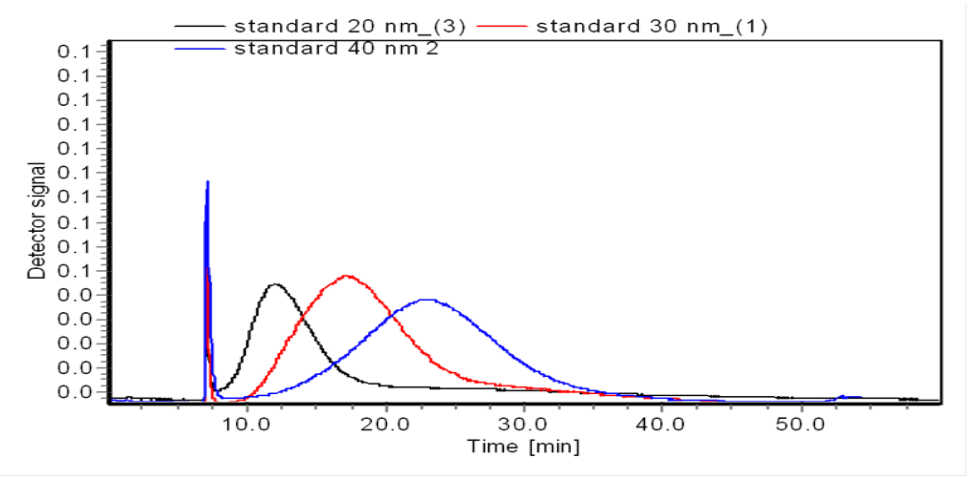

Figure 5-3: Raw data of the three standards as measured with FFF. The bigger the size of the nanoparticles the longer it takes for NPs to get eluted through the FFF column.

The sizes of the samples measured with FFFF show similar range as the DLS size. G2 has DLS z-average size of 18.2 ± 0.4 nm and FFF measured size of 16.0 ± 5.0 nm. Similarly the

G5 has Z-average of 22.6 ± 0.7 nm and FFF size of 19.5 ± 7.5.nm. These data show that the difference between the sizes measured with DLS and FFF is in the margin of error. For sample G2, T-experimental (1.27 calculated from the samples means and the standard deviation) is smaller than T-critical 2.45 (degree of freedom 11) and for sample G5, T-experiemtal is 1.18 < than T-critical 2.45. Thus they are not significantly different.

G1

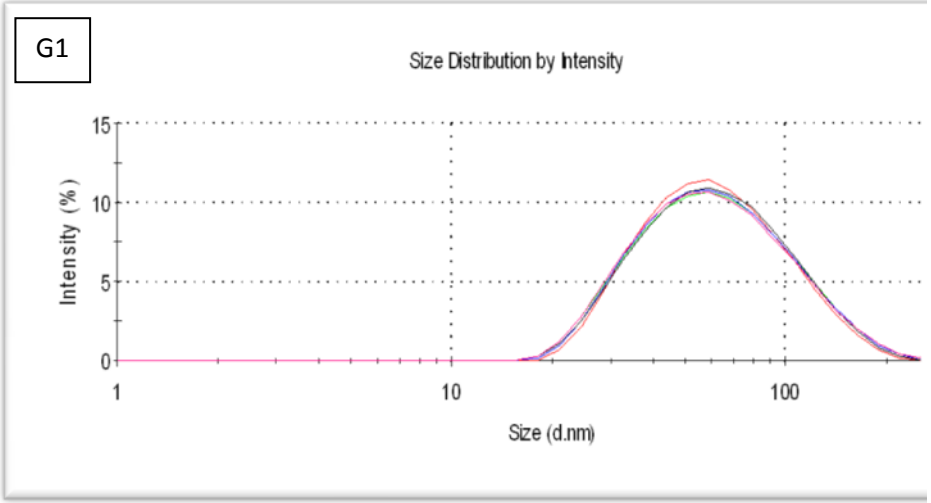
Size Distribution by Intensity
Intensity (%)
15
10
5
0
1
10
100
Size (d.nm)

G4

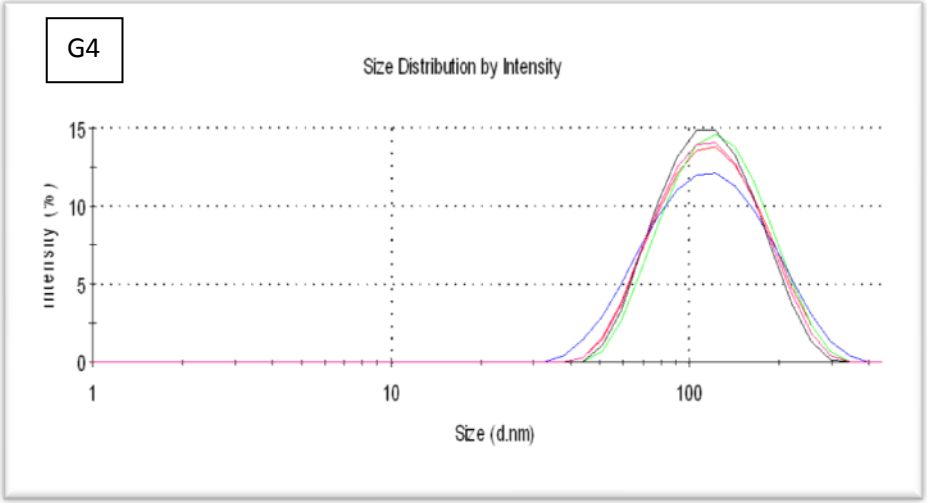
Size Distribution by Intensity
15
10
5
0
1
10
100
Size (d.nm)

G2

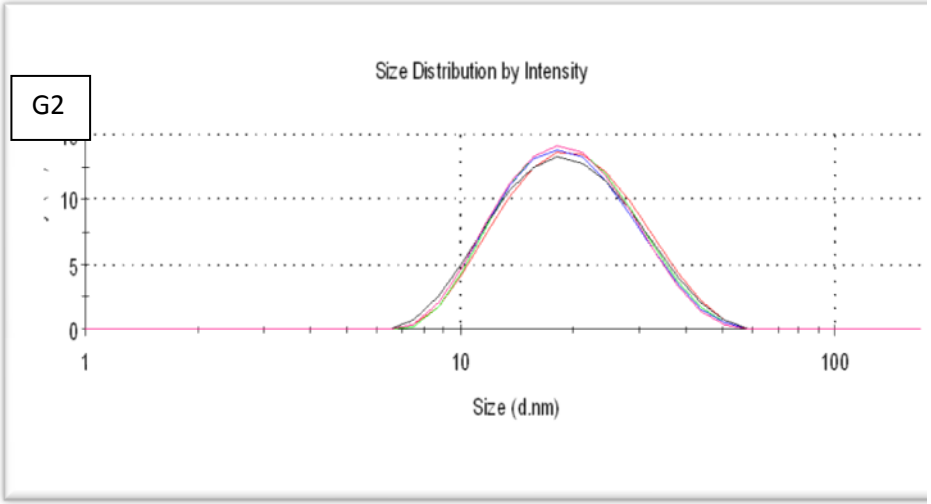
Size Distribution by Intensity
10
5
0
1
10
100
Size (d.nm)

G6

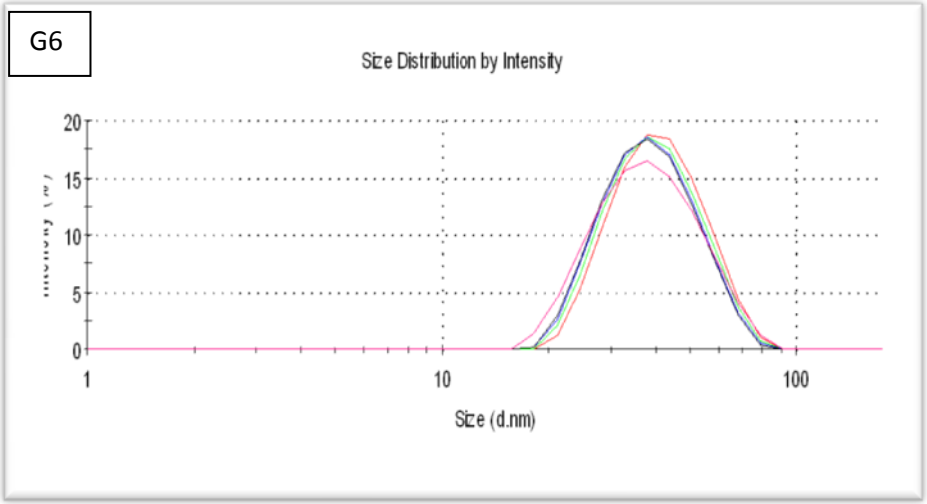
Size Distribution by Intensity
20
15
10
5
0
1
10
100
Size (d.nm)

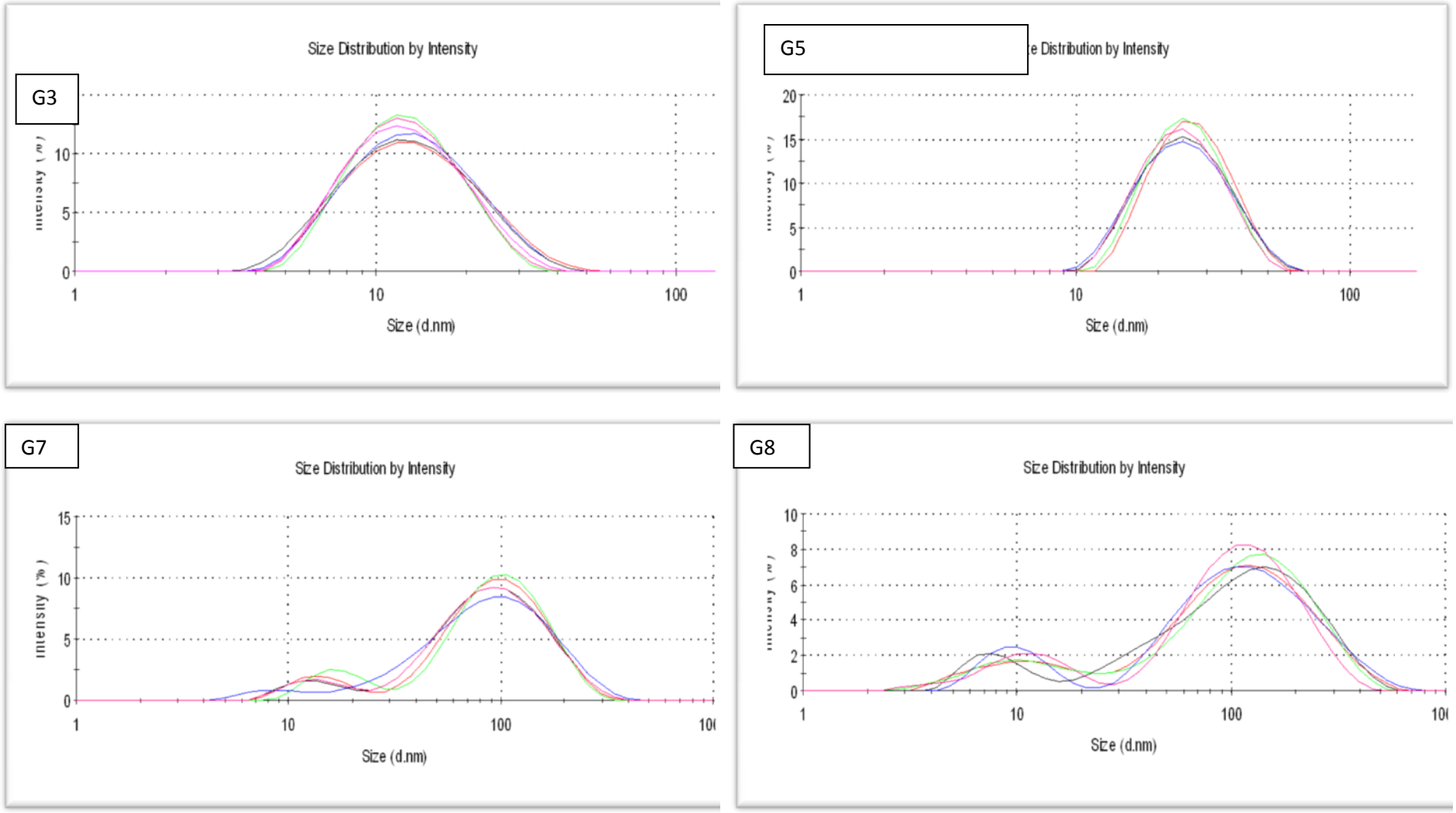

Figure 5-4: DLS diagrams of eight samples illustrating the sizes of the particles. Samples G1.G2 and G3 are stabilised by citrate, samples G4, G5, and G6 are reduced by NaOH and stabilised by PVP while samples G7 and G8 are stabilised PVP. The peaks around 100 nm for the last two samples are big gold particles which shows that the last two samples are clearly more polydispersity than the other samples.

5.2.2.2.2 Colour change analysis.

Synthesised particles demonstrated colours varying from red for smaller particles to purple for larger particles as shown in Figure 5-5. The reason why NPs have different colours can be attributed to the fact that smaller particles (<30 nm) absorb the blue section of the white light spectrum and reflect the red portion which is responsible for their red colour. On the other hand the larger particles due to their size, absorb larger wavelength in the red portion of the spectrum and reflect the blue section which explains why they have purple/blue colour. This property can be used to study the kinetics of size changes phenomena such as agglomeration and aggregation of the particles (de la Rica et al., 2012, Hayden et al., 2012).

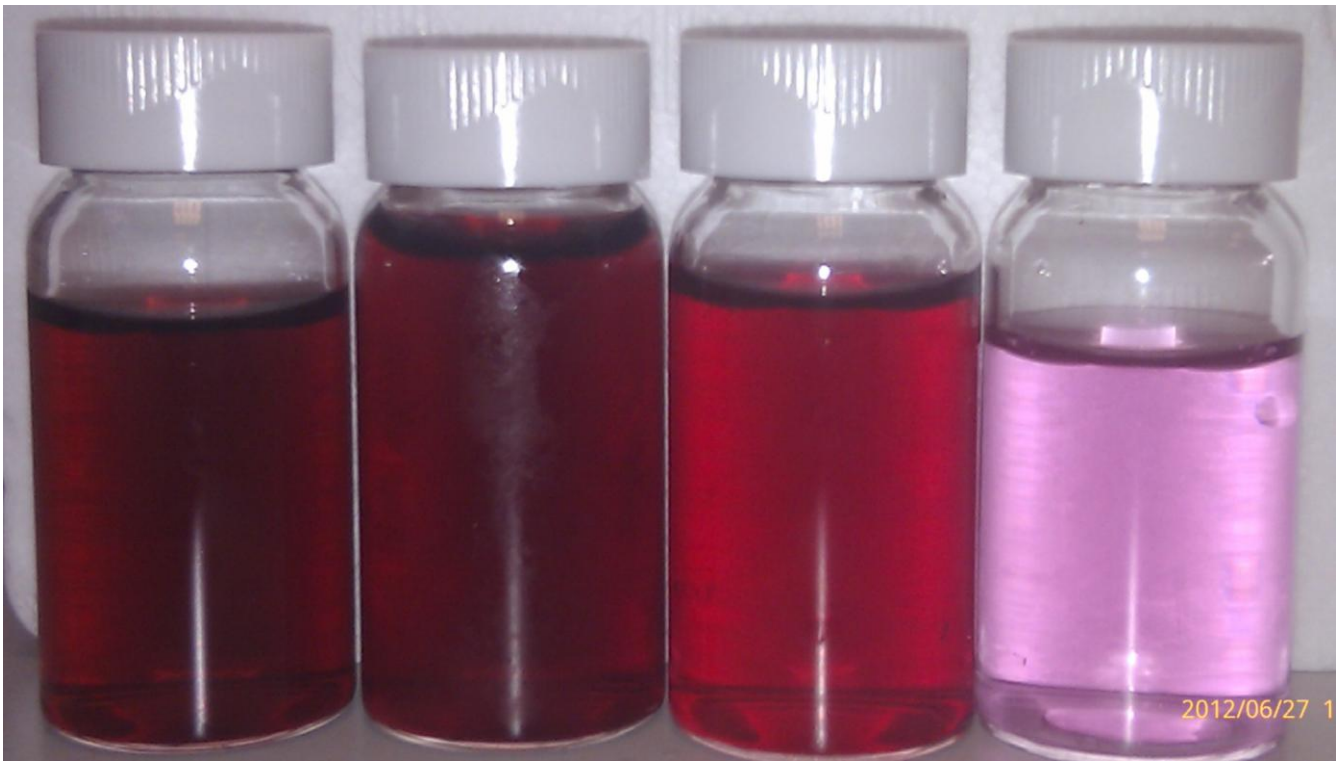

Figure 5-5: Freshly synthesised AuNPs of different sizes. Ruby red colour at the left is for smaller (around 10 nm) AuNPs while the purple colour at the right is manifested by bigger particles (around 45 nm hydrodynamic size).

For further analysis of the particles with different sizes, their surface Plasmon resonance (SPR) properties were recorded and compared among them using modern double beam Uv_vis spectrophotometer technique. As explained in Chapter 4: section 4.4.5 of the materials and

methodology the SPR is the effect of the interaction between the oscillating magnetic/electric fields of the electromagnetic waves including visible light and the delocalised surface electrons of the metallic nanoparticles. The position of the maximum absorbance measured with Uv-vis depends on a number of factors including the shape, the dialectric constant, the surrounding media and the size of the nanoparticle s(Eustis and El-Sayed, 2006).

SPR spectra of AuNPs with range of sizes were recorded and presented in Figure 5-6 a below. Then the hydrodynamice diameters measured with DLS were plotted against the wavelengths corresponding to the maximum absorbance of each particle size and illustrated in Figure 5-6 b below. There is understandable positive correlation between the two variables: the size and the wavelength of the maximum absorbance, with regression constant ($R^2 = 0.94$). Here, Uv-vis data has supported the fact that the synthesised gold nanoparticles have a range of different sizes. It can be clearly seen that the particles with bigger sizes have their maximum absorbance at a relatively higher wavelength toward the red section of the visible light spectrum. The wavelength of the maximum absorbencies of the NPs varied from 517 nm to 529 nm when the z-average values size of the hydrodynamic diameter of particles measured with the DLS varied from 11 nm to 92 nm as can be seen in Figure 5-6 below.

To test the significant of the correlation, t-value was calculation using equation Equation 4-8 in section 4.6 Chapter 4:.

Then tdist(t,freedom,tail) function of the excel software was used to calculate probability value of 4.5E0-^{8} which much smaller than 95% significance value of 0.05. Thus the correlation is not-significant.

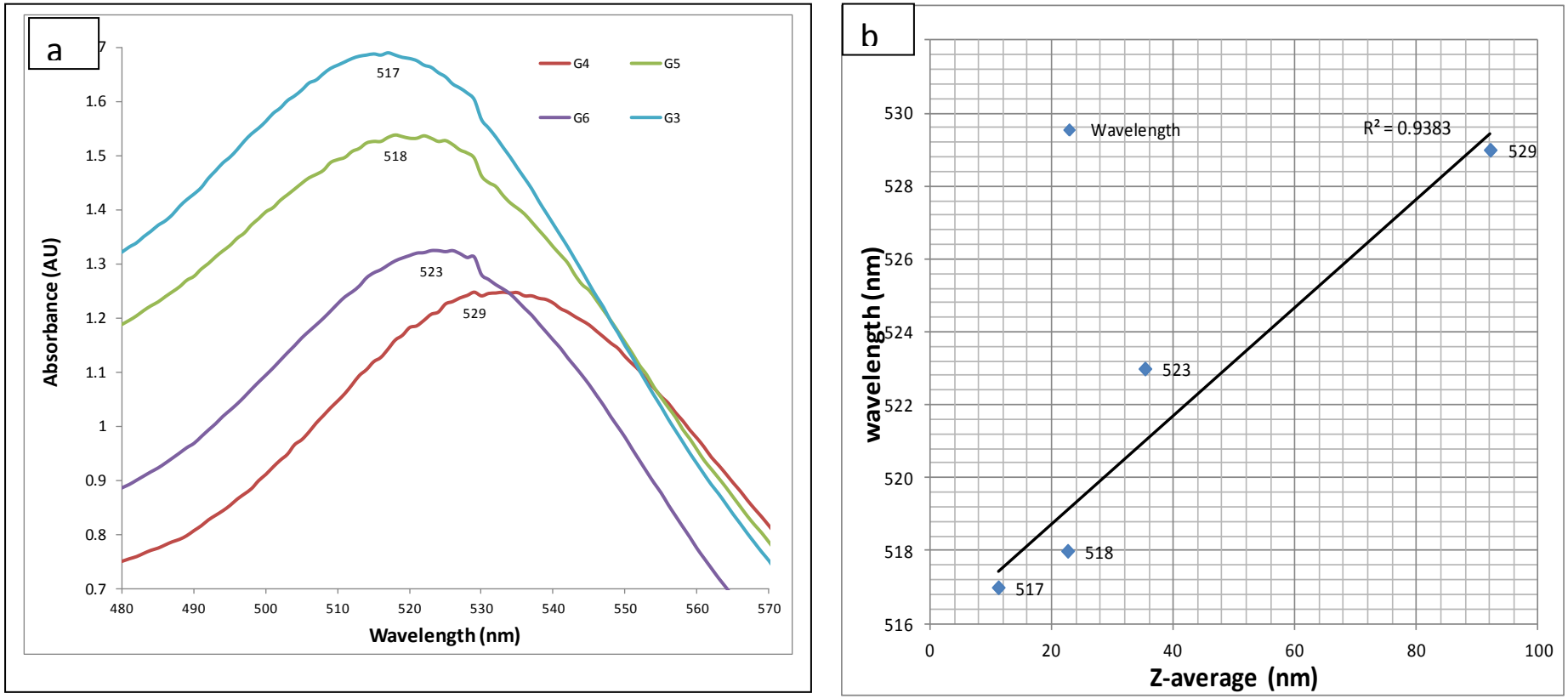

Figure 5-6: Graph showing the relationship between the size and the SPR maximum. The bigger the size of the particles the higher the wave length of the maximum absorption Part a) illustrates the red shift of the maximum SPR due to the increasing size. Part b) presents the positive correlation between z-average and the SPR maximum.

5.2.2.2.3 TEM and AFM measured core sizes.

TEM micrographs of the synthesised particles were measured using TEM jeol1200 (see Chapter 4: section 4.4.2 for the imaging procedure plus sample preparation methods and section 3.1.2 for theoretical background of the TEM technique) and the microgarphs of representative samples are presented in Figure 5-7 for citrate and Figure 5-8 for PVP capped gold samples. Size distributions histograms of the different types of the synthesised gold nanoparticles were also calculated and shown in these graphs. Variations in size were achieved with varying the initial molar ratio between the tetrachloroauric acid and the capping agents (citrate and PVP) (Frens, 1973) (see Table 4-1 in Chapter 4: for the experimental condition and the concentration of the reactants used for the synthesis of the particles).

The average core sizes of citrate capped particles from a minimum number of 100 particles were found to be in the range 7.1 nm to 32.6 nm while PVP-coated particles (minimum 100 particles) have core sizes varying 11.4 nm to around 85 nm (see details with standard deviation in Table 5-1).

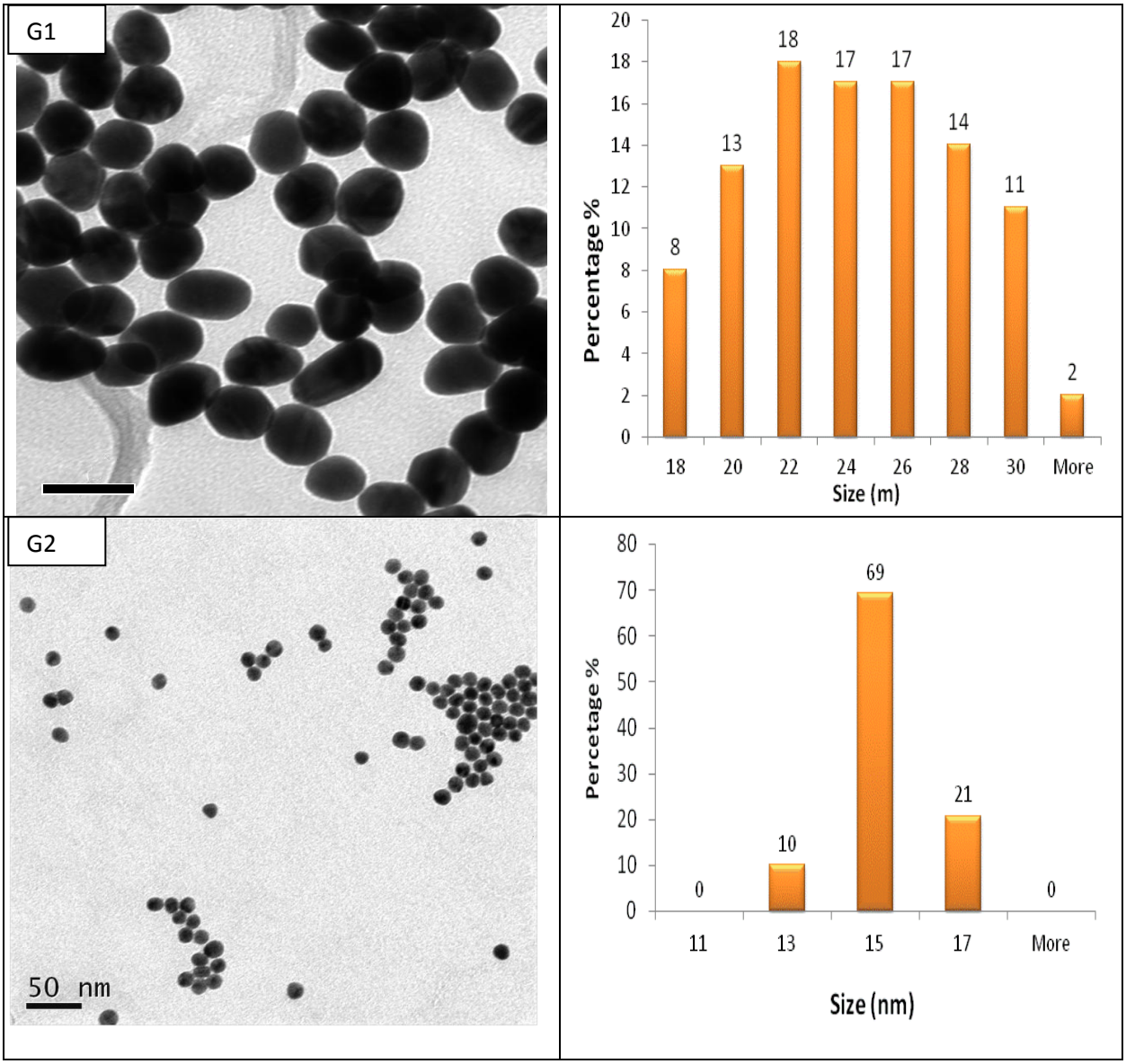

Figure 5-7: TEM images and size distribution histograms of citrate capped AuNPS of two sizes of AuNPs. G1 particles are clearly bigger in size than in G2. See full description of the nanoparticles in Table 5-1.

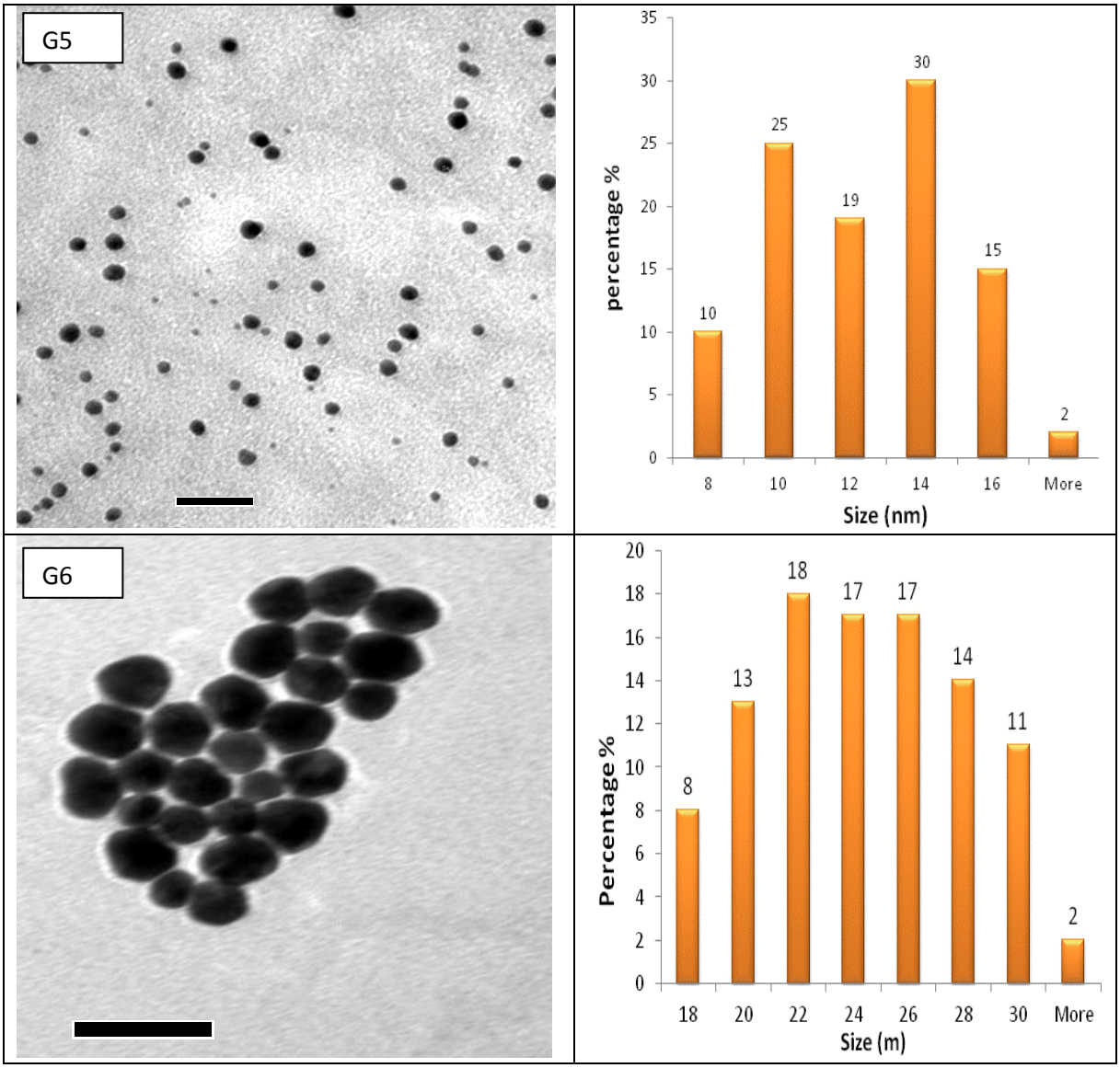

Figure 5-8: TEM images and size distribution histograms of cold method prepared PVP capped AuNPs of different sizes. Right-hand side of the figure is presented with excel calculated size distribution of the particles,

For further analysis of the size of the synthesised gold nanoparticles, samples were immobilised on mica sheet (see section 4.4.3 of Chapter 4: for details of procedures) and AFM topographs were recorded using noncontact mode of the AFM. Average diameter and size distributions of the particles were calculated and illustrated in Figure 5-9 below and recorded in Table 5-1.

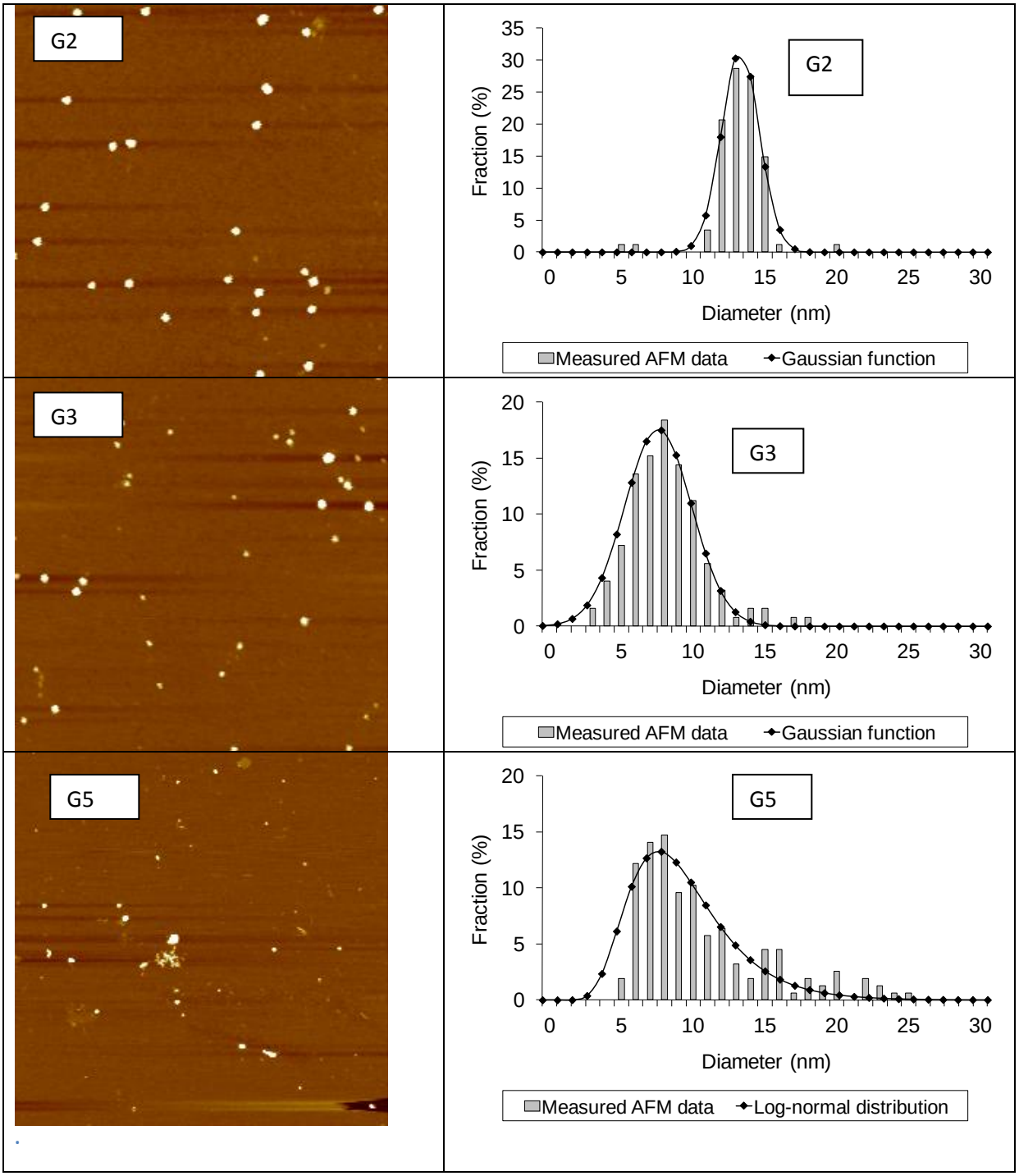

Figure 5-9:Topographs of three different particles as measured with AFM and the corresponding size distribution. AFM images courtesy Dr Mohamed Baalousha.

5.2.2.2.4 Comparison of the sizes measured with different techniques

The size measurements results of the abovementioned techniques were summarised in Table 5-1 below. In addition to the size data, the table gives standard deviation values and other relevant technique specific parameters such as polydispersity index (PDI) for DLS data.

Table 5-1: Hydrodynamic diameters and core sizes of AuNPs as measured with different techniques.

Sample Code	TEM (nm)	AFM (nm)	DLS (nm)	FFF (nm)	DLS-TEM	DLS/TEM	Shape factor
G1	32.6 ± 6.5		41.77± 0.74 (PDI = 0.28)		9.18	1.3	0.84 ± 0.07
G2	14.2 ± 1.0	13.3 ± 1.3	18.27 ± 0.36 (PDI = 0.19)	16.0 ± 5.0	4.07	1.3	0.92 ± 0.05
G3	7.1±2.4	7.1±2.3	11.55 ± 0.42 (PDI = 0.20)	11.8±4.4			0.89±0.05
G4	±		102.00 ±0.17 (PDI = 0.19)				
G5	11.4 ± 2.8	9.5 ± 3.5	22.60 ± 0.70 (PDI = 0.14)	19.5 ± 7.5	11.2	2.0	0.87 ± 0.09
G6	23.3 ± 3.8		35.31 ± 1.02 (PDI = 0.13)		12.01	1.5	0.89 ±0.05
G7	11.6±2.7	-	60.4±0.2 (PDI=0.43)		48.8	5.2	0.80±0.014
G8	7.3+2.2		37.8±0.4 (PDI±0.54)		30.5	5.2	

The data in Table 5-1 shows that the DLS-measured Z-average hydrodynamic diameters of the synthesized particles are always larger than the sizes obtained by TEM and AFM analysis and are fairly comparable with FFF data which also gives a measurement of hydrodynamic diameter calculated from the diffusion coefficient of the particles. To see whether the abovementioned difference is significant, student ttest (P = 0.05) was conducted and the results for citrate capped samples and PVP capped samples were summarised in the following Table 5-2 below. The averages

of DLS measurements were calculated from only 5 replicates while the TEM averages were calculated from at least 100 particles. To find the value of T-critical from statistical tables, the size of the smaller DLS replicates (5 replicates) were used. For nearly all samples analysed t-experimental were larger than the t-critical which means that the difference is significant. This difference between DLS and FFF on one hand and TEM and AFM on the other hand, can be caused by the combination effect of a number of factors including the degree of polydispersity of the particles and type and size of the coating agents. In the sense that the higher the polydispersity the higher the difference between the DLS and TEM/AFM sizes. Regarding coating agents, the organic stabilizer in this case citrate and PVP is transparent to electrons, so TEM gives the size of only more electron dense metallic core of the particles, whereas DLS measures the hydrodynamic diameter of the gold NP calculated from the diffusion coefficient. The DLS size, therefore, includes the core, the capping agent and any associated water (Diegoli et al., 2008). Another important point is that the difference between DLS and TEM is always higher for the PVP stabilised samples than the citrate stabilised samples (see Table 5-1). This is due to the fact that PVP is a long chain polymer while citrate is a much shorter molecule.

Table 5-2: Significant test data for the size difference between TEM core sizes and DLS hydrodynamic diameters.

Sample code	Capping agent	T-experimental	T-critical (degrees of freedom)	Null hypotheis:No difference between sizes measured TEM and DLS
G1	Citrate	5.70	2.78	T-exp > Tcrit = rejected
G2	Citrate	2.50	2.78	T-exp < Tcrit = accepted
G3	Citrate	1.85834	2.78	T-exp <Tcrit = accepted
G5	PVP	4.677171	2.78	T-exp > Tcrit = rejected
G6	PVP	7.524014	2.78	T-exp > Tcrit = rejected

5.2.2.3 Shape of the AuNPs

TEM and AFM images of the freshly synthesised NPs presented in Figure 5-7 and Figure 5-8 above respectively have clearly manifested the spherical shapes of the synthesised nanoparticles. The images clearly show the presence of individual spherical particles in the samples. Quantification of the shapes of the all particles was attempted by calculating their shape factors using Equation 4-1 in Chapter 4: materials and methodology. This equation gives information about the sphericity of the particles. Perfect spherical particles will have shape factor values of 1 while other particles will have values less than 1. The nearer the value to 1 the more round the particle is.

The calculated shape factor values of the synthesised particles were near 1 and higher than 0.8 for all samples as listed in the result Table 5-1 above. Figure 5-10 presents the shapes of the typical PVP capped AuNPs. It is clear from these images that the synthesised AuNPs are of high quality, monodisperse and spherical in shape. This monodispersity in shape of the nanoparticles is an essential for the interpretation, analysis and comparison of any effect-property data caused by another property of the particles such as size, surface charge,etc.

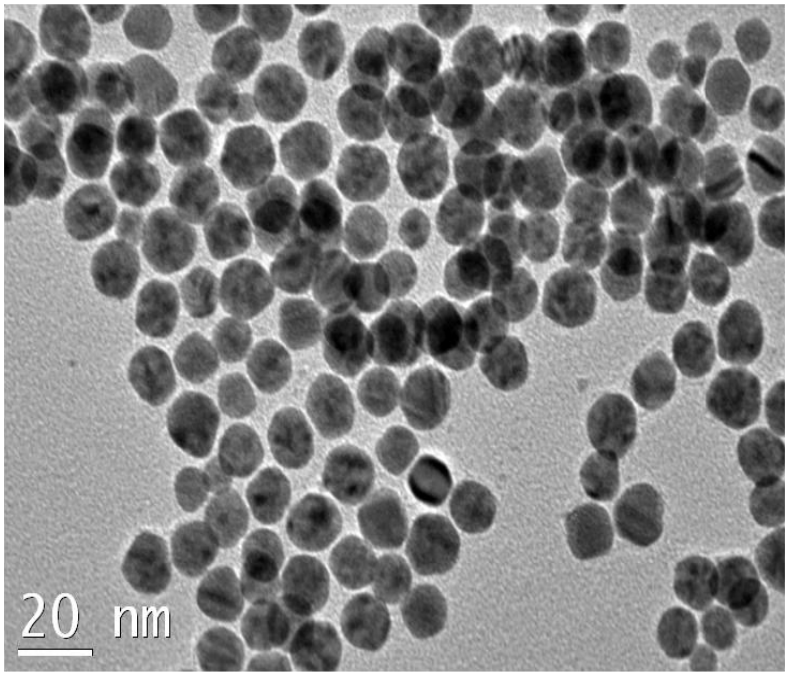

Figure 5-10: Typical TEM images of freshly synthesised gold nanoparticles showing highly spherical monodisperse AuNPs. The particles have an average core size of 10 nm.

For the quantification of the shapes of the synthesised gold nanoparticles, from each sample at least 100 particles were randomly chosen throughout the surface of the TEM copper grid and shape factor distribution diagrams of the particles were plotted and illustrated in Figure 5-11 below. It can be seen from the shape factor distribution diagrams that for all samples 95% of the particles have a shape factor value better than 0.8 which clearly confirms the sphericity of the synthesised AuNPs since this value is not far from the perfect sphere shape factor which is 1.

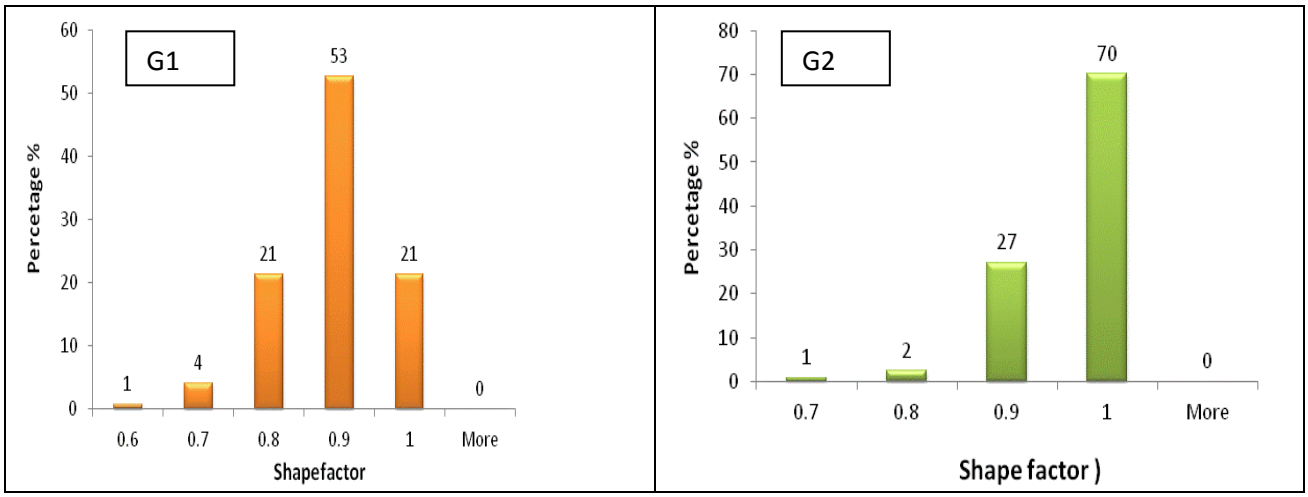

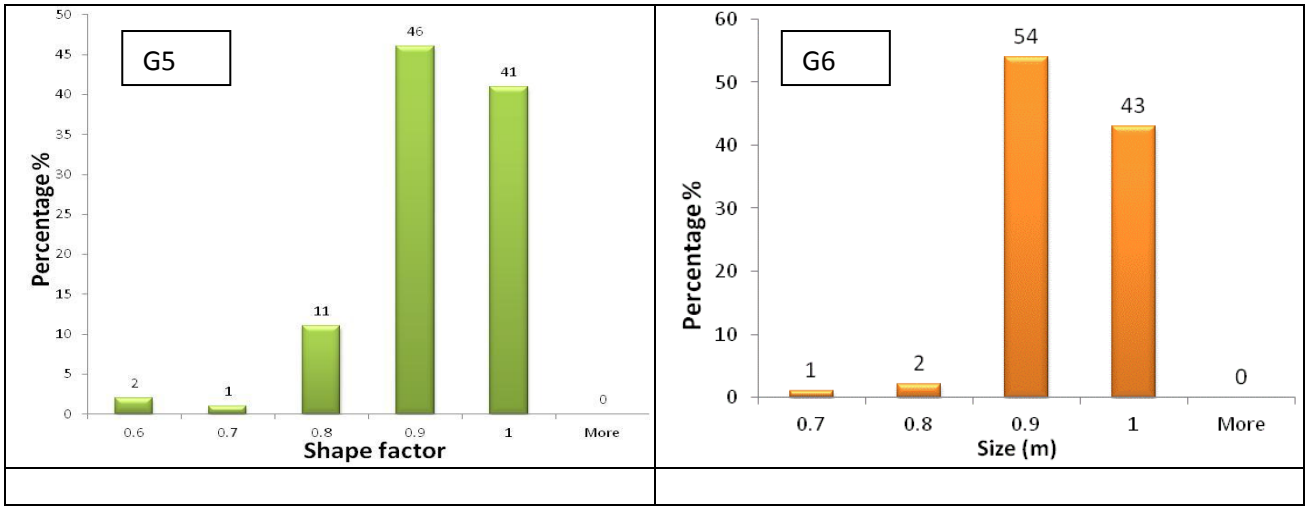

Figure 5-11: Shape factor distribution diagrams of AuNPs calculated from TEM images. G1 and G2 are coated by citrate. G5 and G6 are coated by PVP polymer. Relevant physicochemical properties of the NPs presented in this graph are summarised in table 5.1 above.

5.2.2.4 Surface chemistry

Surface chemistry of NPs is mainly determined by the type of coating agents stabilised with the NPs. Coating agents can have effect on a number of measureable surface properties of NPs such as pH, zeta potential and surface charge. The surface charge of the particles may arbitrate either attraction or repulsion between NPs and other components in the relevant media such as environmental present chemicals, organic materials and organisms. Steric polymerisation may on the other hand affect drastically the size of the coated particles and subsequent transport in the environment. Therefore, surface chemistry is a key property for the ultimate fate and behaviour of the NPs in the environmental relevant conditions including ionic strength, amount of naturally occurring organic matters and microorganisms. For the sake of identifying the surface properties of the NPs, pH, zeta potential and surface charge of the synthesised NPs were measured and presented in the result Table 5-3 below.

Table 5-3: Surface chemistry properties of freshly synthesised AuNPs with different coating agents in terms of surface charge, pH and zeta potential.

Sample code	Zeta potential (mV)	Surface Charge (c/g)	pH
G1	-52.5 ±1.05		6.24
G2	-46.6 ± 2.4	-2180	6.27
G3	-26.0 ± 3.37	-2662	6.43
G4	-20.1 ± 0.0	-	7.45
G5	-19.1 ± 5.0	-	7.53
G6	-18.1 ±0.5	-	7.39
G7	-15.9 ±0.6	-459	4.76
G8	-20.4 ± 1.3	-730	5.23

Zeta potential is a measurement of the overall charge of the particles in media and it indicates the stability of the particles in the sense that the higher the zeta potential the more stable the particles are. It is calculated from electrophoretic mobility of the particles in an applied electric field. From the zeta potential data in Table 5-3 can be seen that the citrate capped particles have higher values of the zeta potential than the PVP capped NPs. Among the PVP stabilised particles, their zeta potential are the same magnitude regardless of the synthesis method (hot or cold) used during the synthesis of the particles which indicates that the zeta potential is mainly determined by the surface coating. The pH of citrate capped NPs are around 6 while the PVP capped samples which were reduced by NaOH have apparently high pH. This can be associated with the fact that NaOH is strong alkaline and thus it raises the pH of the solution.

5.2.2.5 Dissolved and nanoparticles fractions of gold

The synthesis process of the nanoparticles begins with the reduction of gold ions into gold atoms. To quantify the fraction of gold ions which is changed into NPs and the dissolved fraction, the concentrations of both total gold and dissolved gold have been measured using ICP-MS. The

amount of gold atoms that had been changed into nanoparticles was obtained by the difference between total and dissolved fraction of gold. Table 5-4 shows that the percentage dissolved was less than 2.5% for all samples. In addition to that, it demonstrates that there are relatively more dissolved gold ions in the case of the PVP capped samples than the citrate capped particles.

Table 5-4: Concentration of the total and dissolved gold in the samples as prepared and measured with ICP-MS.

Sample Code	Total gold(ppm)	Dissolved gold (ppb)	% dissolved	NPs gold (obtained by difference)
G1	11.07	52.00	0.47%	11.02
G2	22.27	54.50	0.24%	22.21
G3	89.55	43.75	0.05%	89.51
G4	107.10	260.75	0.24%	106.84
G5	105.95	2595.00	2.45%	103.36
G6	93.7	2118.00	2.26%	91.58
G7	106.2	811.00	0.76%	105.39
G8	66.8	243.00	0.36%	66.56

5.2.3 Stability of the AuNPs

Nanoparticles prepared through chemical reaction where metallic ions are reduced to atoms need to be stabilised by suitable coating agents. Lack of appropriate stabilising agents will cause continuous growth of the particles and subsequent aggregation of the NPs. The stability of the synthesised gold nanoparticles has been monitored. The z-average of the hydrodynamic diameter of the NPs was measured using DLS for a period of six months and results are presented in Figure 5-12 below. The three measurements did not reveal any significant size variations in the period studied).

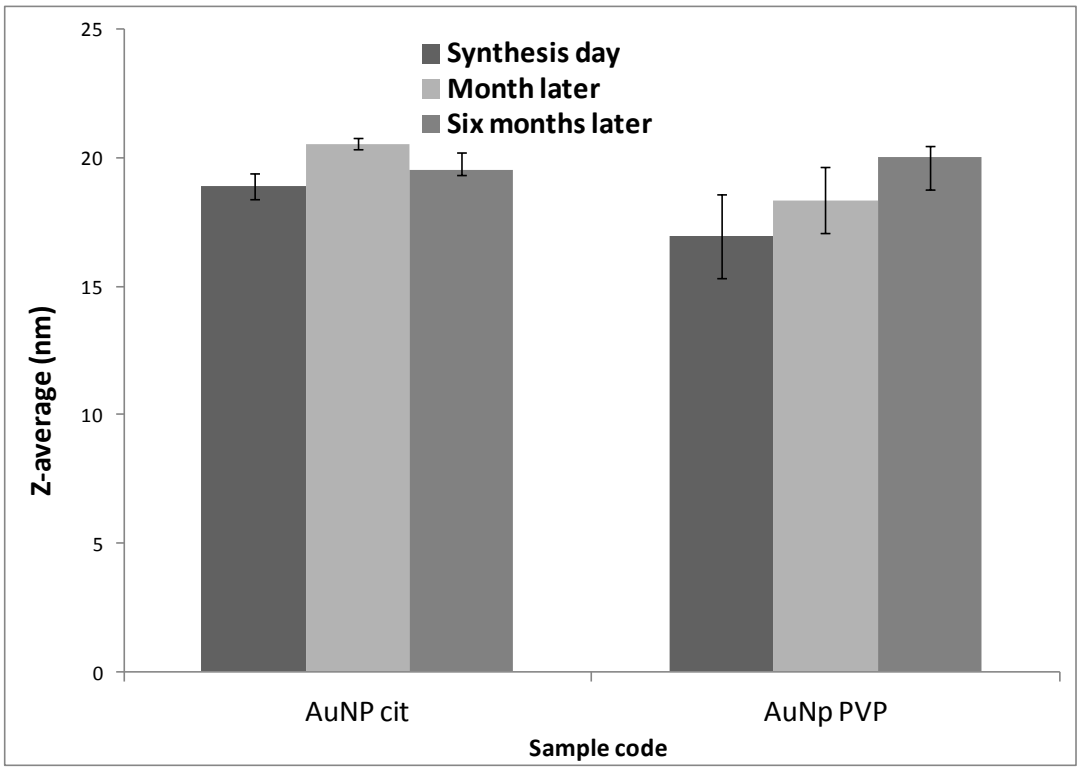

Figure 5-12: Stability of two samples of AuNPs coated with either citrate or PVP is monitored over a period of six months from the synthesis date.

The surface Plasmon resonance (SPR) of the samples was also recorded for a period of six months using Uv-vis spectrophotometer. The results presented in Figure 5-13 showed consistency of the absorption peak in that period and did not reveal any significant change in size which would be manifested as red shift in the six months period of study (see Figure 5-13).

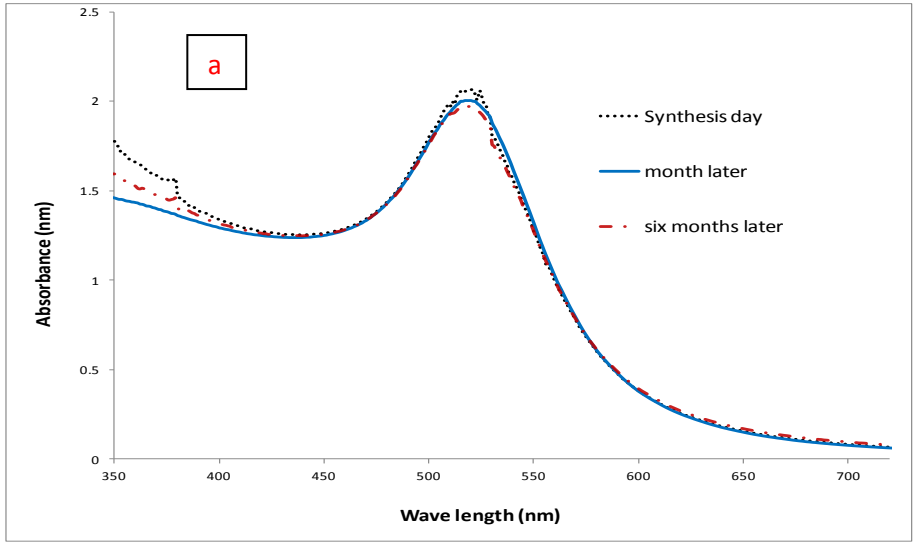

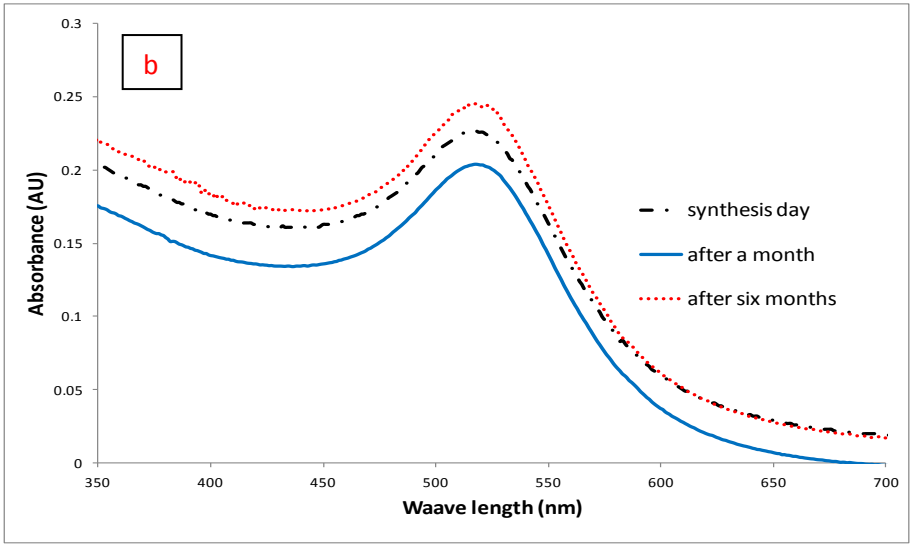

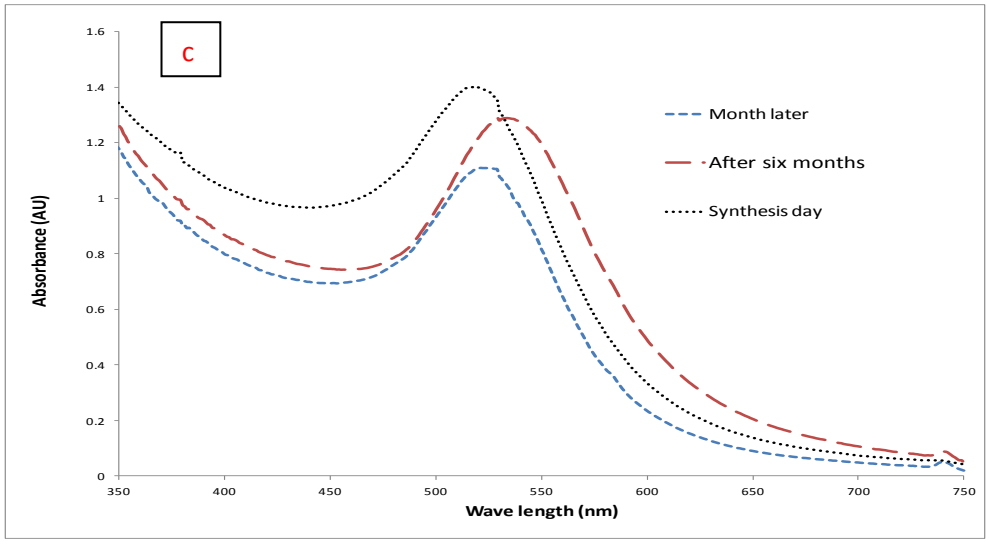

Figure 5-13: SPR spectra showing the stability of AuNP over a period of 6 months a) citrate stabilised NPs b) is stabilised with PVP and prepared through cold method as explained in section 4.2.3.1 and c) are samples prepared through hot method (see section 4.2.3.2) and stabilised by the PVP.

5.2.4 Effect of ionic strength on the stability of the NPs

Apart from the stability of the NPs over time, the effect of the ionic strength of the media on the size of both citrates capped and PVP capped NPs were investigated. Testing NPs in a range of ionic strength is essential for the understanding of the behaviour of the NPs in the environment since environmental relevant conditions may vary in ionic strength. For instance fresh surface water normally contains low concentration of dissolved ions while seawater has relatively higher ionic strength. The variation of the particles sizes as function of the ionic strength was illustrated in Figure 5-14 below. As manifested by the steep gradient of the graph in Figure 5-14 a citrate capped particles are more vulnerable to the ionic strength than the PVP capped ones.

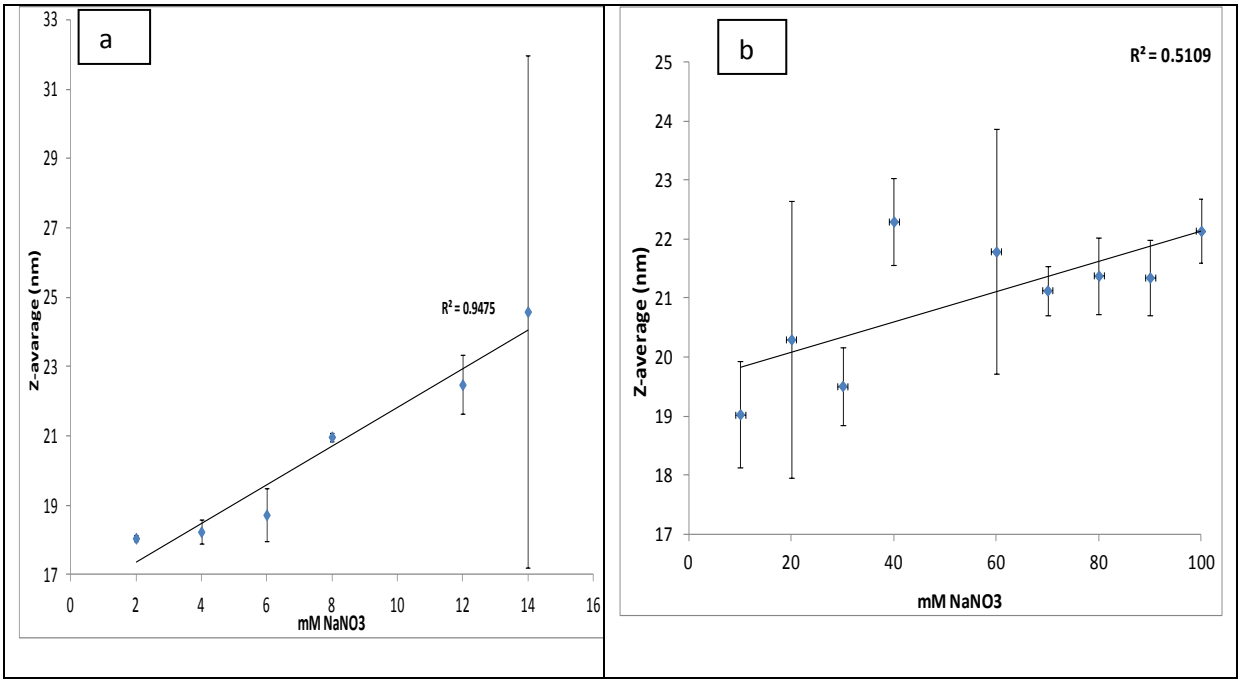

Figure 5-14: The correlation curve of the z-average values of citrate capped NPs and the ionic strength of the media. The media used for this purpose was monovalent electrolyte which is $NaNO_3$. Section a represents citrate capped NP. Section b is PVP capped NP.

The increase in size of the nanoparticles indicates the formation of aggregates in the media. It is worth noting that the PVP coated NPs were tested in ionic strength as high as 100 mM and the increase in size is insignificant since the difference between the sizes is in the error

margin (see Figure 5-14 b above). DLS diagram given in Figure 5-15 below shows the aggregation of the citrate particles caused by ionic strength.

Recently published data has investigated the effect of a) single monovalent and divalent elctrolytes of cations, b) a mixture of electrolytes and c) the anions on aggregation of citrate capped AgNPs Nanoparticles (Baalousha et al., 2013). This research has compared the effect of the above mentions electrolytes and concluded that divalent cations ($Ca(SO_4)$, $Ca(NO_3)_2$, $MgCl_2$ and $MgSO_4$ have stronger influence on aggregation as compared to monvalent cations NaCl, $NaNO_3$, Na_2SO_4. Regarding to the anions, sulphates and nitrates did not manifest any specific ion effect while the addition of chloride ions has enhanced the aggreagation of the NPs. Similarly, El Badawy et al have investigated the effect of monovalent cations $NaNO_3$ and divalent cations $Ca(NO_3)_2$ on Silver nanoparticles of different coating agents (Badawy et al., 2010). Naked silver NPs, Citrate capped silver NPs and Borate capped silver NPs have aggregated at higher ionic strength (100 mM) while the presence of Ca^{2+} cations have resulted in enhanced apparent aggregation at ionic strength as low as 10 mM. Investigation on the aggregations of silver nanoparticles coated with either PVP and citrate has revealed that divalent electrolytes were more efficient in destabilising the citrate coated NPs as indicated by the considerably lower critical coagulation concentrations (2.1 mM CaCl2 and 2.7 mM MgCl2 vs 47.6 mM NaCl) (Huynh and Chen, 2011).

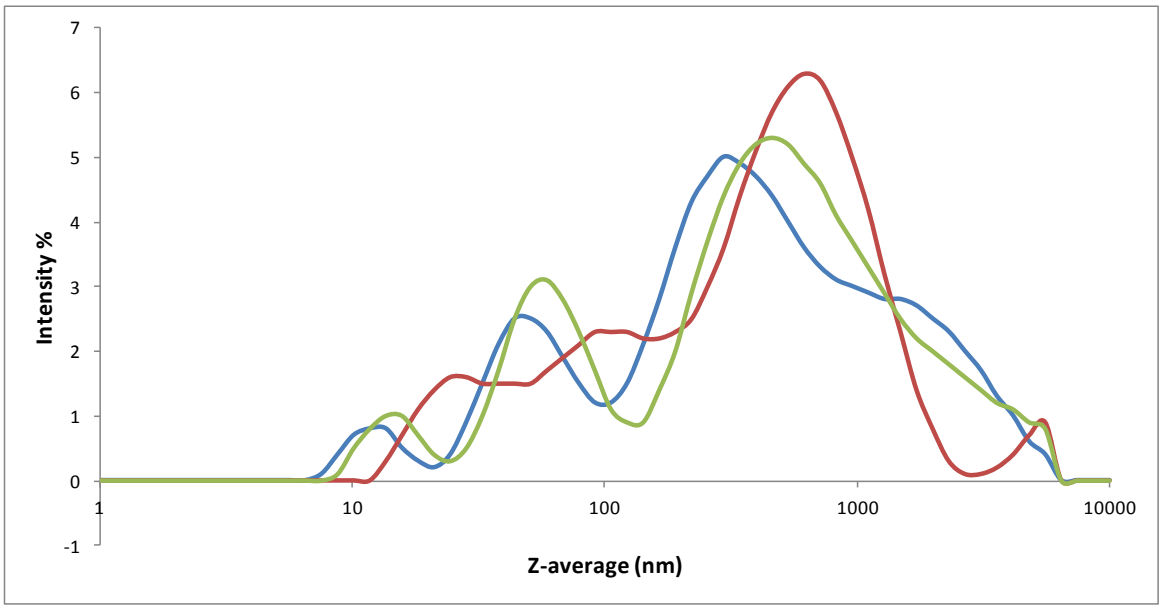

Figure 5-15: DLS diagram of citrate capped NPs in 16 mM $NaNO_3$ solution showing that citrate capped AuNPs particles clearly aggregate at this ionic strength and higher as shown by the mixture of peaks.

Figure 5-16 shows lack of aggregation of PVP coated NPs in high ionic strength solution. The ionic strength of the solution is as high as 80 mM.

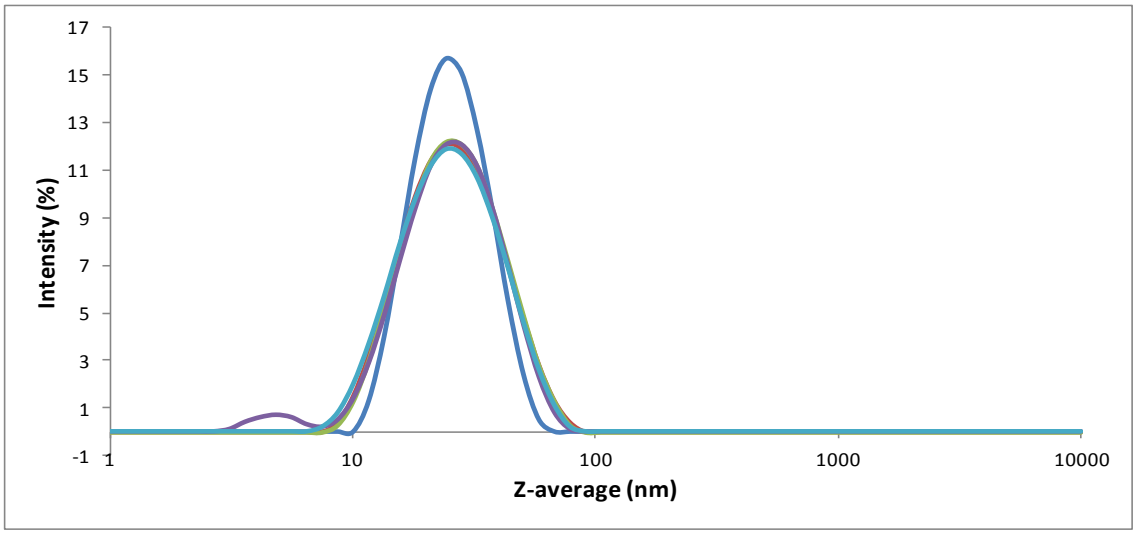

Figure 5-16: DLS diagram of PVP capped NPs in 80 mM $NaNO_3$ solution showing that there is no sign of NPs aggregations in this high ionic strength solutions.

5.3 Conclusion

Prior to any exposure experiment of NPs on the environment, their physicochemical properties need to be studied so that the fate and behaviour of the NPs after exposure can be compared to their original properties. It is the aim of this chapter to synthesise and fully characterise good quality gold NPs of different sizes and different surface chemistries.

Gold nanoparticles were synthesised using wet chemistry methods. Two types of coating agents (citrate and PVP) were used to stabilise freshly synthesised gold nanoparticles. During the synthesis, the first sign for the production of the NPs was manifested in colour change from yellow to ruby red. This was confirmed by the characteristic surface Plasmon resonance peak for gold which is around 520 nm. Multi - method-approach was used to fully characterise the synthesised NPs. Here, a range of different but complementing analytical and imaging techniques helped to measure relevant physicochemical properties of the NPs. In brief, stable, monodisperse, spherical AuNPs with two coating agents and a range of sizes were synthesised using one-step method approach. The NPs are homogenous in size and spherical in shape. Furthermore, the stability of the NPs was monitored and the results showed their stability even after one year from the synthesis date. The core size of citrate capped varies from 7 nm to 32 nm while PVP particles have core sizes ranging from 11nm to 85nm. The shape factors of all samples were near to 1 and better than 0.8. From the ICP_MS measurements, it can be seen that for all samples 97.5% of gold ions were converted into NPs and just a very small fraction (<2.5%) is dissolved in the solution. Between different capping agents, the PVP capped NPs have more dissolved fraction than the citrate capped particles.

Since the size, shape and monodispersity of stabilised gold NPs are fundamental features for their toxicity studies, these fully characterised gold NPs can form a reliable basis for potential

reference materials which help the identification of the ecotoxicological effects caused by certain variables. The range of sizes and coating agents will provide more versatility of these potential reference materials for the study of property-effect relationship in (eco) toxicology studies.

These fully characterised, high quality AuNPs will be used in the following chapters to study their effect/interaction with the planktonic bacteria *Pseudomonas fluorescens.*

Chapter 6: Stability of gold NPs in Minimal Davis Media (MDM) and their Effect on *Pseudomonas fluorescens.*

6.1 Introduction

Nanomaterials behave differently in the different compartments of the environment (Praetorius et al., 2012). Bacterial biomass forms an integral and important part of the environmental living organisms and the interaction between nanoparticles (NPs) and bacteria is an inevitable process(Pelletier et al., 2010). The effect of this interaction on both bacteria and on the behaviour of the nanomaterials is a matter of investigation and available studies remain far from being conclusive (Tong et al., 2007, Johansen et al., 2008, Kumar et al., 2011).

The main task of this chapter is threefold. First the stability and behaviour of the NPs in relevant bacteria growth media will be studied and monitored. The nanoparticles will be fully characterised in the growth media through measuring their physicochemical properties such as sizes, degree of aggregation, concentration, surface plasma and pH of the media which are important parameters for the study of the effect of the nanoparticles on any organisms. If the NPs change their properties in the full strength of the media, the media will be further diluted to preserve the original properties of NPs and special care will be taken so that the diluted media is still able to provide enough nutrients to guarantee the growth of bacteria without being starved. Secondly, the growth inhibition of environmental planktonic bacteria caused by different types of gold NPs will be investigated. Finally the behaviour of NPs after bacteria exposure will also be monitored. The bacteria chosen for this purpose is the environmental bacteria Pseudomonas fluorescens because of its widespread colonising in soil, plant and water. The strain used (SBW25) was received from Professor Christopher

Thomas from the Bioscience School in the University of Birmingham. Detailed information of the Pseudomonas fluorescens in general and the above mentioned strain in particular was given in Chapter 2: sections 2.3.3. In brief, pseudomonas flourescens is a rod shape, motile, non pathogenic, gram-negative aerobic bacteria with flagella as a medium for movement (see Figure 6-1.

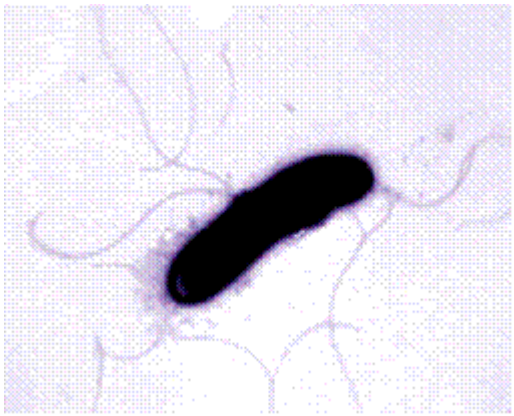

Figure 6-1: TEM images Pseudomonas fluorescens showing its rodshape body and its flagelles(Silby, 2006).

Agar plates were prepared biweekly and bacteria samples were spread on a fresh agar plates to keep them alive (Figure 6-2). As mentioned earlier, prior to the investigation of the effect of gold NPs on bacteria their stability in a liquid bacterial growth media need to be tested. Minimal Davis Media is used for this purpose.

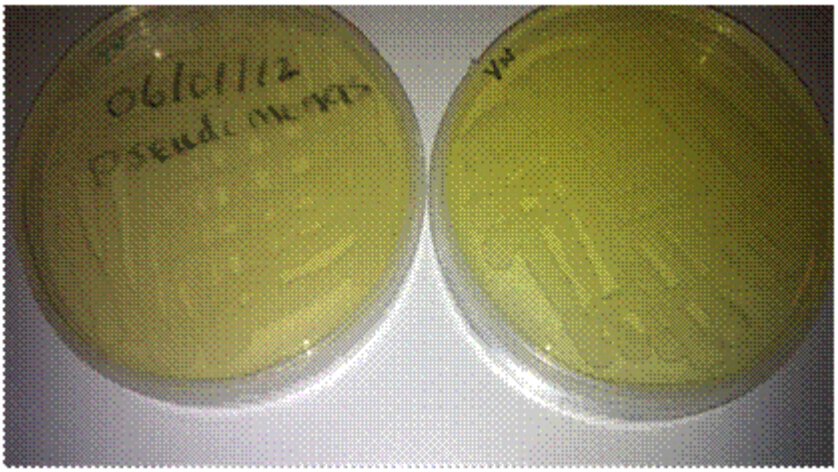

Figure 6-2: *Pseudomonas fluorescens* growing on freshly prepared agar base plate.

6.2 Stability of the gold nanoparticles in Minimal Davis Media

The stability of freshly synthesised samples of gold nanoparticles of the two capping agents (citrate and PVP) in MDM (see section 4.5.1 for the preparation of the media and its ionic strength) of different concentrations was monitored in a period of two weeks. Hydrodynamic size measured with DLS and Surface plasma resonance (SPR) was taken continuously while at the end of the experiment at day 9 samples were imaged with TEM to detect possible aggregations.

6.2.1 Stability of citrate capped NPs in undiluted MDM media

Citrate capped NPs of different sizes were prepared as explained in Chapter 4:section 4.2.2. The capping and stabilising by the citrate is achieved through charge stabilisation mechanism. Citrate is a negatively charged organic ion and by attaching it on the surface of the NPs repulsion forces between particles are created. The same negative sign of the surface of the NPs keeps them separated and thus preventing them from forming aggregates. If the conditions of the surrounding media such as ionic strength change the thickness of the electric double layer around the single particles will change in the sense that the higher ionic strength the thinner the double layer and this will affect the stability of the NPs. The stability of citrate capped 14.8 nm core size AuNPs (hereafter called G2) was tested in three different dilutions of MDM media and the results are summarised in following sections. The detailed physicochemical properties of the synthesised NPs including G2 are tabulated in the result Table 5-1 in Chapter 5: of the thesis.

6.2.1.1 AuNPs capped with citrate in undiluted MDM media.

To study the stability of the NPs, G2 NPs were added into undiluted MDM media and their surface Plasmon resonance (SPR) were continuously recorded for two days using a Uv-vis spectrophotometer. Results were presented in Figure 6-3 below. The decay rate in the table was calculated below using Equation 6-1.

$$R = \frac{\Delta A}{\Delta t}$$

Equation 6-1

Where A is the maximum absorbance (AU) and t is the time (minutes). The unit of R is AU/Minutes.

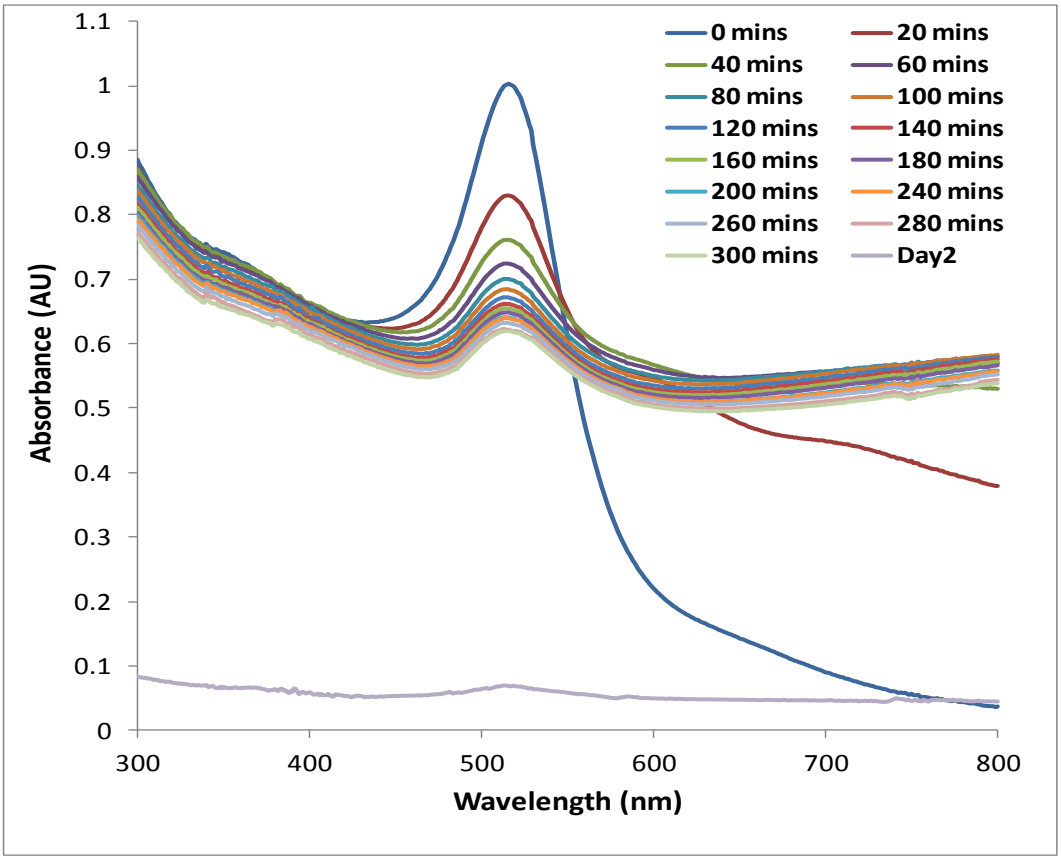

Figure 6-3: Surface plasmon resonance (SPR) of 14.8 nm citrate capped gold NPs in full strength undiluted MDM media measured in a period of 24 hours. Time intervals of 40 minutes were used throughout the first 5 hrs of the experiment.

The surface Plasmon resonance of the freshly synthesised gold NPs changed rapidly in the first 60 minutes of the undiluted MDM media and disappeared completely after 24 hrs after the exposure of the NPs in the undiluted MDM media as is illustrated clearly in the above Figure 6-3. The reason for the disappearance of SPR is due to the formation of aggregates of bulk scale sizes. The maximum absorbance of each spectrum is determined and plotted against time as illustrated in Figure 6-4 below.

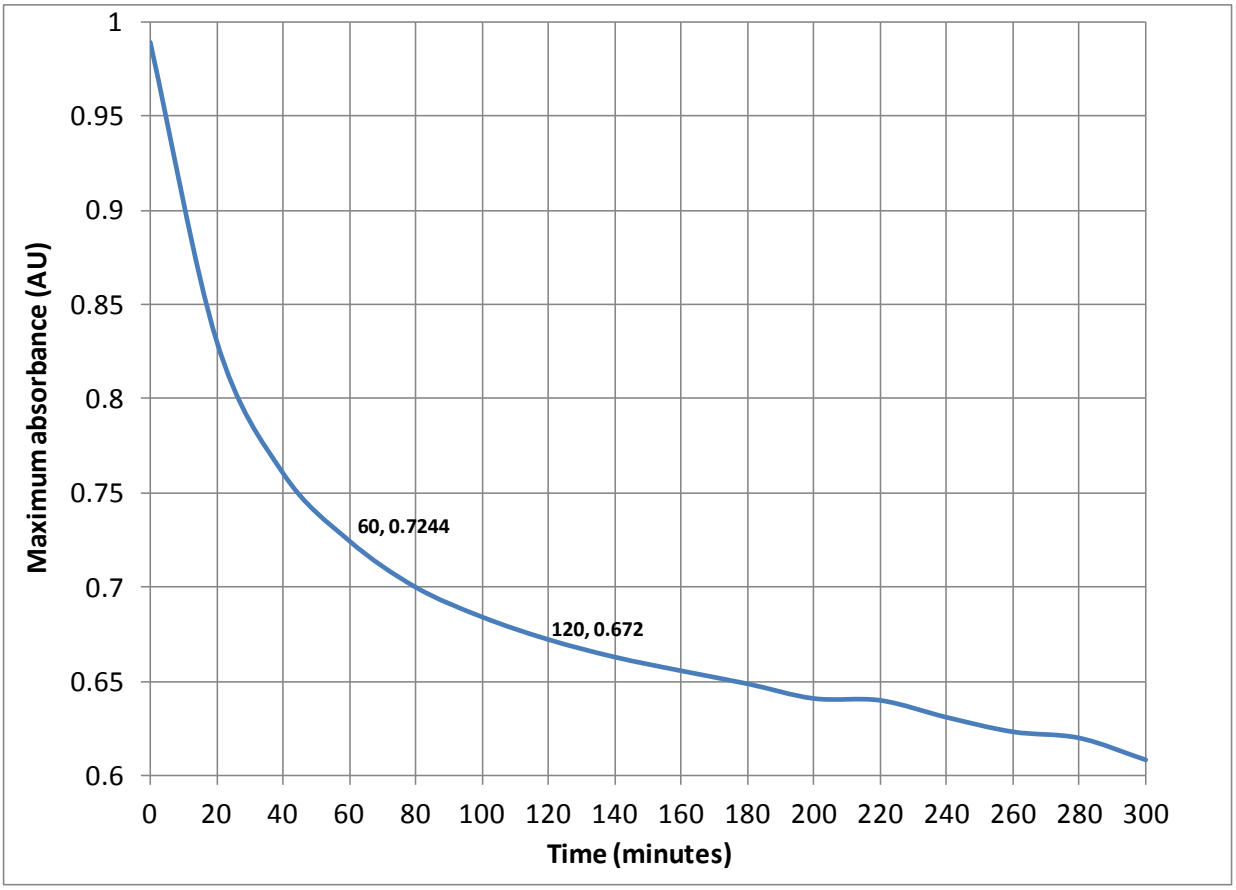

Figure 6-4: Graph showing how the maximum SPR of citrate capped AuNPs of 14.8 nm core size in undiluted MDM changes with the time.

As highlighted in Figure 6-4, the absorbance is decreasing exponentially. The absorbance dropped from 0.9892 AU to 0.7244 AU in the first 60 minutes which corresponds with a decrease of -0.2648 AU. In the following hour the absorbance has fallen to 0.672 AU which corresponds with decrease of just -0.0524 AU. The maximum absorbance has completely

disappeared after 24 hours of exposure which corresponds when all NPs change into aggregates. The colours of the NPs changed from ruby red to black after 30 minutes as illustrated in Figure 6-5 below and after 24 hrs of exposure, huge aggregates of the NPs were visible at the bottom of the container.

Figure 6-5: The characteristic red colour of the freshly synthesised AuNPs has changed into black within the first 30 minutes in the full strength of the Mimimal Davis Media (MDM)

DLS measurements of the above citrate capped AuNPs were performed after 30 minutes of exposing NPs in undiluted MDM and the monomodial narrow peek with z-average of 18.3 ± 0.4 with Polydispersity index (PDI) of 0.19 changed into a mixture of different peeks as illustrated in Figure 6-6 a and b respectively.

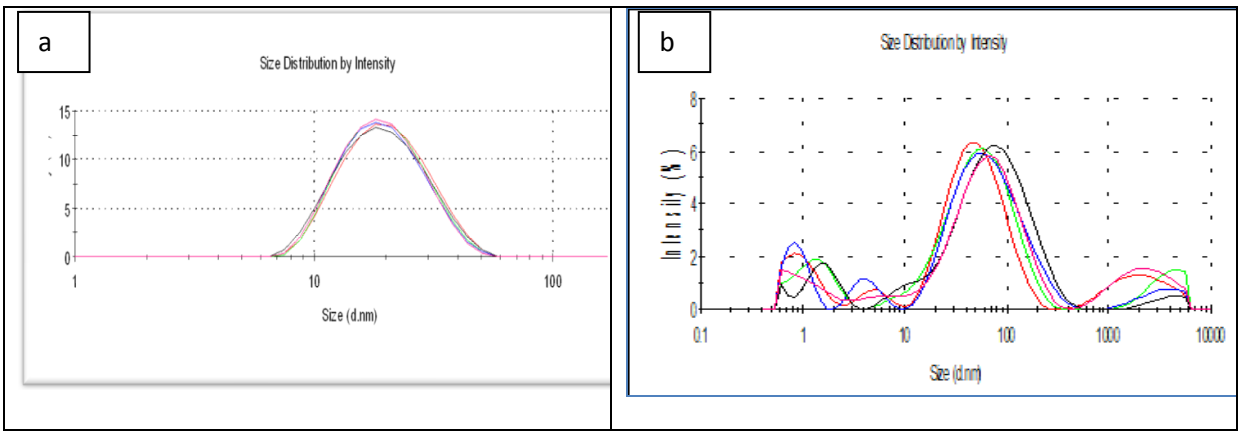

Figure 6-6: DLS graphs showing aggregation of the citrate capped AuNPs (G2) in undiluted MDM media. a) monomodal size distribution by intensity measured with DLS of freshly synthesised 14.8 nm core size citrate capped AuNPs b) same NPs in undiluted media . Measurements were performed about 30 minutes after exposure.

Though the original sample was monomodial the multiple peeks some of them outside the nanoscale in Figure 6-6 b which indicated that aggregations of the NPs have taken place in the media within a period of only 30 minutes.

After 9 days in the media, samples were prepared by the ultracentrigation method described in Chapter 4: section 4.4.1. Then, the grid was washed with milli-q and dried. Images in Figure 6-7 were taken with Jeol1200 TEM (see Chapter 3: section 3.1.2 for the theory of the TEM techniques).

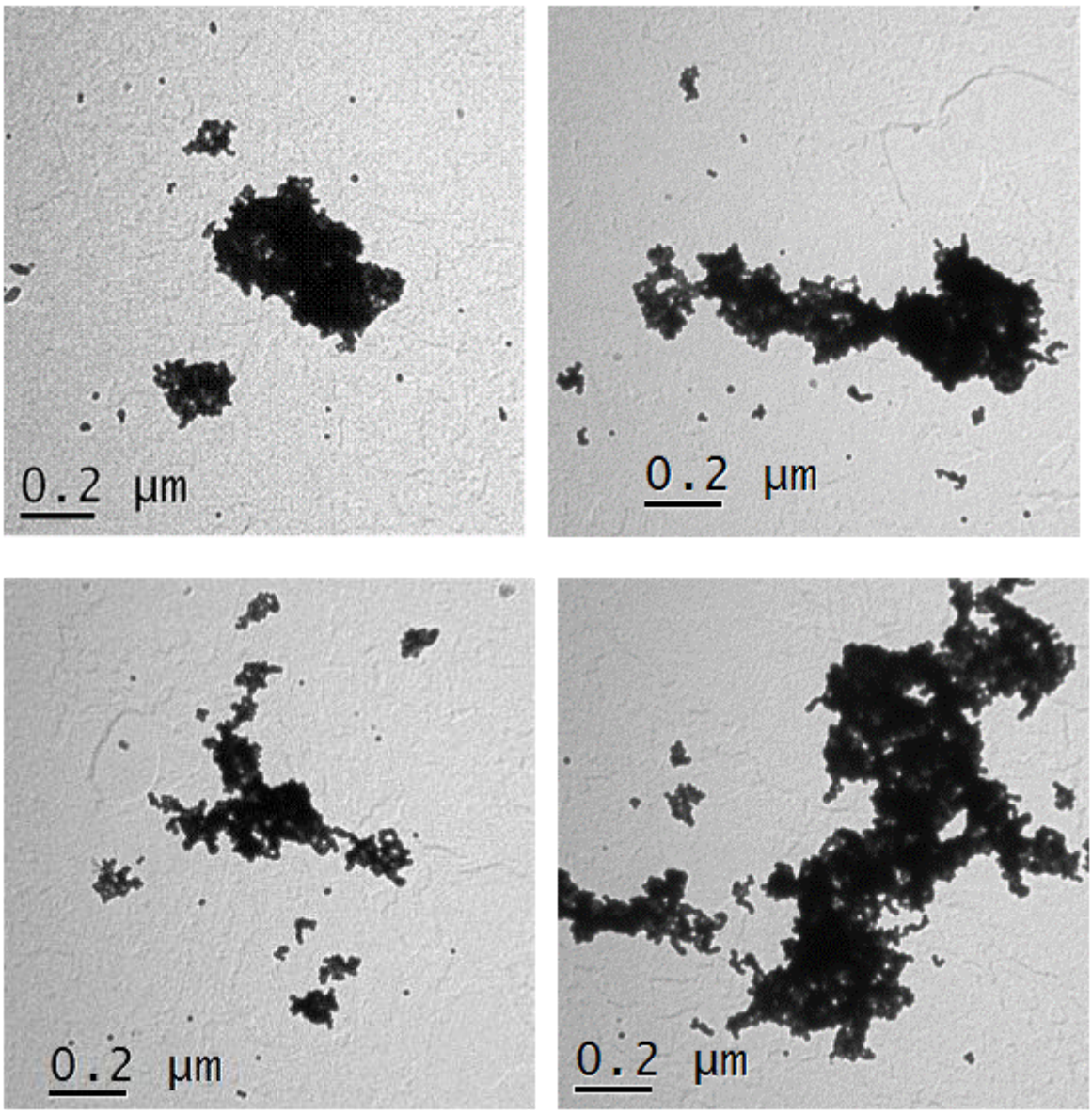

Figure 6-7: TEM images showing aggregates of different sizes of citrate capped AuNPS in undiluted MDM media.

Figure 6-7 exhibits large aggregates with a range of sizes and some single particles of the citrate capped AuNPs in the undiluted MDM media supporting the disappearing SPR spectrum illustrated in Figure 6-3 and the DLS data presented in Figure 6-6.b. The sizes of aggregates larger than 1000 nm were recorded. The results from different techniques presented above for the citrate capped AuNPs in undiluted MDM media clearly revealed that this type of NPs are unstable in this strength of the media. The undiluted media has ionic strength of 19.1 mM as calculated with equation Equation 4-2. It is a well-known phenomenon that charge stabilised NPs aggregate in high ionic strength media (Badawy et al., 2010, Cumberland and Lead, 2009). Consequently, the behaviour of the citrate capped NPs in diluted MDM media was investigated and results are presented in the following sections.

6.2.1.2 AuNPs capped with citrate in 4x diluted MDM media

The behaviour of G2 NPs in 4x diluted MDM media was further studied and characterised with uv-vis, DLS and TEM. The surface Plasmon resonance of the NPs was recorded for 14 days and the data were presented in Figure 6-8 below. SPR of the particles remained unchanged throughout this period of time indicating that the AuNPs particles behaved in a quite stable manner in this 4x diluted MDM media.

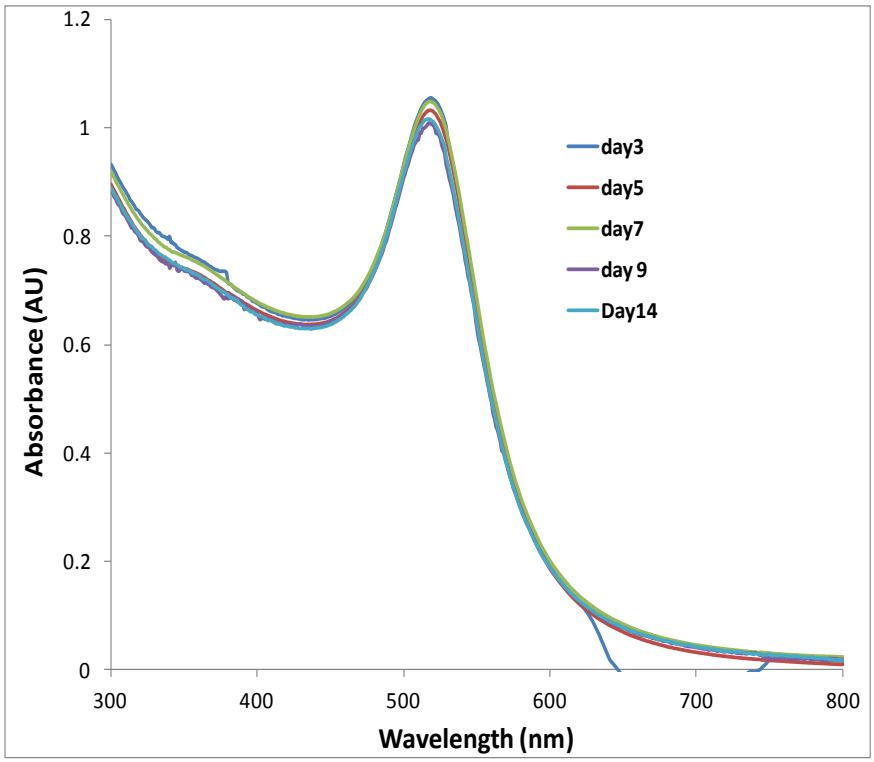

Figure 6-8: Surface plasmon resonance measured with Uv-vis of 14.8 nm core size citrate capped AuNPs in 4x diluted MDM media measured in a period of 14 days.

For further analysis of the citrate capped AuNPs in 4x diluted MDM media, DLS measurements were taken in different days and the results were presented in Figure 6-9, Figure 6-10 Figure 6-11 and Figure 6-11 below.

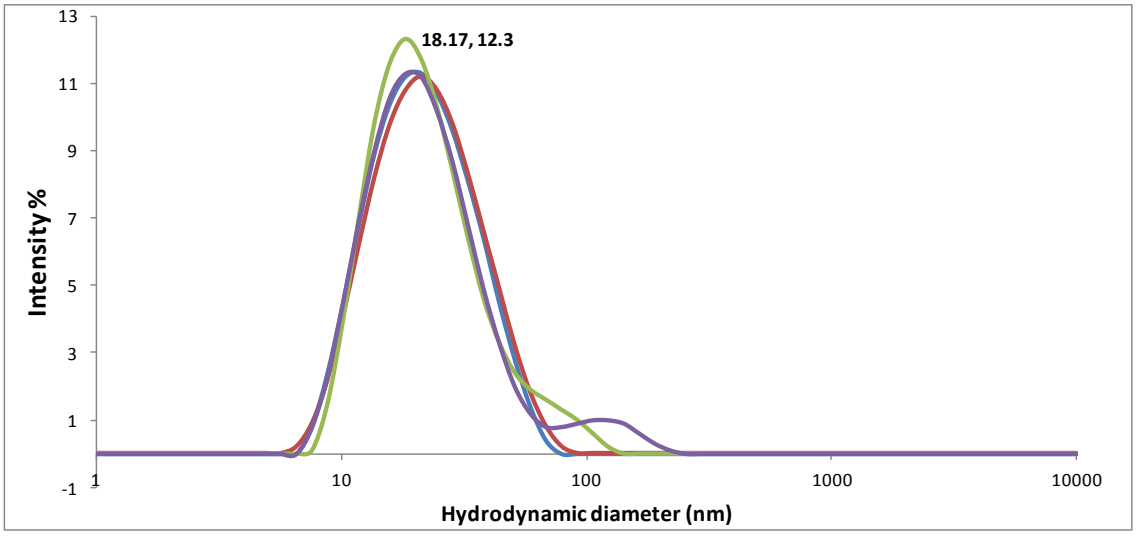

Figure 6-9: Size distribution by intensity measured with DLS of 14.8 nm core size citrate capped AuNPs (G2) in 4x diluted MDM media measured day 1 of the exposure.

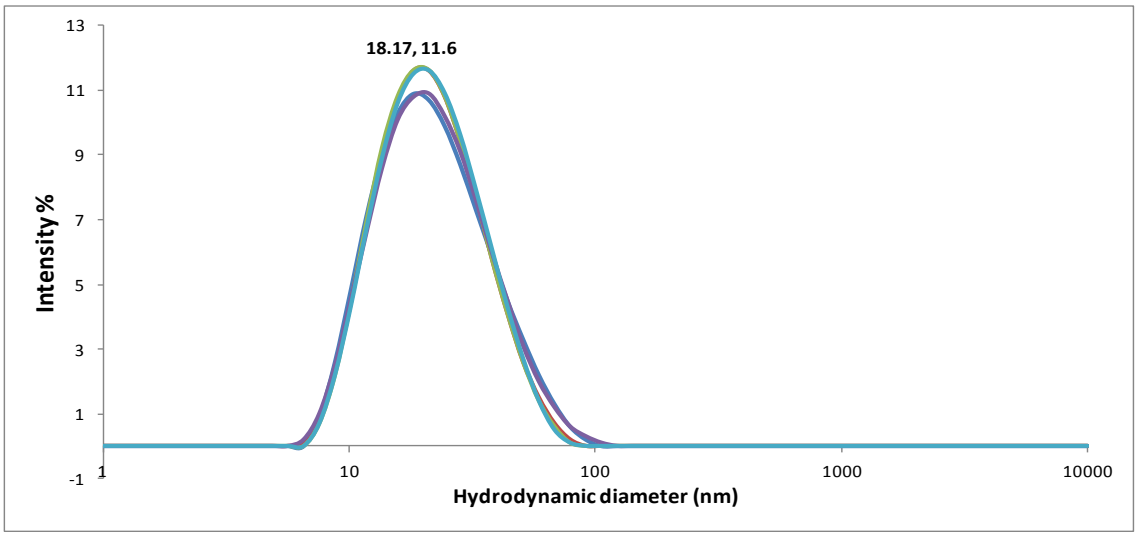

Figure 6-10: Size distribution by intensity measured with DlS of 14.8 nm core size citrate capped AuNPs after 5 days in 4x diluted MDM media.

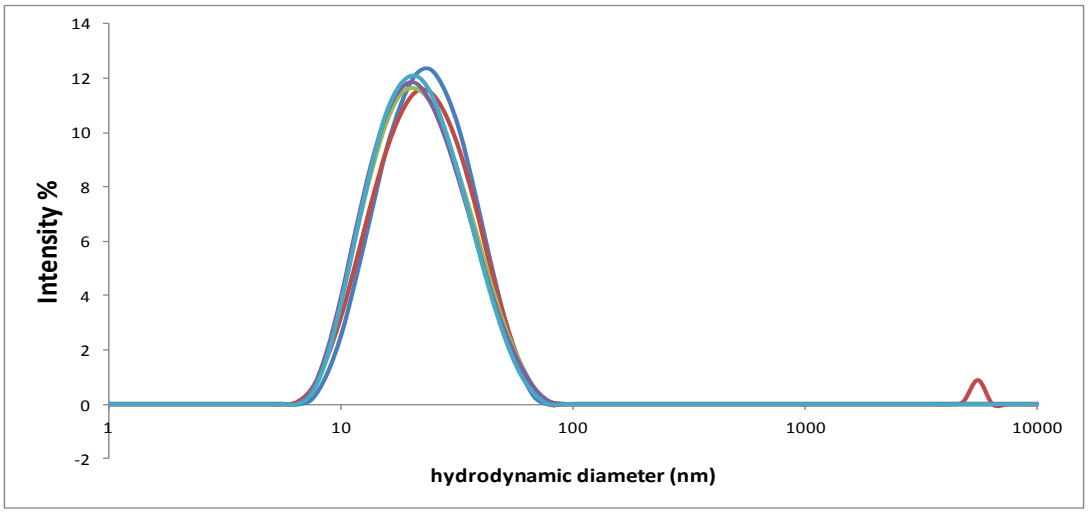

Figure 6-11: size distribution by intensity measured with DLs of 14.8 nm core size citrate capped AuNPs in 4x diluted MDM media. Measurement was taken on day 9 of the exposure.

The above DLS measurements which are spread over a period of 9 days have demonstrated that the size distribution by intensity of the citrate capped AuNPs remained monomodial with comparable polydispersity indices. In all three measurements there were no indications of aggregations taking place in the media since the intensity did not change and there are no peeks in the microscale area. Samples of the citrate capped AuNPs were prepared using ultra

centrifuge method for TEM imaging after 9 days of exposure in 4x diluted MDM media and images of the NPs were illustrated in Figure 6-12.

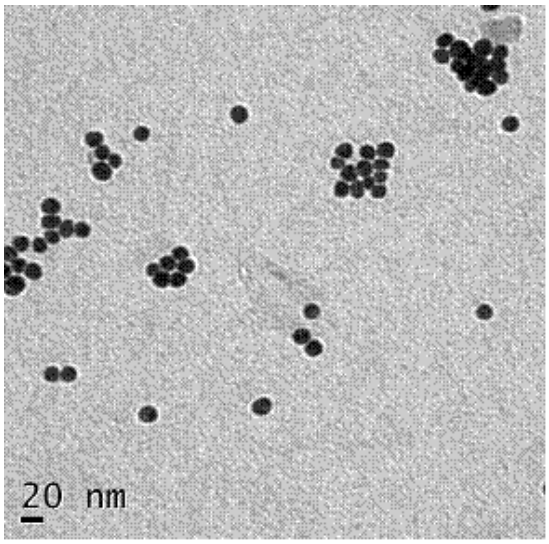

Figure 6-12: TEM images showing stabile single particles of citrate capped AuNPs (G2) after 9 days of exposure in 4x diluted MDM media.

In contrast with the full strength of the MDM media where complete aggregation of the NPs was recorded within 30 minutes (see section 6.2.1) the original spherical shape and size of the AuNPs were preserved (Figure 6-12) which specify the stability of the particles in this strength of the media (ionic strength is 4.78 mM).

6.2.1.3 AuNPs capped with citrate in 10x diluted MDM media

One further step of the dilution of the media was carried out and the stability of the citrate capped AuNPs were tested and characterised. The Uv-vis measurements of the SPR of the particles and TEM images recorded and presented in Figure 6-13 a and b respectively.

Since the citrate capped AuNPs have shown stability in 4x diluted media similar results were expected in the 10x diluted media which was clearly confirmed by both the TEM and Uv-vis measurements.

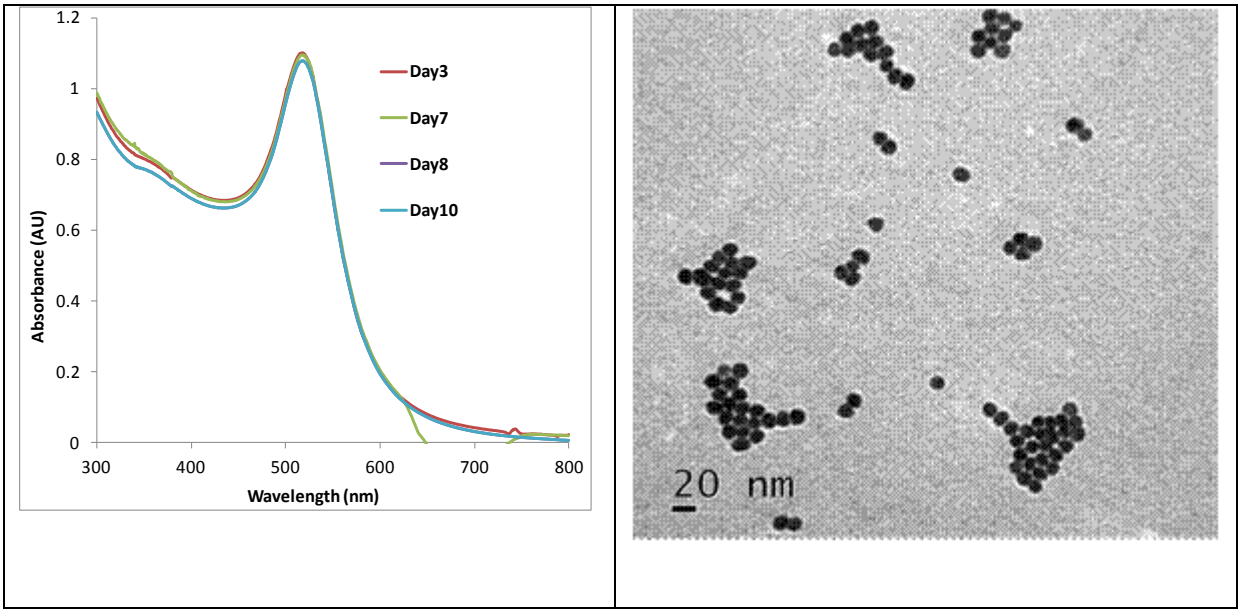

Figure 6-13: a) SPR of citrate capped NPs in 10x diluted MDM media monitored ten days. b) : TEM images of citrate capped NPs after 9 days in 10x diluted media.

6.2.2 Stability of gold NPS capped with PVP in MDM media

The stability of the synthesised NPs is mainly determined by their surface chemistry which is the type of coating agents used to stabilise the NPs. While citrate stabilises through repulsion of the same charge on the surface of the NPs, PVP stabilisation is caused by sterisch effect. The bulk molecule of the PVP polymer separates the NPs and keeps them in the media. The stability of PVP coated NPs was investigated in three different concentration of the MDM media. TEM, DLS and UV-vis analytical techniques were used to study their behaviour in the media and the results are given in the sections below.

6.2.2.1 AuNPs capped with PVP in undiluted MDM media

The stability of PVP capped nanoparticles were studied in a period of 12 days. The surface plasma resonance of the PVP capped samples in undiluted media were recorded and presented in Figure 6-14.

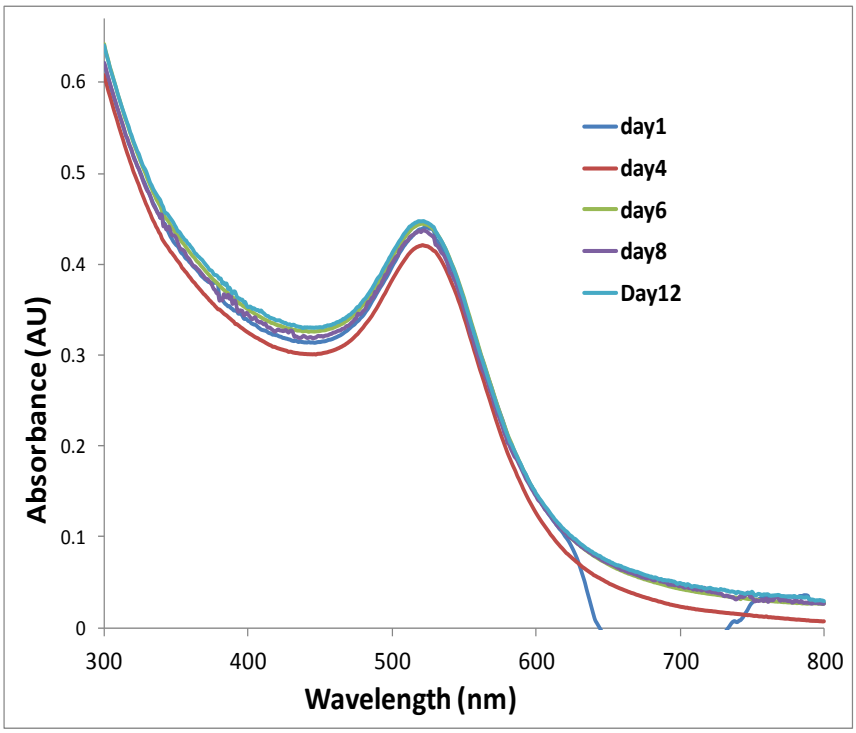

Figure 6-14: The SPR measured with uv-vis of 10 nm core size PVP capped NPs in undiluted MDM media monitored in a period of 12 days.

Unlike citrate capped NPs presented in section 6.2.1.1 where the SPR disappeared within 24 hours in the full strength media the SPR of the PVP stabilised gold NPs remains unchanged for the measured period of 12 days. There is neither shift nor loss of the intensity which showed that PVP capped AuNPs are stable in size and shape in fully concentrated Minimal Davis media (MDM) in the monitored period. For further analysis the TEM samples were prepared on the 9th day in media. It was expected that PVPNPs will stay stable in the diluted media since they are stable in the undiluted media. TEM images of 10 nm core size gold nanoparticles stabilised with PVP in three different strengths of PVP media were illustrated in Figure 6-15 below.

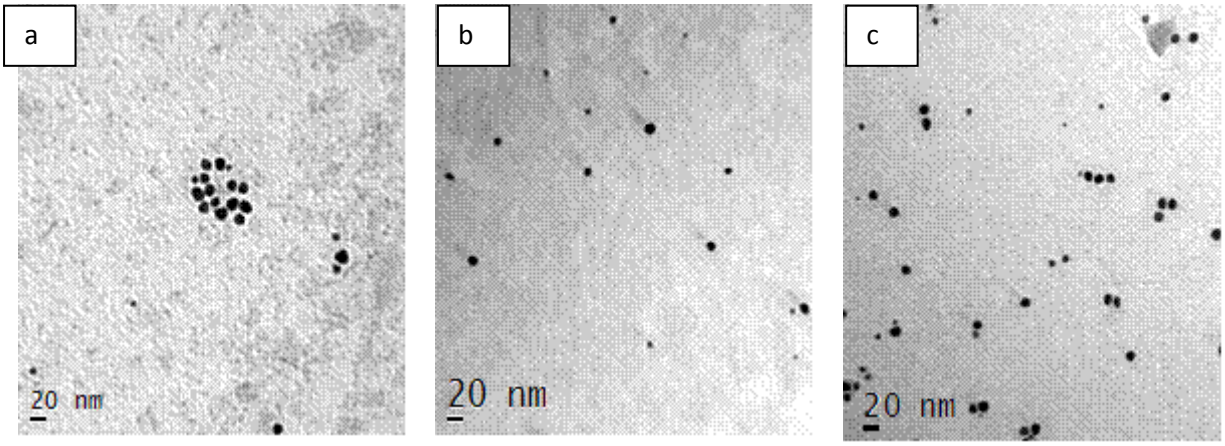

Figure 6-15: TEM images of gold nanoparticles capped with PVP in undiluted MDM media. Image a is in undiluted media, b in 4x diluted media and c in 10 diluted media. Samples were placed on the TEM grid after 9 days in the media.

Figure 6-15 above clearly put on view that gold NPs capped with PVP are stable in all three concentrations of the media including undiluted media. The individual nanoparticles are clearly visible on the grid with no sign of aggregation. This shows that PVP capped NPs are more stable in MDM media and other media with similar ionic strength than citrate capped gold NPs.

After a period of trial and error to decide what strength of the MDM media can be used to maintain both the stability of the NPs and the growth of the bacteria, it was found out that on one hand NPs especially citrate capped NPs are not stable in the full strength of the MDM media (see section 6.2.1 above) while on the other hand bacterial growth in 10 diluted MDM media was practically both time-consuming and incomplete. So 4x diluted media provide enough nutrients for bacterial growth and both types of the NPs (citrate capped and PVP capped) remained quite stable. Therefore, for the remaining studies which are aimed to investigate the bacterial growth inhibition caused by the AuNPs the 4x diluted MDM media will be used.

6.3 Growth curve of *Pseudomonas fluorescens*

Pseudomonas fluorescens was grown in 4x diluted MDM media and placed in a shaking incubator rotating with 120 rpm at 25^{o}C. Optical density at wavelength of 595 nm was recorded using UV-vis for a period of 52 hrs to scan the different growth phases of the bacteria and the results are illustrated in Figure 6-16 below.

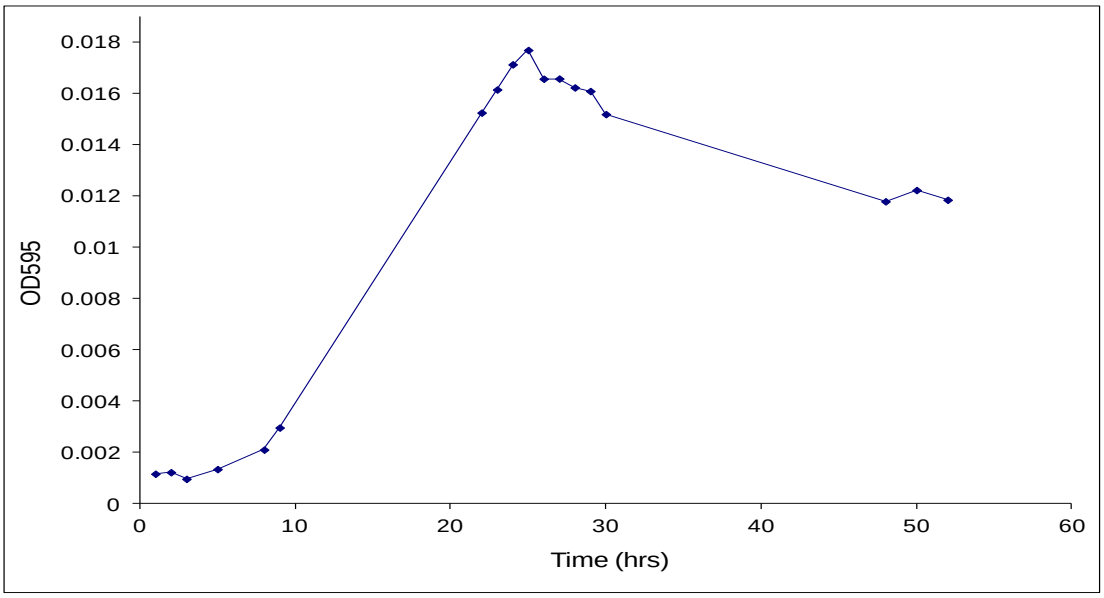

Figure 6-16: Typical growth curve of the psoudomonas flourescencs strain SBW25 in 4x diluted MDM media.

This growth curve is helpful to show the difference phases of bacterial growth. It shows a short lack phase of roughly 3 hours. It clearly displays an exponential phase starting after few hours and ending around 24 hours after the inoculation of the bacteria, which is when the bacteria are most vulnerable to toxicants. It is worth noting that the death phase is not very obvious here since both the dead cells and living cells scatter the light and Uv-vis measures both scatterings.

6.4 Testing the Effect of AuNPs on planktonic bacteria

Generally, the growth of bacteria can be measured directly by counting cells using a cell counter or indirectly by using a spectrophotometer (turbidity measurement). In the

spectrophotometer method, the intensity of the scattered light depends on the number of bacteria cells in the media. The higher the number of cells the cloudier the suspension and more scattered the light. In this investigation, turbidity measurement was used to investigate possible bacterial growth inhibition caused by different types of AuNPs used by taking the optical density (OD) measurements of the bacteria suspension at a wave length of 595 nm. Though the OD method is a quick, non-destructive and easier to carry out than the counting method, one inherent problem of the turbidity measurement method is that the death phase of the curve is less obvious since the dead cells still physically scatter light. The theory and the practical application of the used Uv-vis instruments were given in sections 3.1.6 and 4.4.5 respectively.

High quality gold nanoparticles of different sizes and different capping agents which were synthesised using methods described in Chapter 4: section 4.2 and their stability in different strength of MDM were thoroughly tested and described in the above sections were exposed on *Pseudomonas fluorescens* bacteria growing in a liquid MDM media .The overall aim was to study the interaction of the nanoparticles with the bacteria and monitor the effect of the NPs on the growth of the bacteria. The experiment was divided into two stages which are: first, monitoring bacteria growth with UV-vis and second, characterising the NPs after bacteria exposure by DLS, Uv-sis, and TEM.

6.4.1 Effect of AuNPs on the growth of the *Pseudomonas fluorescens*

In the first stage, the bacteria were grown in MDM media for 12 hrs to reach the middle of the exponential growth phase before any treatment with NPs is administered. This is followed by the continuous monitoring stage in which the growth of the bacteria in untreated media and in the samples treated with 10 ppm gold NPs of different sizes and coating agents were

quantified by measuring the optical density at a wavelength of 595 nm for a period of 30 hours with Uv-vis. The size of the NPs used vary from 100 nm to 5 nm to cover the whole nanoscale range and the inhibition effect of two capping agents citrate and PVP on the bacterial growth were also tested and compared with the untreated samples. The data of this part of the experiment are presented in the following sections starting first with the effect of two separate sizes of citrate capped AuNPs followed by the PVP capped particles and finally the effect caused by the gold ions.

6.4.1.1 Interaction of 14 nm citrate capped on Pseudomonas fluorescens

Freshly synthesised citrate capped gold nanoparticles (G2) (see Table 5-1 in Chapter 5:for the physicochemical properties of G2 particles) were exposed on the *Pseudomonas fluorescens* for a period of two consecutive days to investigate their possible toxicity with bacteria. All experimental handlings were carried out in a clean flow laminar cabinet sterilised with 70% ethanol while the air in the cabinet was kept sterilised by using Bunsen burner. Gold AuNPs were added aseptically to the bacteria suspension by using 0.2 μm filter. Since the effect of NPs is most of the time associated with their small size and their large surface area it was hypnotized that gold NPs may affect the growth of bacteria negatively causing bacterial growth inhibition. To test this hypothesis and to make data reliable two independent tests were carried out in two different days. Results are presented in Figure 6-17 below and each point in the graph is the average values of 5 independent replicates.

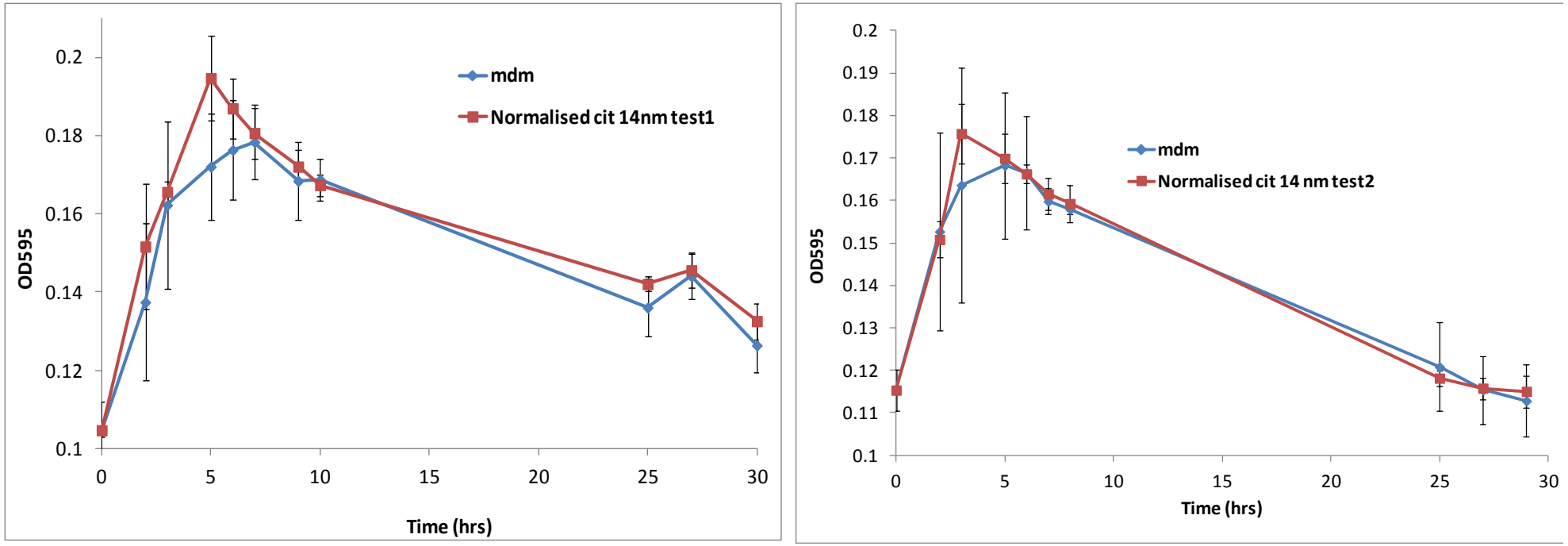

Figure 6-17: Optical density (OD) on 595 nm wavelength measured with Uv-Vis spectrophotometer of the bacteria treated with 14.8 nm AuNPs capped with citrate compared with the OD of the bacteria in the MDM media. Two graphs are for two independent replicates which were recorded in two different days.

The above data in Figure 6-17 imply that the growth of the bacteria was augmented with the presence of gold NPs capped with citrate. This is manifested by the fact that the OD595 of the bacteria treated with NPs in both tests is slightly higher than the MDM only media especially in the exponential growth phase area of the bacteria. This increase in growth caused by citrate capped NPs can be explained since the citrate is one of the nutrients in the MDM media. The NPs solution provides more citrate available for the bacteria to consume and grow. The data also suggest that this type of NPs have no negative effect on the growth of the bacteria. It is worth knowing though that the experimental errors were calculated and the error bars show that the increase of the growth caused by gold NPs solution is not significant since the error bars are overlapping. Similar investigations were carried out for 5 nm core size citrate capped NPs (hereafter called G3) 10 nm core size PVP capped NPs (G5 and 100 nm hydrodynamic sizes PVP capped NPs (G4). Physicochemical properties of these NPs are summarised in the result Table 5-1 in Chapter 5:. Findings are listed in the following sections.

6.4.1.2 Interaction of 5 nm citrate capped on Pseudomonas fluorescens

G3 NPs with final concentration of 10 ppm were exposed on *Pseudomonas fluorescens* growing in MDM media. The optical density was recorded and compared to the untreated sample. Size based toxicity of gold NPs was reported in some literatures where it was found out that the smaller particles manifest some degree of toxicity unlike the bigger particles(Pan et al., 2007). So, it was expected that smaller particles easily penetrate in the bacteria cells and effect its growth. The results from the G3 AuNPs on the growth of the bacteria are presented in Figure 6-18 below and it can be seen similar effect as G2 NPs where the growth of the bacteria is positively affected. This fact implies that the citrate capped particles of sizes between 5 nm and 14.8 nm core sizes have no measureable negative effect on the growth of

the bacteria, instead, they increase slightly the growth since the citrate can be utilised by the bacteria as carbon resource.

.

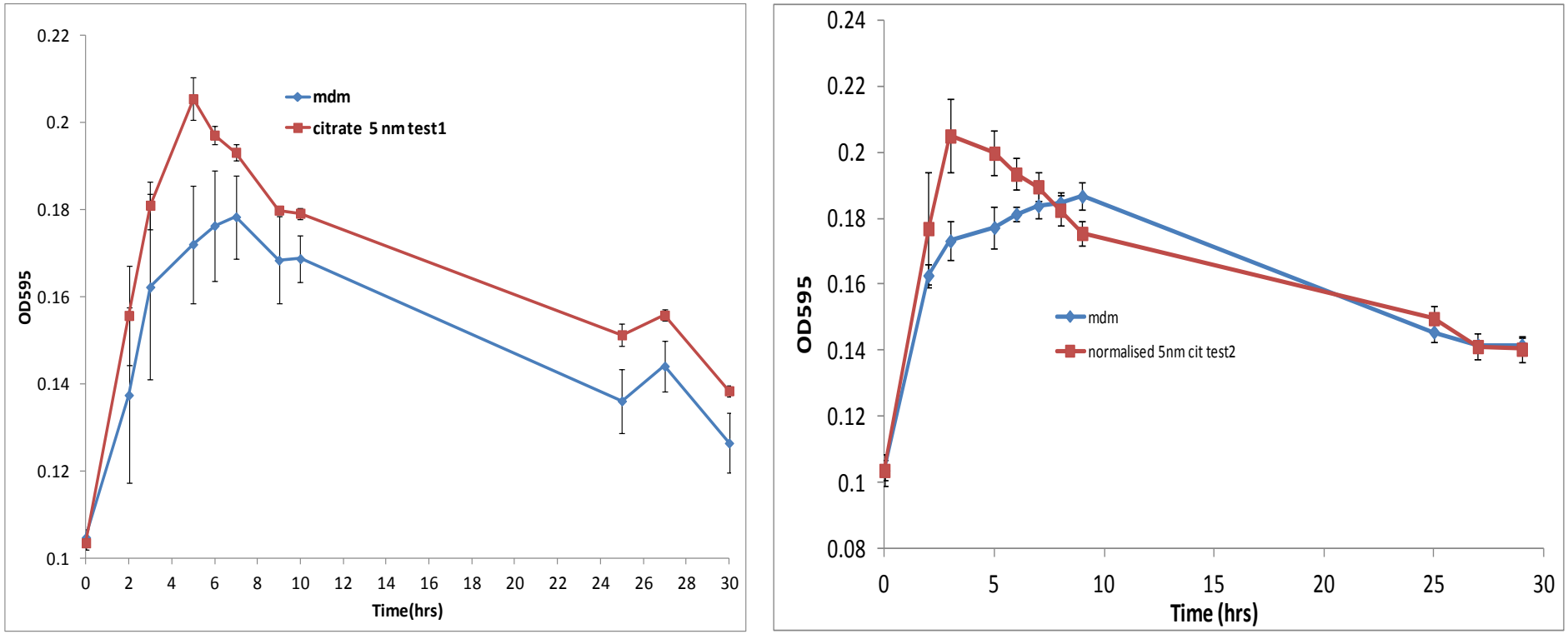

Figure 6-18: Optical density (OD) on 595 nm wavelength measured with Uv-vis spectrophotometer of the bacteria treated with 5 nm citrate capped AuNPs comaped with the OD of the bacteria in the MDM media. The two graphs are for two independent replicates of samples measured in two different days.

The lack of growth inhibition effect of AuNPs on different forms of bacteria was reported earlier in the literature by several previous studies (Hwang et al., 2008, Amin et al., 2009). Amin et al have investigated the effect of 15 nm citrate capped AuNPs on the growth of Esherichia coli and pointed out that there was no significant toxic effect caused by gold nanoparticles. In our study we found that both 14.8 nm core size and 5 nm core size (as measured with TEM) citrate capped AuNPs have no significant inhibition effect on the growth of *Pseudomonas fluorescens*.

6.4.1.3 Interaction of PVP capped NPs of different sizes on Pseudomonas fluorescens.

After preliminary stability investigation of two sizes of PVP capped AuNPs, one from the upper limit of the nanoscale and one near to the lowest limit of the nanoscale were chosen and their interaction with the bacterial samples were tested.

10 nm core size and 100 nm hydrodynamic diameter particles were added to bacteria suspension which is in the exponential phase of its growth phase. The final concentration of the gold in the bacteria suspension was kept at 10 ppm. As measurement of bacterial population, the optical density (OD) of the suspension at a wavelength of 595 nm was continuously recorded in a period of two days. For each size, two independent tests measured in two different days were carried out and each measurement point in the graphs represents the average value of 5 readings. Growth curves normalised on initial readings are illustrated in Figure 6-19 for 10 nm NPs and in Figure 6-20 for the 100 nm PVPAuNPs. The optical density of the bacteria treated with the PVPNPs showed similar growth curve as in the MDM media as illustrated in the Figure 6-19 below.

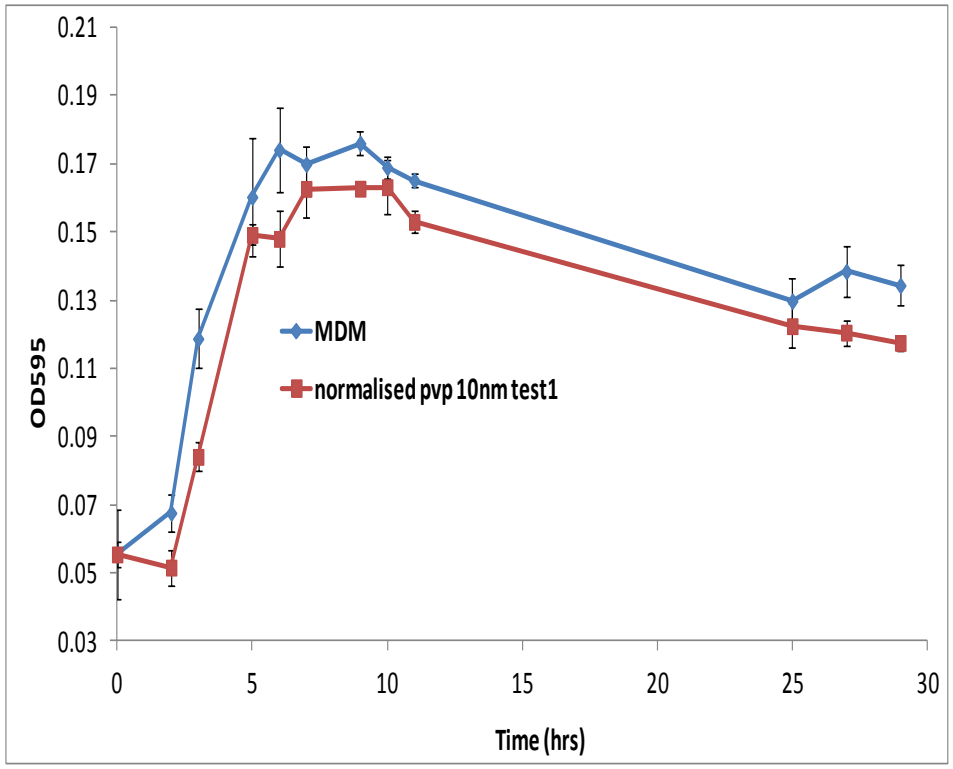

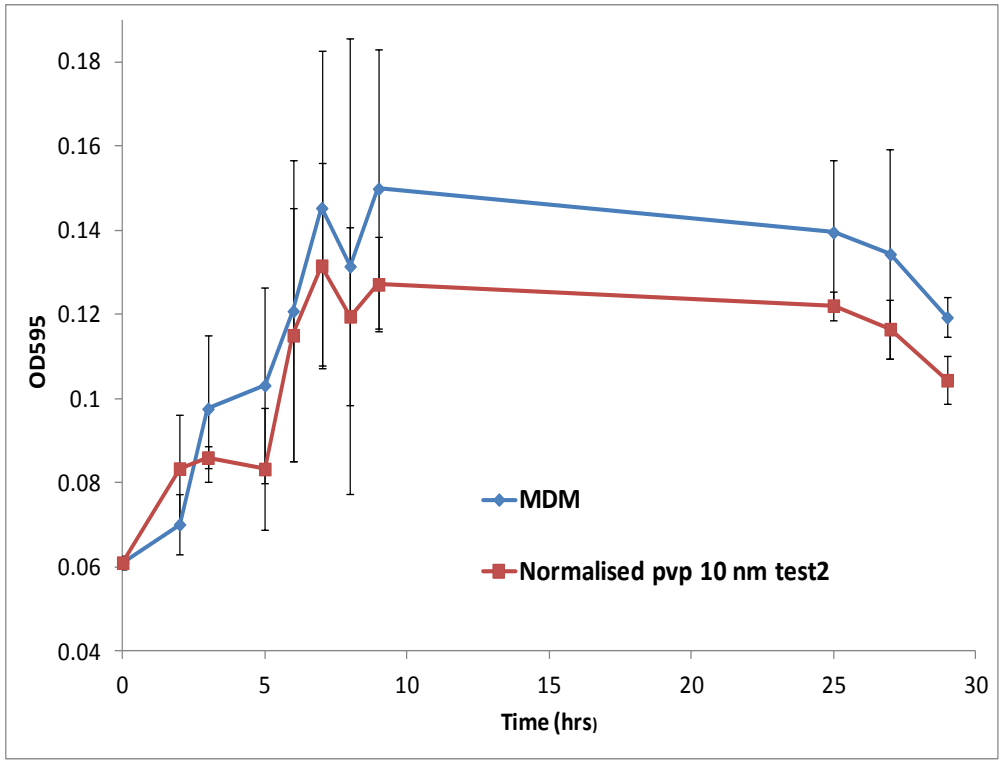

Figure 6-19: Optical density (OD) on 595 nm wavelength measured with Uv-vis spectrophotometer of the bacteria treated with 10 nm PVP capped AuNPs compared with the OD of the bacteria in the MDM media. Two graphs are for two independent replicates of samples measured in two different days.

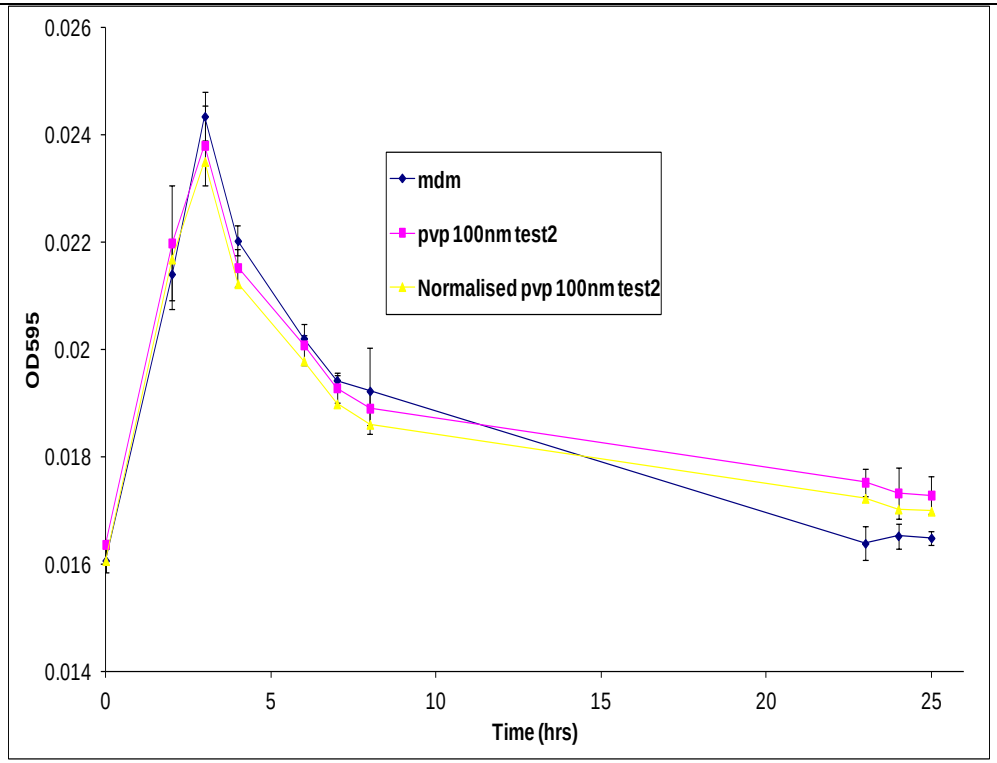

Figure 6-20: Optical density of the bacteria treated with 85 nm PVP capped AuNPs compared with the OD of the bacteria in the MDM media.

The growth with the PVP capped gold nanoparticles is slightly lower than the MDM alone. This implies that the PVP may have some toxic effects on the growth of the bacteria as manifested by lower optical density. It is important to know though that the difference is in the experimental error margin presented by the error bars calculated from 5 independent replicates and thus the difference is not significant. Linear trapezoidal method explained in section 4.5.5 was applied to estimate the area under the growth curve of the bacterial culture. The percentage growth inhibition caused by the PVP capped NPs was quantified using Equation 4-4 and a value of 10% inhibition was calculated for the 10 nm particles.

6.4.1.4 Interaction of gold ions on Pseudomonas fluorescens

Because of its antibacterial activity, the toxicity of silver ions attracted lots of consideration and its toxic effects on a range of different bacterial variety was confirmed by different researchers (Matsumura et al., 2003, Sambhy et al., 2006, Ratte, 1999, Feng et al., 2000). Similar studies for gold ions tested on a different variety of bacteria have indicated the toxicity of gold in the ionic form(Karthikeyan and Beveridge, 2002, Southam and Beveridge, 1994). The experiments described in the previous sections regarding the effect of gold NPs on environmental bacteria pseudomonas fluoresces had not shown any significant change on the growth of the bacteria represented by optical density of the bacteria population. It is worth knowing that the sizes of the AuNPs investigated and represented in the previous sections have almost covered the whole nanoscale range starting from 100 nm all the way down to 5 nm core size. Therefore, one final experiment investigating the effect of gold ions on the growth of bacteria was planned and conducted in a similar way as the nanoparticles experiments. In accordance with previous experiment the final concentration of the gold ions was kept at 10 ppm in the bacterial suspension and ions were added in the media after 12 hrs of incubation which corresponds the exponential growth phase of the bacteria. An optical

density on 595 nm wavelength was recorded continuously in a period of two days. The results of the two independent tests carried out in two different days were plotted in Figure 6-21 below.

The data in Figure 6-21 below were normalised on the initial reading value, the experimental errors were calculated and presented as error bars in the curves. Although the initial reading of the OD in the MDM alone and in the ions - treated samples started on the same point (0.12 AU) there was an increase of OD in the case of the MDM alone and a decrease of the optical density in the case of the ions - treated samples. The decreasing optical density growth curve of the bacteria indicates that the effect of gold ions on the growth of bacteria can be classified as bactericide effect and total inhibition of the growth has occurred. This effect is clearly comparable to the effect of silver ions reported earlier.

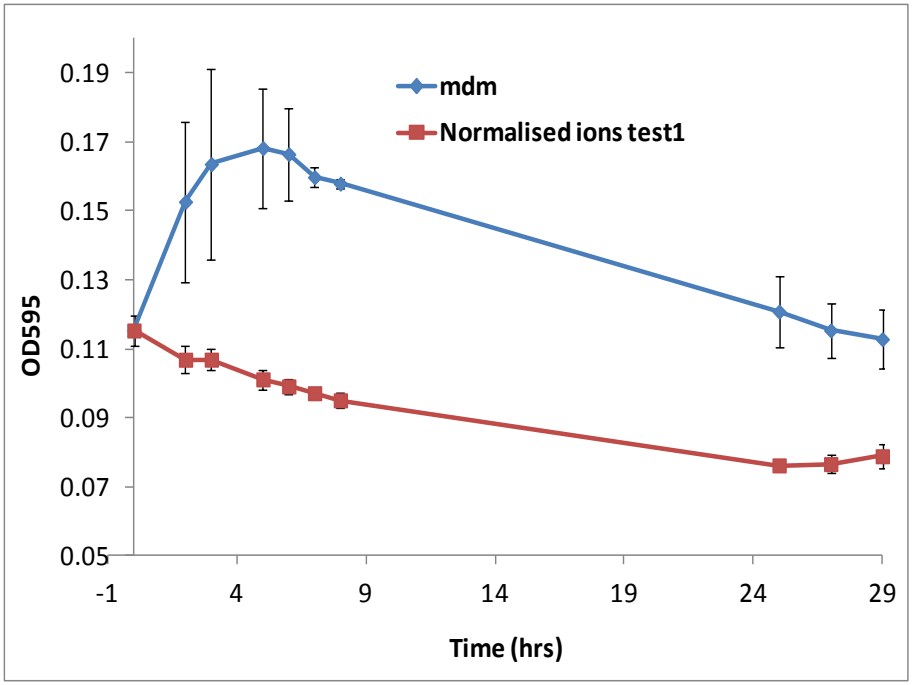

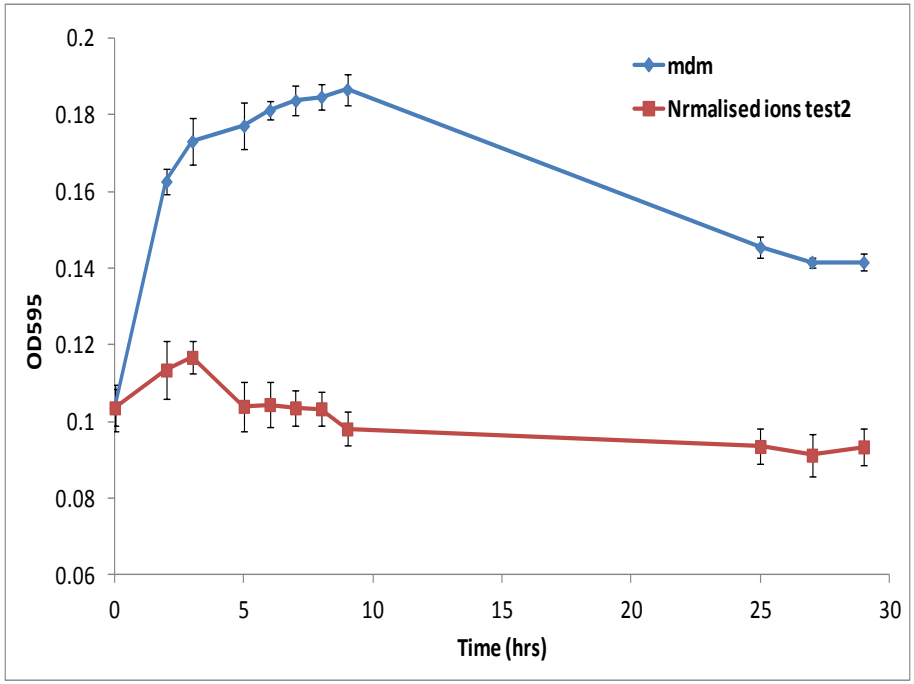

Figure 6-21: Optical density (OD) on 595 nm wavelength measured with Uv-vis spectrophotometer of the bacteria treated with gold ions compared with the OD of the bacteria in the MDM media. Two graphs are for two indepenedent replicates of samples measured in two different days.

6.4.1.5 Citrate and PVP as carbon source for Pseudomonas fluorescens

The results from citrate and PVP capped NPs on the growth of the bacteria presented in the previous sections indicated that the capping agents affected the bacteria growth in different ways. This led to further investigation of the bacteria growing in PVP and citrate media without any other carbon sources. The overall aim of this experiment was to test whether *Pseudomonas fluorescens* can grow in media without carbon resources except the capping agents of the NPs used in this project. The bacteria were incubated in citrate and PVP solutions separately. The concentrations of the capping agents in the solutions were comparable as their concentrations in the AuNPs synthesis media. After one week of incubation, the effect observed was presented in Figure 6-22 below. It can be undoubtedly seen that there is growth of the bacteria in citrate media manifested by the cloudy greenish colour of the solution caused by the bacteria cells producing the characteristic yellow-greenish Pyoverdine, pigment for the Pseudomonas fluorescens (Meyer et al., 2002). In the case of the PVP, there is no sign of growth at all which implies that the bacteria cannot utilise the PVP polymer as carbon source or PVP may have toxic affect on the bacteria which may be the reason why the growth of the bacteria in PVP capped NPs is slightly less than in the MDM media alone.

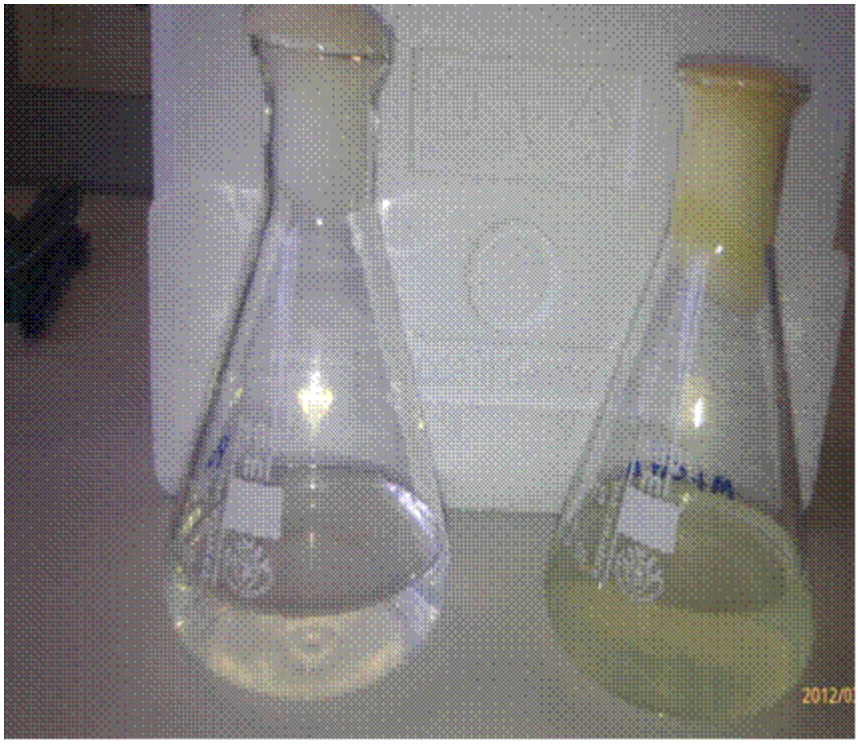

Figure 6-22: Testing the ability of bacteria to consume citrate and PVP as carbon resources. Green liquid shows bacteria growing in citrate solution while clear liquid shows no growth of bacteria in the PVP solution.

6.4.1.6 Comparison between citrate NPs , PVP NPs and gold ions

In summary, the citrate capped NPs have slightly increased the growth of the bacteria. In contrast, the growth was reduced slightly by PVP capped AuNPs. It is worth noting though that both effects described above were not significant since the differences were in the error margins. The effect of gold ions on the bacteria growth was clearly significant. Gold ions had not only stopped the growth but they had a clearly bactericide effect as shown by the decreasing growth curves (see Figure 6-21 above).

6.4.2 Characterisation of AuNPs after exposure on bacteria

Although the AuNPs were stable in the 4x diluted MDM media there is no guarantee that their behaviour will stay the same in the bacterial growth suspension where apart from the media there are also both extracellular polysaccharides produced by bacteria and bacteria

cells. To investigate the fate and behaviour of the NPs in the post exposure period, both citrate and PVP capped NPs have been exposed to bacteria suspension for two days and then fully characterised. TEM images of the NPS with bacteria were recorded; DLS measurements of both unfiltered samples and 100 nm filtered samples were taken. The surface Plasmon resonance (SPR) of NPs was measured. Results are presented in the following sections.

6.4.2.1 Characterisation of citrate capped AuNPs after exposure to bacteria

Characterisation of citrate capped AuNPs after two days exposure on bacterial suspension was conducted using DLS, Uv-vis and TEM. DLS measurements of unfiltered bacterial suspension are illustrated in Figure 6-23 and compared with the measurement carried out after filtering the suspension with 100 nm sterile filter presented in Figure 6-24 and Figure 6-25.

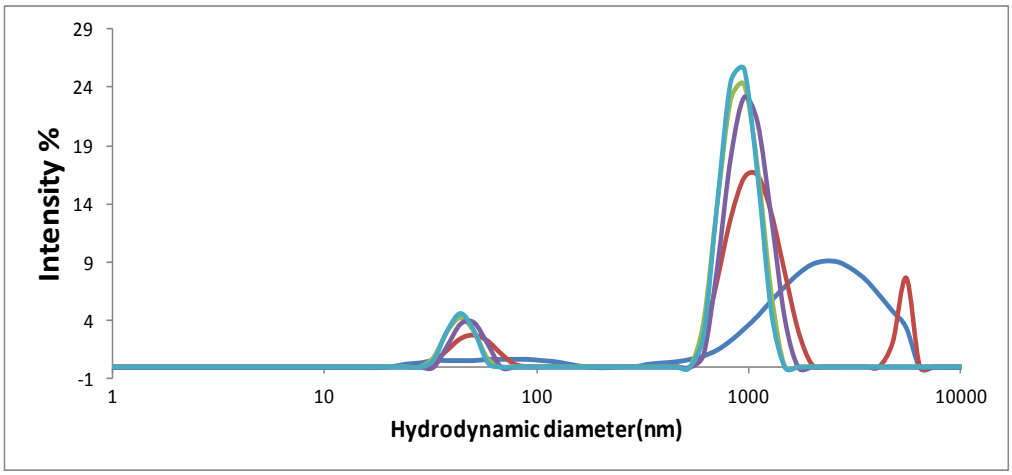

Figure 6-23: Size distribution by intensity measured with DLs of unfiltered bacteria suspension treated with 14.8 nm core size citrate capped AUNPs.

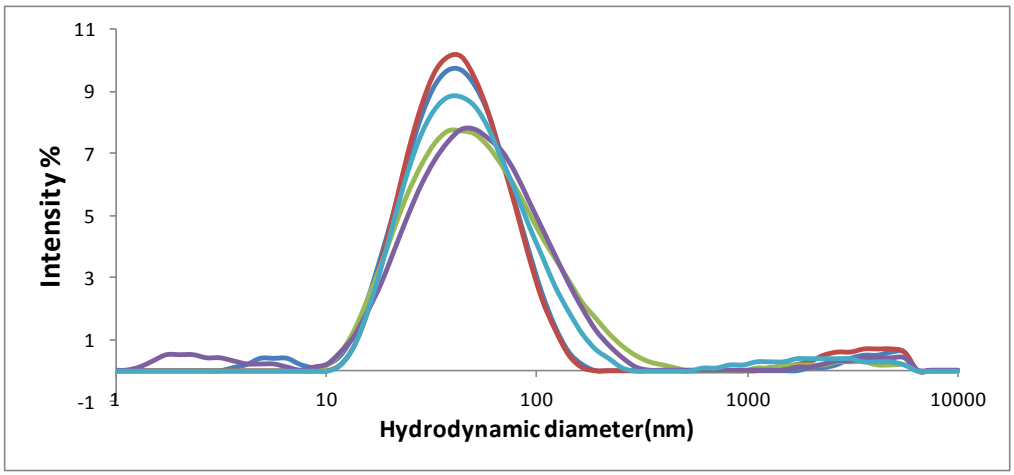

Figure 6-24: Size distribution by intensity measured with DLS filtered with 100 nm filter bacterial suspension treated with 14.8 nm core size citrate capped AuNPs. The measurement was taken view minutes after treating the NPs in the bacterial suspension.

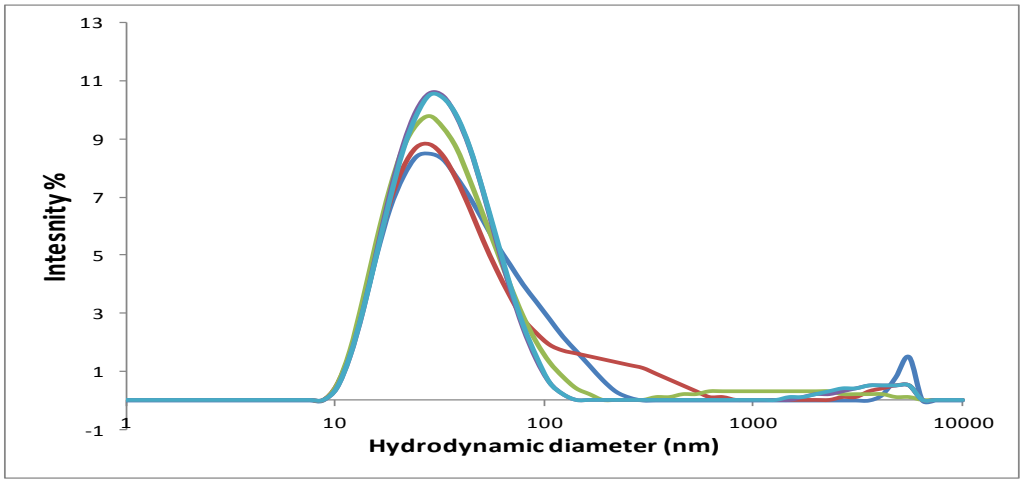

Figure 6-25: Size distribution by intensity of bacterial suspension treated with 14.8 nm core size citrate capped AuNPs and filtered with 100 nm pore size filter. The measurement was taken after two days of exposure at the end of the experiment.

Both the intensity and the place of the DLS peak at the start of the experiment (just after the addition of the NPs to the solution) were compared with its intensity and place at the end of the experiment. The two measurements show fairly comparable results for both the intensity and place of the peaks (see Figure 6-24 and Figure 6-25). The place of the peaks indicates that the size of the NPs did not change during the exposure period while the unchanged intensity implies that no NPs were lost or absorbed by the bacteria. In the case of the unfiltered suspension, the huge peak around 800 nm (Figure 6-23) represents the average hydrodynamic diameter of the bacteria cells. Due to the size of this peak the intensity of gold NPs was

nearly obscured. After filteration of the samples with a 100 nm filter and removing all bacterial cells the AuNP intensity has sharply increased.

To confirm the stability of the NPs indicated by the DLS results, TEM samples were prepared at the end of the exposure period and images were taken directly after. The presence of stable gold NPs can be seen on and around the bacterial cells in the suspension in Figure 6-26. There was no sign of the NPs aggregation in the suspension. The extracellular polysaccharides (EPS) produced by the bacteria cells may have a similar stabilising effect on the NPs as natural organic matter. The effect of different natural humic substances on different NPs was studied previously and was reported that they stabilise NPs by coating them (Deonarine et al., 2011, Akaighe et al., 2011).(Baalousha, 2009, Chen and Elimelech, 2007).

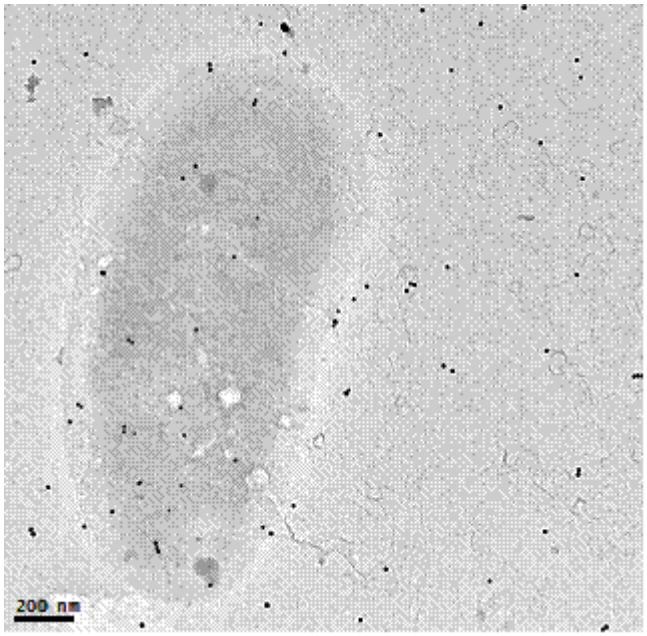

Figure 6-26: TEM images showing stable citrate capped 14.7 nm core size AuNPs randomly distributed on and around the bacteria body. Images were taken after 9 days of exposure.

SPR spectra of the filtered bacteria suspension were recorded both at the start and after two days of exposure of gold NPs. The spectra have shown the characteristic absorption peak of

AuNPs around 520 nm. This peak was absent in the case of positive control (MDM+ bacteria) and the results are summarised in Figure 6-27 below.

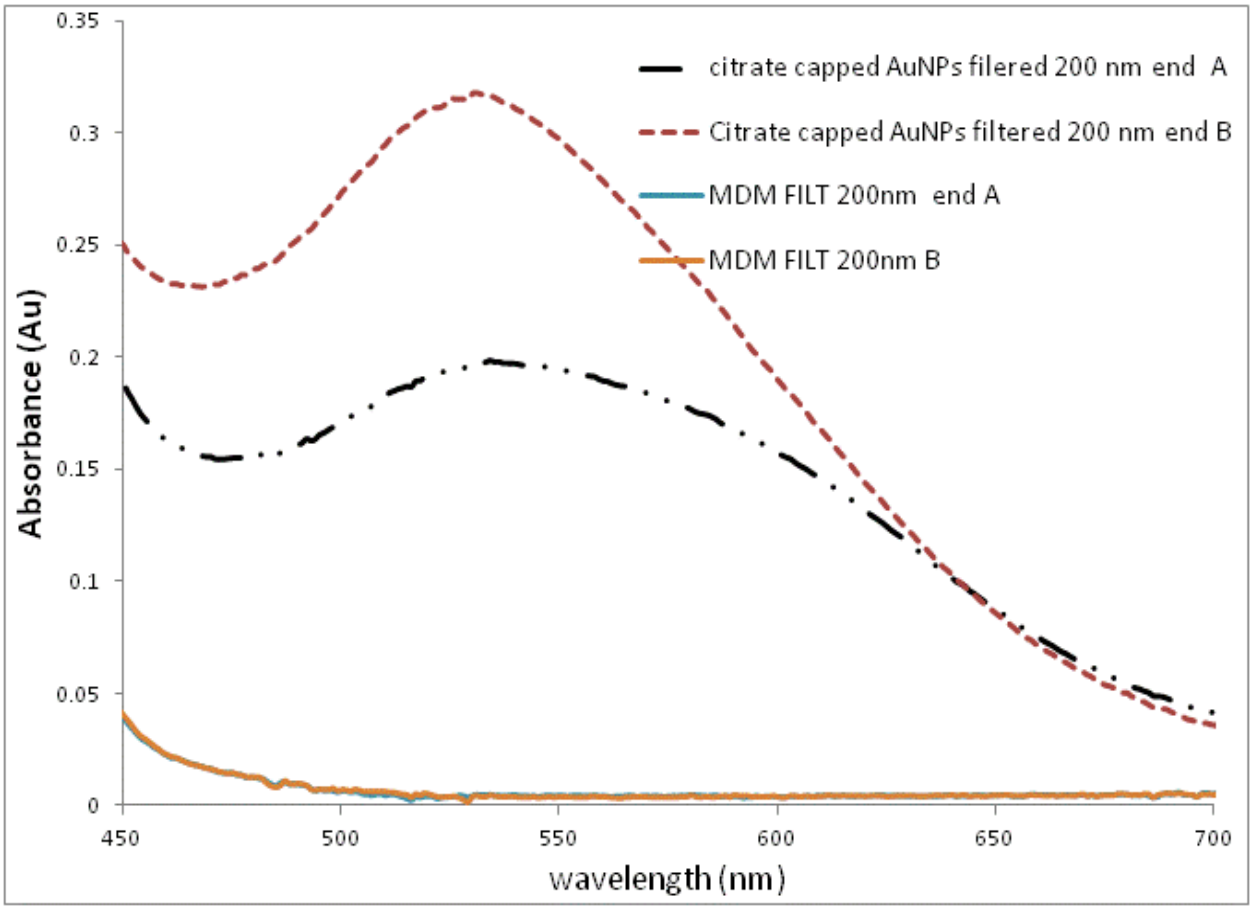

Figure 6-27: **SPR spectra measured with Uv-vis spectrophotometer of the citrate capped 14.8 nm core size AuNPs after exposure to bacteria suspension. All samples were filtered through 0.2 µm filter to remove bacteria cells.**

6.4.2.2 Characterisation of PVP capped AuNPs after exposure to bacteria

Similarly, the PVP capped AuNPs was characterised after exposure time of two days in bacterial suspension. The characterisation techniques used for this purpose were DLS to measure the hydrodynamic diameter and to detect any aggregation that took place during the exposure. TEM was used to image the NPs in the suspension media and Uv-vis to record the surface Plasmon resonance (SPR) of the NPs. The measurement of the SPR serves to confirm

the presence of gold NPs qualitatively. The results from different characterisation techniques are summarised in Figure 6-28 below.

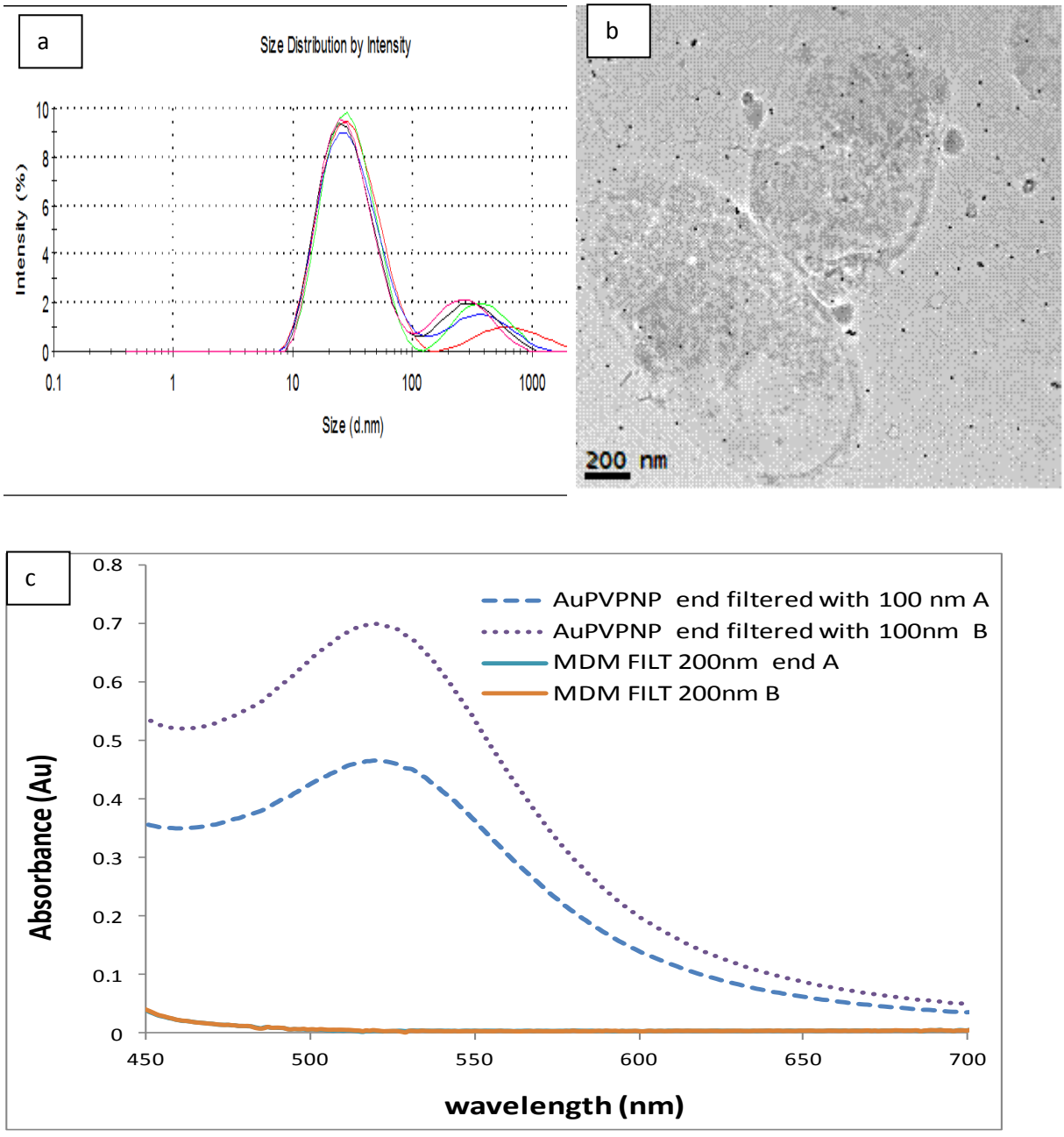

Figure 6-28: Characterisation of 1o nm core size PVP capped AuNP after exposure in bacteria suspension. a) is the DLS size distribution by intensity, b) shows TEM images of both the NPs and bacteria cells, c) is the SPR of the NPs.

Figure 6-28.a shows two peaks for the size distribution by intensity measured with DLS. The more intensity peak above 10 nm corresponds to the scattering of the NPs while the less intensity peak could be caused by loose PVP molecules which can pass through the pore size

of the filter due to their narrow diameter. TEM images illustrated in Figure 6-28 b clearly show the presence of stable, spherical NPs in the suspension media. The images show both the NPs and bacteria cells. The presence of gold NPs at the end of the growth period is confirmed by the surface Plasmon resonance absorbance peak around 520 nm. MDM blank show no absorbance around 500 nm.

6.5 Conclusion

The main purpose of this chapter is to investigate the effect of the both the core size and the surface chemistry of NPs on environmental bacteria. Prior to the exposure to the bacteria, NPs were fully characterised and their stability in the bacterial growth media was investigated. The characterisation of the NPs in media is essential so that their effect on the bacteria cells can be compared and related to their properties in the media. Here, the behaviour of the AuNPs in different dilution of Minimal Davis media (MDM) was studied. The full strength media caused citrate capped NPs to aggregate immediately as confirmed by instantaneous colour change followed by disappearing surface Plasmon which completely vanished within 24 hours. TEM images have also showed big aggregates of the particles while the PVP capped NPs are relatively more stable in the undiluted media. This media has high ionic strength. Therefore, charge stabilised citrate capped NPs normally aggregate in high ionic media. When the media was diluted 4 times or more and the ionic strength was reduced both types of particles (citrate capped and PVP capped) were stable in the diluted media for a period of 2 weeks as measured with DLS and supported by SPR spectra. The stability of the NPs in the diluted MDM media is further confirmed by the TEM images of the samples which clearly showed the presence of single spherical AuNPs in the bacterial suspension media. After completing the stability test investigations, 4x diluted MDM media

was chosen for the investigation of the effect of the gold nanoparticles of different sizes and different coating agents on the *Pseudomonas fluorescens* since this dilution has guaranteed both the stability of the NPs and the bacterial growth. Different types of the NPs have manifested different effects on the bacteria growth. While both sizes (5 and 14.8 nm) citrate capped AuNPs have slightly increased the bacteria growth, the 10 nm PVP capped AuNPs slowed down the growth slightly. This emphasises the importance of the coating agents around the NPs for the bacteria-NPs interaction. Apart from the NP-bacteria interaction, the effect of gold ions on the bacteria was investigated. Gold ions of similar concentration as NPs have completely inhibited the bacteria growth and caused the immediate death of the cells. The important implication for future practice which has been highlighted in this research is the importance of studying the stability of the NPs in the growth media prior to their exposure to the bacteria. Taken together, The results from this research has shown that AuNPs of similar core size may affect differently on the growth of bacterial cultures due to their different surface chemistry which is determined by the type of coating agents.

Chapter 7: Interaction of gold NPs on Pseudomonas Fluoroscens

7.1 Introduction

Bacterial cells are delimited by their cell wall and membrane which consists of outer and inner cytoplasm membrane. The outer membrane is the barrier which normally has a direct contact with the environmental surrounding wherein the bacteria are living (Figure 7-1). The physicochemical properties of the wall and outer membrane are crucial and determine how substrates including NPs interact with bacterial cells. Equally important are the nature and properties of the surface chemistry of the NPs presented by the coating agents though the importance of this outer layer is many times ignored (Luo et al., 2010).

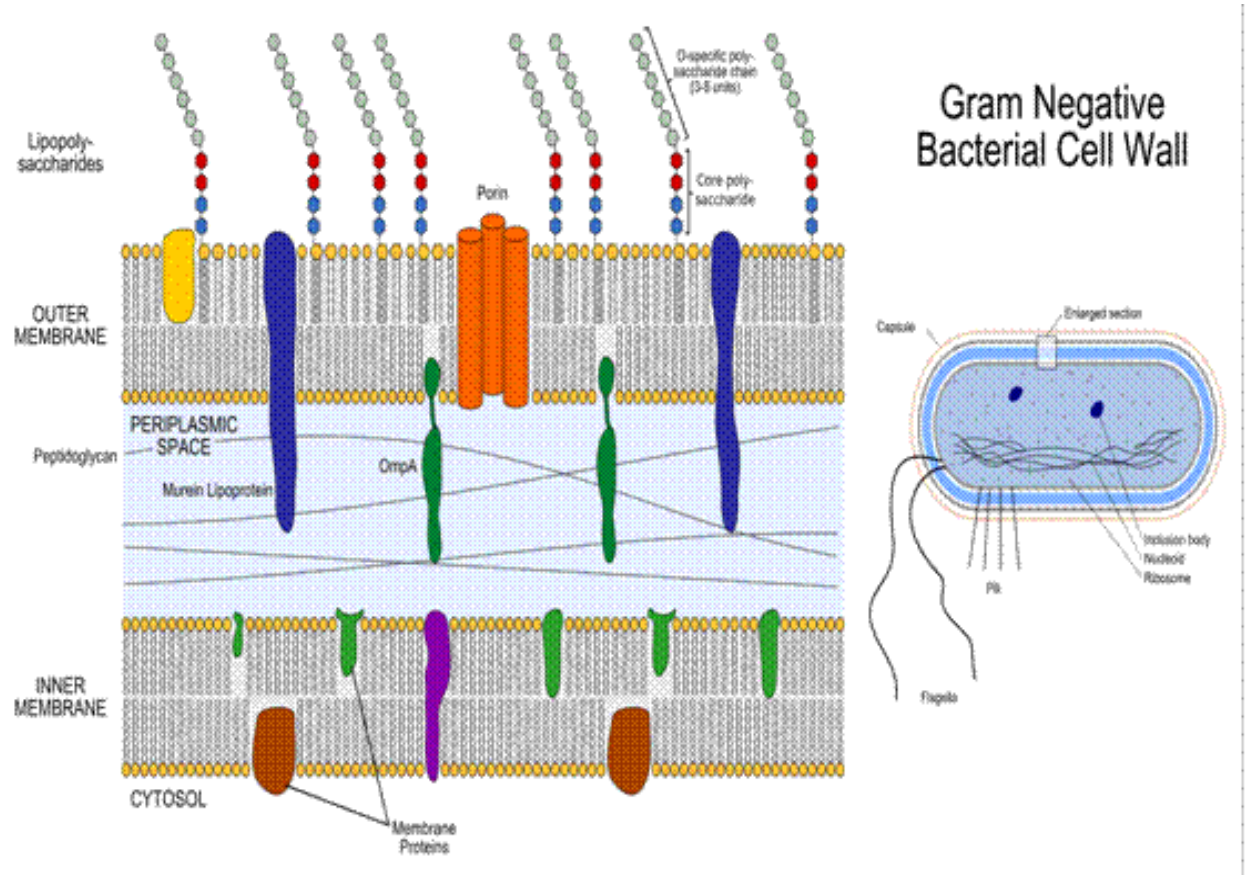

Figure 7-1: Schematic diagram showing details of gram negative bacterial cell wall, outer and inner membrane.(Dahl, 2008)

Any possible bacteria-NPs interaction is usually initialised by the interaction of outer membrane and the capping agents (Luo et al., 2010, Kang et al., 2007, Thill et al., 2006). This interaction may be the result of electrostatic forces based on the charge of the approaching surfaces (Stoimenov et al., 2002). The overall surface charge of the two types of bacteria gram positive and gram negative is negative charge due to the surface chemistry of the outer membrane. The outer membrane of the gram positive bacteria has carboxyl groups which by deprotonation form a negatively charged surface (Yee et al., 2004). Similarly the charge of the gram negative is originated by lipopolysaccharides which together with phospholipids are the main constituents of the outer cell membrane (De Castro et al., 2008, Raetz, 1990). This means that NPs with similar core sizes and shape may have different effects on the bacteria due to their different surface chemistry caused by their coating agents which is the main means of keeping NPs dispersed and preventing them from aggregation.

Depending on the type and surface structure of the NPs on one hand and on the type of bacterial cell membrane on the other hand the interaction effect may be manifested in different structural changes of the membrane including blebbing and tubule formation (Stachowiak et al., 2010) and enlargements of the membrane defects (Leroueil et al., 2007).

Because of their long known antimicrobial effect, silver nanoparticles (Ag-NP) have been widely studied and previous studies on their interaction with the different bacteria have shown different effects on the surface of the bacteria. Bovine serum stabilised silver nanoparticles (Ag-NP) have repeatedly disrupted and damaged the outer cell membrane of E.coli bacteria as studied by Pal et al (Pal et al., 2007). Membrane damages and formation of pits on the bacteria cell membrane caused by Ag-NP were reported by Sondi et al (Sondi and Salopek-Sondi, 2004).

Apart from the Ag-NPs, the interaction of bacteria with different surfaces and other types of nanoparticles were studied. The very abundant soil and water bacteria pseudomonas aurigenosa has developed a rigid cellular outer membrane on hydrophilic surfaces while the membrane become relatively soft in hydrophobic substrates (Luo et al., 2010). The disruption of the cell membrane of the pseudomonas aurigenosa and the subsequent uncontrolled leakage of cell DNA was reported after interacting with diaminopyrimidineethiol-functionalised, cationic 3 nm AuNPs (Zhao et al., 2010). Other studies (Stoimenov et al., 2002, Zhang et al., 2007) on ZnO have revealed similar effects on the bacterial cell membrane where alterations of membrane architecture and its permeability were reported. For a more complete list of the effect of nanoparticles on different types of bacteria can be referred to the Table 2-3 and Table 2-4 in chapter 2.

Despite the above mentioned isolated findings the exact mechanisms of how both natural and engineered NPs interact with bacterial outer membrane still remain a matter of investigation and are not yet well understood (Hayden et al., 2012). In this study gold nanoparticles with two different capping agents (PVP and citrate) were exposed on Pseudomonas flourescens bacteria growing in a liquid Minimal Davis Media (MDM). The bacteria-AuNPs interaction was investigated using TEM (see sections 3.1.2 for a detailed theoretical background of these techniques). The overall aims of this research were threefold.

1) To study the distribution of the NPs on the surface of the bacteria,

2) To observe any changes on the bacterial outer membrane

3) To investigate whether NPs are internalised in the bacteria cells.

Furthermore, any observed effect of the different surface chemistry of AuNPs on the bacteria membrane will be discussed and compared.

7.2 Results and discussion

Prior to any effect caused by nanoparticles on the bacteria, the interaction between the outer cell membrane and the coating agents of the nanoparticls needs to take place. This bacteria-NPs interaction is mediated by the properties of the outer membrane and the surface chemistry of the nanoparticls. The overall charge of the approaching surfaces may play a crucial role in this interaction. To confirm the charge of both AuNPs and Pseudomonas flourescens cells, the first measurement carried out prior to the bacteria- AuNPs interaction investigation was the measurement of the zeta potential as described in the following paragraphs.

7.2.1 Zetapotential measurement of the AuNPs and pseudomonas flouresencs

Charged particles in a solution are surrounded by ions of opposite charge which form a fixed layer around the charged particles. Beyond this fixed layer, there is an electrically neutral diffusive layer. When charged particles are placed in an electric field they move toward the oppositely charged electrode together with the fixed layer and small portion of the diffusive layer called sliding surface. Zeta potential is the electrical potential on the sliding surface and it is a measurement of the stability of the charged particles in the sense that the higher the zeta potential is the more stable the particles in the solution are. Aggregation of the particles occurs when the value of the zeta potential tends to zero(Elimelech et al., 1995). The zeta potential of the freshly synthesised AuNPs, the bacterial growth media and the purified bacteria cells through washing with milli-Q and centrifugating three times with 5000 rpm for 10 minutes were measured and summarised in Table 7-1 below.

Table 7-1: Electrokinetic properties of freshly synthesised AuNPs of different coating agents and bacteria cells both purified and in the growth media.

Sample type	Zetapotential N= 5	pH	Mobility N =5
Freshly prepared citrate capped AuNPs	-46.6 ± 2.4		-3.65 ± 0.19
Freshly prepared PVP capped AuNPs	-11.6 ± 1.3	7.63	-0.91 ± 0.10
Bacteria in 4x diluted Minimal Davis Media (MDM)	-29.0 ± 0.5	7.72	-2.27 ± 0.04
Purified bacteria in Milli-Q (see above)	-52.6 ± 0.8	6.79	-4.12 ± 0.07
4x diluted MDM	-34.3 ± 1.34	6.75	-2.69 ±0.10

.

The data in Table 7-1 shows that the zeta potential of citrate capped AuNPs are more negatively charged than the PVP capped AuNPs. This difference can be associated with the nature of the capping agents. Citrate is negatively charged ion dissociates from the three sodium citrate salt while PVP is long polymer with a limited dissociable functional groups (see Figure 7-2 below for the structure of citrate and PVP molecules).

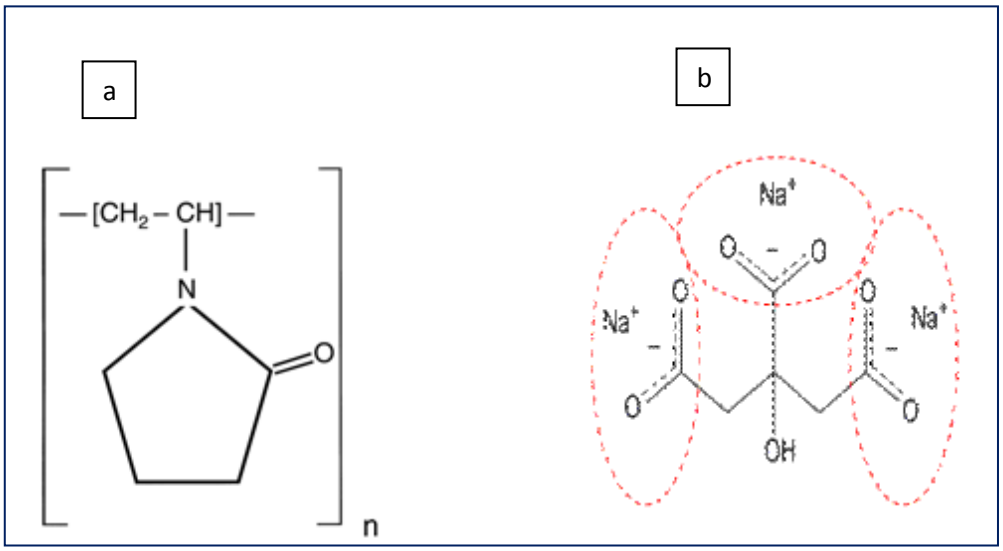

Figure 7-2: Structure of the a) PVP and B) citrate showing that citrate has three charged carboxyl functional groups while PVP has no charged functional group (Fooladi, 2009)

Further, it is worth value to know that the overall charge on the surface of the purified bacteria cells presented by their zeta potential is highly negatively charged more than both types of the NPs used.

7.2.2 Interaction of citrate capped AuNPs with the Pseudomonas flourescens

Citrate capped gold nanoparticles (G2 see Table 4-1 for the experimental conditions and Table 5-1 for detailed characterisation results of the sample) were added to the bacterial growth suspension in its exponential phase. After an incubation period of 2 days TEM samples were prepared through the drop method described in section 4.4.2 of the materials and methodology chapter and TEM images were recorded using both TEM JEOL 2100 and Jeol 1200. The findings were summarised in the following two sections.

7.2.2.1 Distribution of Citrate capped AuNPs on the surface body of the bacteria

It is worth value to know that in contrast to recently published findings where the accumulation of cationic monolayer protected AuNP on specific location on the membrane of Escherichia coli (Hayden et al., 2012) here the distribution of the AuNPs is completely random on and around the surface of the body of the bacteria. There were no localised accumulation of the NPs nor were there any signs of aggregation observed as can be seen by 8000x magnified images in Figure 7-3. This lack of self-organisation distribution of AuNP on the surface of bacteria (Staphylococus aureus) was previously reported by Chwalibog (Chwalibog, 2010).

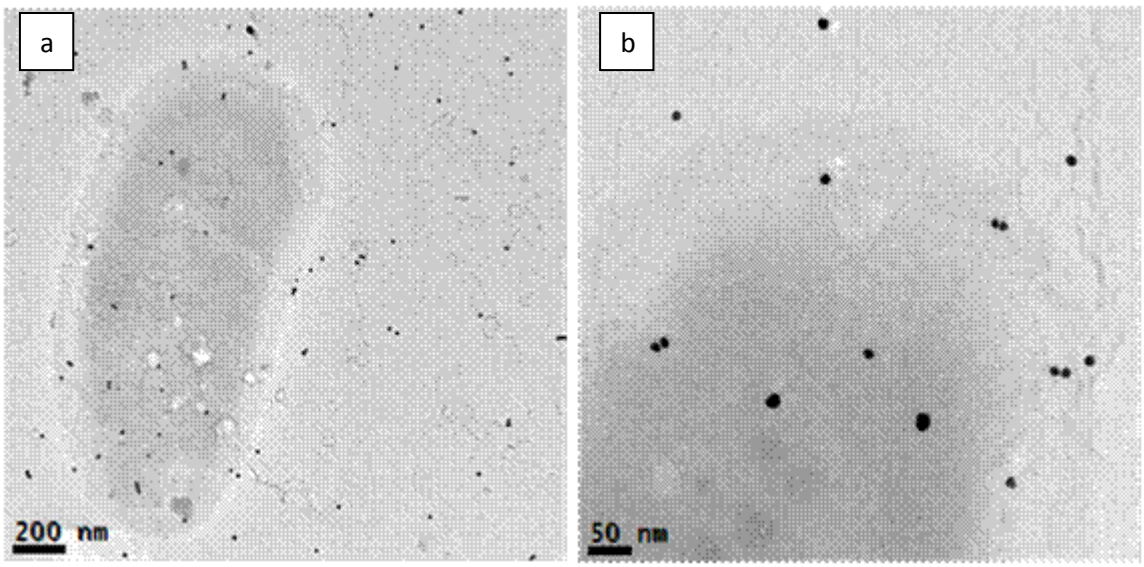

Figure 7-3:TEM images showing the random distribution of stable citrate capped AuNPs on and around the surface of the un-sectioned whole bacterial body a) 8000x magnified images b) 25000x magnified image.

This random distribution added to the lack of aggregation became more obvious through the images taken with higher magnification of 25000x (Figure 7-3 b) which shows single rounded AuNPs on and around the curvature of smooth, undamaged cell membrane. The stability of the AuNPs in the bacteria suspension is clearly confirmed.

7.2.2.2 Effect of citrate capped AuNPs on the outer membrane of the bacteria

Figure 7-4 below illustrates bacterial samples treated with G2 AuNPs. Different images represent different magnifications. Special attention was paid to detect any structural changes of the outer membrane of the bacterial cells. The smooth, undamaged outer membrane demonstrated by all images indicates that citrate capped gold nanoparticles have no effect on the structure of the membrane. Although it may be expected that due to the electrostatic repulsion between the negatively charged nanoparticles and negatively charged cell membrane (as shown by the zeta potential in Table 7-1 above) close membrane-NP interaction does not occur, Figure 7-4 below shows AuNPs touching on the membrane as indicated by arrows. Another important point of finding is that the citrate on the surface of nanoparticles

was not used as carbon source by the Pseudomonas flourescens bacteria. If the citrate capped molecules on the surface of the nanoparticle were consumed and removed by bacteria, aggregation of AuNPs was inevitable but the very stable nanoparticles in the suspension throughout the exposure period clearly show that they remained coated and stabilised by the citrate.

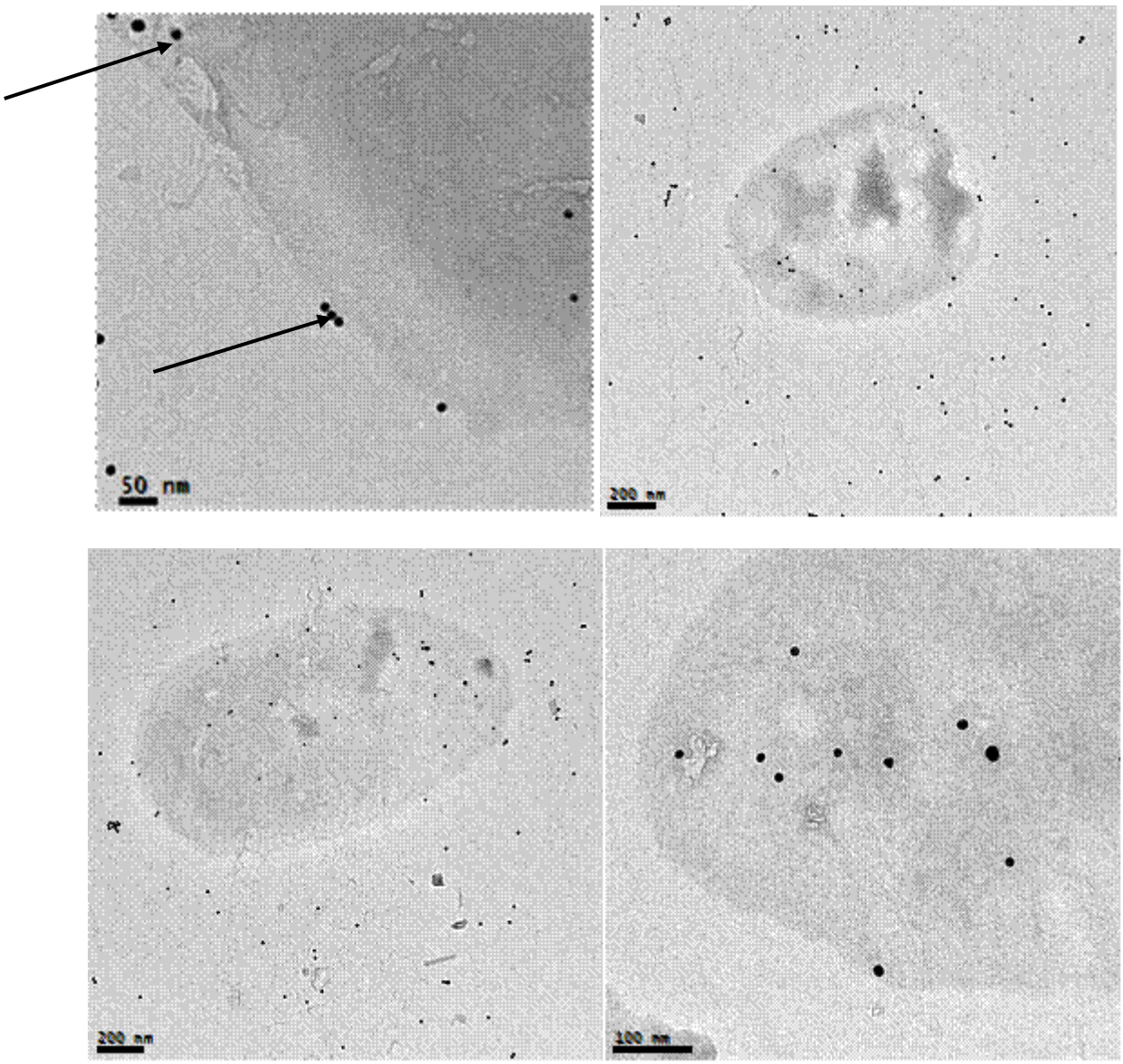

Figure 7-4: Images of bacterial cells treated with AuNPs capped with citrate. Arrows are indicating the stable AuNPs on the smooth, undamaged curvature of the bacterial cells.

7.2.3 Interaction of PVP capped NPs with the bacteria

The first observation is that PVP capped AuNPs are quite stable in the bacterial growth suspension and there were neither aggregation nor shape transformations observable (Figure 7-5). Furthermore, as in the case of citrate capped particles, the PVP capped particles are randomly distributed on and around the outer membrane of the bacteria cells. Again here there are no localised accumulations of the NPs on specific areas of the bacteria body. Another important observation is that these cells treated with PVP capped NPs (Figure 7-5 below) have produced more extracellular polysaccharides (EPS) pointed to with arrows between and around cells than the cells growing in blank media (see Figure 7-9 below for comparison).

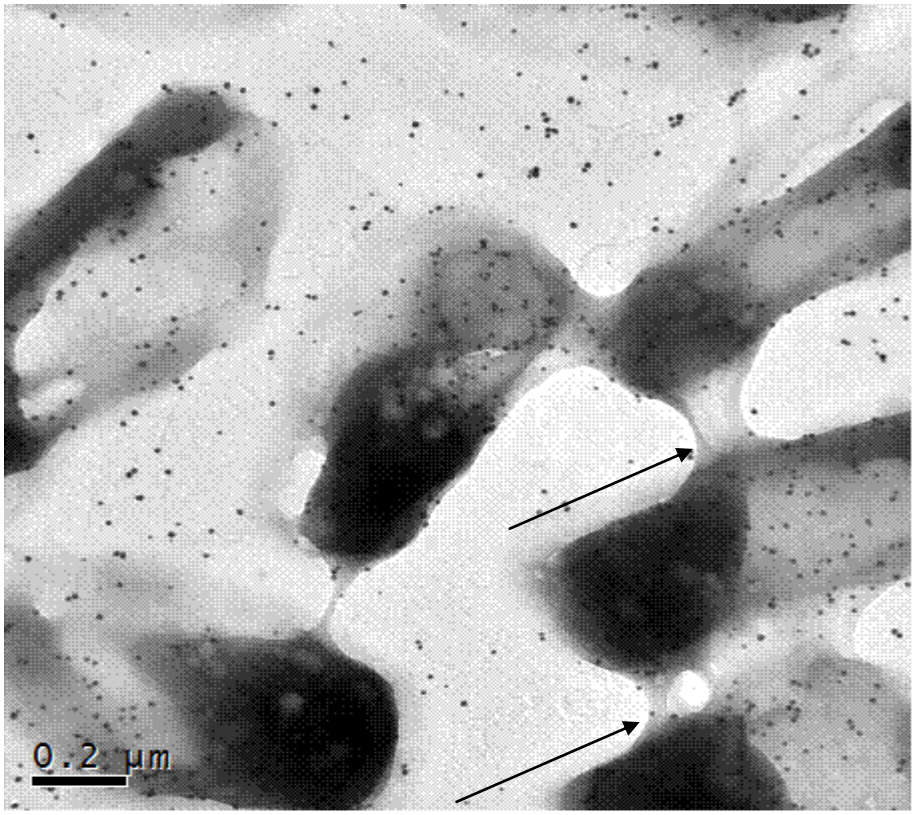

Figure 7-5: PVP capped AuNPs randomly distributed on and around *Pseudomonas fluorescens* cells. No aggregation of the NPs is visible in the bacteria growth media.

Unlike citrate capped AuNPs which have not shown any effect on the outer membrane of the bacterial cells, the effect of the PVP capped gold nanoparticles on the surface of the bacteria cells was apparent as can be seen in the following sections.

7.2.3.1 Holes on the surface of the bacteria

The severe damage on the outer membrane of the bacteria cells caused by the PVP capped AuNPs was manifested by the formation of wide holes on the surface of the membrane as presented with the TEM images in fFigure 7-6igure 6.6 below which are clearly showing this effect. Those holes which were absent in the images taken after the treatment of citrate capped AuNPs are much wider than the NPs (10 nm core size) treated. These wide holes may possibly facilitate the subsequent internalisation of the PVP capped gold nanoparticles in the cell. Similar effects caused by silver NPs on Escherichia coli were reported previously (Li et al., 2010b). Though the PVP molecules are slightly negatively charged, the electrostatic repulsion forces between the PVP capped gold nanoparticles and the outer membrane of the bacterial cells were not strong enough to prevent the adhesion of the PVP coated NPs on the outer-membrane facilitating the bacteria NPs interaction and the subsequent damage of the cell membrane.

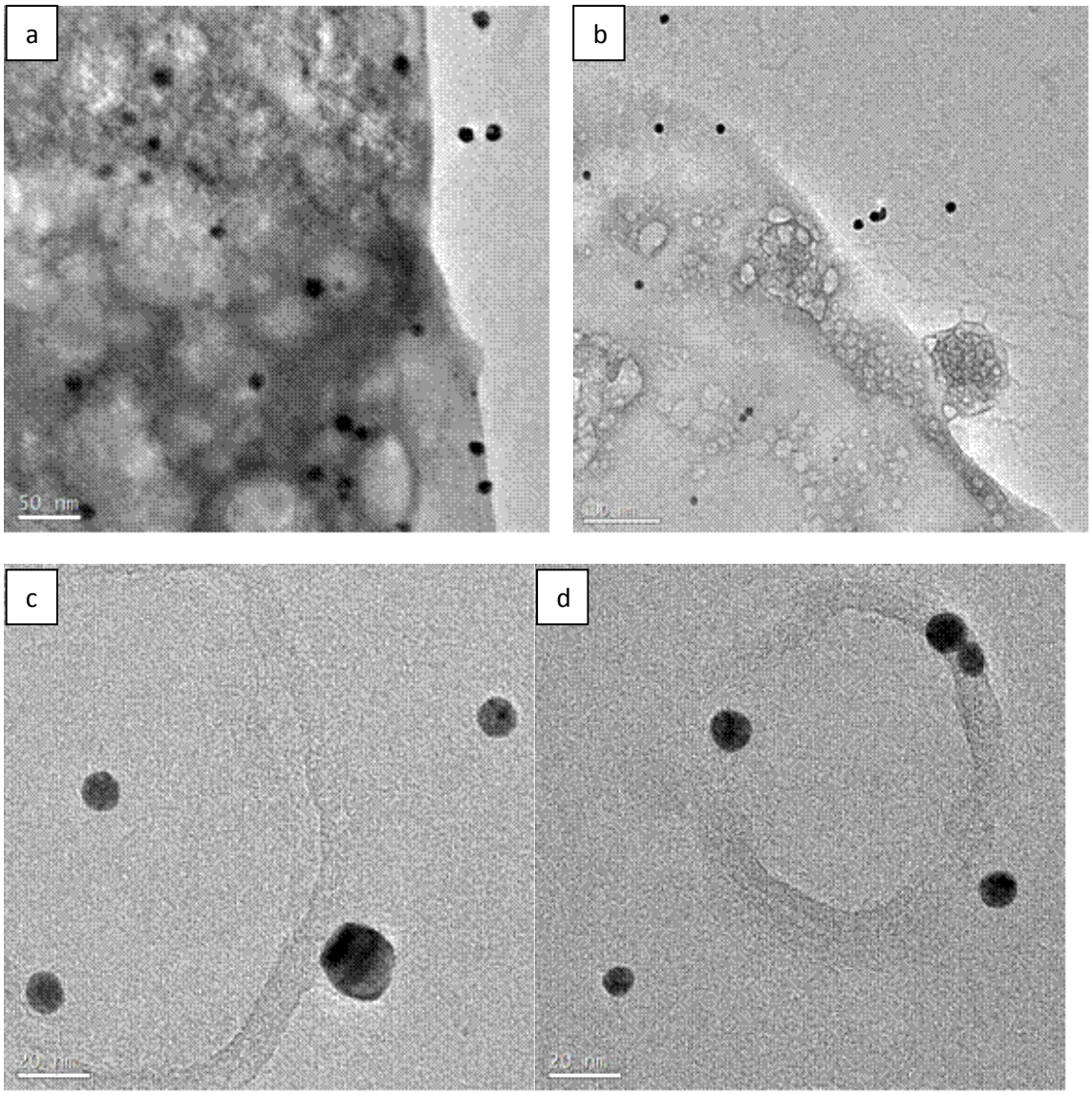

Figure 7-6: Apparent pits and wide holes on the surface of the outer membrane of the Pseudomonas fluorescens caused by PVP capped AuNPs. Images a and b are 8000x times magnified. c and d are 25000x magnified.

7.2.3.2 Blebbing on the surface of the bacteria

Another apparent effect on the surface of the outer- membrane of the bacteria cells caused by PVP capped AuNPs is the formation of blebbings which are abnormal vesicular outgrowths of the outer-membrane of the bacterial cells (indicated with arrows in Figure 7-7 below). Blebbings are clearly wider than NPs and some are around 100 nm in diameter (Figure 7-7 e.). Most Blebbings are more electron-dense then the rest of the bacteria cells which may indicate accumulation of NPs and the damaged material of the cell membrane.

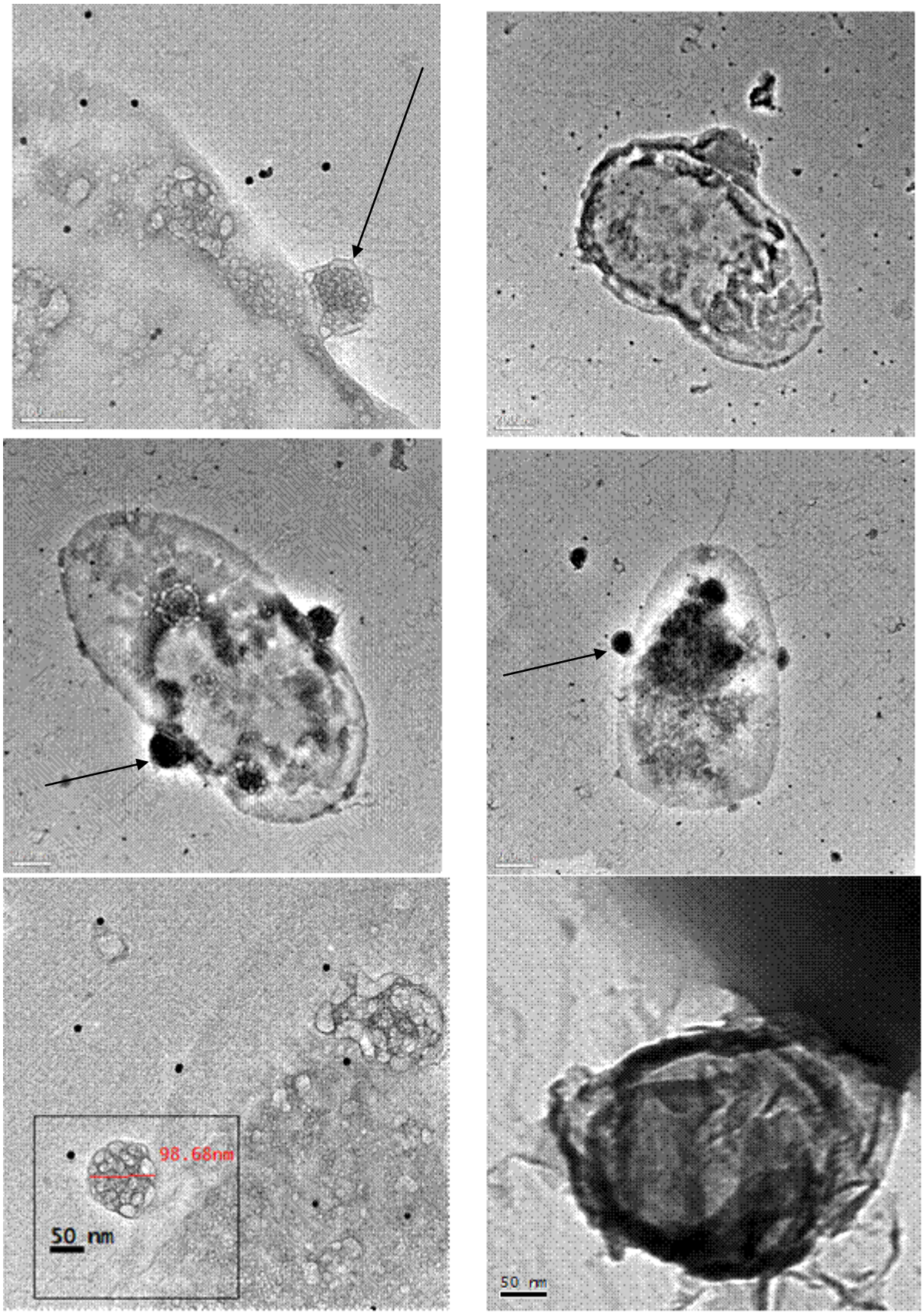

Figure 7-7: TEM images showing the Blebbings on the surface of *Pseudomonas fluorescens* cell membrane as effect of PVP capped AuNPs. Arrows are pointing to the places of the blebbing on the surface of bacterial cells.

7.2.3.3 Bursting bacterial cells and tubular formations

A more rigorous cell architecture damages than the previously mentioned blebbing formations are the complete bursting of some bacterial cells and the formation of long tubular structures on the surface of the outer membrane of the bacterial cells as shown in Figure 7-8 below. Both of these damages were manifested by the bacterial cells treated with PVP capped gold NPs unlike the citrate capped and blank samples inFigure 7-9.

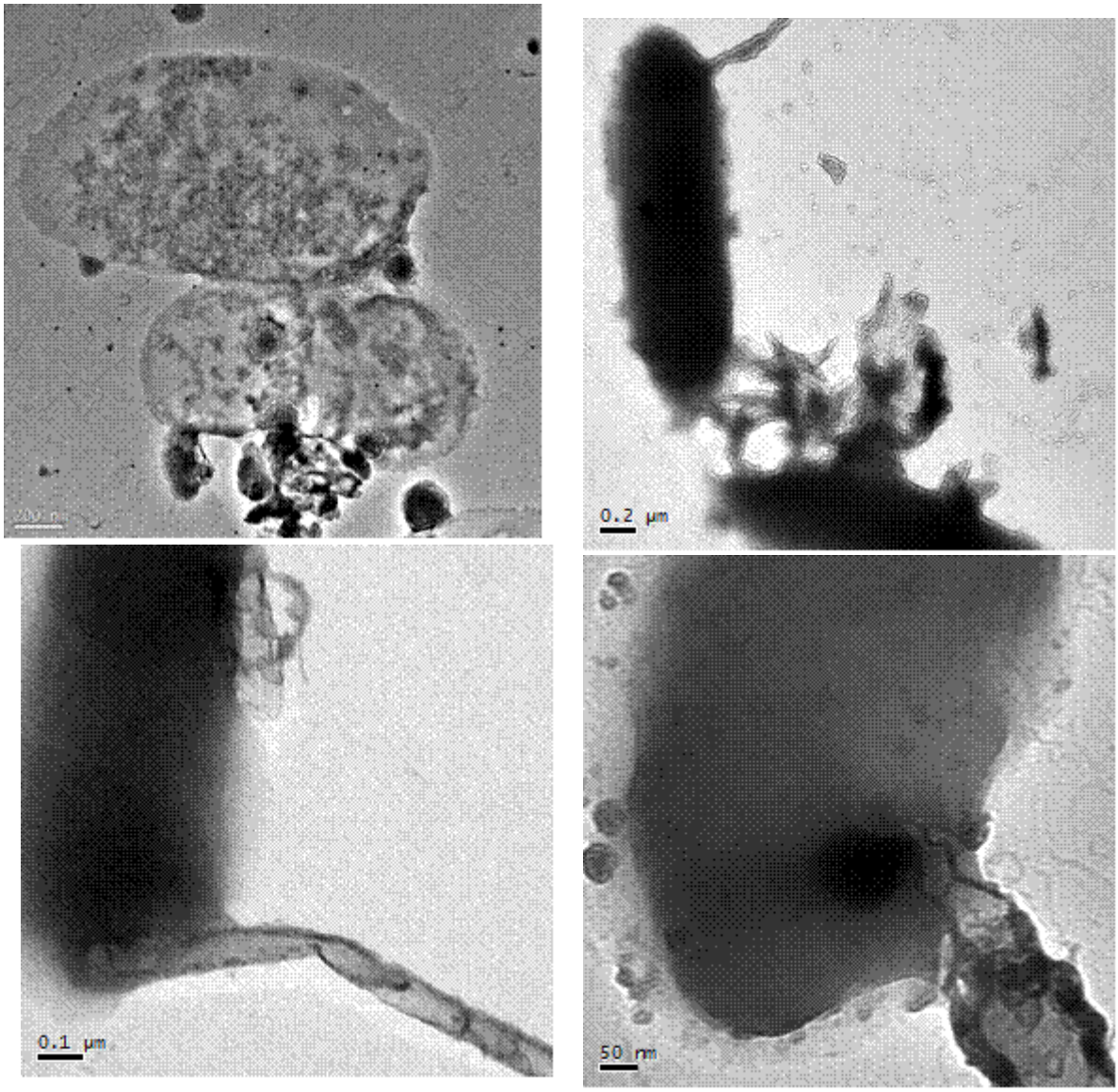

Figure 7-8: Bursting bacterial cell top row and tubular structures on the surface of the cell membrane bottom row caused by the AuNPs capped with PVP.

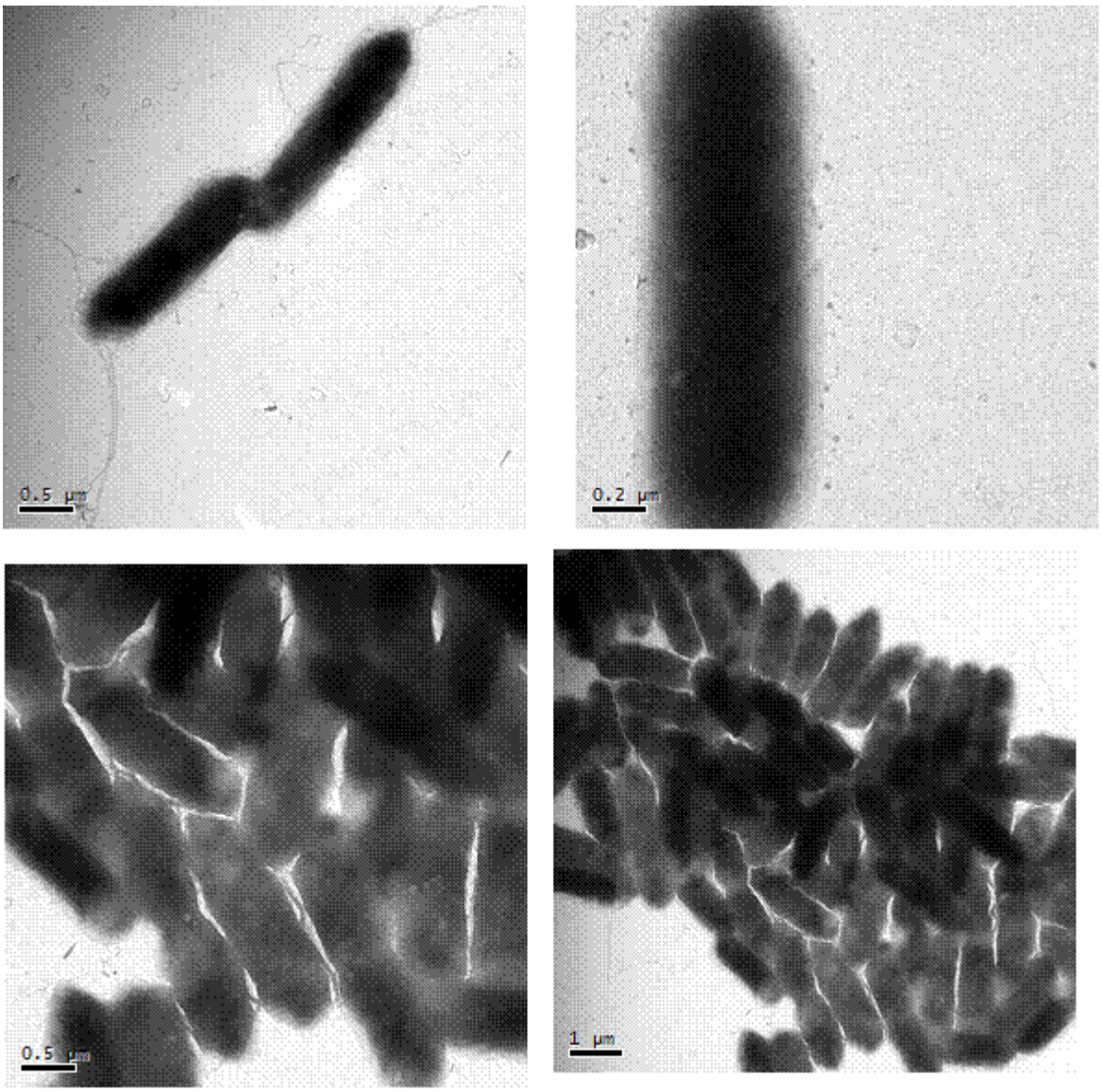

Figure 7-9:TEM images of bacterial cells grown in blank Minimum Davis Media (MDM). Cell membranes are smooth and undamaged.

7.2.4 Internalisation of the NPs in the bacteria cells

The toxicity of the NPs on the bacteria was many times attributed to the dissolved ions which easily follow through the cell membrane and manifest their toxicity in the cytoplasm (Ratte, 1999, Sambhy et al., 2006). This toxicity of the ions was supported by the data presented in chapter 5 section 6.4.1.4 which shows complete inhibition of the bacteria growth after the

treatment of final concentration of 10 ppm gold ions. However, recent studies have reported the actual internalisation of the NPs in the bacterial cells and the presence of both Ag-NPs (Morones et al., 2005b) and metaloxides (ZnO and MgO) (Sinha et al., 2011, Stoimenov et al., 2002) inside bacterial cells were confirmed.

The wide holes on the outer membrane of the bacteria caused by the PVP capped NPs described above in section 7.2.3.1 may form easy pathways for the NPs to get inside the bacteria cells. To study these effect, bacterial cells in their exponential growth phase were treated with PVP capped NPs. After an 8-hour exposure bacterial cells were fixed using phosphate buffered non-coagulant dialdehyde glutaraldehyde fixative which stops all biochemical reaction through forming a covalent bonding bridge between proteins in the cells and making them insoluble. In this way, all biological activities were frozen and the structure of the samples was preserved. The so prepared samples were then sectioned into ultra-thin-sections using ultra-microtone and stained with uranylacetate to provide contrast for the followed TEM imaging. Sections were placed on TEM copper grid and analysed using jeol2100 operating with 200KV (see section 3.1.2 in the methodology chapter for detailed description of the TEM microscope). Results were presented in Figure 7-10 below. 8 hours was chosen as exposure time since bacteria cells may die naturally if much longer time is waited and their membrane may get damaged if the time allocated for exposure is longer.

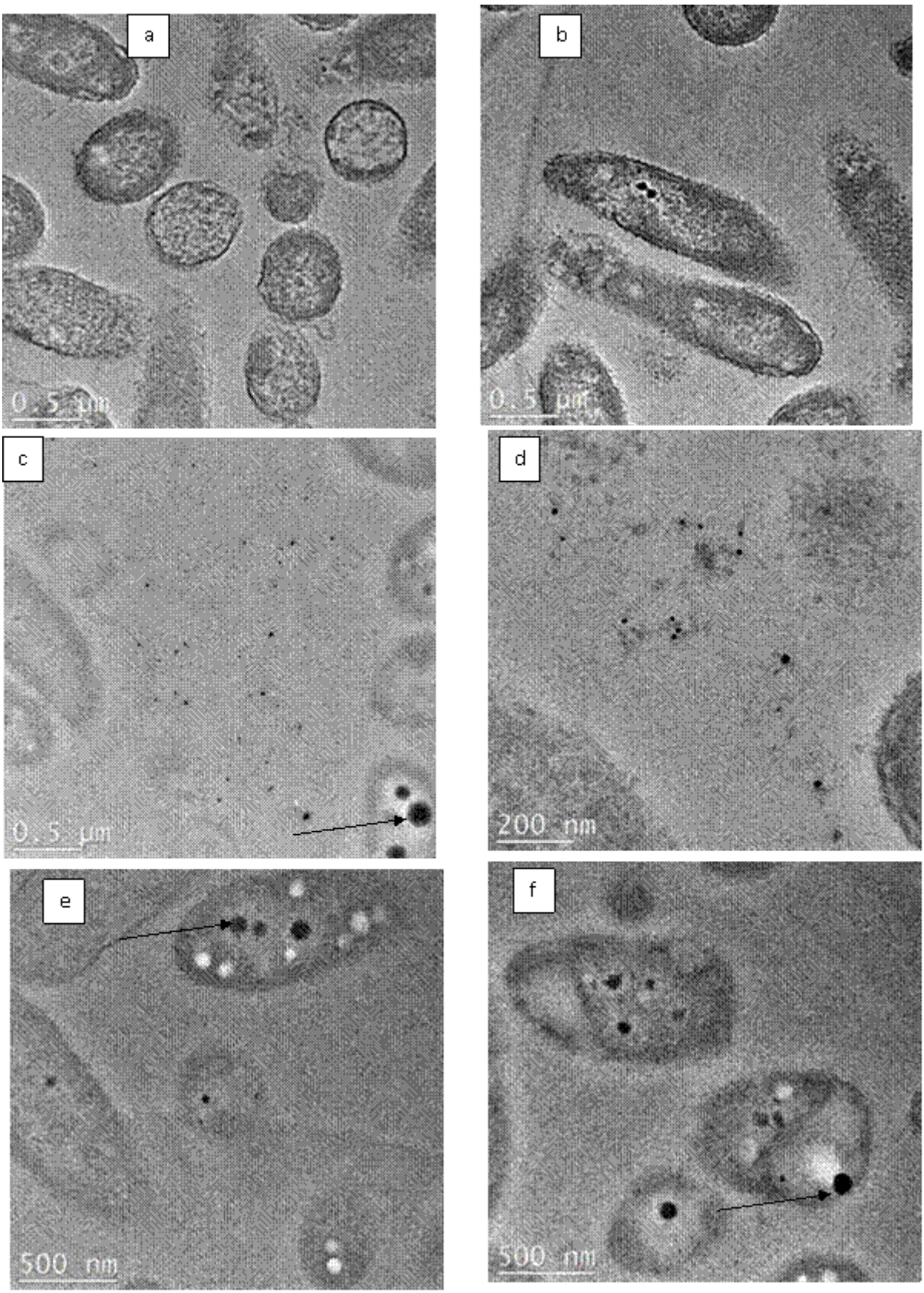

Figure 7-10: TEM images showing the sections of bacterial cells. Image c shows stable AuNPs outside the cells. Images c, e and f represent different magnifications and all show aggregates of more electron dense dark materials in the cells as pointed with arrows. Sections d shows atable AuNPs distributed outside bacteria cells. Sections a and b are lower magnifications and they only show bacterial cell sections.

Sections of the bacterial cells can be particularly seen in the top row of Figure 7-10. Bacterial cells were sectioned randomly in different positions. Some of them longitudinally in the whole length of the rode shape bacterial cells while others were sectioned halfway through or just the top of the cell was trimmed. The presence of stable gold NPs in extracellular media between sections of the bacterial cells can easily be seen in Figure 7-10 c and d as indicated with arrows. What is more interesting to observe are the darker electro-dense areas in some cells as shown in Figure 7-10 c, e and f and indicated with arrows. These can be aggregates of the NPs in the cells. To confirm whether or not the more electron-dense dots inside the sections of the bacterial cells are aggregates of AuNPs, EDX spectrum of a normal point in the cell was recorded (Figure 7-11 below) and compared with EDX spectra of the some black dots (Figure 7-12 below).

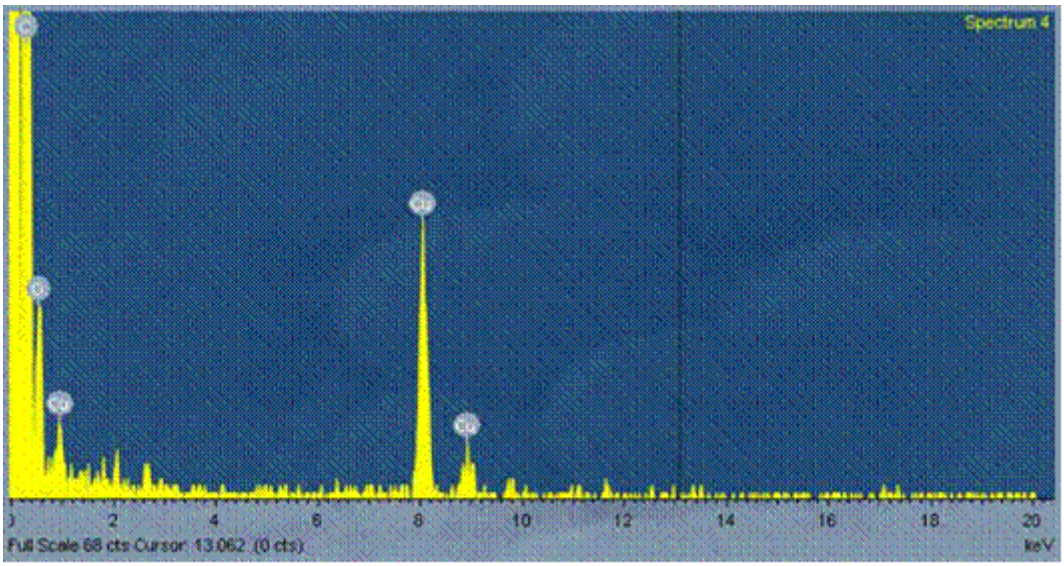

Figure 7-11: EDX spectrum of a normal point inside the cell but outside the more electron-dense black areas in the bacterial cells. EDX spectrum were taken with Jeol 2100 TEM.

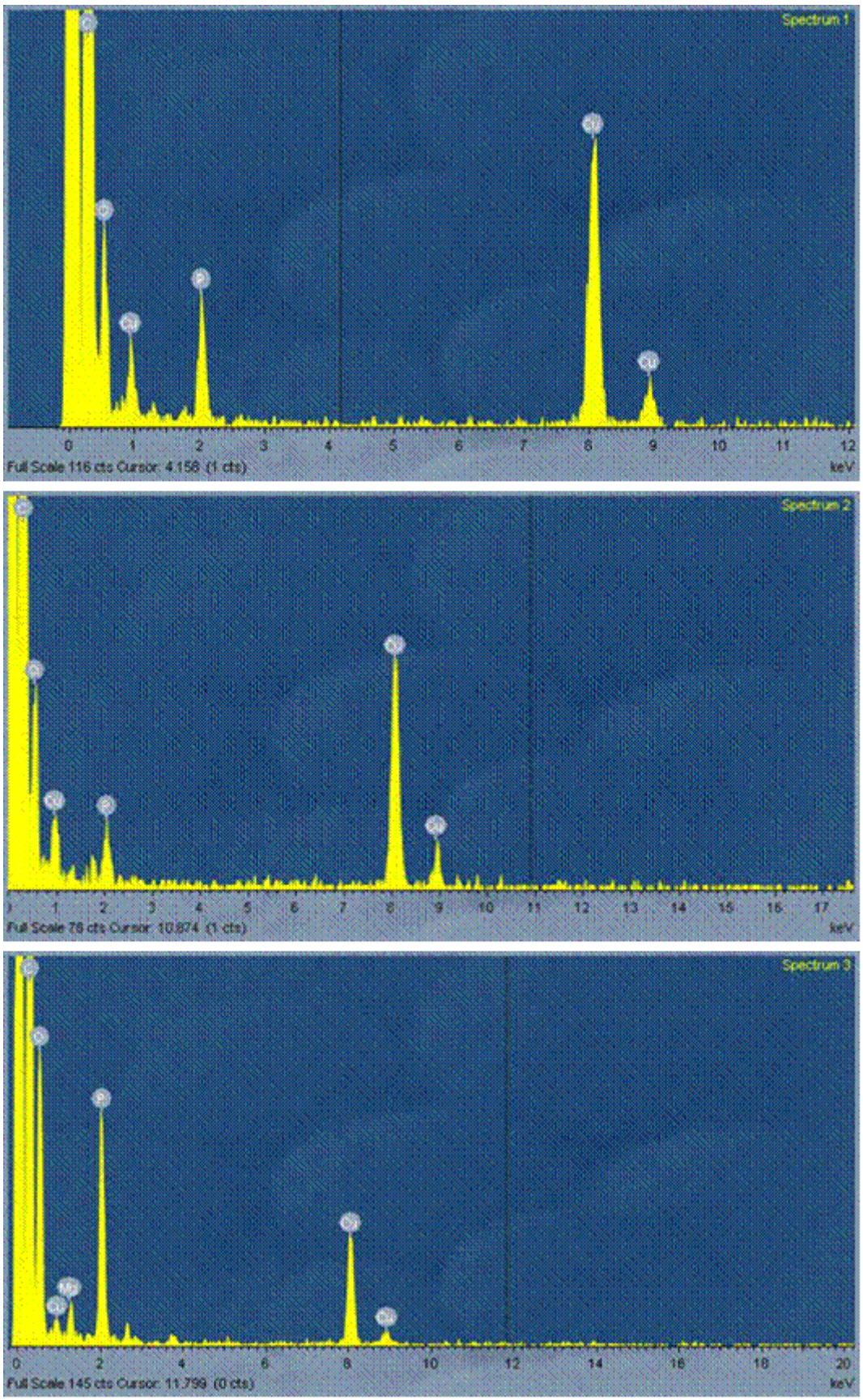

Figure 7-12: EDX spectra of black more electron-dense areas inside the bacterial cells sections.

The EDX spectra of the black dots which were presumably supposed to represent aggregations of AuNPs, have not shown the presence of gold element. Similarly, the EDX spectrum taken outside the black more electron-dense areas did not show any gold NPs. Since the main element present in the EDX analysis and shown in the spectra is copper, it is probably copper from the TEM grid that presents the black dots. Therefore, it can be concluded that internalisation of gold NPs in the Pseudomonas flourescens bacteria cells did not take place.

7.3 Conclusion

Finally, this study has shown that both citrate capped AuNPs and PVP capped AuNPs are very stable in the bacteria growth suspension. There were no aggregation or shape changes observable. Furthermore, unlike citrate capped AuNPs which have not affected the membrane of the bacteria PVP capped AuNPs have a significant effect on the morphological structure of the outer membrane leading to the formation of wide holes, blebbing, tubular formation on the surface of bacteria membrane and complete bursting of the affected bacterial cells. Since citrate capped AuNPs are much more negatively charged than the PVP capped ones previous studies (Stoimenov et al., 2002, Hamouda and Baker, 2000) speculated the importance of electrostatic interaction for the bacteria-NPs interaction but in this study the actual contact of citrate capped NPs on the surface of the cell membrane is visualised. The two types of NPs used here were both spherical in shape and had similar sizes they do only differ in the coating agents. The environmental implication of this finding is that the effect of environmental NPs on microorganism is mainly determined by the type and surface chemistry of the coating agents such as organic humid substances.

Chapter 8: Conclusion and further work

Nanotechnology is a quite recent and promising field due to the novel and useful applications of the nanomaterials (NM)) which form the basis for many technological fields and scientific areas. This field has opened the door for the production of uncountable new materials due to the discovery of fascinating and unique properties of the matter in the nanoscale. The influence of the nanotechnology on modern society is both explained and justified by the scale of the variety of scientific and technological applications using nano-based ideas. It is very clear that these products will sooner or later reach the environment. Although engineered nanoparticles are designed to fulfil a special purpose and we may have an idea about their original properties during their production, the fate and properties of the NPs, once released in the environment, may differ partially or completely from their original physicochemical properties due to a number of possible reasons: they may form aggregates of macroscale, get coated with organic matter in the environment or interact with other inorganic nanosized particles in nature.

One of the most noteworthy facts to consider regarding nanoparticles is their impact on the natural environment both in short and long term exposures. It is interesting to note that the scientific community is more than ever ready and willing to know and assess the possible adverse effects of nanotechnology on the environment in order not to commit the past mistakes of producing, using and releasing new products (such as asbestos, plastic) into the environment without knowing their impact on different compartments of our planet. In fact, among all environmental compartments, the biomass population is by far the most vulnerable to the effects of the released products into the environment.

As part of the scientific curiosity of understanding the effects of the NPs in the environment, this study was set out to explore the effects of the NPs on planktonic bacteria abundant in the environment. The overall aim of the study was to investigate both the bacterial growth and the inhibition effect of the NP and the interaction of NPs on lab - grown bacteria and interpret this interaction in terms of property-response relationship. Special attention was paid to the effect of both core size and surface chemistry of the NPs on the bacteria by producing well constrained nanomaterials in terms of size, shape, dispersion and stability. Nanoparticles with core sizes varying from 5 nm to 85 nm and with two different coating agents were synthesised using wet chemistry bottom up synthesis methods. A comprehensive list of analytical and imaging techniques was used to fully characterise these freshly - synthesised NPs. Since the size, shape and monodispersity of gold NPs are fundamental features of their effect on the living organisms, these fully - characterised gold NPs can form a reliable basis for a potential reference material which helps the identification of the ecotoxicological effects caused by certain nano-property. The range of sizes and coating agents will provide more versatility for the study of property – effect relationship in (eco) toxicology studies. The stability of the AuNPs for a period of at least six months was monitored. The NPs showed no change in size and shape. The need for testing the stability of the NPs in the bacterial growth media and for fully characterising them in the media in terms of their original physicochemical properties - such as size and shape prior to the exposure process - is profoundly important since the media conditions may alter the intrinsic properties of the NPs and, therefore, make it difficult to interpret any possible effect.

After extensive characterisation of the NPs in the coating agent media and bacterial growth media (Minimal Davis Media), the effect of the size and coating agents on environmental abundant bacteria *Pseudomonas fluorescens* were investigated. Nanoparticles of comparable

size and concentration but with different coating agents were exposed to the bacteria. It was found out that NPs with different coating agents of similar final concentrations manifested different effects on the bacteria exposed. PVP coated 10 nm core sizes gold NPs with final concentration of 10 ppm have reduced the growth of bacteria compared to the Minimum Davis Media blank. This adverse effect was manifested by the bacterial cells in the form of outer membrane damage as confirmed by the TEM images of the cells. Blebbings and tubular formation on the surface of the bacterial outer membrane and wide holes on the membrane were signs of membrane damages after NPs exposure. Complete bursting of effected bacterial cells was also visualised. In contrast, citrate - capped NPs of similar concentration and core size as the aforementioned PVP coated NPs have slightly increased the growth of the bacteria This finding supports the idea that surface chemistry of the NPs is a very important factor in terms of the effect of the NPs on the bacterial cells. Any interaction between the NPs and the bacterial cells starts with the contact of the coating agent of the NPs on the outer cell membrane. Consequently, the bacteria was grown in both PVP and citrate solution without any other carbon source. It was found out that bacteria can utilise citrate as carbon source but not the PVP. This finding has explained why bacteria growth was slightly increased in the citrate - capped NPs solution. Finally, gold ions of similar concentration as the above - mentioned NPs solutions have completely inhibited the bacteria growth and caused the immediate death of the bacterial cells.

What makes this research unique and different from many ecotoxicology studies is the four - step process employed here:

- ✓ Synthesising well - constrained NPs.
- ✓ Fully characterising them and studying their stability for the relevant period of time.

- ✓ Characterising the NPs in the bacterial growth media prior to the bacterial exposure to ensure any change of the physicochemical properties of the NPs in the media since any property change may complicate the data interpretation after exposure.

- ✓ Post exposure characterisation of both NPs and bacterial cells.

The aforementioned four steps are necessary to carry out in order to relate NPs property to the cell response. Although it is possible that some researches have characterised the NPs after synthesis, studies that sought to fully characterise the NPs both in the growth media and after exposure are rare or non – existent.

Notwithstanding the fact that the effect of the coating agents on the outer cell membrane is visualised in the form of blebbing and wide wholes on the surface of the membrane, the nature and the mechanisms of the interaction between NPs and cells need further research. The bacterial population in the environment can exist either as unicellular planktonic or in more sessile communities in the form of biofilm. Therefore, both the transport of the NPs in the biofilm and their effects on the structure of the biofilm will be an interesting area for further investigation and will contribute to our understanding of this relatively new technology on the natural environment.

References

ABELIOVICH, A. 1992. Transformations of ammonia and the environmental impact of nitrifying bacteria. *Biodegradation,* 3**,** 255-264.

ADAMS, L. K., LYON, D. Y. & ALVAREZ, P. J. J. 2006. Comparative eco-toxicity of nanoscale TiO2, SiO2, and ZnO water suspensions. *Water Research,* 40**,** 3527-3532.

AHMAD, T., WANI, I. A., MANZOOR, N., AHMED, J. & ASIRI, A. M. 2013. Biosynthesis, structural characterization and antimicrobial activity of gold and silver nanoparticles. *Colloids and Surfaces B-Biointerfaces,* 107**,** 227-234.

AITKEN, R. J., CHAUDHRY, M. Q., BOXALL, A. B. A. & HULL, M. 2006. Manufacture and use of nanomaterials: current status in the UK and global trends. *Occupational Medicine,* 56**,** 300-306.

AKAIGHE, N., MACCUSPIE, R. I., NAVARRO, D. A., AGA, D. S., BANERJEE, S., SOHN, M. & SHARMA, V. K. 2011. Humic Acid-Induced Silver Nanoparticle Formation Under Environmentally Relevant Conditions. *Environmental Science & Technology,* 45**,** 3895-3901.

ALBRECHT, T. R., MIZES, H. A., NOGAMI, J., PARK, S.-I. & QUATE, C. F. 1988. Observation of tilt boundaries in graphite by scanning tunneling microscopy and associated multiple tip effects. *Applied Physics Letters,* 52**,** 362-364.

ALIVISATOS, A. P. 1996. Semiconductor Clusters, Nanocrystals, and Quantum Dots. *Science,* 271**,** 933-937.

ALLISON, D. G., GILBERT, P., LAPPIN-SCOTT, H.M., AND WILSON,M. 2000. *Community Structure and Co-orporation in Biofilms,* London, Cambridge University Press.

AMIN, R. M., MOHAMED, M. B., RAMADAN, M. A., VERWANGER, T. & KRAMMER, B. 2009. Rapid and sensitive microplate assay for screening the effect of silver and gold nanoparticles on bacteria. *Nanomedicine,* 4**,** 637-643.

AMMANN, A. A. 2007. Inductively coupled plasma mass spectrometry (ICP MS): a versatile tool. *Journal of Mass Spectrometry,* 42**,** 419-427.

AMMERMAN, J. W. 2003a. Phosphorus Cycling in Aquatic Environments: Role of Bacteria. *Encyclopedia of Environmental Microbiology.* John Wiley & Sons, Inc.

AMMERMAN, J. W. 2003b. Phosphorus Cycling in Aquatic Environments: Role of Bacteria. *Encyclopedia of Environmental Microbiology*. New York, USA: John Wiley & Sons, Inc.

ANGUS, J. C., MORROW, D. L., DUNNING, J. W. & FRENCH, M. J. 1969. MOTION MEASUREMENT BY LASER DOPPLER TECHNIQUES. *Industrial & Engineering Chemistry,* 61**,** 8-20.

ARBAB, A. S., BASHAW, L. A., MILLER, B. R., JORDAN, E. K., LEWIS, B. K., KALISH, H. & FRANK, J. A. 2003. Characterization of Biophysical and Metabolic Properties of Cells Labeled with Superparamagnetic Iron Oxide Nanoparticles and Transfection Agent for Cellular MR Imaging1. *Radiology,* 229**,** 838-846.

ARNAOUT, C. L. & GUNSCH, C. K. 2012. Impacts of Silver Nanoparticle Coating on the Nitrification Potential of Nitrosomonas europaea. *Environmental Science & Technology,* 46**,** 5387-5395.

ASAHARA, T., KOSEKI, H., TSURUMOTO, T., SHIRAISHI, K., SHINDO, H., BABA, K., TAODA, H. & TERASAKI, N. 2009. The bactericidal efficacy of a photocatalytic TiO2 particle mixture with oxidizer against Staphylococcus aureus. *Japanese Journal of Infectious Diseases,* 62**,** 378-380.

ATES, M., DANIELS, J., ARSLAN, Z. & FARAH, I. O. 2013. Effects of aqueous suspensions of titanium dioxide nanoparticles on Artemia salina: assessment of nanoparticle aggregation, accumulation, and toxicity. *Environmental Monitoring and Assessment,* 185**,** 3339-3348.

ATOMICWORLD. 2012. *Basic principle of transmission electron microscope* [Online].

BAALOUSHA, M.JU-NAM, Y., COLE, P. S., V. , FERNANDES, T., JEPSON, M. A., LEAD, J., HIRILJAC, J. A. & JONES, I. P. 2012a. Characterization of cerium oxide nanoparticles. Part 1: Size measurements. Environ.Toxicol.Chem.(Accepted) . 2012b. . *Environ.Toxicol.Chem.*

BAALOUSHA, M. 2009. Aggregation and disaggregation of iron oxide nanoparticles: Influence of particle concentration, pH and natural organic matter. *Science of The Total Environment,* 407**,** 2093-2101.

BAALOUSHA, M., JU-NAM, Y., COLE, P., STONE, V., FERNANDES, T., JEPSON, M. A. & LEAD, J. 2012b. Characterization of cerium oxide nanoparticles. Part 2: non-size properties. Environ.Toxicol.Chem.(Accepted) . 2012a. *Environ.Toxicol.Chem.*

BAALOUSHA, M., MANCIULEA, A., CUMBERLAND, S., KENDALL, K. & LEAD, J. R. 2008. Aggregation and surface properties of iron oxide nanoparticles: Influence of ph and natural organic matter. *Environmental Toxicology and Chemistry,* 27**,** 1875-1882.

BAALOUSHA, M., NUR, Y., RÖMER, I., TEJAMAYA, M. & LEAD, J. R. 2013. Effect of monovalent and divalent cations, anions and fulvic acid on aggregation of citrate-coated silver nanoparticles. *Science of The Total Environment,* 454–455**,** 119-131.

BAALOUSHA, M., STOLPE, B. & LEAD, J. R. 2011. Flow field-flow fractionation for the analysis and characterization of natural colloids and manufactured nanoparticles in environmental systems: A critical review. *Journal of Chromatography A,* 1218**,** 4078-4103.

BABALOLA, O. 2010. Beneficial bacteria of agricultural importance. *Biotechnology Letters,* 32**,** 1559-1570.

BABYNIN, E. V., NURETDINOV, I. A., GUBSKAYA, V. P. & BARABANSHCHIKOV, B. I. 2002. Study of mutagenic activity of fullerene and some of its derivatives using his plus reversions of Salmonella typhimurium as an example. *Russian Journal of Genetics,* 38**,** 359-363.

BADAWY, A. M. E., LUXTON, T. P., SILVA, R. G., SCHECKEL, K. G., SUIDAN, M. T. & TOLAYMAT, T. M. 2010. Impact of Environmental Conditions (pH, Ionic Strength, and Electrolyte Type) on the Surface Charge and Aggregation of Silver Nanoparticles Suspensions. *Environmental Science & Technology,* 44**,** 1260-1266.

BAGRII, E. I. & KARAULOVA, E. N. 2001. New in fullerene chemistry (a review). *Petroleum Chemistry,* 41**,** 295-313.

BAILEY, R. E. & NIE, S. 2003. Alloyed Semiconductor Quantum Dots: Tuning the Optical Properties without Changing the Particle Size. *Journal of the American Chemical Society,* 125**,** 7100-7106.

BALDASSARI, S., KOMARNENI, S., MARIANI, E. & VILLA, C. 2005. Microwave-hydrothermal process for the synthesis of rutile. *Materials Research Bulletin,* 40**,** 2014-2020.

BAMWENDA, G. R. & ARAKAWA, H. 2000. Cerium dioxide as a photocatalyst for water decomposition to O2 in the presence of Ceaq4+ and Feaq3+ species. *Journal of Molecular Catalysis A: Chemical,* 161**,** 105-113.

BANFIELD, J. F., WELCH, S. A., ZHANG, H., EBERT, T. T. & PENN, R. L. 2000. Aggregation-Based Crystal Growth and Microstructure Development in Natural Iron Oxyhydroxide Biomineralization Products. *Science,* 289**,** 751-754.

BARNES, R. J., RIBA, O., GARDNER, M. N., SCOTT, T. B., JACKMAN, S. A. & THOMPSON, I. P. 2010. Optimization of nano-scale nickel/iron particles for the reduction of high concentration chlorinated aliphatic hydrocarbon solutions. *Chemosphere,* 79**,** 448-454.

BASSO, M., GIARRE, L., DAHLEH, M. & MEZIC, I. Numerical analysis of complex dynamics in atomic force microscopes. Control Applications, 1998. Proceedings of the 1998 IEEE International Conference on, 1-4 Sep 1998 1998. 1026-1030 vol.2.

BAUGHMAN, R. H., ZAKHIDOV, A. A. & DE HEER, W. A. 2002. Carbon Nanotubes--the Route Toward Applications. *Science,* 297**,** 787-792.

BEEK, W. J. E., WIENK, M. M. & JANSSEN, R. A. J. 2004. Efficient Hybrid Solar Cells from Zinc Oxide Nanoparticles and a Conjugated Polymer. *Advanced Materials,* 16**,** 1009-1013.

BELLLONI, J. 1996. Metal Nanocolloids. *Current Opinion in Colloid & Interface Science,* 1**,** 184-196.

BELSER, L. W. 1979. POPULATION ECOLOGY OF NITRIFYING BACTERIA. *Annual Review of Microbiology,* 33**,** 309-333.

BERNE, B. J. & PECORA, R. 2000. *Dynamic Light Scat*terin, New York, USA**,** Dover Publications.

BETTMER, J., JAKUBOWSKI, N. & PRANGE, A. 2006. Elemental tagging in inorganic mass spectrometric bioanalysis. *Analytical and Bioanalytical Chemistry,* 386**,** 7-11.

BIANCO, A. & PRATO, M. 2003. Can Carbon Nanotubes be Considered Useful Tools for Biological Applications? *Advanced Materials,* 15**,** 1765-1768.

BINNIG, G., QUATE, C. F. & GERBER, C. 1986. Atomic Force Microscope. *Physical Review Letters,* 56**,** 930.

BINNIG, G. & ROHRER, H. 1987. Scanning tunneling microscopy—from birth to adolescence. *Reviews of Modern Physics,* 59**,** 615-625.

BINNIG, G., ROHRER, H., GERBER, C. & WEIBEL, E. 1982a. Surface Studies by Scanning Tunneling Microscopy. *Physical Review Letters,* 49**,** 57-61.

BINNIG, G., ROHRER, H., GERBER, C. & WEIBEL, E. 1982b. Tunneling through a controllable vacuum gap. *Applied Physics Letters,* 40**,** 178-180.

BISWAS, P. & WU, C. Y. 2005. 2005 Critical Review: Nanoparticles and the environment. *Journal of the Air & Waste Management Association,* 55**,** 708-746.

BLACKMAN, G. S., MATE, C. M. & PHILPOTT, M. R. 1990. Interaction forces of a sharp tungsten tip with molecular films on silicon surfaces. *Physical Review Letters,* 65**,** 2270-2273.

BLOCK, S. S., SENG, V. P. & GOSWAMI, D. W. 1997. Chemically Enhanced Sunlight for Killing Bacteria. *Journal of Solar Energy Engineering,* 119**,** 85-91.

BONDARENKO, O., IVASK, A., KAKINEN, A. & KAHRU, A. 2012. Sub-toxic effects of CuO nanoparticles on bacteria: Kinetics, role of Cu ions and possible mechanisms of action. *Environmental Pollution,* 169**,** 81-89.

BÖNNEMANN, H. & RICHARDS, RYAN M. 2001. Nanoscopic Metal Particles − Synthetic Methods and Potential Applications. *European Journal of Inorganic Chemistry,* 2001**,** 2455-2480.

BORN, M. & WOLF, E. 1999. *Principles of optics* Oxford UK, Pergamon.

BOS, J. & TIJSSEN, R. 1995. Chapter 4 Hydrodynamic chromatography of polymers.

BOSI, S., DA ROS, T., CASTELLANO, S., BANFI, E. & PRATO, M. 2000. Antimycobacterial activity of ionic fullerene derivatives. *Bioorganic & Medicinal Chemistry Letters,* 10**,** 1043-1045.

BRADFORD, A., HANDY, R. D., READMAN, J. W., ATFIELD, A. & MÜHLING, M. 2009. Impact of Silver Nanoparticle Contamination on the Genetic Diversity of Natural Bacterial Assemblages in Estuarine Sediments. *Environmental Science & Technology,* 43**,** 4530-4536.

BRUST, M. & KIELY, C. J. 2002. Some recent advances in nanostructure preparation from gold and silver particles: a short topical review. *Colloids and Surfaces A: Physicochemical and Engineering Aspects,* 202**,** 175-186.

BRUST, M., WALKER, M., BETHELL, D., SCHIFFRIN, D. J. & WHYMAN, R. 1994. Synthesis of thiol-derivatised gold nanoparticles in a two-phase Liquid-Liquid system. *Journal of the Chemical Society, Chemical Communications***,** 801-802.

BUCHER, J., MASTEN, S., B., M., POWERS, K., ROBERTS, S. & WALKER, N. 2004. Developing Expereimental Approaches for the Evaluation of Toxicological Interaction of nanoscale Materials. Final workshop Report. Gainesville, Florida: National Institute of Environmental health Sciences and University of Florida.

BUFFLE, J., WILKINSON, K. J., STOLL, S., FILELLA, M. & ZHANG, J. 1998. A Generalized Description of Aquatic Colloidal Interactions: The Three-colloidal Component Approach. *Environmental Science & Technology,* 32**,** 2887-2899.

BUSECK, P. R. 2002. Geological fullerenes: review and analysis. *Earth and Planetary Science Letters,* 203**,** 781-792.

BUTLER, O. T., CAIRNS, W., COOK, J. M. & DAVIDSON, C. M. 2011. Atomic spectrometry update. Environmental analysis. *Journal of Analytical Atomic Spectrometry,* 26**,** 250-286.

BUTT, H.-J., CAPPELLA, B. & KAPPL, M. 2005. Force measurements with the atomic force microscope: Technique, interpretation and applications. *Surface Science Reports,* 59**,** 1-152.

BUZEA, C., PACHECO, I. I. & ROBBIE, K. 2007. Nanomaterials and nanoparticles: Sources and toxicity. *Biointerphases,* 2**,** MR17-MR71.

CALDWELL, K. D., KESNER, L. F., MYERS, M. N. & GIDDINGS, J. C. 1972. Electrical Field-Flow Fractionation of Proteins. *Science,* 176**,** 296-298.

CALDWELL, K. D., NGUYEN, T. T., MYERS, M. N. & GIDDINGS, J. C. 1979. Observations on Anomalous Retention in Steric Field-Flow Fractionation. *Separation Science and Technology,* 14**,** 935-946.

CALLOW, J. A. & CALLOW, M. E. 2006. Biofilms. *Prog Mol Subcell Biol,* 42**,** 141-69.

CAO, Q. & ROGERS, J. A. 2009. Ultrathin Films of Single-Walled Carbon Nanotubes for Electronics and Sensors: A Review of Fundamental and Applied Aspects. *Advanced Materials,* 21**,** 29-53.

CHA, J. N., BARTL, M. H., WONG, M. S., POPITSCH, A., DEMING, T. J. & STUCKY, G. D. 2003. Microcavity Lasing from Block Peptide Hierarchically Assembled Quantum Dot Spherical Resonators. *Nano Letters,* 3**,** 907-911.

CHAN, W. C. W., MAXWELL, D. J., GAO, X., BAILEY, R. E., HAN, M. & NIE, S. 2002. Luminescent quantum dots for multiplexed biological detection and imaging. *Current Opinion in Biotechnology,* 13**,** 40-46.

CHATTERJEE, S., BANDYOPADHYAY, A. & SARKAR, K. 2011. Effect of iron oxide and gold nanoparticles on bacterial growth leading towards biological application. *Journal of Nanobiotechnology,* 9**,** 34.

CHEN, F. & GERION, D. 2004. Fluorescent CdSe/ZnS Nanocrystal−Peptide Conjugates for Long-term, Nontoxic Imaging and Nuclear Targeting in Living Cells. *Nano Letters,* 4**,** 1827-1832.

CHEN, J. P. & YANG, R. T. 1993. Selective Catalytic Reduction of NO with NH3 on SO-24/TiO2 Superacid Catalyst. *Journal of Catalysis,* 139**,** 277-288.

CHEN, K. L. & ELIMELECH, M. 2007. Influence of humic acid on the aggregation kinetics of fullerene (C60) nanoparticles in monovalent and divalent electrolyte solutions. *Journal of Colloid and Interface Science,* 309**,** 126-134.

CHEN, S. F. & ZHANG, H. Y. 2013. Aggregation and Dissolution Kinetics of Nanosilver in Seawater. *Asian Journal of Chemistry,* 25**,** 2886-2888.

CHINNAPONGSE, S. L., MACCUSPIE, R. I. & HACKLEY, V. A. 2011. Persistence of singly dispersed silver nanoparticles in natural freshwaters, synthetic seawater, and simulated estuarine waters. *Science of The Total Environment,* 409**,** 2443-2450.

CHMELIK, J. 2007. Applications of field-flow fractionation in proteomics: Presence and future. *PROTEOMICS,* 7**,** 2719-2728.

CHOI, O., KIM, J., KIM, J.-G., JEONG, Y., MOON, J. S., PARK, C. S. & HWANG, I. 2008. Pyrroloquinoline Quinone Is a Plant Growth Promotion Factor Produced by Pseudomonas fluorescens B16. *Plant Physiology,* 146**,** 657-668.

CHRISTIAN G, D. 2004. Non-regulated water contaminants: emerging research. *Environmental Impact Assessment Review,* 24**,** 711-732.

CHRISTOF, M. N. 2001. Nanoparticles, Proteins, and Nucleic Acids: Biotechnology Meets Materials Science. *Angewandte Chemie International Edition,* 40**,** 4128-4158.

CHWALIBOG, A. S., E. HOTOWY, A. 2010. Visualization of interaction between inorganic nanoparticles and bacteria or fungi. *International Journal of Nanomedicine,* 5**,** 1085-1094.

CIGANG, X. & ET AL. 2006. A combined top-down bottom-up approach for introducing nanoparticle networks into nanoelectrode gaps. *Nanotechnology,* 17**,** 3333.

CLESCERI, L. S., GREENBERG, A. E. & EATON, A. D. 1998. *Standard Methods for the Examinat*ion of Water and Wastewater, Washington DC, USA, American Public Health Association.

CLOSE, G. F., YASUDA, S., PAUL, B., FUJITA, S. & WONG, H. S. P. 2008. A 1 GHz Integrated Circuit with Carbon Nanotube Interconnects and Silicon Transistors. *Nano Letters,* 8**,** 706-709.

COMMISSION, E. 2006. The appropriateness of existing methodologies to assess the potential risks associated with engineered and adventitious products of nanotechnologies. European Commission Health & Consumer Protection

COSTERTON, J. W., LEWANDOWSKI, Z., CALDWELL, D. E., KORBER, D. R. & LAPPIN-SCOTT, H. M. 1995. Microbial Biofilms. *Annual Review of Microbiology,* 49**,** 711-745.

COSTERTON, J. W., STEWART, P. S. & GREENBERG, E. P. 1999. Bacterial Biofilms: A Common Cause of Persistent Infections. *Science,* 284**,** 1318-1322.

CUMBERLAND, S. A. & LEAD, J. R. 2009. Particle size distributions of silver nanoparticles at environmentally relevant conditions. *Journal of Chromatography A,* 1216**,** 9099-9105.

DAHL, J. 2008. *Gram negative bacterial cell wall* [Online]. Wikipedia: Dahl, J. Available: http://en.wikipedia.org/wiki/File:Gram_negative_cell_wall.SVg [Accessed 06/03/2013 2012].

DANIEL, M.-C. & ASTRUC, D. 2003. Gold Nanoparticles: Assembly, Supramolecular Chemistry, Quantum-Size-Related Properties, and Applications toward Biology, Catalysis, and Nanotechnology. *Chemical Reviews,* 104**,** 293-346.

DARIO, M. T. & BACHIORRINI, A. 1999. Interaction of mullite with some polluting oxides in diesel vehicle filters. *Ceramics International,* 25**,** 511-516.

DAVIDSON, E. A. & JANSSENS, I. A. 2006. Temperature sensitivity of soil carbon decomposition and feedbacks to climate change. *Nature,* 440**,** 165-173.

DE CASTRO, C., MOLINARO, A., LANZETTA, R., SILIPO, A. & PARRILLI, M. 2008. Lipopolysaccharide structures from Agrobacterium and Rhizobiaceae species. *Carbohydrate Research,* 343**,** 1924-1933.

DE LA RICA, R., AILI, D. & STEVENS, M. M. 2012. Enzyme-responsive nanoparticles for drug release and diagnostics. *Advanced Drug Delivery Reviews*.

DE WINDT, W., BOON, N., VAN DEN BULCKE, J., RUBBERECHT, L., PRATA, F., MAST, J., HENNEBEL, T. & VERSTRAETE, W. 2006. Biological control of the size and reactivity of catalytic Pd(0) produced by Shewanella oneidensis. *Antonie Van Leeuwenhoek International Journal of General and Molecular Microbiology,* 90**,** 377-389.

DEONARINE, A., LAU, B. L. T., AIKEN, G. R., RYAN, J. N. & HSU-KIM, H. 2011. Effects of Humic Substances on Precipitation and Aggregation of Zinc Sulfide Nanoparticles. *Environmental Science & Technology,* 45**,** 3217-3223.

DERYAGIN, B. V. & LANDOU, L. D. 1941. Theory of the stability of strongly charged lyophobic sols and of the adhesion of strongly charged particles in solutions of electrolytes. *acta phsicochim,* 14.

DEY, R., PAL, K. K., BHATT, D. M. & CHAUHAN, S. M. 2004. Growth promotion and yield enhancement of peanut (Arachis hypogaea L.) by application of plant growth-promoting rhizobacteria. *Microbiological Research,* 159**,** 371-394.

DHAWAN, G. 2012. *back to basics* [Online]. Available: http://www.appliedmembranes.com/about_ultrafiltration.htm [Accessed 10/04/2012 2012].

DIEGOLI, S., MANCIULEA, A. L., BEGUM, S., JONES, I. P., LEAD, J. R. & PREECE, J. A. 2008. Interaction between manufactured gold nanoparticles and naturally occurring organic macromolecules. *Science of The Total Environment,* 402**,** 51-61.

DOMINGOS, R. F., BAALOUSHA, M. A., JU-NAM, Y., REID, M. M., TUFENKJI, N., LEAD, J. R., LEPPARD, G. G. & WILKINSON, K. J. 2009a. Characterizing Manufactured Nanoparticles in the Environment: Multimethod Determination of Particle Sizes. *Environmental Science & Technology,* 43**,** 7277-7284.

DOMINGOS, R. F., TUFENKJI, N. & WILKINSON, K. J. 2009b. Aggregation of Titanium Dioxide Nanoparticles: Role of a Fulvic Acid. *Environmental Science & Technology,* 43**,** 1282-1286.

DONALDSON, K., AITKEN, R., TRAN, L., STONE, V., DUFFIN, R., FORREST, G. & ALEXANDER, A. 2006. Carbon Nanotubes: A Review of Their Properties in Relation to Pulmonary Toxicology and Workplace Safety. *Toxicological Sciences,* 92**,** 5-22.

DOOREN DE JONG, L. E. D. 1926. *Bijdrage tot de kennis van het mineralisatieproces.* van Ditmar.

DOWLING, A. 2005. *Nanoscience and Nanaotechnologies: Opportunities and uncertainties.* , London, UK, Royal Society/Royal Academy of Engineering.

DUFRÊNE, Y. F. 2002. Atomic Force Microscopy, a Powerful Tool in Microbiology. *Journal of Bacteriology,* 184**,** 5205-5213.

DULOG, L. & SCHAUER, T. 1996. Field flow fractionation for particle size determination. *Progress in Organic Coatings,* 28**,** 25-31.

DUNNE, W. M., JR. 2002. Bacterial Adhesion: Seen Any Good Biofilms Lately? *Clin. Microbiol. Rev.,* 15**,** 155-166.

DUNPHY GUZMAN, K. A., FINNEGAN, M. P. & BANFIELD, J. F. 2006. Influence of Surface Potential on Aggregation and Transport of Titania Nanoparticles. *Environmental Science & Technology,* 40**,** 7688-7693.

DÜRIG, U., GIMZEWSKI, J. K. & POHL, D. W. 1986. Experimental Observation of Forces Acting during Scanning Tunneling Microscopy. *Physical Review Letters,* 57**,** 2403-2406.

EILERS, H. & KORFF, J. 1940. The significance of the phenomenon of the electrical charge on the stability of hydrophobic dispersions. *Transactions of the Faraday Society,* 35**,** 229-241.

EINSTEIN, A. 1905. Theory of Brownian Motion. *Ann. der Physik*

ELIMELECH, M., GREGORY, J., JIA, X. & WILLIAMS, R. A. 1995. *Particle Deposition & Aggregation: Measurement, Modelling and Simulation,* Woburn, USA, Butterworth-Heinemann.

ELZEY, S. & GRASSIAN, V. 2010. Agglomeration, isolation and dissolution of commercially manufactured silver nanoparticles in aqueous environments. *Journal of Nanoparticle Research,* 12**,** 1945-1958.

EPA. 2002. Health Assessment for Diesel Exhaust Washungton, DC, USA. U.S. Environmental Protection Agency.

EUROPEAN, C. 2011. What is a "nanomaterial"

European Commission breaks new ground with a common definition, European Commission press release, 18 oct. 2011.

EUSTIS, S. & EL-SAYED, M. A. 2006. Why gold nanoparticles are more precious than pretty gold: Noble metal surface plasmon resonance and its enhancement of the radiative and nonradiative properties of nanocrystals of different shapes. *Chemical Society Reviews,* 35**,** 209-217.

EUSTIS, S., HSU, H.-Y. & EL-SAYED, M. A. 2005. Gold Nanoparticle Formation from Photochemical Reduction of Au3+ by Continuous Excitation in Colloidal Solutions.

A Proposed Molecular Mechanism. *The Journal of Physical Chemistry B,* 109**,** 4811-4815.

FABREGA, J., FAWCETT, S. R., RENSHAW, J. C. & LEAD, J. R. 2009. Silver Nanoparticle Impact on Bacterial Growth: Effect of pH, Concentration, and Organic Matter. *Environmental Science & Technology,* 43**,** 7285-7290.

FABREGA, J., LUOMA, S. N., TYLER, C. R., GALLOWAY, T. S. & LEAD, J. R. 2011. Silver nanoparticles: behaviour and effects in the aquatic environment. *Environment International,* 37**,** 517-531.

FARADAY, M. 1857. The Bakerian Lecture: Experimental Relations of Gold (and Other Metals) to Light. *Philosophical Transactions of the Royal Society of London,* 147**,** 145-181.

FENG, Q. L., WU, J., CHEN, G. Q., CUI, F. Z., KIM, T. N. & KIM, J. O. 2000. A mechanistic study of the antibacterial effect of silver ions on Escherichia coli and Staphylococcus aureus. *Journal of Biomedical Materials Research,* 52**,** 662-668.

FERRARI, M. 2005. Cancer nanotechnology: opportunities and challenges. *Nat Rev Cancer,* 5**,** 161-171.

FILELLA, M. & BUFFLE, J. 1993. Factors controlling the stability of submicron colloids in natural waters. *Colloids and Surfaces A: Physicochemical and Engineering Aspects,* 73**,** 255-273.

FINDLAY, A. D., THOMPSON, D. W. & TIPPING, E. 1996. The aggregation of silica and haematite particles dispersed in natural water samples. *Colloids and Surfaces A: Physicochemical and Engineering Aspects,* 118**,** 97-105.

FLAHAUT, E. 2010. Introduction to the special focus issue: environmental toxicity of nanoparticles. *Nanomedicine,* 5**,** 949-950.

FLORIDAUNIVERSITY. 2012. *Potentiometric Titration of an Acid Mixture : Introduction*

[Online]. Available: http://www.chem.fsu.edu/chemlab/chm3120l/acid/intro.html [Accessed 12/02/2013 2013].

FOOLADI, E. 2009. *My first spherification* [Online]. Available: www.fooducation.org/2009/02/my-first-spherification.html [Accessed 01/12/2012 2012].

FREITAG, M., TSANG, J. C., KIRTLEY, J., CARLSEN, A., CHEN, J., TROEMAN, A., HILGENKAMP, H. & AVOURIS, P. 2006. Electrically Excited, Localized Infrared Emission from Single Carbon Nanotubes. *Nano Letters,* 6**,** 1425-1433.

FRENCH, R. A., JACOBSON, A. R., KIM, B., ISLEY, S. L., PENN, R. L. & BAVEYE, P. C. 2009. Influence of Ionic Strength, pH, and Cation Valence on Aggregation Kinetics of Titanium Dioxide Nanoparticles. *Environmental Science & Technology,* 43**,** 1354-1359.

FRENS, G. 1973. Controlled nucleation for the regulation of the particle size in monodisperse gold suspensions. *Nature Phys. Sci.* , 241**,** 20 - 22.

GADD, G. E., BLACKFORD, M., MORICCA, S., WEBB, N., EVANS, P. J., SMITH, A. M., JACOBSEN, G., LEUNG, S., DAY, A. & HUA, Q. 1997. The World's Smallest Gas Cylinders? *Science,* 277**,** 933-936.

GAGOTSI, Y. 2006. *Nanomaterials Handbook,* Newyork, Taylor & Francis Group.

GAO, J., YOUN, S., HOVSEPYAN, A., LLANEZA, V. N. L., WANG, Y., BITTON, G. & BONZONGO, J.-C. J. 2009. Dispersion and Toxicity of Selected Manufactured Nanomaterials in Natural River Water Samples: Effects of Water Chemical Composition. *Environmental Science & Technology,* 43**,** 3322-3328.

GIDDINGS, J. 1993a. Field-flow fractionation: analysis of macromolecular, colloidal, and particulate materials. *Science,* 260**,** 1456-1465.

GIDDINGS, J. C. 1966. A New Separation Concept Based on a Coupling of Concentration and Flow Nonuniformities. *Separation Science,* 1**,** 123-125.

GIDDINGS, J. C. 1973. The conceptual basis of field flow fractionation *J. Chem. Educ,* 50.

GIDDINGS, J. C. 1993b. Field-flow fractionation: Analysis of macromolecular, colloidal, and particulate materials. *Science,* 260**,** 1456-1465.

GIDDINGS, J. C., YANG, F. J. & MYERS, M. N. 1976. Theoretical and experimental characterization of flow field-flow fractionation. *Analytical Chemistry,* 48**,** 1126-1132.

GIDDINGS, J. C., YANG, F. J. & MYERS, M. N. 1977. Flow field-flow fractionation: new method for separating, purifying, and characterizing the diffusivity of viruses. *Journal of Virology,* 21**,** 131-138.

GIDDINGS, J. C., YANG, F. J. F. & MYERS, M. N. 1974. Sedimentation field-flow fractionation. *Analytical Chemistry,* 46**,** 1917-1924.

GIDDINGS, J. C., YANG, F. J. F. & MYERS, M. N. 1975. Application of Sedimentation Field-Flow Fractionation to Biological Particles: Molecular Weights and Separation. *Separation Science,* 10**,** 133-149.

GLASAUER, S., LANGLEY, S. & BEVERIDGE, T. J. 2002. Intracellular Iron Minerals in a Dissimilatory Iron-Reducing Bacterium. *Science,* 295**,** 117-119.

GOODMAN, C. M., MCCUSKER, C. D., YILMAZ, T. & ROTELLO, V. M. 2004. Toxicity of gold nanoparticles functionalized with cationic and anionic side chains. *Bioconjugate Chemistry,* 15**,** 897-900.

GORDON II, J. G. & ERNST, S. 1980. Surface plasmons as a probe of the electrochemical interface. *Surface Science,* 101**,** 499-506.

GOTTSCHALK, F., SONDERER, T., SCHOLZ, R. W. & NOWACK, B. 2009. Modeled Environmental Concentrations of Engineered Nanomaterials (TiO2, ZnO, Ag, CNT,

Fullerenes) for Different Regions. *Environmental Science & Technology,* 43**,** 9216-9222.

GRAN, G. 1950. Determination of the Equivalent Point in Potentiometric Titrations. *Acta Chemica Scandinavica* 4**,** 559-577.

GRAN, G. 1952. Determination of the equivalence point in potentiometric titrations. Part II. *Analyst,* 77**,** 661-671.

GRANCHAROV, S. G., ZENG, H., SUN, S., WANG, S. X., O'BRIEN, S., MURRAY, C. B., KIRTLEY, J. R. & HELD, G. A. 2005. Bio-functionalization of Monodisperse Magnetic Nanoparticles and Their Use as Biomolecular Labels in a Magnetic Tunnel Junction Based Sensor. *The Journal of Physical Chemistry B,* 109**,** 13030-13035.

GUARDIA, P., PÉREZ, N. S., LABARTA, A. & BATLLE, X. 2009. Controlled Synthesis of Iron Oxide Nanoparticles over a Wide Size Range. *Langmuir,* 26**,** 5843-5847.

GUO, L., YANG, S., YANG, C., YU, P., WANG, J., GE, W. & WONG, G. K. L. 2000. Synthesis and Characterization of Poly(vinylpyrrolidone)-Modified Zinc Oxide Nanoparticles. *Chemistry of Materials,* 12**,** 2268-2274.

HAMAKER, H. C. 1937. The London—van der Waals attraction between spherical particles. *Physica,* 4**,** 1058-1072.

HAMOUDA, T. & BAKER, J. R. 2000. Antimicrobial mechanism of action of surfactant lipid preparations in enteric Gram-negative bacilli. *Journal of Applied Microbiology,* 89**,** 397-403.

HANSEL, C. M., BENNER, S. G., NICO, P. & FENDORF, S. 2004. Structural constraints of ferric (hydr)oxides on dissimilatory iron reduction and the fate of Fe(II). *Geochimica et Cosmochimica Acta,* 68**,** 3217-3229.

HARDMAN, R. 2006. A toxicologic review of quantum dots: Toxicity depends on physicochemical and environmental factors. *Environmental Health Perspectives,* 114**,** 165-172.

HAYDEN, S. C., ZHAO, G., SAHA, K., PHILLIPS, R. L., LI, X., MIRANDA, O. R., ROTELLO, V. M., EL-SAYED, M. A., SCHMIDT-KREY, I. & BUNZ, U. H. F. 2012. Aggregation and Interaction of Cationic Nanoparticles on Bacterial Surfaces. *Journal of the American Chemical Society,* 134**,** 6920-6923.

HEIMANN, M. & REICHSTEIN, M. 2008. Terrestrial ecosystem carbon dynamics and climate feedbacks. *Nature,* 451**,** 289-292.

HENRY, D. C. 1931. The Cataphoresis of Suspended Particles. Part I. The Equation of Cataphoresis. *Proceedings of the Royal Society of London. Series A,* 133**,** 106-129.

HERIVEL, J. W. 1960. Newton's Discovery of the Law of Centrifugal Force. *Isis,* 51**,** 546-553.

HERNÁNDEZ-SIERRA, J. F., RUIZ, F., CRUZ PENA, D. C., MARTÍNEZ-GUTIÉRREZ, F., MARTÍNEZ, A. E., DE JESÚS POZOS GUILLÉN, A., TAPIA-PÉREZ, H. & MARTÍNEZ CASTAÑÓN, G. 2008. The antimicrobial sensitivity of Streptococcus mutans to nanoparticles of silver, zinc oxide, and gold. *Nanomedicine: Nanotechnology, Biology and Medicine,* 4**,** 237-240.

HIRNER, A. 2006. Speciation of alkylated metals and metalloids in the environment. *Analytical and Bioanalytical Chemistry*, 385**,** 555-567.

HIRSCH, T., ZHARNIKOV, M., SHAPORENKO, A., STAHL, J., WEISS, D., WOLFBEIS, O. S. & MIRSKY, V. M. 2005. Size-Controlled Electrochemical Synthesis of Metal Nanoparticles on Monomolecular Templates. *Angewandte Chemie International Edition,* 44**,** 6775-6778.

HOCHELLA, M. F., LOWER, S. K., MAURICE, P. A., PENN, R. L., SAHAI, N., SPARKS, D. L. & TWINING, B. S. 2008. Nanominerals, Mineral Nanoparticles, and Earth Systems. *Science,* 319**,** 1631-1635.

HOFFMANN, M. R., MARTIN, S. T., CHOI, W. & BAHNEMANN, D. W. 1995. Environmental Applications of Semiconductor Photocatalysis. *Chemical Reviews,* 95**,** 69-96.

HONIGMANN, B. 1970. Dispersions of Powders in Liquids, with Special Reference to Pigments. Von G. D. Parfitt. Elsevier Publishing Company, Amsterdam-London-New York 1969. 1. Aufl., XIII, 354 S., zahlr. Abb. u. Tab., geb. Dfl. 52.00. *Angewandte Chemie,* 82**,** 329-330.

HOU, P.-X., YANG, Q.-H., BAI, S., XU, S.-T., LIU, M. & CHENG, H.-M. 2002. Bulk Storage Capacity of Hydrogen in Purified Multiwalled Carbon Nanotubes. *The Journal of Physical Chemistry B,* 106**,** 963-966.

HOUK, R. S., FASSEL, V. A., FLESCH, G. D., SVEC, H. J., GRAY, A. L. & TAYLOR, C. E. 1980. Inductively coupled argon plasma as an ion source for mass spectrometric determination of trace elements. *Analytical Chemistry,* 52**,** 2283-2289.

HTTP://PUBLICATIONS.NIGMS.NIH.GOV/CHEMHEALTH/COOL.HTM. 2011. *Cool Tools* [Online]. http://publications.nigms.nih.gov/chemhealth/cool.htm: National institute of general medical sciences. Available: http://publications.nigms.nih.gov/chemhealth/cool.htm [Accessed 22/01/2013 2013].

HU, X., GUO, T., FU, X. & HU, X. 2003. Nanoscale oxide structures induced by dynamic electric field on Si with AFM. *Applied Surface Science,* 217**,** 34-38.

HUANG, L., LI, D. Q., LIN, Y. J., WEI, M., EVANS, D. G. & DUAN, X. 2005. Controllable preparation of nano-MgO and investigation of its bactericidal properties. *Journal of Inorganic Biochemistry,* 99**,** 986-993.

HUANG, M. H., MAO, S., FEICK, H., YAN, H., WU, Y., KIND, H., WEBER, E., RUSSO, R. & YANG, P. 2001. Room-Temperature Ultraviolet Nanowire Nanolasers. *Science,* 292**,** 1897-1899.

HUCZKO, A. & BYSZEWSKI, P. 1998. Characteristics of Fullerines carbon nanotubes *Fullerines 1*. Wroclaw Poland Wiadomosci Chemiczne

HUTCHINGS, G. J., BRUST, M. & SCHMIDBAUR, H. 2008. Gold-an introductory perspective. *Chemical Society Reviews,* 37**,** 1759-1765.

HUTTER, J. L. & BECHHOEFER, J. 1993. Calibration of atomic‐force microscope tips. *Review of Scientific Instruments,* 64**,** 1868-1873.

HUYNH, K. A. & CHEN, K. L. 2011. Aggregation Kinetics of Citrate and Polyvinylpyrrolidone Coated Silver Nanoparticles in Monovalent and Divalent Electrolyte Solutions. *Environmental Science & Technology,* 45**,** 5564-5571.

HWANG, E. T., LEE, J. H., CHAE, Y. J., KIM, Y. S., KIM, B. C., SANG, B.-I. & GU, M. B. 2008. Analysis of the Toxic Mode of Action of Silver Nanoparticles Using Stress-Specific Bioluminescent Bacteria. *Small,* 4**,** 746-750.

HYUNG, H., FORTNER, J. D., HUGHES, J. B. & KIM, J.-H. 2006. Natural Organic Matter Stabilizes Carbon Nanotubes in the Aqueous Phase. *Environmental Science & Technology,* 41**,** 179-184.

IIJIMA, S. 1991. Helical microtubules of graphitic carbon. *Nature,* 354**,** 56-58.

IIJIMA, S. & ICHIHASHI, T. 1993. Single-shell carbon nanotubes of 1-nm diameter. *Nature,* 363**,** 603-605.

INOUE, S. & SPRING, K. R. 1997. *Video Microscopy the fundamentals* New york, Plenium press.

JALILI, N. & LAXMINARAYANA, K. 2004. A review of atomic force microscopy imaging systems: application to molecular metrology and biological sciences. *Mechatronics,* 14**,** 907-945.

JAMIESON, T., BAKHSHI, R., PETROVA, D., POCOCK, R., IMANI, M. & SEIFALIAN, A. M. 2007. Biological applications of quantum dots. *Biomaterials*, 28**,** 4717-4732.

JANA, N. R., SAU, T. K. & PAL, T. 1998. Growing Small Silver Particle as Redox Catalyst. *The Journal of Physical Chemistry B,* 103**,** 115-121.

JARVIS, K. E. 1988. Inductively coupled plasma mass spectrometry: A new technique for the rapid or ultra-trace level determination of the rare-earth elements in geological materials. *Chemical Geology,* 68**,** 31-39.

JENWAY. 2012. Jenway. Available: http://www.jenway.com/product.asp?dsl=300 [Accessed 12/03/2012 2012].

JIANG, W., MASHAYEKHI, H. & XING, B. 2009. Bacterial toxicity comparison between nano- and micro-scaled oxide particles. *Environmental Pollution,* 157**,** 1619-1625.

JOHANSEN, A., PEDERSEN, A. L., JENSEN, K. A., KARLSON, U., HANSEN, B. M., SCOTT-FORDSMAND, J. J. & WINDING, A. 2008. Effects of C60 fullerene nanoparticles on soil bacteria and protozoans. *Environmental Toxicology and Chemistry,* 27**,** 1895-1903.

JONER, E. J., HARTNIK, T. & AMUNDSEN, C. E. 2008. Norwegian Pollution Control Authority (2008) Environmental fate and ecotoxicity of engineered nanoparticles. Bioforsk, Norway.

JONES, N., RAY, B., RANJIT, K. T. & MANNA, A. C. 2008. Antibacterial activity of ZnO nanoparticle suspensions on a broad spectrum of microorganisms. *FEMS Microbiology Letters,* 279**,** 71-76.

JU-NAM, Y. & LEAD, J. R. 2008. Manufactured nanoparticles: An overview of their chemistry, interactions and potential environmental implications. *Science of The Total Environment,* 400**,** 396-414.

KAI, Y., KOMAZAWA, Y., MIYAJIMA, A., MIYATA, N. & YAMAKOSHI, Y. 2003. [60]Fullerene as a Novel Photoinduced Antibiotic. *Fullerenes, Nanotubes and Carbon Nanostructures,* 11**,** 79-87.

KAMAT, P. V. 1993. Photochemistry on nonreactive and reactive (semiconductor) surfaces. *Chemical Reviews,* 93**,** 267-300.

KANG, S., MAUTER, M. S. & ELIMELECH, M. 2009. Microbial Cytotoxicity of Carbon-Based Nanomaterials: Implications for River Water and Wastewater Effluent. *Environmental Science & Technology,* 43**,** 2648-2653.

KANG, S., PINAULT, M., PFEFFERLE, L. D. & ELIMELECH, M. 2007. Single-walled carbon nanotubes exhibit strong antimicrobial activity. *Langmuir,* 23**,** 8670-8673.

KAPITZA, H. G. 1994. *Microscopy From The Very Beginning,* Oberkochen, Germany, Carl Zeiss,.

KAPLAN, J. B., MEYENHOFER, M. F. & FINE, D. H. 2003. Biofilm Growth and Detachment of Actinobacillus actinomycetemcomitans. *J. Bacteriol.,* 185**,** 1399-1404.

KARTHIKEYAN, S. & BEVERIDGE, T. J. 2002. Pseudomonas aeruginosa biofilms react with and precipitate toxic soluble gold. *Environmental Microbiology,* 4**,** 667-675.

KATAOKA, K., HARADA, A. & NAGASAKI, Y. 2001. Block copolymer micelles for drug delivery: design, characterization and biological significance. *Advanced Drug Delivery Reviews,* 47**,** 113-131.

KAWAI-NAKAMURA, A., SATO, T., SUE, K., TANAKA, S., SAITOH, K., AIDA, K. & HIAKI, T. 2008. Rapid and continuous hydrothermal synthesis of metal and metal

oxide nanoparticles with a microtube-reactor at 523 K and 30 MPa. *Materials Letters,* 62**,** 3471-3473.

KELLER, A. A., WANG, H., ZHOU, D., LENIHAN, H. S., CHERR, G., CARDINALE, B. J., MILLER, R. & JI, Z. 2010. Stability and Aggregation of Metal Oxide Nanoparticles in Natural Aqueous Matrices. *Environmental Science & Technology,* 44**,** 1962-1967.

KHAYDAROV, R. R., KHAYDAROV, R. A., EVGRAFOVA, S., WAGNER, S. & CHO, S. Y. 2011. Environmental and Human Health Issues of Silver Nanoparticles Applications. Environmental Security and Ecoterrorism. *In:* ALPAS, H., BERKOWICZ, S. M. M. & ERMAKOVA, I. (eds.). Springer Netherlands.

KILZ, S., LENZ, C., FUCHS, R. & BUDZIKIEWICZ, H. 1999. A fast screening method for the identification of siderophores from fluorescent Pseudomonas spp. by liquid chromatography/electrospray mass spectrometry. *Journal of Mass Spectrometry,* 34**,** 281-290.

KIM, J. H., LEE, G.-D., PARK, S. S. & HONG, S.-S. 2006. Hydrothermal synthesis of titanium dioxides using acidic and basic peptizing agents and their photocatalytic activity on the decomposition of orange II. *In:* HYUN-KU RHEE, I.-S. N. & JONG MOON, P. (eds.) *Studies in Surface Science and Catalysis.* Elsevier.

KIM, S.-Y., LIM, T.-H., CHANG, T.-S. & SHIN, C.-H. 2007a. Photocatalysis of methylene blue on titanium dioxide nanoparticles synthesized by modified sol-hydrothermal process of TiCl<sub>4</sub&gt. *Catalysis Letters,* 117**,** 112-118.

KIM, S. N., RUSLING, J. F. & PAPADIMITRAKOPOULOS, F. 2007b. Carbon Nanotubes for Electronic and Electrochemical Detection of Biomolecules. *Advanced Materials,* 19**,** 3214-3228.

KING, S., HYUNH, K. & TANNENBAUM, R. 2003. Kinetics of Nucleation, Growth, and Stabilization of Cobalt Oxide Nanoclusters. *The Journal of Physical Chemistry B,* 107**,** 12097-12104.

KIRCHNER, C., LIEDL, T., KUDERA, S., PELLEGRINO, T., JAVIER, A. M., GAUB, H. E., STOLZLE, S., FERTIG, N. & PARAK, W. J. 2005. Cytotoxicity of colloidal CdSe and CdSe/ZnS nanoparticles. *Nano Letters,* 5**,** 331-338.

KIRKLAND, J. J., LIEBALD, W. & UNGER, K. K. 1990. Characterization of diesel soot by sedimentation field flow fractionation. *Journal of Chromatographic Science,* 28**,** 374-378.

KISER, M. A., LADNER, D. A., HRISTOVSKI, K. D. & WESTERHOFF, P. K. 2012. Nanomaterial Transformation and Association with Fresh and Freeze-Dried Wastewater Activated Sludge: Implications for Testing Protocol and Environmental Fate. *Environmental Science & Technology,* 46**,** 7046-7053.

KLAINE, S. J., ALVAREZ, P. J. J., BATLEY, G. E., FERNANDES, T. F., HANDY, R. D., LYON, D. Y., MAHENDRA, S., MCLAUGHLIN, M. J. & LEAD, J. R. 2008. Nanomaterials in the environment: Behavior, fate, bioavailability, and effects. *Environmental Toxicology and Chemistry,* 27**,** 1825-1851.

KLOEPFER, J. A., MIELKE, R. E. & NADEAU, J. L. 2005. Uptake of CdSe and CdSe/ZnS quantum dots into bacteria via purine-dependent mechanisms. *Applied and Environmental Microbiology,* 71**,** 2548-2557.

KLOEPPER, J. W., LEONG, J., TEINTZE, M. & SCHROTH, M. N. 1980. Enhanced plant growth by siderophores produced by plant growth-promoting rhizobacteria. *Nature,* 286**,** 885-886.

KNOLL, M. & RUSKA, E. 1932. Electron Microscope. *Z. Phys,* 78**,** 318 - 339.

KORDÁS, K., TÓTH, G., MOILANEN, P., KUMPUMÄKI, M., VÄHÄKANGAS, J., UUSIMÄKI, A., VAJTAI, R. & AJAYAN, P. M. 2007. Chip cooling with integrated carbon nanotube microfin architectures. *Applied Physics Letters,* 90.

KREIBIG, U. & VOLLMER, M. 1995. *Optical properties of metal clusters,* Berlin, Germany, Springer.

KRETZSCHMAR, R., BARMETTLER, K., GROLIMUND, D., YAN, Y.-D., BORKOVEC, M. & STICHER, H. 1997. Experimental determination of colloid deposition rates and collision efficiencies in natural porous media. *Water Resour. Res.,* 33**,** 1129-1137.

KROTO, H. W., HEATH, J. R., O'BRIEN, S. C., CURL, R. F. & SMALLEY, R. E. 1985. C60: Buckminsterfullerene. *Nature,* 318**,** 162-163.

KRUMOV, N., PERNER-NOCHTA, I., ODER, S., GOTCHEVA, V., ANGELOV, A. & POSTEN, C. 2009. Production of Inorganic Nanoparticles by Microorganisms. *Chemical Engineering & Technology,* 32**,** 1026-1035.

KUENEN, J. G. & ROBERTSON, L. A. 1994. Combined nitrification-denitrification processes. *FEMS Microbiology Reviews,* 15**,** 109-117.

KUMAR, N., SHAH, V. & WALKER, V. K. 2011. Perturbation of an arctic soil microbial community by metal nanoparticles. *Journal of Hazardous Materials,* 190**,** 816-822.

KUMAR, S., GANDHI, K. S. & KUMAR, R. 2006. Modeling of Formation of Gold Nanoparticles by Citrate Methodâ€ *Industrial & Engineering Chemistry Research,* 46**,** 3128-3136.

KUO, T.-R., WU, C.-L., HSU, C.-T., LO, W., CHIANG, S.-J., LIN, S.-J., DONG, C.-Y. & CHEN, C.-C. 2009. Chemical enhancer induced changes in the mechanisms of transdermal delivery of zinc oxide nanoparticles. *Biomaterials,* 30**,** 3002-3008.

KVITEK, L., PANAČEK, A., SOUKUPOVA, J., KOLAR, M., VEČEROVA, R., PRUCEK, R., HOLECOVA, M. & ZBORIL, R. 2008. Effect of Surfactants and Polymers on

Stability and Antibacterial Activity of Silver Nanoparticles (NPs). *The Journal of Physical Chemistry C,* 112**,** 5825-5834.

LAI, L., LIN, C., XIAO, C.-Q., XU, Z.-Q., HAN, X.-L., FU, L., LI, D.-W., MEI, P., JIANG, F.-L., GUO, Q.-L. & LIU, Y. 2013. Adhesion of quantum dots-induced membrane damage of Escherichia coli. *Journal of Colloid and Interface Science,* 389**,** 61-70.

LANG, C., SCHÜLER, D. & FAIVRE, D. 2007. Synthesis of Magnetite Nanoparticles for Bio- and Nanotechnology: Genetic Engineering and Biomimetics of Bacterial Magnetosomes. *Macromolecular Bioscience,* 7**,** 144-151.

LAPRESTA-FERNÁNDEZ, A., FERNÁNDEZ, A. & BLASCO, J. 2012. Nanoecotoxicity effects of engineered silver and gold nanoparticles in aquatic organisms. *TrAC Trends in Analytical Chemistry,* 32**,** 40-59.

LARACHI, F., PIERRE, J., ADNOT, A. & BERNIS, A. 2002. Ce 3d XPS study of composite CexMn1-xO2-y wet oxidation catalysts. *Applied Surface Science,* 195**,** 236-250.

LAURENT, S., FORGE, D., PORT, M., ROCH, A., ROBIC, C., VANDER ELST, L. & MULLER, R. N. 2008. Magnetic Iron Oxide Nanoparticles: Synthesis, Stabilization, Vectorization, Physicochemical Characterizations, and Biological Applications. *Chemical Reviews,* 108**,** 2064-2110.

LEAD, J. R. 2010. Manufactured nanoparticles in the environment. *Environmental Chemistry,* 7**,** 1-2.

LEAD, J. R. & WILKINSON, K. J. 2006. Aquatic Colloids and Nanoparticles: Current Knowledge and Future Trends. *Environmental Chemistry,* 3**,** 159-171.

LECOANET, H. F., BOTTERO, J.-Y. & WIESNER, M. R. 2004. Laboratory Assessment of the Mobility of Nanomaterials in Porous Media. *Environmental Science & Technology,* 38**,** 5164-5169.

LEE, H. J. & JEONG, S. H. 2005. Bacteriostasis and Skin Innoxiousness of Nanosize Silver Colloids on Textile Fabrics. *Textile Research Journal,* 75**,** 551-556.

LEE, I., HAN, S. W. & KIM, K. 2001. Simultaneous preparation of SERS-active metal colloids and plates by laser ablation. *Journal of Raman Spectroscopy,* 32**,** 947-952.

LEE, S. W., LIANG, D., GAO, X. P. A. & SANKARAN, R. M. 2011. Direct Writing of Metal Nanoparticles by Localized Plasma Electrochemical Reduction of Metal Cations in Polymer Films. *Advanced Functional Materials,* 21**,** 2155-2161.

LEROUEIL, P. R., HONG, S., MECKE, A., BAKER, J. R., ORR, B. G. & BANASZAK HOLL, M. M. 2007. Nanoparticle Interaction with Biological Membranes: Does Nanotechnology Present a Janus Face? *Accounts of Chemical Research,* 40**,** 335-342.

LEWIS, J. A. 2000. Colloidal Processing of Ceramics. *Journal of the American Ceramic Society,* 83**,** 2341-2359.

LEWIS, L. N. 1993. Chemical catalysis by colloids and clusters. *Chemical Reviews,* 93**,** 2693-2730.

LI, H., DUAN, X., LIU, G., JIA, X. & LIU, X. 2008. Morphology controllable synthesis of TiO2 by a facile hydrothermal process. *Materials Letters,* 62**,** 4035-4037.

LI, M., POKHREL, S., JIN, X., MÄDLER, L., DAMOISEAUX, R. & HOEK, E. M. V. 2010a. Stability, Bioavailability, and Bacterial Toxicity of ZnO and Iron-Doped ZnO Nanoparticles in Aquatic Media. *Environmental Science & Technology,* 45**,** 755-761.

LI, W.-R., XIE, X.-B., SHI, Q.-S., ZENG, H.-Y., OU-YANG, Y.-S. & CHEN, Y.-B. 2010b. Antibacterial activity and mechanism of silver nanoparticles on <i>Escherichia coli</i&gt. *Applied Microbiology and Biotechnology,* 85**,** 1115-1122.

LI, X. & LENHART, J. J. 2012. Aggregation and Dissolution of Silver Nanoparticles in Natural Surface Water. *Environmental Science & Technology,* 46**,** 5378-5386.

LIU, J. & HURT, R. H. 2010. Ion Release Kinetics and Particle Persistence in Aqueous Nano-Silver Colloids. *Environmental Science & Technology,* 44**,** 2169-2175.

LIU, Y., ROSENFIELD, E., HU, M. & MI, B. 2013. Direct observation of bacterial deposition on and detachment from nanocomposite membranes embedded with silver nanoparticles. *Water Research*.

LIZ-MARZÃ¡N, L. M. 2005. Tailoring Surface Plasmons through the Morphology and Assembly of Metal Nanoparticles. *Langmuir,* 22**,** 32-41.

LOGOTHETIDIS, S., PATSALAS, P. & CHARITIDIS, C. 2003. Enhanced catalytic activity of nanostructured cerium oxide films. *Materials Science and Engineering: C,* 23**,** 803-806.

LOHRKE, J., BRIEL, A. & MÄDER, K. 2008. Characterization of superparamagnetic iron oxide nanoparticles by asymmetrical flow-field-flow-fractionation. *Nanomedicine,* 3**,** 437-452.

LOVERN, S. B., STRICKLER, J. R. & KLAPER, R. 2007. Behavioral and Physiological Changes in Daphnia magna when Exposed to Nanoparticle Suspensions (Titanium Dioxide, Nano-C60, and C60HxC70Hx). *Environmental Science & Technology,* 41**,** 4465-4470.

LOWRY, G. V., GREGORY, K. B., APTE, S. C. & LEAD, J. R. 2012. Transformations of Nanomaterials in the Environment. *Environmental Science & Technology,* 46**,** 6893-6899.

LU, Y., YIN, Y., MAYERS, B. T. & XIA, Y. 2002. Modifying the Surface Properties of Superparamagnetic Iron Oxide Nanoparticles through A Sol−Gel Approach. *Nano Letters,* 2**,** 183-186.

LUGTENBERG, B. & KAMILOVA, F. 2009. Plant-growth -promoting Rhizobacteria. *Annual Review Microbiology,* 63**,** 541-556.

LUO, J., CHAN, W.-B., WANG, L. & ZHONG, C.-J. 2010. Probing interfacial interactions of bacteria on metal nanoparticles and substrates with different surface properties. *International Journal of Antimicrobial Agents,* 36**,** 549-556.

LUO, J., MAYE, M. M., KARIUKI, N. N., WANG, L., NJOKI, P., LIN, Y., SCHADT, M., NASLUND, H. R. & ZHONG, C.-J. 2005. Electrocatalytic oxidation of methanol: carbon-supported gold-platinum nanoparticle catalysts prepared by two-phase protocol. *Catalysis Today,* 99**,** 291-297.

LYON, D. Y., ADAMS, L. K., FALKNER, J. C. & ALVAREZ, P. J. J. 2006. Antibacterial Activity of Fullerene Water Suspensions: Effects of Preparation Method and Particle Size†. *Environmental Science & Technology,* 40**,** 4360-4366.

M.N, M. 2006. Do nanoparticles present ecotoxicological risks for the health of the aquatic environment? *Environment International,* 32**,** 967-976.

MADHUSUDAN REDDY, K., GOPAL REDDY, C. V. & MANORAMA, S. V. 2001. Preparation, Characterization, and Spectral Studies on Nanocrystalline Anatase TiO2. *Journal of Solid State Chemistry,* 158**,** 180-186.

MAFUNÉ, F., KOHNO, J.-Y., TAKEDA, Y., KONDOW, T. & SAWABE, H. 2000. Structure and Stability of Silver Nanoparticles in Aqueous Solution Produced by Laser Ablation. *The Journal of Physical Chemistry B,* 104**,** 8333-8337.

MAKINO, T., CHIA, C. H., SEGAWA, Y., KAWASAKI, M., OHTOMO, A., TAMURA, K., MATSUMOTO, Y. & KOINUMA, H. 2002. High-throughput optical characterization for the development of a ZnO-based ultraviolet semiconductor-laser. *Applied Surface Science,* 189**,** 277-283.

MALVERN 2001. Zeta Potential: An introduction in 30 minutes. Worcester: Malvern instrument.

MALVERN 2004. *Zetasizer Nano Series User Manual* Worcester Uk, Malvern Instrument.

MALVERN 2007. zetasizer Nano User Manual.

MALVERN. 2012. *Principle Behind Dynamic Light Scattering* [Online]. Available: http://www.malvern.com/labeng/technology/dynamic_light_scattering/dynamic_light_scattering.htm [Accessed 14/03/2012 2012].

MASHINO, T., NISHIKAWA, D., TAKAHASHI, K., USUI, N., YAMORI, T., SEKI, M., ENDO, T. & MOCHIZUKI, M. 2003a. Antibacterial and antiproliferative activity of cationic fullerene derivatives. *Bioorganic & Medicinal Chemistry Letters,* 13**,** 4395-4397.

MASHINO, T., OKUDA, K., HIROTA, T., HIROBE, M., NAGANO, T. & MOCHIZUKI, M. 1999. Inhibition ofE. coli growth by fullerene derivatives and inhibition mechanism. *Bioorganic & Medicinal Chemistry Letters,* 9**,** 2959-2962.

MASHINO, T., USUI, N., OKUDA, K., HIROTA, T. & MOCHIZUKI, M. 2003b. Respiratory chain inhibition by fullerene derivatives: Hydrogen peroxide production caused by fullerene derivatives and a respiratory chain system. *Bioorganic & Medicinal Chemistry,* 11**,** 1433-1438.

MATSUMURA, Y., YOSHIKATA, K., KUNISAKI, S. & TSUCHIDO, T. 2003. Mode of bactericidal action of silver zeolite and its comparison with that of silver nitrate. *Applied and Environmental Microbiology,* 69**,** 4278-4281.

MCWHIRTER, M. J., MCQUILLAN, A. J. & BREMER, P. J. 2002. Influence of ionic strength and pH on the first 60 min of Pseudomonas aeruginosa attachment to ZnSe and to TiO2 monitored by ATR-IR spectroscopy. *Colloids and Surfaces B: Biointerfaces,* 26**,** 365-372.

MEHTA, R. & THAKRAL, S. 2006. Fullerenes: An introduction and overview of their biological properties. *Indian Journal of Pharmaceutical Sciences,* 68**,** 13-19.

MELLOR, J. W. 1923. *A Comprehensive Treasise on inorganic and Theoretical Chemistry,,* London, Longmans, Green and Co.

MENDES, G. C. C., BRANDÃO, T. R. S. & SILVA, C. L. M. 2007. Ethylene oxide sterilization of medical devices: A review. *American Journal of Infection Control,* 35**,** 574-581.

MESSAUD, F. A., SANDERSON, R. D., RUNYON, J. R., OTTE, T., PASCH, H. & WILLIAMS, S. K. R. 2009. An overview on field-flow fractionation techniques and their applications in the separation and characterization of polymers. *Progress in Polymer Science,* 34**,** 351-368.

MEYER, E. 1992. Atomic force microscopy. *Progress in Surface Science,* 41**,** 3-49.

MEYER, J.-M. 2000. Pyoverdines: pigments, siderophores and potential taxonomic markers of fluorescent<SMALL> Pseudomonas</SMALL> species. *Archives of Microbiology,* 174**,** 135-142.

MEYER, J. M., GEOFFROY, V. A., BAIDA, N., GARDAN, L., IZARD, D., LEMANCEAU, P., ACHOUAK, W. & PALLERONI, N. J. 2002. Siderophore typing, a powerful tool for the identification of fluorescent and nonfluorescent pseudomonads. *Applied and Environmental Microbiology,* 68**,** 2745-2753.

MEYER, J. M. & HORNSPERGER, J. M. 1978. Role of PyoverdinePf, the Iron-binding Fluorescent Pigment of Pseudomonas fluorescens, in Iron Transport. *Journal of General Microbiology,* 107**,** 329-331.

MILLER, J. C. & MILLER, J. N. 1993. Statistics for Analytical Chemistry, 3rd edition, New york, USA. Ellis Harwood limited.

MIRKIN, C. A., LETSINGER, R. L., MUCIC, R. C. & STORHOFF, J. J. 1996. A DNA-based method for rationally assembling nanoparticles into macroscopic materials. *Nature,* 382**,** 607-609.

MISRA, S. K., DYBOWSKA, A., BERHANU, D., LUOMA, S. N. & VALSAMI-JONES, E. 2012. The complexity of nanoparticle dissolution and its importance in nanotoxicological studies. *Science of The Total Environment,* 438**,** 225-232.

MIZES, H. A., PARK, S.-I. & HARRISON, W. A. 1987. Multiple-tip interpretation of anomalous scanning-tunneling-microscopy images of layered materials. *Physical Review B,* 36**,** 4491-4494.

MOISAN, M., BARBEAU, J., CREVIER, M., PELLETIER, J., PHILIP, N. & SAOUDI, B. 2002. Plasma sterilization. Methods and mechanisms. *Pure Appl. Chem.,,* 74**,** 349.

MOLDOVAN, M., KRUPP, E. M., HOLLIDAY, A. E. & DONARD, O. F. X. 2004. High resolution sector field ICP-MS and multicollector ICP-MS as tools for trace metal speciation in environmental studies: a review. *Journal of Analytical Atomic Spectrometry,* 19**,** 815-822.

MONROE, D. 2007. Looking for Chinks in the Armor of Bacterial Biofilms. *PLoS Biol,* 5**,** e307.

MONTASER, A. 1998. InductivelyCoupled PlasmaMass Spectrometry., New York, USA. Wiley VCH:.

MORNET, S., VASSEUR, S., GRASSET, F. & DUGUET, E. 2004. Magnetic nanoparticle design for medical diagnosis and therapy. *Journal of Materials Chemistry,* 14**,** 2161-2175.

MORONES, J. R., ELECHIGUERRA, J. L., CAMACHO, A., HOLT, K., KOURI, J. B., RAMIREZ, J. T. & YACAMAN, M. J. 2005a. The bactericidal effect of silver nanoparticles. *Nanotechnology,* 16**,** 2346-2353.

MORONES, J. R., ELECHIGUERRA, J. L., CAMACHO, A., HOLT, K., KOURI, J. B., RAMÍREZ, J. T. & YACAMAN, M. J. 2005b. The bactericidal effect of silver nanoparticles. *Nanotechnology,* 16**,** 2346.

MUELLER, N. C. & NOWACK, B. 2008. Exposure Modeling of Engineered Nanoparticles in the Environment. *Environmental Science & Technology,* 42**,** 4447-4453.

MÜLLER, J. & WEIßENRIEDER, S. 1994. ZnO-thin film chemical sensors. *Fresenius' Journal of Analytical Chemistry,* 349**,** 380-384.

MURRAY, H. H. 2000. Gold: Progress in Chemistry, Biochemistry and Technology Edited by Hubert Schmidbaur (Technical University of Munich, Germany). John Wiley & Sons: New York. 1999. ISBN 0-471-97369-6. *Journal of the American Chemical Society,* 122**,** 4534-4534.

MYERS, M. N. 1997. Overview of field-flow fractionation. *Journal of Microcolumn Separations,* 9**,** 151-162.

NAVALADIAN, S., VISWANATHAN, B., VISWANATH, R. & VARADARAJAN, T. 2006. Thermal decomposition as route for silver nanoparticles. *Nanoscale Research Letters,* 2**,** 44 - 48.

NAVARRO, E., BAUN, A., BEHRA, R., HARTMANN, N., FILSER, J., MIAO, A.-J., QUIGG, A., SANTSCHI, P. & SIGG, L. 2008. Environmental behavior and ecotoxicity of engineered nanoparticles to algae, plants, and fungi. *Ecotoxicology,* 17**,** 372-386.

NEAL, A. 2008. What can be inferred from bacterium–nanoparticle interactions about the potential consequences of environmental exposure to nanoparticles? *Ecotoxicology,* 17**,** 362-371.

NEL, A., XIA, T., MÄDLER, L. & LI, N. 2006. Toxic Potential of Materials at the Nanolevel. *Science,* 311**,** 622-627.

NELLIST, P. D., CHISHOLM, M. F., DELLBY, N., KRIVANEK, O. L., MURFITT, M. F., SZILAGYI, Z. S., LUPINI, A. R., BORISEVICH, A., SIDES, W. H. &

PENNYCOOK, S. J. 2004. Direct Sub-Angstrom Imaging of a Crystal Lattice. *Science,* 305**,** 1741.

NELMS, S. 2005. *Inductively Coupled PlasmaMass Spectrometry Handbook,* Carlton, Victoria, Blackwell.

NIEMEYER, C. M. 2001. Nanoparticles, Proteins, and Nucleic Acids: Biotechnology Meets Materials Science. *Angewandte Chemie International Edition,* 40**,** 4128-4158.

NIU, C., SICHEL, E. K., HOCH, R., MOY, D. & TENNENT, H. 1997. High power electrochemical capacitors based on carbon nanotube electrodes. *Applied Physics Letters,* 70**,** 1480-1482.

NOWACK, B. & BUCHELI, T. D. 2007. Occurrence, behavior and effects of nanoparticles in the environment. *Environmental Pollution,* 150**,** 5-22.

NYBERG, L., TURCO, R. F. & NIES, L. 2008. Assessing the impact of nanomaterials on anaerobic microbial communities. *Environmental Science & Technology,* 42**,** 1938-1943.

O'KEEFE, J. A. 1956. Resolving Power of Visible Light. *J. Opt. Soc. Am.,* 46**,** 359-359.

O'TOOLE, G. A. 2003. To Build a Biofilm. *J. Bacteriol.,* 185**,** 2687-2689.

OSKAM, G. 2006. Metal oxide nanoparticles: synthesis, characterization and application. *Journal of Sol-Gel Science and Technology,* 37**,** 161-164.

PADMAVATHY, N. & VIJAYARAGHAVAN, R. 2011. Interaction of ZnO Nanoparticles with MicrobesA Physio and Biochemical Assay. *Journal of Biomedical Nanotechnology,* 7**,** 813-822.

PAL, S., TAK, Y. K. & SONG, J. M. 2007. Does the Antibacterial Activity of Silver Nanoparticles Depend on the Shape of the Nanoparticle? A Study of the Gram-Negative Bacterium Escherichia coli. *Applied and Environmental Microbiology,* 73**,** 1712-1720.

PALLERONI, N. J., KUNISAWA, R., CONTOPOULOU, R. & DOUDOROFF, M. 1973. Nucleic Acid Homologies in the Genus Pseudomonas. *International Journal of Systematic Bacteriology,* 23**,** 333-339.

PALLERONI, N. J. D., M. 1974. The Genus Pseudomonas. In Bergey's Manual of Determinitive Bacteriology In: GIBBONS, R. E. B. N. E. (ed.) In Bergey's Manual of Determinitive Bacteriology. 8th edition ed. Baltimore, USA. Williams & Wilkins

PAN, Y., NEUSS, S., LEIFERT, A., FISCHLER, M., WEN, F., SIMON, U., SCHMID, G., BRANDAU, W. & JAHNEN-DECHENT, W. 2007. Size-Dependent Cytotoxicity of Gold Nanoparticles. *Small,* 3**,** 1941-1949.

PANDEY, P. A., BELL, G. R., ROURKE, J. P., SANCHEZ, A. M., ELKIN, M. D., HICKEY, B. J. & WILSON, N. R. 2011. Physical Vapor Deposition of Metal Nanoparticles on Chemically Modified Graphene: Observations on Metal–Graphene Interactions. *Small,* 7**,** 3202-3210.

PAOLO PENGO, S. P., MARINO BATTAGLIARIN, LUCIA PASQUATO AND PAOLO SCRIMIN 2003. Synthesis, characterization and properties of water-soluble gold nanoparticles with tunable core size. *Journal of Materials Chemistry***,** 2471 -2478.

PARIKH, S. J. & CHOROVER, J. 2006. ATR-FTIR Spectroscopy Reveals Bond Formation During Bacterial Adhesion to Iron Oxide. *Langmuir,* 22**,** 8492-8500.

PELLETIER, D. A., SURESH, A. K., HOLTON, G. A., MCKEOWN, C. K., WANG, W., GU, B., MORTENSEN, N. P., ALLISON, D. P., JOY, D. C., ALLISON, M. R., BROWN, S. D., PHELPS, T. J. & DOKTYCZ, M. J. 2010. Effects of Engineered Cerium Oxide Nanoparticles on Bacterial Growth and Viability. *Applied and Environmental Microbiology,* 76**,** 7981-7989.

PERCIVAL, S., T., WALKER, J, T., AND HUNTER, P,R. 2000. *Microbiologial aspects of Biofilms and Drinking Water.,* Florida, CRC Press.

PEREZ, J. M. 2007. Iron oxide nanoparticles: Hidden talent. *Nat Nano,* 2**,** 535-536.

PEREZ, J. M., O'LOUGHIN, T., SIMEONE, F. J., WEISSLEDER, R. & JOSEPHSON, L. 2002. DNA-Based Magnetic Nanoparticle Assembly Acts as a Magnetic Relaxation Nanoswitch Allowing Screening of DNA-Cleaving Agents. *Journal of the American Chemical Society,* 124**,** 2856-2857.

PERKINELMER 2011. The 30 minutes guide to ICP_MS. Waltham, USA.

PETER, J. S. 2000. Gold - Progress in Chemistry, Biochemistry and Technology. H. Schmidbaur (ed.) John Wiley & Sons, Chichester, 1999 ISBN 0-471-97369-6. *Applied Organometallic Chemistry*, 14**,** 171.

PETER , P. E. & JOHN MEURIG, T. 2007. Gold in a Metallic Divided State - From Faraday to Present-Day Nanoscience13. *Angewandte Chemie International Edition,* 46**,** 5480-5486.

PETTEYS, M. P. & SCHIMPF, M. E. 1998. Characterization of hematite and its interaction with hurnic material using flow field-flow fractionation. *J. Chromatogr. A,* 816.

PHARM_VIRGINIA. 2012. *Atomic Force MIcroscope (AFM)* [Online]. Available: http://pharm.virginia.edu/AFM.html [Accessed 04/02/2013 2013].

PHILIP WONG, H. S. 2005. Beyond the conventional transistor. *Solid-State Electronics,* 49**,** 755-762.

PICCAPIETRA, F., SIGG, L. & BEHRA, R. 2011. Colloidal Stability of Carbonate-Coated Silver Nanoparticles in Synthetic and Natural Freshwater. *Environmental Science & Technology*.

POCKRAND, I., SWALEN, J. D., GORDON II, J. G. & PHILPOTT, M. R. 1978. Surface plasmon spectroscopy of organic monolayer assemblies. *Surface Science,* 74**,** 237-244.

POLTE, J. R., ERLER, R., THUÌˆNEMANN, A. F., SOKOLOV, S., AHNER, T. T., RADEMANN, K., EMMERLING, F. & KRAEHNERT, R. 2010. Nucleation and Growth of Gold Nanoparticles Studied via in situ Small Angle X-ray Scattering at Millisecond Time Resolution. *ACS Nano,* 4**,** 1076-1082.

PONG, B.-K., ELIM, H. I., CHONG, J.-X., JI, W., TROUT, B. L. & LEE, J.-Y. 2007. New Insights on the Nanoparticle Growth Mechanism in the Citrate Reduction of Gold(III) Salt: Formation of the Au Nanowire Intermediate and Its Nonlinear Optical Properties. *The Journal of Physical Chemistry C,* 111**,** 6281-6287.

POOL, R. 1990. The Children of the STM. *Science,* 247**,** 634-636.

PRADEEP, T. & ANSHUP 2009. Noble metal nanoparticles for water purification: A critical review. *Thin Solid Films,* 517**,** 6441-6478.

PRAETORIUS, A., SCHERINGER, M. & HUNGERBÜHLER, K. 2012. Development of Environmental Fate Models for Engineered Nanoparticles—A Case Study of TiO2 Nanoparticles in the Rhine River. *Environmental Science & Technology,* 46**,** 6705-6713.

PRATIM, B. & CHANG-YU, W. 2005. 2005 critical review: nanoparticles and the environment. *Journal Name: Journal of the Air and Waste Management Association; Journal Volume: 55; Journal Issue: 6***,** Medium: X; Size: page(s) 708-746.

PRATSINIS, S. E., ZHU, W. & VEMURY, S. 1996. The role of gas mixing in flame synthesis of titania powders. *Powder Technology,* 86**,** 87-93.

RAETZ, C. R. H. 1990. Biochemistry of Endotoxins. *Annual Review of Biochemistry,* 59**,** 129-170.

RAKHI, R. B., SETHUPATHI, K. & RAMAPRABHU, S. 2008. Synthesis and hydrogen storage properties of carbon nanotubes. *International Journal of Hydrogen Energy,* 33**,** 381-386.

RAMASWAMY, V., JAGTAP, N. B., VIJAYANAND, S., BHANGE, D. S. & AWATI, P. S. 2008. Photocatalytic decomposition of methylene blue on nanocrystalline titania prepared by different methods. *Materials Research Bulletin,* 43**,** 1145-1152.

RAO, N. N. & DUBE, S. 1996. Photocatalytic degradation of mixed surfactants and some commercial soap/detergent products using suspended TiO2 catalysts. *Journal of Molecular Catalysis A: Chemical,* 104**,** L197-L199.

RASHIDZADEH, M. 2008. Synthesis of High-Thermal Stable Titanium Dioxide Nanoparticles. *International Journal of Photoenergy,* 2008.

RATANATHANAWONGS WILLIAMS, S. K., BENINCASA, M.-A. & ASHAMES, A. A. 2006. Field Flow Fractionation in Analysis of Polymers and Rubbers. *Encyclopedia of Analytical Chemistry.* John Wiley & Sons, Ltd.

RATTE, H. T. 1999. Bioaccumulation and toxicity of silver compounds: A review. *Environmental Toxicology and Chemistry,* 18**,** 89-108.

RAY, P. C., YU, H. & FU, P. P. 2009. Toxicity and Environmental Risks of Nanomaterials: Challenges and Future Needs. *Journal of Environmental Science and Health, Part C,* 27**,** 1-35.

RAY, S. J., ANDRADE, F., GAMEZ, G., MCCLENATHAN, D., ROGERS, D., SCHILLING, G., WETZEL, W. & HIEFTJE, G. M. 2004. Plasma-source mass spectrometry for speciation analysis: state-of-the-art. *Journal of Chromatography A,* 1050**,** 3-34.

RESCHIGLIAN, P., ZATTONI, A., RODA, B., MICHELINI, E. & RODA, A. 2005. Field-flow fractionation and biotechnology. *Trends in Biotechnology,* 23**,** 475-483.

RINCON, A. G. & PULGARIN, C. 2004a. Bactericidal action of illuminated TiO2 on pure Escherichia coli and natural bacterial consortia: post-irradiation events in the dark and

assessment of the effective disinfection time. *Applied Catalysis B-Environmental,* 49**,** 99-112.

RINCON, A. G. & PULGARIN, C. 2004b. Effect of pH, inorganic ions, organic matter and H2O2 on E-coli K12 photocatalytic inactivation by TiO2 - Implications in solar water disinfection. *Applied Catalysis B-Environmental,* 51**,** 283-302.

ROCO, M. 2011. The Long View of Nanotechnology Development: The National Nanotechnology Initiative at 10 Years. *Nanotechnology Research Directions for Societal Needs in 2020.* Springer Netherlands.

ROCO, M. C. 2005. Environmentally Responsible Development of Nanotechnology. *Environmental Science & Technology,* 39**,** 106A-112A.

RODUNER, E. 2006. Size matters: why nanomaterials are different. *Chemical Society Reviews,* 35**,** 583-592.

ROZHKOV, S. P., GORYUNOV, A. S., SUKHANOVA, G. A., BORISOVA, A. G., ROZHKOVA, N. N. & ANDRIEVSKY, G. V. 2003. Protein interaction with hydrated C60 fullerene in aqueous solutions. *Biochemical and Biophysical Research Communications,* 303**,** 562-566.

SALATA, O. 2004. Applications of nanoparticles in biology and medicine. *Journal of Nanobiotechnology,* 2**,** 3.

SALEH, N., KIM, H.-J., PHENRAT, T., MATYJASZEWSKI, K., TILTON, R. D. & LOWRY, G. V. 2008. Ionic Strength and Composition Affect the Mobility of Surface-Modified Fe0 Nanoparticles in Water-Saturated Sand Columns. *Environmental Science & Technology,* 42**,** 3349-3355.

SAMBHY, V., MACBRIDE, M. M., PETERSON, B. R. & SEN, A. 2006. Silver Bromide Nanoparticle/Polymer Composites: Dual Action Tunable Antimicrobial Materials. *Journal of the American Chemical Society,* 128**,** 9798-9808.

SAPKOTA, A., WILLIAMS, D. A. & BUCKLEY, T. J. 2005. Tollbooth Workers and Mobile Source-Related Hazardous Air Pollutants: How Protective Is the Indoor Environment? *Environmental Science & Technology,* 39**,** 2936-2943.

SARDAR, R., FUNSTON, A. M., MULVANEY, P. & MURRAY, R. W. 2009. Gold Nanoparticles: Past, Present, and Futureâ€ *Langmuir,* 25**,** 13840-13851.

SAWAI, J., IGARASHI, H., HASHIMOTO, A., KOKUGAN, T. & SHIMIZU, M. 1995. EFFECT OF CERAMIC POWDER SLURRY ON SPORES OF BACILLUS-SUBTILIS. *Journal of Chemical Engineering of Japan,* 28**,** 556-561.

SAWAI, J., IGARASHI, H., HASHIMOTO, A., KOKUGAN, T. & SHIMIZU, M. 1996. Effect of particle size and heating temperature of ceramic powders on antibacterial activity of their slurries. *Journal of Chemical Engineering of Japan,* 29**,** 251-256.

SAYES, C. M., FORTNER, J. D., GUO, W., LYON, D., BOYD, A. M., AUSMAN, K. D., TAO, Y. J., SITHARAMAN, B., WILSON, L. J., HUGHES, J. B., WEST, J. L. & COLVIN, V. L. 2004. The Differential Cytotoxicity of Water-Soluble Fullerenes. *Nano Letters,* 4**,** 1881-1887.

SCENIHR 2007. Sceintific Committee on Emerging and Newly Identified Health Risks. Opinion on the sceintific aspects of the existing and proposed definitions relating to products of nanoscience and nanotechnologies. Brussels, Belgium: : European Commission.

SCHÜLER, D. & FRANKEL, R. B. 1999. Bacterial magnetosomes: microbiology, biomineralization and biotechnological applications. *Applied Microbiology and Biotechnology,* 52**,** 464-473.

SHAFIROVICH, E., DIAKOV, V. & VARMA, A. 2006. Combustion of novel chemical mixtures for hydrogen generation. *Combustion and Flame,* 144**,** 415-418.

SHAFIROVICH, E., DIAKOV, V. & VARMA, A. 2007. Combustion-assisted hydrolysis of sodium borohydride for hydrogen generation. *International Journal of Hydrogen Energy*, 32**,** 207-211.

SHANMIN, G. & ET AL. 2003. Preparation of CuAlO 2 nanocrystalline transparent thin films with high conductivity. *Nanotechnology*, 14**,** 538.

SHENDRUK, T. N. & SLATER, G. W. 2012. Operational-modes of field-flow fractionation in microfluidic channels. *Journal of Chromatography A*, 1233**,** 100-108.

SHENHAR, R. & ROTELLO, V. M. 2003. Nanoparticles: Scaffolds and Building Blocks. *Accounts of Chemical Research*, 36**,** 549-561.

SHIELDS, S. P., RICHARDS, V. N. & BUHRO, W. E. 2010. Nucleation Control of Size and Dispersity in Aggregative Nanoparticle Growth. A Study of the Coarsening Kinetics of Thiolate-Capped Gold Nanocrystals. *Chemistry of Materials*.

SHTYKOVA, E. V., HUANG, X., REMMES, N., BAXTER, D., STEIN, B., DRAGNEA, B., SVERGUN, D. I. & BRONSTEIN, L. M. 2007. Structure and Properties of Iron Oxide Nanoparticles Encapsulated by Phospholipids with Poly(ethylene glycol) Tails. *The Journal of Physical Chemistry C*, 111**,** 18078-18086.

SHUGUANG WANG, LAWSON, R., RAY, P. C. & HONGTAO YU 2011. Toxic effects of gold nanoparticles on Salmonella typhimurium bacteria. *Toxicology and Industrial Health*, 27**,** 547-554.

SILBY, M. L., S. 2006. *Pseudomonas Flourescens* [Online]. Available: http://genome.jgi-psf.org/psefl/psefl.home.html [Accessed 05/12/2012 2012].

SINGHAL, A., YANG, J. C. & GIBSON, J. M. 1997. STEM-based mass spectroscopy of supported Re clusters. *Ultramicroscopy*, 67**,** 191-206.

SINHA, R., KARAN, R., SINHA, A. & KHARE, S. K. 2011. Interaction and nanotoxic effect of ZnO and Ag nanoparticles on mesophilic and halophilic bacterial cells. *Bioresource Technology,* 102**,** 1516-1520.

SIOUTAS, C., DELFINO, R. J. & SINGH, M. 2005. Exposure Assessment for Atmospheric Ultrafine Particles (UFPs) and Implications in Epidemiologic Research. *Environ Health Perspect,* 113.

SLAVEYKOVA, V. I., STARTCHEV, K. & ROBERTS, J. 2009. Amine- and Carboxyl-Quantum Dots Affect Membrane Integrity of Bacterium Cupriavidus metallidurans CH34. *Environmental Science & Technology,* 43**,** 5117-5122.

SMOLUCHOWSKI, M. 1903. *Bull. Int. Acad. SCi. ,* 184.

SMOLUCHOWSKI, M. V. 1918. *Z. Phys. Chem.,* 92.

SOLOMON, T. 2001. The Definition and Unit of Ionic Strength. *Journal of Chemical Education,* 78**,** 1691.

SOLOV'EV, A., POTEKHINA, T., CHERNOVA, I. & BASIN, B. 2007. Track membrane with immobilized colloid silver particles. *Russian Journal of Applied Chemistry,* 80**,** 438-442.

SONDI, I. & SALOPEK-SONDI, B. 2004. Silver nanoparticles as antimicrobial agent: a case study on E. coli as a model for Gram-negative bacteria. *Journal of Colloid and Interface Science,* 275**,** 177-182.

SOTO, K. F., CARRASCO, A., POWELL, T. G., GARZA, K. M. & MURR, L. E. 2005. Comparative <i>in vitro</i> cytotoxicity assessment of some manufacturednanoparticulate materials characterized by transmissionelectron microscopy. *Journal of Nanoparticle Research,* 7**,** 145-169.

SOUTHAM, G. & BEVERIDGE, T. J. 1994. The in vitro formation of placer gold by bacteria. *Geochimica et Cosmochimica Acta,* 58**,** 4527-4530.

STACHOWIAK, J. C., HAYDEN, C. C. & SASAKI, D. Y. 2010. Steric confinement of proteins on lipid membranes can drive curvature and tubulation. *Proceedings of the National Academy of Sciences,* 107**,** 7781-7786.

STANIER, R. Y., PALLERONI, N. J. & DOUDOROFF, M. 1966. The Aerobic Pseudomonads a Taxonomic Study. *Journal of General Microbiology,* 43**,** 159-271.

STANKUS, D. P., LOHSE, S. E., HUTCHISON, J. E. & NASON, J. A. 2010. Interactions between Natural Organic Matter and Gold Nanoparticles Stabilized with Different Organic Capping Agents. *Environmental Science & Technology,* 45**,** 3238-3244.

STOIMENOV, P. K., KLINGER, R. L., MARCHIN, G. L. & KLABUNDE, K. J. 2002. Metal Oxide Nanoparticles as Bactericidal Agents. *Langmuir,* 18**,** 6679-6686.

STOLPE, B. & HASSELLÖV, M. 2007. Changes in size distribution of fresh water nanoscale colloidal matter and associated elements on mixing with seawater. *Geochimica et Cosmochimica Acta,* 71**,** 3292-3301.

STONE, V., NOWACK, B., BAUN, A., VAN DEN BRINK, N., VON DER KAMMER, F., DUSINSKA, M., HANDY, R., HANKIN, S., HASSELLÖV, M., JONER, E. & FERNANDES, T. F. 2010. Nanomaterials for environmental studies: Classification, reference material issues, and strategies for physico-chemical characterisation. *Science of The Total Environment,* 408**,** 1745-1754.

SUN, X., SHENG, Z. & LIU, Y. 2013. Effects of silver nanoparticles on microbial community structure in activated sludge. *Science of The Total Environment,* 443**,** 828-835.

SUZUKI, Y., KELLY, S. D., KEMNER, K. M. & BANFIELD, J. F. 2002. Radionuclide contamination: Nanometre-size products of uranium bioreduction. *Nature,* 419**,** 134-134.

TAGMATARCHIS, N. & SHINOHARA, H. 2001. Fullerenes in Medicinal Chemistry and their Biological Applications. *Mini Reviews in Medicinal Chemistry,* 1**,** 339-348.

TARASENKO, N., NEVAR, A. & NEDELKO, M. 2010. Properties of zinc-oxide nanoparticles synthesized by electrical-discharge technique in liquids. *physica status solidi (a),* 207**,** 2319-2322.

TAYEL, A., A, EL-TRAS, W., F, MOUSA, S., EL-BAZ, A. F., MAHROUS, H., SALEM, M. F. & BRIMER, L. 2011. Antibacterial action of zinc oxide nanoparticles against foodborne pathogens. *Journal of food safety,* 31**,** 211 -218.

TAYLOR, J. June 2002,. New Dimensions for Manufacturing A UKStrategy for Nanotechnology. Department of Trade and Industry and Office of Science and Technology.

TEMPLETON, A. C., WUELFING, W. P. & MURRAY, R. W. 1999. Monolayer-Protected Cluster Molecules. *Accounts of Chemical Research,* 33**,** 27-36.

TERSOFF, J. & RUOFF, R. S. 1994. Structural Properties of a Carbon-Nanotube Crystal. *Physical Review Letters,* 73**,** 676.

THENG, B. K. G. & YUAN, G. 2008. Nanoparticles in the Soil Environment. *ELEMENTS,* 4**,** 395-399.

THEODORE, L. K., G. L. 2005. *Nanotechnology Environmental Implications and Solutions,* New Jersey, John Wiley & Sons.

THILL, A., ZEYONS, O., SPALLA, O., CHAUVAT, F., ROSE, J., AUFFAN, M. & FLANK, A. M. 2006. Cytotoxicity of CeO2 nanoparticles for Escherichia coli. Physico-chemical insight of the cytotoxicity mechanism. *Environmental Science & Technology,* 40**,** 6151-6156.

THOMAS, R. 2004. Practical guide to ICP_MS, New york, USA. Marcel Dekker.

TIAN, N., ZHOU, Z.-Y., SUN, S.-G., DING, Y. & WANG, Z. L. 2007. Synthesis of Tetrahexahedral Platinum Nanocrystals with High-Index Facets and High Electro-Oxidation Activity. *Science,* 316**,** 732-735.

TIMMER, J. M. K., SPEELMANS, M. P. J. & VAN DER HORST, H. C. 1998. Separation of amino acids by nanofiltration and ultrafiltration membranes. *Separation and Purification Technology,* 14**,** 133-144.

TIPPING, E. 1981. The adsorption of aquatic humic substances by iron oxides. *Geochimica et Cosmochimica Acta,* 45**,** 191-199.

TOENNIES, G. & GALLANT, D. L. 1949. The relation between photometric turbidity and bacterial concentration. *Growth,* 13**,** 7-20.

TOLAYMAT, T. M., EL BADAWY, A. M., GENAIDY, A., SCHECKEL, K. G., LUXTON, T. P. & SUIDAN, M. 2010. An evidence-based environmental perspective of manufactured silver nanoparticle in syntheses and applications: A systematic review and critical appraisal of peer-reviewed scientific papers. *Science of The Total Environment,* 408**,** 999-1006.

TONG, M., DING, J., SHEN, Y. & ZHU, P. 2010. Influence of biofilm on the transport of fullerene (C60) nanoparticles in porous media. *Water Research,* 44**,** 1094-1103.

TONG, Z., BISCHOFF, M., NIES, L., APPLEGATE, B. & TURCO, R. F. 2007. Impact of Fullerene (C60) on a Soil Microbial Community. *Environmental Science & Technology,* 41**,** 2985-2991.

TOUHAMI, A., JERICHO, M. H. & BEVERIDGE, T. J. 2004. Atomic Force Microscopy of Cell Growth and Division in Staphylococcus aureus. *Journal of Bacteriology,* 186**,** 3286-3295.

TREFRY, J. C., MONAHAN, J. L., WEAVER, K. M., MEYERHOEFER, A. J., MARKOPOLOUS, M. M., ARNOLD, Z. S., WOOLEY, D. P. & PAVEL, I. E. 2010.

Size Selection and Concentration of Silver Nanoparticles by Tangential Flow Ultrafiltration for SERS-Based Biosensors. *Journal of the American Chemical Society,* 132**,** 10970-10972.

TROJANOWICZ, M. 2006. Analytical applications of carbon nanotubes: a review. *TrAC Trends in Analytical Chemistry,* 25**,** 480-489.

TSAO, N., LUH, T. Y., CHOU, C. K., WU, J. J., LIN, Y. S. & LEI, K. Y. 2001. Inhibition of group A streptococcus infection by carboxyfullerene. *Antimicrobial Agents and Chemotherapy,* 45**,** 1788-1793.

TSCHARNUTER, W. 2006. Photon Correlation Spectroscopy in Particle Sizing. Encyclopedia of Analytical Chemistry. Larkspur, CA, USA. John Wiley & Sons, Ltd.

TURKEVICH, P. C. S., J. HILLER 1951. A study of the Nucleation and Growth Processes in the Synthesis of Colloidal Gold. *Discussions of the Faraday Society,* 11**,** 55-75.

ULRICH, A., MOOR, C., VONMONT, H., JORDI, H.-R. & LORY, M. 2004. ICP–MS trace-element analysis as a forensic tool. *Analytical and Bioanalytical Chemistry,* 378**,** 1059-1068.

URS, G. & ET AL. 2011. Magnetic properties of nanomagnetic and biomagnetic systems analyzed using cantilever magnetometry. *Nanotechnology*, 22**,** 285715.

VERWEY, J. W. & OVERBEEK, J. T. G. 1948. *Theory of the Stability of Lyophobic Colloids,* New york, USA. Elsavier.

VOYLES, P. M., MULLER, D. A., GRAZUL, J. L., CITRIN, P. H. & GOSSMANN, H. J. L. 2002. Atomic-scale imaging of individual dopant atoms and clusters in highly n-type bulk Si. *Nature,* 416**,** 826-829.

WALLACE, L. 1998. *industrial centrifugation Technology* New york, USA. McGraw-Hill.

WALLACE, L. 2007. *Centrifugal separation in Biochemistry,* Oxford, Academic press.

WANG, C., WANG, L., WANG, Y., LIANG, Y. & ZHANG, J. 2012. Toxicity effects of four typical nanomaterials on the growth of Escherichia coli, Bacillus subtilis and Agrobacterium tumefaciens. *Environmental Earth Sciences,* 65**,** 1643-1649.

WANG, W.-N., LENGGORO, I. W., TERASHI, Y., KIM, T. O. & OKUYAMA, K. 2005. One-step synthesis of titanium oxide nanoparticles by spray pyrolysis of organic precursors. *Materials Science and Engineering: B,* 123**,** 194-202.

WANG, Z. L. & SONG, J. 2006. Piezoelectric Nanogenerators Based on Zinc Oxide Nanowire Arrays. *Science,* 312**,** 242-246.

WEI, C., LIN, W. Y., ZAINAL, Z., WILLIAMS, N. E., ZHU, K., KRUZIC, A. P., SMITH, R. L. & RAJESHWAR, K. 1994. Bactericidal Activity of TiO2 Photocatalyst in Aqueous Media: Toward a Solar-Assisted Water Disinfection System. *Environmental Science & Technology,* 28**,** 934-938.

WEI, Y. & ET AL. 2007. Magnetic polymer microspheres with polymer brushes and the immobilization of protein on the brushes. *Journal of Materials Chemistry,* 17**,** 3812.

WICK, P., MANSER, P., LIMBACH, L. K., DETTLAFF-WEGLIKOWSKA, U., KRUMEICH, F., ROTH, S., STARK, W. J. & BRUININK, A. 2007. The degree and kind of agglomeration affect carbon nanotube cytotoxicity. *Toxicology Letters,* 168**,** 121-131.

WIDDER, K. J., SENYEL, A. E. & SCARPELLI, G. D. 1978. Magnetic microspheres: a model system of site specific drug delivery in vivo. *Proceedings of the Society for Experimental Biology and Medicine. Society for Experimental Biology and Medicine (New York, N.Y.),* 158**,** 141-6.

WIESNER, M. R., LOWRY, G. V., JONES, K. L., HOCHELLA, J. M. F., DI GIULIO, R. T., CASMAN, E. & BERNHARDT, E. S. 2009. Decreasing Uncertainties in

Assessing Environmental Exposure, Risk, and Ecological Implications of Nanomaterial. *Environmental Science & Technology,* 43**,** 6458-6462.

WIGGINTON, N. S., HAUS, K. L. & HOCHELLA JR, M. F. 2007. Aquatic environmental nanoparticles. *Journal of Environmental Monitoring,* 9**,** 1306-1316.

WIKIPEDIA , F. E. 2012. *Diagram of zeta potential and slipping planeV2.svg* [Online]. Available: http://en.wikipedia.org/wiki/Zeta_potential [Accessed 20/04/2012 2012].

WILHELM, C., GAZEAU, F., ROGER, J., PONS, J. N. & BACRI, J. C. 2002. Interaction of Anionic Superparamagnetic Nanoparticles with Cells: Kinetic Analyses of Membrane Adsorption and Subsequent Internalization. *Langmuir,* 18**,** 8148-8155.

WILLETS, K. A. & VAN DUYNE, R. P. 2007. Localized Surface Plasmon Resonance Spectroscopy and Sensing. *Annual Review of Physical Chemistry,* 58**,** 267-297.

WILLIAMS, D. B. & CARTER, C. B. 1996. *Transmission electron microscopy- a text book for material science* New York, USA. Plenum Press.

WILSON, K. & WALKER, J. 2010. *Practical Biochemistry; Principles and techniques,* New York, USA. Cambridge University Press.

WINKELMAN, G. 1991. *Handbook of microbiological iron chelates.* , Tupingen, Germany. Boca Raton, CRC press.

WITTGREN, B. & WAHLUND, K. G. 1997. Fast molecular mass and size characterization of polysaccharides using asymmetrical flow field-flow fractionation-multiangle light scattering. *J. Chromatogr., A,* 760.

WOLF, S. 2004. *Microchip Manufacturing,* Sunset Beach, Lattice Press.

WOLFRUM, E. J., HUANG, J., BLAKE, D. M., MANESS, P. C., HUANG, Z., FIEST, J. & JACOBY, W. A. 2002. Photocatalytic oxidation of bacteria, bacterial and fungal spores, and model biofilm components to carbon dioxide on titanium dioxide-coated surfaces. *Environmental Science & Technology,* 36**,** 3412-3419.

WOODROW_WILSON_CENTRE. 2007. *Woodrow Wilson Nanotechnology Consumer Products* [Online]. Available: http://www.nanotechproject.org/inventories/consumer/ [Accessed 24/01/2013 2013].

WUILLOUD, R. G. & ALTAMIRANO, J. C. 2006. Speciation Analysis of Non-Metallic Elements Using Plasma-Based Atomic Spectrometry for Detection. *Current Analytical Chemistry,* 2**,** 353-377.

WUM, P. 2012. *Inductively Coupled Plasma - Mass Spectrometer* [Online]. Washington: Washington University in St. Louis. Available: http://eecelabs.seas.wustl.edu/ICP-MS.aspx [Accessed 04/05/2012.

XU, S., LIAO, Q. & SAIERS, J. E. 2008. Straining of Nonspherical Colloids in Saturated Porous Media. *Environmental Science & Technology,* 42**,** 771-778.

YANG, H., WANG, Y., LAI, S., AN, H., LI, Y. & CHEN, F. 2007. Application of Atomic Force Microscopy as a Nanotechnology Tool in Food Science. *Journal of Food Science,* 72**,** R65-R75.

YANG, L. & WATTS, D. J. 2005. Particle surface characteristics may play an important role in phytotoxicity of alumina nanoparticles. *Toxicology Letters,* 158**,** 122-132.

YEE, N., FOWLE, D. A. & FERRIS, F. G. 2004. A Donnan potential model for metal sorption onto Bacillus subtilis. *Geochimica et Cosmochimica Acta,* 68**,** 3657-3664.

YUAN, Z., LI, J., CUI, L., XU, B., ZHANG, H. & YU, C.-P. 2012. Interaction of silver nanoparticles with pure nitrifying bacteria. *Chemosphere*.

ZEISLER, R., MURPHY, K., BECKER, D., DAVIS, W., KELLY, W., LONG, S. & SIEBER, J. 2006. Standard Reference Materials® (SRMs) for measurement of inorganic environmental contaminants. *Analytical and Bioanalytical Chemistry*, 386**,** 1137-1151.

ZHANG, L., JIANG, Y., DING, Y., POVEY, M. & YORK, D. 2007. Investigation into the antibacterial behaviour of suspensions of ZnO nanoparticles (ZnO nanofluids). *Journal of Nanoparticle Research,* 9**,** 479-489.

ZHANG, Y., CHEN, Y., WESTERHOFF, P., HRISTOVSKI, K. & CRITTENDEN, J. C. 2008. Stability of commercial metal oxide nanoparticles in water. *Water Research,* 42**,** 2204-2212.

ZHAO, Y., TIAN, Y., CUI, Y., LIU, W., MA, W. & JIANG, X. 2010. Small Molecule-Capped Gold Nanoparticles as Potent Antibacterial Agents That Target Gram-Negative Bacteria. *Journal of the American Chemical Society,* 132**,** 12349-12356.

ZHAROV, V. P., MERCER, K. E., GALITOVSKAYA, E. N. & SMELTZER, M. S. 2006. Photothermal nanotherapeutics and nanodiagnostics for selective killing of bacteria targeted with gold nanoparticles. *Biophysical Journal,* 90**,** 619-627.

ZHOU, M., WANG, B., ROZYNEK, Z., XIE, Z., FOSSUM, J. O., YU, X. & RAAEN, S. 2009. Minute synthesis of extremely stable gold nanoparticles. *Nanotechnology,* 20**,** 505606.

ZHOU, Y., KONG, Y., KUNDU, S., CIRILLO, J. & LIANG, H. 2012. Antibacterial activities of gold and silver nanoparticles against Escherichia coli and bacillus Calmette-Guerin. *Journal of Nanobiotechnology,* 10**,** 19.

ZONG, R. L., ZHOU, J., LI, B., FU, M., SHI, S. K. & LI, L. T. 2005. Optical properties of transparent copper nanorod and nanowire arrays embedded in anodic alumina oxide. *Journal of Chemical Physics,* 123**,** 5.

APPENDIX A: TEM images of the synthesised gold nanoparticles: one sample from each coating agents

Appendix A1: TEM images of G2 (citrate capped)

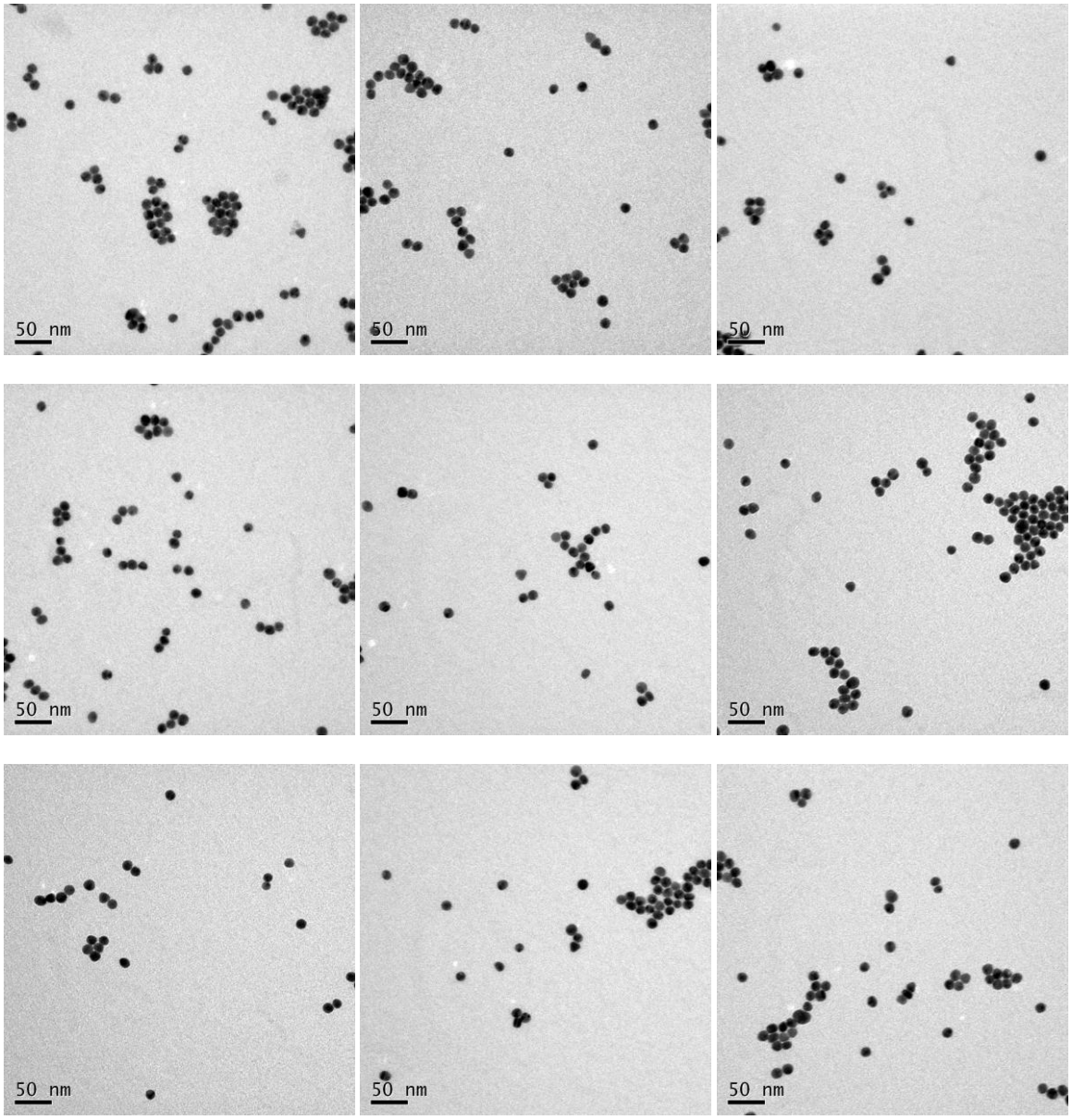

Appendix A2: TEM images of G5 (PVP capped)